Cooperative Transmission Techniques in Wireless Communication Networks

A Thesis Submitted
to the College of Graduate Studies and Research
in Partial Fulfillment of the Requirements
for the Degree of Doctor of Philosophy
in the Department of Electrical and Computer Engineering
University of Saskatchewan

by

Ha X. Nguyen

Saskatoon, Saskatchewan, Canada

Permission To Use

In presenting this thesis in partial fulfillment of the requirements for a Postgraduate degree from the University of Saskatchewan, it is agreed that the Libraries of this University may make it freely available for inspection. Permission for copying of this thesis in any manner, in whole or in part, for scholarly purposes may be granted by the professors who supervised this thesis work or, in their absence, by the Head of the Department of Electrical and Computer Engineering or the Dean of the College of Graduate Studies and Research at the University of Saskatchewan. Any copying, publication, or use of this thesis, or parts thereof, for financial gain without the written permission of the author is strictly prohibited. Proper recognition shall be given to the author and to the University of Saskatchewan in any scholarly use which may be made of any material in this thesis.

Request for permission to copy or to make any other use of material in this thesis in whole or in part should be addressed to:

Head of the Department of Electrical and Computer Engineering
57 Campus Drive
University of Saskatchewan
Saskatoon, Saskatchewan, Canada
S7N 5A9

Acknowledgments

In my four years in Saskatoon, I have been fortunate to get help and support from many people. These few lines are not enough to express my gratitude to all of them.

First and foremost, I would like to express my deepest appreciation to my supervisor, Prof. Ha Hoang Nguyen, for his constant inspiration, support, and guidance during my Ph.D. program at the University of Saskatchewan. I have benefited tremendously from his enthusiasm and constructive criticism. I am indebted to him for carefully reading my manuscripts and patiently working with me on my writing. I would not have been able to complete this thesis without the benefit of his vast knowledge, experience, and valuable comments.

I would also like to thank my co-supervisor, Prof. Tho Le-Ngoc (McGill University), for his collaboration on my research projects. Through our conversations, his deep and broad knowledge of life has been a great source of inspiration to me.

I would like to extend my appreciation to Profs. Eric Salt, Seokbum Ko, Ralph Deters, Anh Dinh, and Prof. Paul Ho from Simon Fraser University for serving on my doctoral committee and providing valuable feedback. Special thanks go to Prof. Eric Salt for many non-technical conversations. Undoubtedly, I have enjoyed every single moment talking with him.

I would like to thank all my past and current colleagues: Son Hoang, Tung Pham, Nam Vien, Tran Nguyen, Duy Nguyen, Quang Duong, Zohreh Andalibi, and Simin Bokharaiee, for the wonderful time at the Communication Theory Research Group (CTRG). I have enjoyed many discussions with them on various technical and non-technical topics.

I gratefully acknowledge the Natural Sciences and Engineering Research Council (NSERC) and the Department of Electrical and Computer Engineering at the Uni-

versity of Saskatchewan for their financial support. Without it, I would not have been able to study in Canada and complete my Ph.D. program.

My deepest gratitude and love belongs to all of my family members, especially my beloved wife and son, for their tremendous understanding, support, care, encouragement, and love during this long-term study. Without them, this thesis would have not been completed. I also thank my mother, mother-in-law, father-in-law, for their constant love and support.

Finally, I would like to dedicate this thesis in honor of my late father. I have deep regret that he will not see the completed thesis. His unconditional love is something I can never pay back.

Abstract

Cooperative communication networks have received significant interests from both academia and industry in the past decade due to its ability to provide spatial diversity without the need of implementing multiple transmit and/or receive antennas at the end-user terminals. These new communication networks have inspired novel ideas and approaches to find out what and how performance improvement can be provided with cooperative communications. The objective of this thesis is to design and analyze various cooperative transmission techniques under the two common relaying signal processing methods, namely decode-and-forward (DF) and amplify-and-forward (AF).

For the DF method, the thesis focuses on providing performance improvement by mitigating detection errors at the relay(s). In particular, the relaying action is implemented adaptively to reduce the phenomenon of error propagation: whether or not a relay's decision to retransmit depends on its decision variable and a predefined threshold. First, under the scenario that unequal error protection is employed to transmit different information classes at the source, a relaying protocol in a single-relay network is proposed and its error performance is evaluated. It is shown that by setting the optimal signal-to-noise ratio (SNR) thresholds at the relay for different information classes, the overall error performance can be significantly improved. Second, for multiple-relay networks, a relay selection protocol, also based on SNR thresholds, is proposed and the optimal thresholds are also provided. Third, an adaptive relaying protocol and a low-complexity receiver are proposed when binary frequency-shift-keying (FSK) modulation is employed and neither the receiver nor the transmitter knows the fading coefficients. It is demonstrated that large performance improvements are possible when the optimal thresholds are implemented at the relays and destination. Finally, under the scenario that there is information feedback from the destination to the relays, a novel protocol is developed to achieve the maximum transmission throughput over a multiple-relay network while the bit-error rate satisfies a given constraint.

With the AF method, the thesis examines a fixed-gain multiple-relay network in which the channels are temporally-correlated Rayleigh flat fading. Developed is a general framework for maximum-ratio-combining detection when M-FSK modulation is used and no channel state information is available at the destination. In particular, an upper-bound expression on the system's error performance is derived and used to verify that the system achieves the maximal diversity order. Simulation results demonstrate that the proposed scheme outperforms the existing schemes for the multiple-relay network under consideration.

Table of Contents

List of Tables

List of Figures

List of Abbreviations

M-FSK	Multiple Frequency-Shift Keying
AF	Amplify-and-Forward
ASK	Amplitude-Shift Keying
AWGN	Additive White Gaussian Noise
BER	Bit-Error-Rate
BFSK	Binary Frequency-Shift Keying
C-MRC	Cooperative Maximum-Ratio-Combining
CF	Compress-and-Forward
CSI	Channel State Information
DF	Decode-and-Forward
DPSK	Differential Phase-Shift Keying
DSTC	Distributed Space-Time Coding
FSK	Frequency-Shift Keying
i.i.d.	independent and identically distributed
OOK	On-Off Keying
PSK	Phase-Shift Keying
QAM	Quadrature Amplitude Modulation
RF	Radio Frequency
RV	Random Variable

SNR	Signal-to-Noise Ratio
UEP	Unequal Error Protection

1. Introduction and Organization of The Dissertation

1.1 Introduction

The introduction of mobile and wireless communication systems in the late 20th century has radically changed the life of human being, especially in the economical and social aspects. In addition to the more traditional services such as speech, video, and data, the pervasive use of wireless communication systems can also provide other services to improve the quality of life, including health care, home automation, etc. Nevertheless, the main challenge in designing and operating a wireless communication system is to be able to provide a high throughput transmission with good reliability under limited radio spectrum, interference, and time variation of the wireless channel. With the rapidly growing demand for various services of the next-generation wireless communication systems, such as high-speed wireless Internet access and wireless television, the requirements for high data transmission rates and reliable communications over wireless channels become even more pressing. In fact, the past decades have witnessed explosive interest and development from both industry and research community in the design of wireless communication systems to increase the data transmission, improve reliability and optimize power consumption. Such interest and development promise to continue for years to come.

Unlike many other communication channels, the signals transmitted over a wireless channel arrive at the destination through multiple paths, which at certain frequencies can add destructively and result in a serious performance degradation [C1-1, C1-2, C1-3]. This phenomenon experienced in wireless transmission is commonly referred to

as *fading*. Fading causes very poor performance and a low data rate of a wireless communication system. The most effective technique to mitigate the fading effects in wireless communications is *diversity*. The basic idea of any diversity techniques is to provide the receiver with independently faded copies of the transmitted signal. Diversity techniques that have been studied in the literature and applied in practice include time diversity, frequency diversity, spatial diversity, signal space diversity, etc. Moreover, one can combine several types of diversity to further improve the system performance [C1-1, C1-2, C1-3]. Among the mentioned diversity techniques, *spatial diversity* that is provided with the use of multiple transmit and/or receive antennas has been intensively studied in the last fifteen years.

However, in many emerging wireless applications, such as ad-hoc networks, implementing multiple transmit and/or receive antennas to provide diversity might not be possible due to the size and cost limitations. A new diversity method has recently been proposed to overcome the above limitations [C1-4, C1-5]. The basic idea of the new method is that a source node transmits information data to the destination through multiple nodes (or relays). In this way, the destination receives the transmitted data with multiple copies that are generally affected by different and statistically independent fading paths. The destination then combines all the received signals to obtain diversity. Diversity obtained through multihop transmissions with the assistance of relays is commonly referred to as *cooperative diversity* [C1-4, C1-5, C1-6, C1-7].

Depending on the type of signal processing performed at relays, cooperative diversity schemes can be classified as Amplify-and-Forward (AF), Decode-and-Forward (DF), Estimate-and-Forward, etc. The two cooperative schemes that are extensively studied in the literature are AF and DF. With AF, relays receive noisy versions of the source's data, amplify and re-transmit to the destination. The AF protocol is further categorized as variable-gain or fixed-gain relaying based on the availability of channel state information (CSI) at the relays. The variable-gain AF relaying scheme requires the instantaneous CSI of the source-relay link at the corresponding relay to maintain a fixed transmit power at all time. On the other hand, the fixed-gain AF

relaying scheme does not need the instantaneous CSI, but the average signal-to-noise ratio of the source-relay link in order to maintain a fixed average transmit power at each relay. With DF, relays decode the source's data, re-encode and re-transmit to the destination [C1-4, C1-5, C1-6, C1-7, C1-8, C1-9, C1-10].

A cooperative diversity network can be designed and implemented coherently. For AF relaying, coherent implementation requires that the destination has the CSI of all the transmission links involved in the cooperation. With DF, the destination needs the CSI of the link between the source and the destination and between the relays and the destination. In order to satisfy such CSI requirements, training data from the source and the relays are required, which might still be unrealistic in a fast fading environment. Moreover, the complexity of channel estimation increases with the number of relays in the network.

To bypass the need of CSI at the relays and/or destination, noncoherent modulation and demodulation can be used. Popular noncoherent techniques include differential phase-shift keying (DPSK), on-off keying (OOK), and frequency-shift keying (FSK) [C1-11]. The basic idea of DPSK is to use the phase of the previous channel symbol as a phase reference for the phase of the current channel symbol, thus a coherent phase reference at the receiver is not necessary. With this technique, the phase differences between consecutive symbols carry the information [C1-12]. For OOK, since the information is sent by turning on or turning off a sinusoidal carrier, the information can be demodulated by measuring the energy of the received signal to a fixed threshold. On the other hand, due to the orthogonal property of the FSK modulation, the detection of information is done by comparing the energy of the received signal at each frequency. The receiver outputs the information bits corresponding to the frequency of the signal that has the highest energy [C1-12].

An important consideration in many communication systems is the quality of services under a wide range of channel conditions. Typically, data can be divided into different important classes, which require different degrees of protection. In poor channel conditions, the receiver can recover the more important classes (known as

basic or coarse data) with an acceptable reliability while the less important classes (known as refinement or enhancement data) are recovered from better channel conditions. For example, multimedia data such as audio, images and video exhibit unequal error sensitivity for different bits. It is wasteful if all of the bits are protected equally. In contrast, the unequal error protection (UEP) scheme protects the data according to the system requirements. The bit stream of the source data is divided into two or more groups and different protection levels are applied to these groups. To achieve UEP in point-to-point communications, nonuniform amplitude-shift keying (ASK), quadrature amplitude modulation (QAM) and phase-shift keying (PSK) constellations have been studied [C1-13, C1-14].

There are many different criteria that can be used to evaluate the performance of a communication system, such as average signal-to-noise ratio (SNR), outage probability, average bit-error-rate (BER), etc. The average BER, which quantifies the reliability of the entire communication system from "bits in" to "bits out", is of primary interest since it is most revealing about the nature of the system behavior [C1-12][1]. As a matter of fact, the main challenge of the system designer in wireless communications is to develop new communication systems with improved BER performance as compared to existing systems under similar constraints such as power, bandwidth, complexity, etc.

This thesis focuses on various techniques to improve the performance of cooperative communication systems over wireless channels. In particular, the thesis first examines unequal error protection techniques in coherent DF cooperative networks. Then various relaying protocols are investigated in noncoherent DF/AF cooperative networks in order to improve the error/throughput performance. The introduction, motivation, and contribution of each particular research topic will be given in the following section and also in each individual chapter.

[1]It should be emphasized here that the average BER is a performance measure that is the most difficult to compute analytically.

1.2 Organization of the Dissertation

This thesis is organized in a manuscript style. Therefore, it includes published, accepted, or submitted manuscripts. There is one chapter, namely Chapter 2, which describes the basic concepts of wireless communications, cooperative communications, unequal error protection, and noncoherent communications that are useful for the understanding of the various techniques in the included manuscripts. It should be pointed out that each chapter has its own reference list. The letter C (stands for "Chapter") and chapter number are added at the beginning of each reference item in the list. Also there are footnotes added to provide answers and/or add clarifications to the external examiner's questions and comments. Since these revisions are not in the original versions of the included manuscripts, they are formatted in sans serif font.

In what follows, a brief introduction to each manuscript is given.

The first manuscript included in Chapter 3 studies a relaying technique based on the signal-to-noise ratio (SNR) threshold in cooperative networks which employ a single relay and use hierarchical modulation for two different information classes at the source, namely a hierarchical 2/4-ASK constellation. First, the manuscript reviews some research works that focus on UEP in cooperative networks. It then introduces a novel relaying technique that can improve the error performance of the cooperative networks with hierarchical modulation. The manuscript provides the approximated BER of each information class. Numerical and simulation results are also presented to validate the advantages of the proposed technique.

The second manuscript included in Chapter 4 is a further development of the manuscript in Chapter 3. It is concerned with a *multiple-relay* network employing a hierarchical 2/4-ASK constellation for unequal error protection of two different information classes at the source. A single relay selection scheme is employed to overcome the throughput loss in cooperative networks. The approximated BER of each information class is also derived. Numerical and simulation results confirm that the proposed cooperative scheme improves the BER performance significantly.

The manuscript in Chapter 5 considers a cooperative network in which binary frequency-shift-keying (BFSK) modulation is employed to facilitate noncoherent communications. First, the manuscript reviews and discusses the disadvantages of related research works on noncoherent cooperative communications. It then proposes an adaptive noncoherent cooperative scheme. The average BER is derived in a closed-form expression for a two-relay network. The problems of selecting optimal thresholds or jointly optimal thresholds and power allocation to minimize the average BER are investigated. Simulation results show that the proposed scheme yields a superior performance under a wide range of channel conditions when optimal thresholds or jointly optimal thresholds and power allocation are employed.

The manuscript in Chapter 6 studies throughput maximization in noncoherent cooperative networks. It presents an incremental relaying protocol based on the adaptive DF relaying scheme for a cooperative wireless network in which BFSK modulation is employed. Both the average BER and throughput analysis is obtained for the proposed protocol via very-tight closed-form upper bounds. Based on the obtained BER and throughput expressions, the problem of choosing optimal thresholds to maximize the throughput while the BER meets a given constraint is investigated. The results show that the proposed protocol achieves a considerable improvement in the performance of cooperative diversity systems.

The last manuscript in Chapter 7 develops a detection scheme based on implicit pilot-symbol-assisted architecture for non-coherent AF relay networks. An upper-bound on the BER is derived in a closed-form expression for a multiple-relay network with BFSK. The manuscript also shows that the developed system can always achieve a full diversity order. Compared to previously proposed schemes, the proposed scheme can significantly improve the BER performance under different channel conditions.

Chapter 8 summarizes the contributions of this thesis and gives some suggestions for further studies.

References

[C1-1] D. Tse and P. Viswanath, *Fundamentals of Wireless Communications*. Cambridge University Press, 2005.

[C1-2] A. Goldsmith, *Wireless Communications*. Cambridge University Press, 2005.

[C1-3] T. M. Duman and A. Ghrayeb, *Coding for MIMO Communication Systems*. Wiley, 2007.

[C1-4] A. Sendonaris, E. Erkip, and B. Aazhang, "User cooperation diversity, Part I: System description," *IEEE Trans. Commun.*, vol. 51, no. 11, pp. 1927–1938, November 2003.

[C1-5] A. Sendonaris, E. Erkip, and B. Aazhang, "User cooperation diversity, Part II: Implementation aspects and performance analysis," *IEEE Trans. Commun.*, vol. 51, no. 11, pp. 1939–1948, November 2003.

[C1-6] J. Laneman and G. Wornell, "Distributed space-time-coded protocols for exploiting cooperative diversity in wireless networks," *IEEE Trans. Inform. Theory*, vol. 49, pp. 2415–2425, October 2003.

[C1-7] J. Laneman, D. Tse, and G. Wornell, "Cooperative diversity in wireless networks: Efficient protocols and outage behavior," *IEEE Trans. Inform. Theory*, vol. 50, pp. 3062–3080, December 2004.

[C1-8] M. Hasna and M.-S. Alouini, "A performance study of dual-hop transmissions with fixed gain relays," *IEEE Trans. Wireless Commun.*, vol. 3, pp. 1963–1968, November 2004.

[C1-9] R. Nabar, H. Bolcskei, and F. Kneubuhler, "Fading relay channels: performance limits and space-time signal design," *IEEE J. Select. Areas in Commun.*, vol. 22, pp. 1099–1109, August 2004.

[C1-10] D. Chen and J. Laneman, "Modulation and demodulation for cooperative diversity in wireless systems," *IEEE Trans. Wireless Commun.*, vol. 5, pp. 1785–1794, July 2006.

[C1-11] H. H. Nguyen and E. Shwedyk, *A First Course in Digital Communications*. Cambridge University Press, 2009.

[C1-12] M. K. Simon and M.-S. Alouini, *Digital Communication over Fading Channels*. Wiley, 2005.

[C1-13] A. Calderbank and N. Seshadri, "Multilevel codes for unequal error protection," *IEEE Trans. Inform. Theory*, vol. 39, pp. 1234–1248, July 1993.

[C1-14] M. Pursley and J. Shea, "Nonuniform phase-shift-key modulation for multimedia multicast transmission in mobile wireless networks," *IEEE J. Select. Areas in Commun.*, vol. 17, pp. 774–783, May 1999.

2. Background and System Model

The primary purpose of this chapter is to briefly review the principal knowledge in the field of study. To this end, this chapter provides important background on wireless fading channels and diversity techniques, as well as discusses fundamental concepts of cooperative communications, unequal error protection, and noncoherent communications.

2.1 Overview of Communications Systems

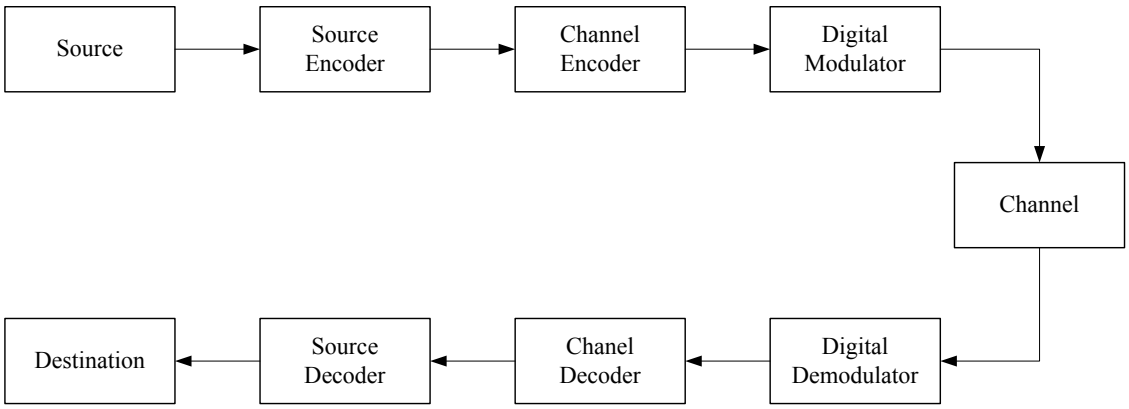

Figure 2.1 Basic elements of a digital communication system.

Fig. 2.1 illustrates the block diagram of a digital communication system, in which information is transmitted from one point to another. The source generates either analog signals such as speech, audio, and video, or digital data such as text or multimedia. The message produced by the source is converted into a binary sequence by the source encoder. The binary sequence is then passed to the channel encoder, which introduces redundancy into the binary sequence in order to overcome the effects of noise and interference encountered during the transmission. The channel-encoded

binary sequence (or coded sequence) is then modulated by the digital modulator to generate waveforms for transmission over a physical channel link, such as a telephone line, an optical fiber cable, or a high frequency radio link. At the receiver side, the above procedures are reversed so that the destination can restore the original source information.

For a wireless channel, the communication occurs in a bandwidth W around a center frequency f_c, i.e., in a passband of $[f_c - W/2, f_c + W/2]$. The signal transmitted at the carrier frequency f_c is called the passband signal. In the special case, when $f_c \approx 0$, the transmitted signal is called the baseband signal. In typical wireless applications, the digital modulator performed at the transmitter side (at the last stage) has to "up-convert" the signal to the carrier frequency f_c, i.e., generates the passband signal and transmits it via an antenna. Similarly, the digital demodulator performed at the receiver side (at the first stage) would typically "down-convert" the radio-frequency (RF) signal to a baseband signal before making any further processing. Furthermore, most of the processing, such as coding/decoding, modulation/demodulation, synchronization, etc., is actually carried out at the baseband. Therefore, the baseband equivalent model is usually used to study and analyze a wireless communication system since it is more convenient than the passband model. It should be noted that studying the baseband equivalent model basically suppresses the issues of frequency up-conversion and down-conversion, i.e., making it independent of carrier frequencies [C2-1, Chapter 2], [C2-2, Chapter 4].

The baseband equivalent signal for a passband signal should be such that when shifted up by f_c, one should obtain the passband signal. In general, the relationship between the passband signal $x_{\mathrm{PB}}(t)$ and the equivalent baseband signal $x(t)$ can be written as [C2-1]:

$$x_{\mathrm{PB}}(t) = \mathcal{R}\left\{x(t)\exp\left(j2\pi f_c t\right)\right\} \tag{2.1}$$

where $\mathcal{R}\{\cdot\}$ takes the real part of the signal. The relationship between the spectrum of $x_{\mathrm{PB}}(t)$ and $x(t)$ is illustrated in Fig. 2.2.

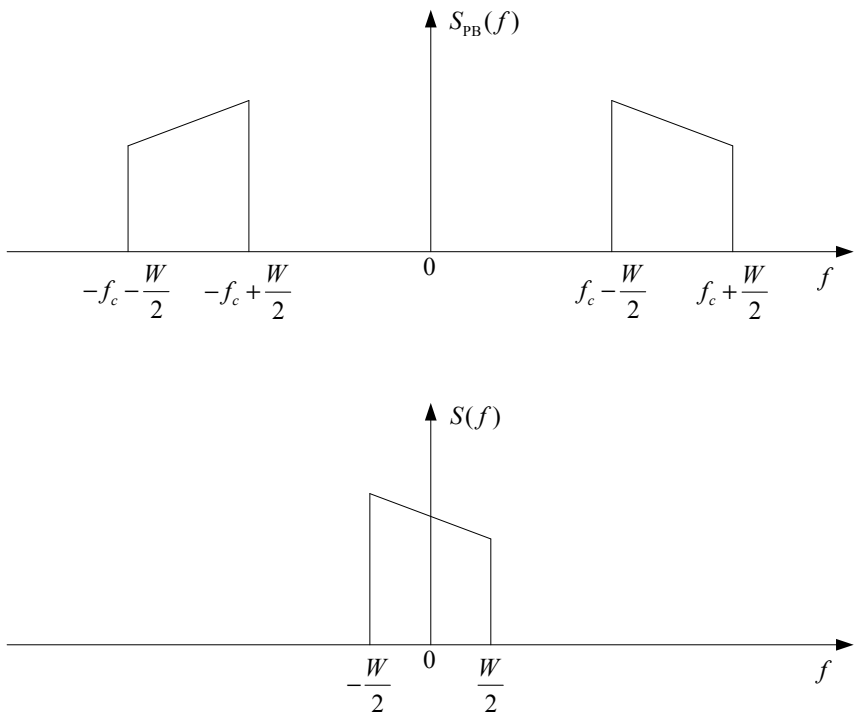

Figure 2.2 Illustration of the relationship between passband spectrum $S_{\mathrm{PB}}(f)$ and its equivalent baseband spectrum $S(f)$.

In what follows, we discuss the wireless channel and its baseband equivalent channel model. Such a model is largely used in this thesis.

2.2 Wireless Channels

The key distinction between wireless and wireline communications lies in the physical properties of the channels. When a radio-frequency (RF) signal is transmitted over a wireless channel, due to the presence of multiple propagation paths between the transmitter and receiver, there are multiple copies of the transmitted signal at the receiver. The multiple paths arise due to reflections, scattering, diffractions from objects in the environment as illustrated in Fig. 2.3. The combination of multiple copies of the transmitted signal affects many characteristics of the received signal. In general, the effects of a wireless channel can be categorized into two types: large-scale fading (or path loss, attenuation) and small-scale fading (typically referred simply to as fading). The large-scale fading is due to signal attenuation by large objects such as

buildings, hills, etc. The small-scale fading is due to the constructive and destructive combinations of the multiple signals arrived over different propagation paths at the receiver. Dealing with small-scale fading is one of the most challenging issues in designing a robust wireless communication system. Hence, in what follows, we discuss a channel model for the wireless link that is affected by the small-scale fading.

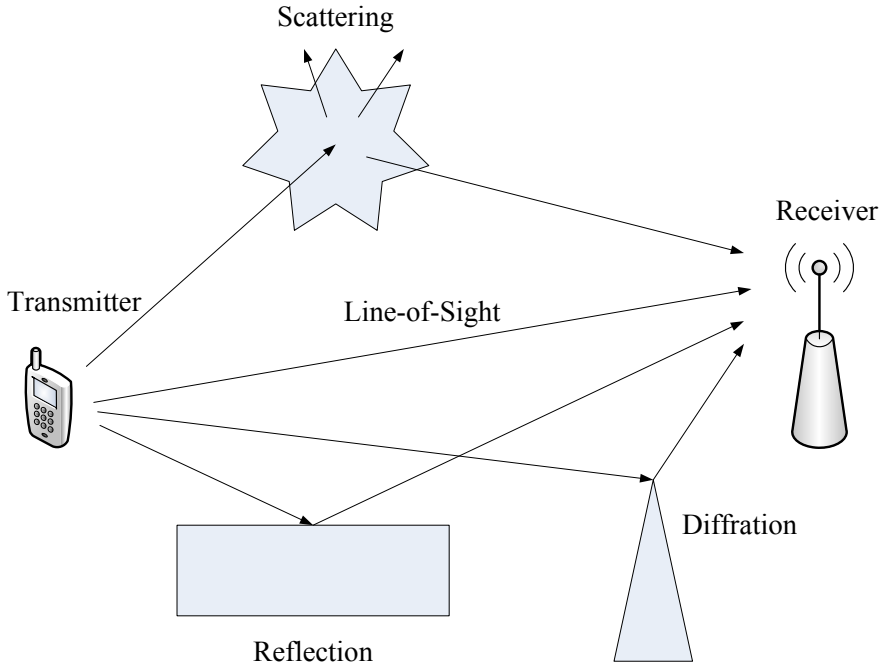

Figure 2.3 Example of a wireless channel in which there are multiple propagation paths between the transmitter and receiver.

2.2.1 Input/Output Model of a Wireless Channel

Consider a communication system in which one source communicates with one destination over a wireless fading channel. Given the baseband input signal $x(t)$, which is assumed to be bandlimited to $W/2$ Hz, and ignoring the interference by other users in the system, the continuous-time baseband received signal at the destination can be mathematically expressed as [C2-1, Chapter 2], [C2-2, Chapter 14]

$$y(t) = \sum_i a_i(t) \exp(-j2\pi f_c \tau_i(t)) x(t - \tau_i(t)) + z(t), \tag{2.2}$$

where $a_i(t)$ and $\tau_i(t)$ are the overall attenuation and propagation delay at time t from the source to the destination on path i, respectively. The term $z(t)$ represents ambient

noise and is typically modeled as zero-mean additive white Gaussian noise (AWGN) with two-sided power spectral density $N_0/2$. It can be seen that the baseband output is a sum, over each path, of the delayed replicas of the baseband input and the noise. Without the noise component, the input/output relationship in (2.2) is that of a linear time-varying system, i.e., it can be described by the baseband equivalent channel impulse response $h(\tau, t)$ at time t to an impulse transmitted at time $(t - \tau)$. In terms of $h(\tau, t)$, the input/output relationship is written as

$$y(t) = \int_{-\infty}^{\infty} h(\tau, t)x(t - \tau)\mathrm{d}\tau + z(t). \tag{2.3}$$

Comparing (2.2) and (2.3), one can see that the baseband equivalent channel impulse response $h(\tau, t)$ is a weighted sum of delta functions (see Fig. 2.4). That is

$$h(\tau, t) = \sum_i a_i(t) \exp(-j2\pi f_c \tau_i(t))\delta(\tau - \tau_i(t)), \tag{2.4}$$

where $\delta(\cdot)$ denotes the Dirac delta function.

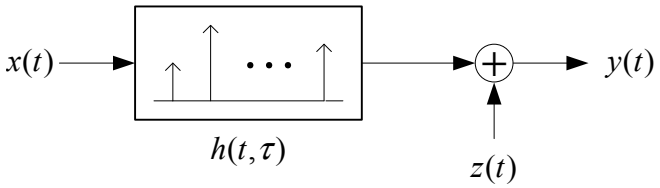

Figure 2.4 Channel model in a wireless communication system.

The next step is to convert the continuous-time baseband equivalent model to a discrete-time baseband equivalent model since it is more useful and relevant to the design, analysis as well as digital-signal-processing (DSP) implementation. The baseband equivalent input can be represented as

$$x(t) = \sum_m x[m]\mathrm{sinc}(Wt - m), \tag{2.5}$$

where $x[m]$ is given by $x(m/W)$ and $\mathrm{sinc}(t) = \frac{\sin(\pi t)}{\pi t}$ is the band-limited interpolating function. The baseband equivalent output in (2.2) is rewritten as

$$y(t) = \sum_m x[m] \sum_i a_i(t) \exp(-j2\pi f_c \tau_i(t))\mathrm{sinc}(Wt - W\tau_i(t) - m) + z(t). \tag{2.6}$$

When $y(t)$ is sampled at multiples of $1/W$, the output is given by

$$y[n] = \sum_m x[m] \sum_i a_i\,(n/W) \exp\left(-j2\pi f_c \tau_i(n/W)\right) \operatorname{sinc}\left[n - m - W\tau_i(n/W)\right] + z[n]. \tag{2.7}$$

Let $l = n - m$, then

$$y[n] = \sum_l x[n-l] \sum_i a_i\,(n/W) \exp\left(-j2\pi f_c \tau_i(n/W)\right) \operatorname{sinc}\left[l - W\tau_i(n/W)\right] + z[n]. \tag{2.8}$$

By defining

$$h[l,n] = \sum_i a_i\,(n/W) \exp\left(-j2\pi f_c \tau_i(n/W)\right) \operatorname{sinc}\left[l - W\tau_i(n/W)\right], \tag{2.9}$$

the discrete-time baseband equivalent model of (2.2) can be mathematically given in the following form [C2-1, Chapter 2]:

$$y[n] = \sum_l h[l,n]x[n-l] + z[n]. \tag{2.10}$$

In (2.10) n and l are the discrete time index and the tap index, respectively, of the linear filter that models the fading effects. The signals $x[n]$ and $y[n]$ are the baseband equivalent channel input and output, respectively, whereas $z[n]$ is additive Gaussian noise. The noise is modeled as circularly symmetric complex Gaussian random variable (RV) with variance N_0, denoted as $\mathcal{CN}(0, N_0)$. It means that the real and imaginary components of $z[n]$ are independent and identically distributed (i.i.d.) Gaussian RVs with means zero and variances $N_0/2$. The quantity $h[l,n]$ is the lth complex channel tap at time n.[1]

Delay spread is an important characteristic of a multipath channel. It is measured by the time duration between the arrival of the first signal component and the last signal component. Depending on the delay spread and the signal duration[2], the wireless fading channel can be classified as frequency-selective or frequency non-selective

[1]It should be pointed out that the discrete-time input/output model in (2.10) was derived using the sampling representation in (2.5) of the baseband input signal $x(t)$. However, the same model would be obtained by representing the baseband input signal $x(t)$ as a linear combination of orthonormal basis functions, a representation commonly used for digital modulated signals.

[2]Here the signal duration refers to the duration of one modulated symbol.

(or flat fading) channel. For frequency-selective fading, the delay spread is larger than the signal duration. Hence, different signal components experience different fading and it is represented by multiple taps as shown in (2.2), i.e., the discrete-time baseband equivalent model is as in (2.10). In contrast, for frequency non-selective fading, the delay spread is considerably less than the signal duration. Therefore, all the multipath components are arrived roughly during one signal duration. As a result, the impulse response $h(t, \tau)$ can be approximated by a delta function at $\tau = 0$ that has a time-varying amplitude, i.e.,

$$h(t, \tau) = a(t)\delta(\tau). \tag{2.11}$$

It follows that the discrete-time baseband equivalent input/output model for a flat fading channel can be written as

$$y[n] = h[n]x[n] + z[n]. \tag{2.12}$$

The fading channel can also be categorized as *slow* or *fast* fading. The channel is called slow fading if its channel impulse response changes at a rate much slower than the transmitted signal (i.e., the symbol rate) and the channel is assumed to be static over one or several signal durations. On the other hand, the channel is considered to be fast fading when the channel impulse response changes quickly within a signal duration.

In this thesis, only slow and frequency non-selective channel model is considered.

2.2.2 Representation of Digital Modulated Signals

As discussed before (see Fig. 2.1), the digital information needs to be mapped to analog signals for transmission over a communication channel through a digital modulator. The mapping is generally performed by taking a group of $k = \log_2 M$ bits and selecting one of $M = 2^k$ waveforms, $x_{\mathrm{PB},m}(t)$, $m = 1, 2, \ldots, M$. The signal waveforms may differ in either amplitude, phase or frequency, or some combination of two or more signal parameters. Also, the signal waveforms are usually passband

signals that are suitable for transmission over a wireless radio channel [C2-2]. In what follows, we discuss popular digital modulation methods. Since the discrete-time baseband equivalent input/output model is used in the following chapters, the discrete-time baseband equivalent input, represented by $x[n]$ in (2.10) and (2.12), for each modulation scheme, shall be described.

Amplitude-Shift Keying (ASK)

With ASK, information bits are encoded (or mapped) in the amplitude of the sinusoidal carrier. The M-ASK signal waveforms may be expressed as

$$\begin{aligned} x_{\mathrm{PB},m}(t) &= \mathcal{R}\left\{x_m(t)\exp\left(j2\pi f_c t\right)\right\} = \mathcal{R}\left\{A_m g(t)\exp\left(j2\pi f_c t\right)\right\} \\ &= A_m g(t)\cos(2\pi f_c t), \quad 0 \le t \le T_s \end{aligned} \tag{2.13}$$

where $g(t)$ is a signal pulse shape of symbol duration T_s and $\{A_m, m = 1, 2, \ldots, M\}$ denotes the set of M possible amplitudes corresponding to $M = 2^k$ possible k-bit symbols. The signal amplitudes A_m take the discrete values

$$A_m = (2m - 1 - M)d, \quad m = 1, 2, \ldots, M \tag{2.14}$$

where $2d$ is the distance between adjacent signal amplitudes. Clearly the above set of signal waveforms is represented by one orthonormal function, namely

$$\phi_1(t) = \sqrt{\frac{2}{E_g}}g(t)\cos(2\pi f_c t), \quad 0 \le t \le T_s. \tag{2.15}$$

where E_g denotes the energy of the pulse $g(t)$. One has

$$x_{\mathrm{PB},m}(t) = A_m\sqrt{\frac{E_g}{2}}\phi_1(t), \quad m = 1, 2, \ldots, M. \tag{2.16}$$

Equivalently, the M-ASK signal waveform $x_{\mathrm{PB},m}(t)$ can be represented by the following one-dimensional vector $\mathbf{x}_m$:

$$\mathbf{x}_m = A_m\sqrt{\frac{E_g}{2}}, \quad m = 1, 2, \ldots, M. \tag{2.17}$$

In other words, the signal space diagrams of M-ASK includes M signal points spaced on a line. Compared to the input/output model in (2.10) and (2.12), the input $x[n]$ is equivalent to $\mathbf{x}_m$, i.e., the input $x[n]$ takes values in the set of $\left\{A_m\sqrt{\frac{E_g}{2}}, \quad m = 1, 2, \ldots, M\right\}$.

It should be pointed out that the mapping from k information bits to the M possible signal waveforms can be done in many ways. The so-called Gray mapping is such that the adjacent symbols (when presented in the signal space diagram) differ in only one bit. This is a very desirable property since the most likely errors caused by noise involve the erroneous selection of a signal adjacent to the true signal. Hence with a Gray mapping, most symbol errors cause only a single bit error. For illustration, the signal space diagrams (or constellation diagrams) with Gray mappings for M-ASK, $M = 2, 4, 8$, are shown in Fig. 2.5 [C2-2].

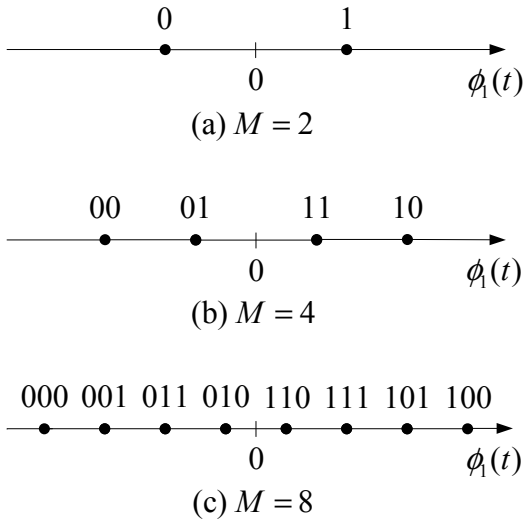

Figure 2.5 Examples of M-ASK constellations with (a) $M = 2$, (b) $M = 4$, and (c) $M = 8$.

Phase-Shift Keying (PSK)

With PSK, information bits are encoded in the phase of the sinusoid carrier. Specifically, the M-PSK signal waveforms are given by

$$\begin{aligned} x_{\mathrm{PB},m}(t) &= \mathcal{R}\left\{g(t)\exp\left(j\frac{2\pi(m-1)}{M}\right)\exp\left(j2\pi f_c t\right)\right\}, \quad 0 \le t \le T_s \qquad (2.18) \\ &= g(t)\cos\left(\frac{2\pi}{M}(m-1)\right)\cos(2\pi f_c t) - g(t)\sin\left(\frac{2\pi}{M}(m-1)\right)\sin(2\pi f_c t) \end{aligned}$$

It can be seen that each signal waveform is expressed as a linear combination of two orthonormal functions, $\phi_1(t)$ and $\phi_2(t)$, i.e.,

$$x_{\mathrm{PB},m}(t) = \sqrt{\frac{E_g}{2}}\cos\left(\frac{2\pi}{M}(m-1)\right)\phi_1(t) + \sqrt{\frac{E_g}{2}}\sin\left(\frac{2\pi}{M}(m-1)\right)\phi_2(t) \qquad (2.19)$$

where

$$\phi_1(t) = \sqrt{\frac{2}{E_g}}\cos(2\pi f_c t), \tag{2.20}$$

$$\phi_2(t) = -\sqrt{\frac{2}{E_g}}\sin(2\pi f_c t). \tag{2.21}$$

Therefore the M-PSK signal waveform $x_{\mathrm{PB},m}(t)$ can be represented by the two-dimensional vector $\mathbf{x}_m = [\ x_{m1},\ \ x_{m2}\ ]$ given by

$$\mathbf{x}_m = \left[\ \sqrt{\tfrac{E_g}{2}}\cos\tfrac{2\pi}{M}(m-1),\ \ \sqrt{\tfrac{E_g}{2}}\sin\tfrac{2\pi}{M}(m-1)\ \right], \quad m = 1, 2, \ldots, M. \tag{2.22}$$

Alternatively, each M-PSK signal waveform can be represented by a signal point $x_m = x_{m1} + jx_{m2}$, $m = 1, 2, \ldots, M$. It is simple to see that the set of M-PSK waveforms consists of M signal points equally spaced on a circle of radius $\sqrt{E_g/2}$ (see Fig. 2.6). Furthermore, the value of x_m is the input $x[n]$ in the input/output model in (2.10) and (2.12). It should be noted that in the case of binary PSK ($M = 2$), the signal waveforms can be represented by the one-dimensional vectors (since the second component of the vector $\mathbf{x}_m$ equals to 0 for $m = 1, 2$), which are identical to binary ASK signals.

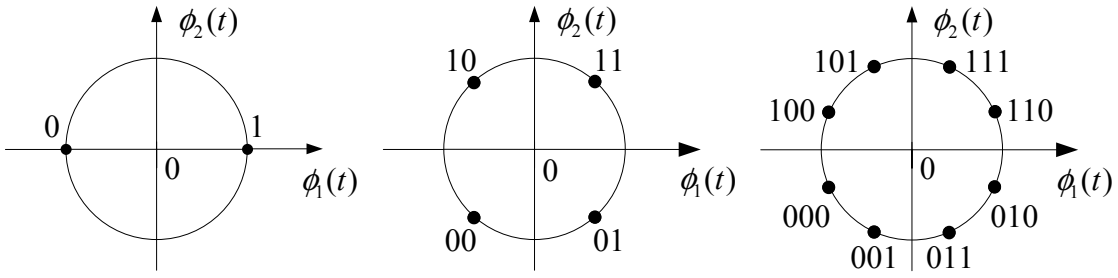

Figure 2.6 Examples of M-PSK constellations with (a) $M = 2$, (b) $M = 4$, and (c) $M = 8$.

Quadrature amplitude modulation (QAM)

With QAM, information bits are encoded in both the amplitude and phase of the sinusoid carrier, i.e., the M-QAM signal waveforms are expressed as

$$\begin{aligned} x_{\mathrm{PB},m}(t) &= \mathcal{R}\left\{A_m \mathrm{e}^{j\theta_m} g(t) \exp\left(j2\pi f_c t\right)\right\}, \quad 0 \le t \le T_s \\ &= A_{m1} g(t)\cos(2\pi f_c t) - A_{m2} g(t)\sin(2\pi f_c t), \quad m = 1, \ldots, M, \end{aligned} \tag{2.23}$$

where A_{m1} and A_{m2} are the information-bearing discrete amplitudes of two quadrature carriers. As in the case of PSK signals, the QAM signal waveforms can be expressed as a linear combination of two orthonormal functions, $\phi_1(t)$ and $\phi_2(t)$, i.e.,

$$x_{\mathrm{PB},m}(t) = A_{m1}\sqrt{\frac{E_g}{2}}\phi_1(t) + A_{m2}\sqrt{\frac{E_g}{2}}\phi_2(t) \tag{2.24}$$

where $\phi_1(t)$ and $\phi_2(t)$ are defined as in (2.47) and (2.21), respectively. Then the two-dimensional vector $\mathbf{x}_m$ representing the M-QAM signal waveform $x_{\mathrm{PB},m}(t)$ can be written as

$$\mathbf{x}_m = [\ x_{m1},\ \ x_{m2}\ ] = \left[\ A_{m1}\sqrt{\tfrac{E_g}{2}},\ \ A_{m2}\sqrt{\tfrac{E_g}{2}}\ \right], \quad m = 1, 2, \ldots, M \tag{2.25}$$

In the case when the amplitudes A_{m1} and A_{m2} take values independently from two discrete sets, the QAM constellation has a rectangular structure and hence it is called *rectangular* QAM. Viewed differently, a rectangular QAM signal can be obtained from two ASK signals in quadrature carriers. Fig. 2.7 shows rectangular QAM constellations with Gray mappings for $M = 2, 4, 8$. Similar to the case of PSK, the input $x[n]$ in the input/output model in (2.10) and (2.12) is equivalent to $x_m = x_{m1} + jx_{m2}$.

Unequal Error Protection

The constellations shown in Figs. 2.5, 2.6, and 2.7 are uniform constellations, i.e., constellations with uniformly spaced signal points. Such constellations protect the information bits equally. However, as mentioned in Chapter 1, UEP is a scheme that protects the data according to the information classes. It is useful for applications

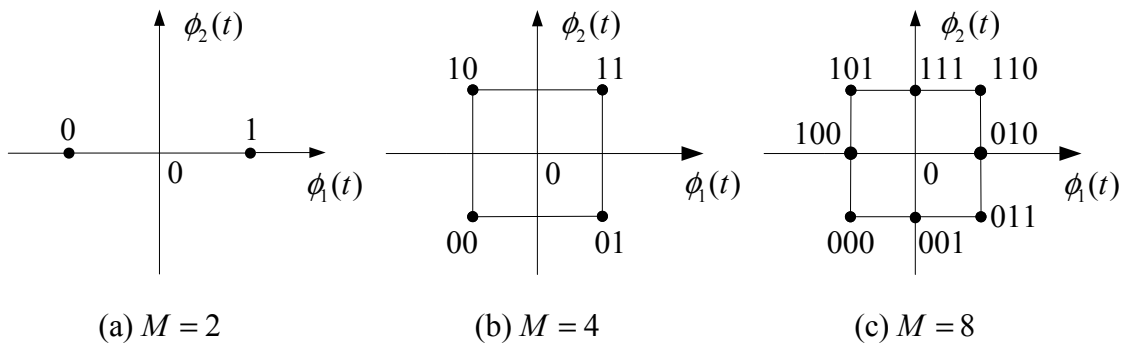

Figure 2.7 Examples of M-QAM constellations with (a) $M = 2$, (b) $M = 4$, and (c) $M = 8$.

which require different degrees of protection for different data classes. Nonuniform constellation is a practical way to achieve UEP for different information classes. In what follows, we discuss how to construct nonuniform constellations.

As an example, Fig. 2.8 illustrates a hierarchical 2/4-ASK constellation. As shown in the figure, the distances in the constellation evolve in a hierarchy. The quantity $2d_1$ represents the distance between the points in the fictitious 2-ASK constellation. It is referred to as the first level of hierarchy. In the second level of hierarchy, $2d_2$ represents the distance between the points in the actual 2-ASK constellation. For a generalized hierarchical 2^m-ASK constellation, $2d_k$ represents the distance between points in the kth level of hierarchy, $k = 1, \ldots, m$. The bits are assigned as follows. The highest priority bit is assigned to the most significant bit position. The lower priority bit is assigned to the subsequent position of lower significance and so on. This can be viewed as $2/4/.../M$-ASK ($M = 2^m$). In Fig. 2.8, there are two different classes. The first bit from the first class is assigned to the most significant bit position. Similarly, the second bit from the second class is assigned to the least significant bit position [C2-3].

As mentioned earlier, a rectangular QAM constellation can be obtained from two ASK constellations in quadrature carriers. Hence the construction of a nonuniform QAM constellation is similar to that of a nonuniform ASK constellation. With hierarchical QAM constellations, the bits are assigned as follows. The two highest

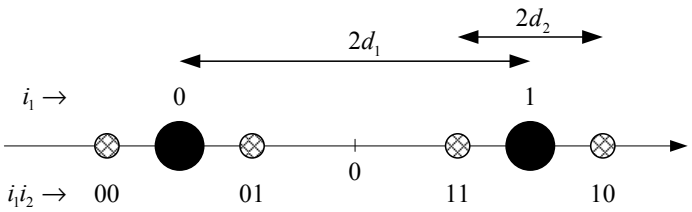

Figure 2.8 Generalized hierarchical 2/4-ASK constellation.

priority bits are assigned to the most significant bits in the in-phase (I) and quadrature (Q) carriers (or channels), respectively. The two lower priority bits are assigned to the subsequent positions of lower significance and so on. This can be viewed as 4/16/64.../M-QAM ($M = 2^{2m}$). Fig. 2.9 illustrates a hierarchical 4/16-QAM constellation. In the figure, there are two different classes and each class contains two bits. Two bits from the first class are assigned to the most significant bits in the I and Q channels. Similarly, two bits from the second class are assigned to the least significant bits in the I and Q channels [C2-3].

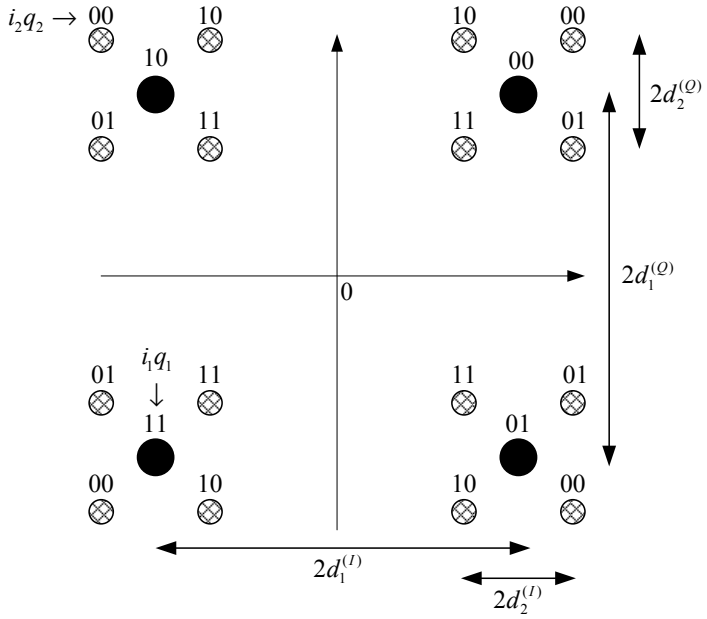

Figure 2.9 Generalized hierarchical 4/16-QAM constellation.

A nonuniform 2^m-PSK constellation can also be constructed from a uniform 2^{m-1}-PSK constellation in order to provide two classes. Specifically, each point in a uniform 2^{m-1}-PSK constellation is split into two *half points* and then rotated in opposite directions from the original point by an angle α. Fig. 2.10 shows a nonuniform 4-

PSK constellation. It is constructed from a binary PSK constellation by splitting and rotating by an angle α. The angles of the 4-PSK signals are then α, $-\alpha$, $\pi + \alpha$, and $\pi - \alpha$. Similarly, one can construct a nonuniform 2^m-PSK constellation for m different classes.

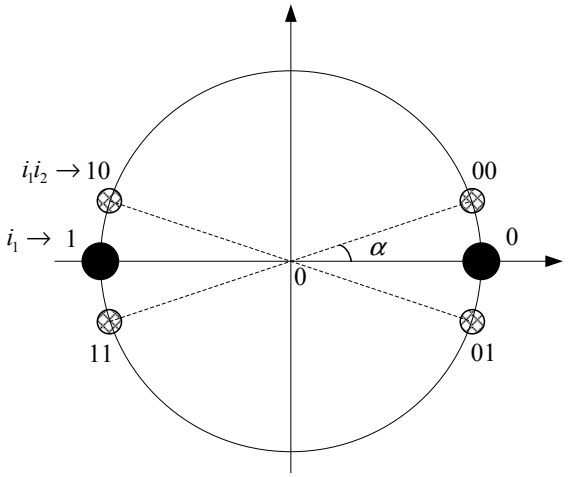

Figure 2.10 Nonuniform 4-PSK constellation.

2.2.3 Statistical Model for Fading

It has been described how the fading channels can be modeled by discrete-time baseband input-output relations as in (2.10) and (2.12). However, a precise mathematical description of fading channels is either unknown or too complex for tractable analysis. Therefore, statistical models are necessary to evaluate the quality of information transmission over a fading channel. Depending on the nature of the environment, there are many different statistical models to describe a fading channel. In what follows, we discuss Rayleigh, Rician, and Nakagami-m fading since they are the most popular statistical models.

Rayleigh fading is the simplest and most popular statistical model for the fading channel when there is no direct line-of-sight (LOS) path between the transmitter and receiver. Let's consider the case of flat fading, i.e., the discrete-time baseband equivalent model is as in (2.12). As mentioned earlier, in a wireless multipath channel, transmitting a signal results in receiving the sum of a large number of signals from

different paths. Therefore, each channel coefficient $h[n]$ is a summation of a large number of independent circularly symmetric random variables. By the central limit theorem, $h[n]$ can be modeled as a zero-mean complex Gaussian RV [C2-1, C2-4]. The probability density function (pdf) of the magnitude of the channel coefficient, $|h[n]|$, converges toward the Rayleigh distribution. Specifically, the Rayleigh pdf that describes the random channel fading magnitude can be represented as follows:

$$p_{|h[n]|}(x) = \frac{2x}{\Omega} \exp\left(-\frac{x^2}{\Omega}\right), \quad x \geq 0 \tag{2.26}$$

where Ω is the average fading power, i.e., $E\{|h[n]|^2\} = \Omega$. In essence, the parameter Ω defines the average power attenuation from the transmitter to the receiver, which largely depends on the distance from from the transmitter to the receiver. It can be shown that the instantaneous received signal-to-noise ratio, $\gamma = (E_s/N_0)|h[n]|^2$, where E_s is the energy of the transmitted signal, is exponential distributed. The pdf of γ is given by

$$p_\gamma(x) = \frac{1}{\overline{\gamma}} \exp\left(-\frac{x}{\overline{\gamma}}\right), \quad x \geq 0 \tag{2.27}$$

where $\overline{\gamma} = \Omega E_s/N_0$ is the mean value of γ.

When the LOS path exits and is much stronger than other paths connecting the transmitter and receiver, the Rician fading channel model is more applicable (Fig. 2.11). The channel magnitude $|h[n]|$ has the following distribution:

$$p_{|h[n]|}(x) = \frac{2(1+K)x}{\Omega} \exp\left(-K - \frac{(1+K)x^2}{\Omega}\right) I_0\left(2x\sqrt{\frac{K(1+K)}{\Omega}}\right), \quad x \geq 0 \tag{2.28}$$

where $I_0(\cdot)$ is the zeroth-order modified Bessel function of the first kind and is given by [C2-5]

$$I_0(z) = \frac{1}{\pi}\int_0^\pi \exp(z\cos(\phi))\mathrm{d}\phi \approx \begin{cases} \frac{\exp(z)}{\sqrt{2\pi z}}, & z \gg 1, \\ 1 + \frac{z^2}{4}, & z \ll 1. \end{cases} \tag{2.29}$$

The Rician K factor represents the ratio of the power in the LOS component to the power in the non line-of-sight components (NLOS) and ranges from 0 to ∞. For $K = 0$, the LOS path is completely obstructed, causing equation (2.28) to revert to

equation (2.26), i.e., the case $K = 0$ corresponds to Rayleigh fading. On the other hand, for $K = \infty$, the LOS path is the only path, i.e., the case $K = \infty$ gives a non-fading channel. The received signal-to-noise ratio γ follows a distribution given as [C2-6]:

$$p_\gamma(x) = \frac{1+K}{\overline{\gamma}} \exp\left(-K - \frac{(1+K)x}{\overline{\gamma}}\right) I_0\left(2\sqrt{\frac{K(1+K)x}{\overline{\gamma}}}\right). \tag{2.30}$$

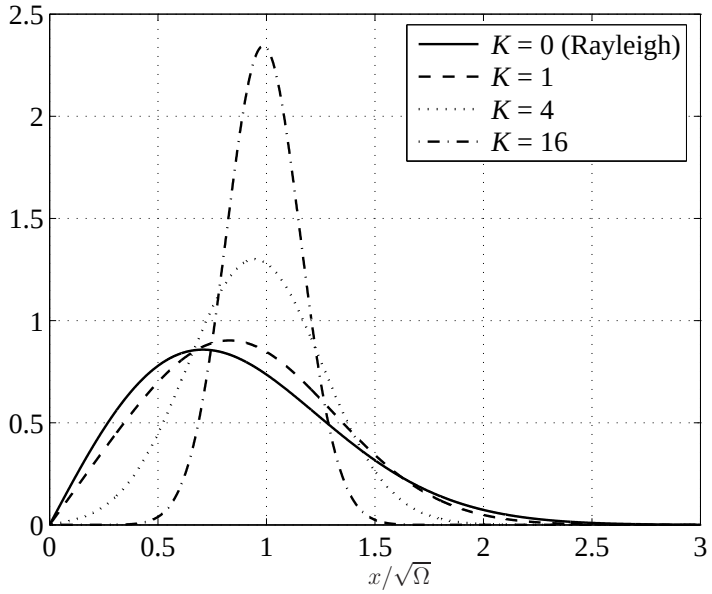

Figure 2.11 Rician distribution.

Another fading model, called Nakagami-m, is mainly applied in environments where the size of clusters of scatters is comparable to the signal wavelength [C2-6]. For this fading model, the pdf of the channel fading magnitude can be represented as follows:

$$p_{|h[n]|}(x) = \frac{2m^m x^{2m-1}}{\Omega^m \Gamma(m)} \exp\left(-\frac{mx^2}{\Omega}\right), \quad x \geq 0 \tag{2.31}$$

where m is the Nakagami-m fading parameter which ranges from $\frac{1}{2}$ to ∞. Tha Gamma function, $\Gamma(\cdot)$, is given by

$$\Gamma(m) = \int_0^\infty t^{m-1} \exp(-t) \mathrm{d}t = (m-1)! \quad \text{for } m \text{ integer.} \tag{2.32}$$

The pdf of γ is

$$p_\gamma(x) = \frac{m^m x^{m-1}}{\overline{\gamma}^m \Gamma(m)} \exp\left(-\frac{m\gamma}{\overline{\gamma}}\right), \quad x \geq 0 \tag{2.33}$$

In terms of the distribution of the fading channel magnitude, the Nakagami-m fading model generalizes many other fading models considered in the literature by adjusting its fading parameter m (Fig. 2.12). For example, it includes the one-sided Gaussian (the worst-case fading) and the Rayleigh fading models when $m = \frac{1}{2}$ and $m = 1$, respectively. Also, for $m \to \infty$, the Nakagami-m fading channel converges to a non-fading channel.

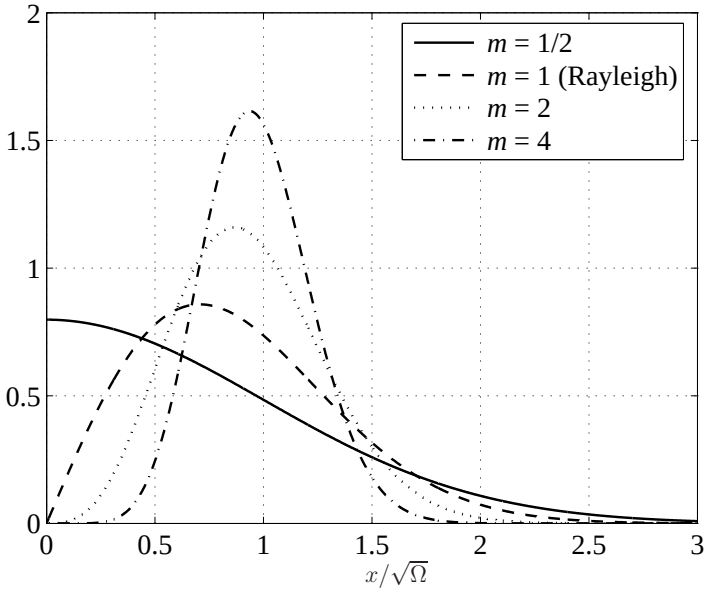

Figure 2.12 Nakagami-m distribution.

As mentioned earlier, Rayleigh fading is the most popular statistical model studied in the literature since having no LOS path is the worse-case situation. As such, the Rayleigh fading model shall be used in the next section to illustrate the performance of information transmission over a wireless fading channel.

2.2.4 Performance Comparison between AWGN and Rayleigh Fading Channels

In order to illustrate the detrimental effect of fading in wireless transmission, this section presents performance analysis and comparison of BPSK modulation over AWGN and flat Rayleigh fading channels.

First, for BPSK the discrete-time baseband equivalent input $x[n]$ in (2.12) is either $+\sqrt{E_b}$ or $-\sqrt{E_b}$ where E_b is the average transmitted bit energy, i.e., $E_b = E_g/2$. The discrete-time baseband output in the nth signal interval can be written as:

$$y[n] = x[n] + z[n] = \begin{cases} +\sqrt{E_b} + z[n], & \text{if a "1" is transmitted} \\ -\sqrt{E_b} + z[n], & \text{if a "0" is transmitted} \end{cases} \tag{2.34}$$

where $z[n]$ is a zero-mean Gaussian random variable with variance $N_0/2$. The conditional pdfs for the two possible transmitted signals are

$$p\left(y[n]\middle|x[n] = +\sqrt{E_b}\right) = \frac{1}{\sqrt{\pi N_0}} \exp\left(-\frac{(y[n] - \sqrt{E_b})^2}{N_0}\right) \tag{2.35}$$

$$p\left(y[n]\middle|x[n] = -\sqrt{E_b}\right) = \frac{1}{\sqrt{\pi N_0}} \exp\left(-\frac{(y[n] + \sqrt{E_b})^2}{N_0}\right) \tag{2.36}$$

We wish to design a detector such that the probability of making a correct decision is maximized. The decision rule based on the computation of the *posterior* probabilities (also known as the likelihood ratio test) is

$$\frac{P\left(x[n] = +\sqrt{E_b}\middle|y[n]\right)}{P\left(x[n] = -\sqrt{E_b}\middle|y[n]\right)} \underset{0}{\overset{1}{\gtrless}} 1 \tag{2.37}$$

Using Bayes' rule, the *posterior* probabilities can be calculated as

$$P\left(x[n]\middle|y[n]\right) = \frac{p\left(y[n]\middle|x[n]\right) P(x[n])}{p(y[n])} \tag{2.38}$$

where $P(x[n])$ is the a *priori* probability of the signal $x[n]$ being transmitted. With the assumption of equal priori probabilities, the decision rule in (2.37) can be rewritten as

$$\frac{p\left(y[n]\middle|x[n] = +\sqrt{E_b}\right)}{p\left(y[n]\middle|x[n] = -\sqrt{E_b}\right)} \underset{0}{\overset{1}{\gtrless}} 1 \tag{2.39}$$

The conditional pdf $p\left(y[n]\middle|x[n]\right)$ is usually called the likelihood function. The detector based on the maximum of the likelihood function $p\left(y[n]\middle|x[n]\right)$ is called the maximum-likelihood detector. The detection rule in (2.39) can be simplified to

$$y[n] \underset{0}{\overset{1}{\gtrless}} 0 \tag{2.40}$$

The optimal detection rule is simply to decide that "bit 1 was transmitted" if $y[n] \geq 0$ and "bit 0 was transmitted" if $y[n] < 0$. With such a detection rule, the error probability can be determined as [C2-2]

$$\begin{aligned} \mathrm{BER}_{\text{AWGN, BPSK}} &= \frac{1}{2}\int_{-\infty}^{0} p\left(y[n]\middle|x[n]=+\sqrt{E_b}\right)\mathrm{d}y[n] \\ &+ \frac{1}{2}\int_{0}^{\infty} p\left(y[n]\middle|x[n]=-\sqrt{E_b}\right)\mathrm{d}y[n] = Q\left(\sqrt{\frac{2E_b}{N_0}}\right) \end{aligned} \quad (2.41)$$

where the Q function is defined as

$$Q(x) = \int_{x}^{\infty} \frac{1}{\sqrt{2\pi}} \exp^{-\frac{t^2}{2}} \mathrm{d}t. \quad (2.42)$$

Observe that the detection error probability decays exponentially in the average received signal-to-noise ratio. This is a very favorable behavior since it implies that the system performance can be improved drastically by increasing the transmitted power. Unfortunately, as will be seen shortly, this behavior only holds for an AWGN channel, not fading channels.

When using BPSK over a Rayleigh fading channel, the discrete-time baseband equivalent input/output model can be written as:

$$y[n] = h[n]x[n] + z[n] = \begin{cases} +\sqrt{E_b}h[n] + z[n], & \text{if a "1" is transmitted} \\ -\sqrt{E_b}h[n] + z[n], & \text{if a "0" is transmitted} \end{cases} \quad (2.43)$$

where $h[n]$ denotes the channel fading coefficient in the nth signal interval. Since the channel is assumed to be Rayleigh flat fading, the pdf of the channel magnitude $|h[n]|$ is as in (2.26).

When the fading channel coefficient, $h[n]$, can be perfectly estimated at the receiver (i.e., coherent detection), one can multiple both sides of (2.40) with $h^*[n]/|h[n]|$ where the superscript $(\cdot)^*$ stands for conjugate operation. This gives

$$\frac{y[n]h^*[n]}{|h[n]|} = \begin{cases} +\sqrt{E_b}|h[n]| + w[n], & \text{if a "1" is transmitted} \\ -\sqrt{E_b}|h[n]| + w[n], & \text{if a "0" is transmitted} \end{cases} \quad (2.44)$$

where $w[n] = \frac{z[n]h^*[n]}{|h[n]|} \sim \mathcal{CN}(0, N_0)$. Taking the real part of both sides of (2.44), one has

$$\mathcal{R}\left\{\frac{y[n]h^*[n]}{|h[n]|}\right\} = \begin{cases} +\sqrt{E_b}|h[n]| + \mathcal{R}\{w[n]\}, & \text{if a "1" is transmitted} \\ -\sqrt{E_b}|h[n]| + \mathcal{R}\{w[n]\}, & \text{if a "0" is transmitted} \end{cases} \tag{2.45}$$

Here $\mathcal{R}\{w[n]\}$ is a real zero-mean Gaussian random variable with variance $N_0/2$. One can see that the optimum detector for the case of non-fading channel in (2.40) is still applicable for the case of fading channel in (2.45), i.e., the decision rule is

$$\mathcal{R}\left\{y[n]h^*[n]\right\} \underset{0}{\overset{1}{\gtrless}} 0 \tag{2.46}$$

From (2.45), compared to (2.34), one can see that the fading channel coefficient is incorporated into the energy term. Specifically, the received energy term in (2.45) is $E_b|h[n]|^2$. Therefore, the error probability for BPSK over a Rayleigh fading channel is given by [C2-2]

$$\begin{aligned} \text{BER}_{\text{Rayleigh fading, BPSK}} &= \mathbb{E}\left\{Q\left(\sqrt{\frac{2E_b|h[n]|^2}{N_0}}\right)\right\} \\ &= \int_0^\infty Q\left(\sqrt{\frac{2E_b|h[n]|^2}{N_0}}\right) p\left(|h[n]|\right) \mathrm{d}|h[n]| \\ &= \frac{1}{2}\left(1 - \sqrt{\frac{\overline{\gamma}}{1+\overline{\gamma}}}\right) \end{aligned} \tag{2.47}$$

where $p\left(|h[n]|\right)$ is the pdf of $|h[n]|$, $\mathbb{E}\{x\}$ denotes the expectation of random variable x, and $\overline{\gamma}$ is the average received signal-to-noise ratio, i.e., $\overline{\gamma} = \Omega E_b/N_0$. The expression of error probability in (2.47) clearly indicates that the error probability decays inversely with the average received signal-to-noise ratio in the fading channel!

The error probabilities of BPSK over AWGN and Rayleigh fading channels determined by (2.41) and (2.47), respectively, are plotted in Fig. 2.13. As can be seen, the AWGN channel is clearly more favorable than the Rayleigh fading channel since there is a large performance degradation experienced in the Rayleigh channel. Performance degradation in Rayleigh fading channels is attributed to the high probability of having very small channel gains (see Figs. 2.11 and 2.12), i.e., fading is the main cause

for the poor performance in wireless channels. To circumvent this problem, the most effective technique is *diversity*. A brief discussion of diversity techniques is given in the next section.

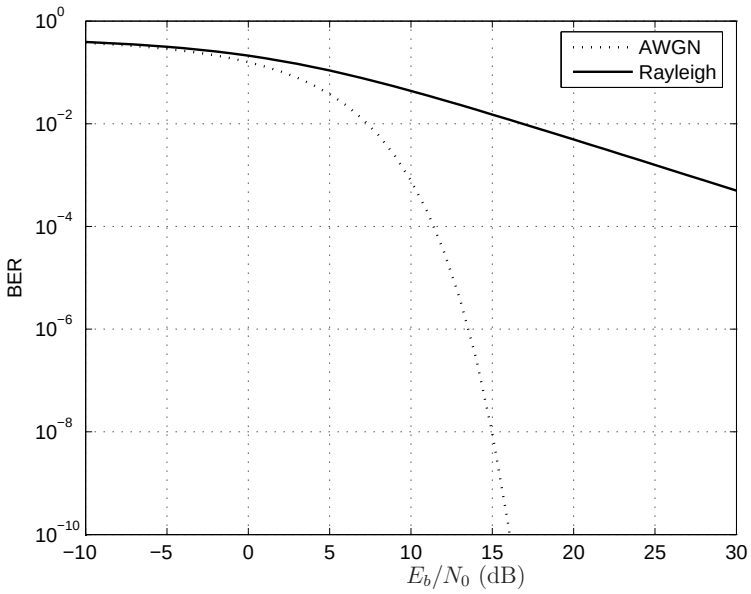

Figure 2.13 Error performance comparison for coherent BPSK under AWGN and Rayleigh fading channels.

2.3 Diversity Techniques in Wireless Channels

The channel model in (2.12) implies that the error performance of a communication system depends on the strength (quality) of a single channel tap. Unfortunately, this tap can be in a deep fade with a significant probability. When this happens, the channel magnitude drops dramatically due to the destructive addition of multipath signals. When the channel tap is in deep fade, any communication scheme will likely suffer from errors. A natural solution to improve the performance is to ensure that the transmitted signal arrives at the destination through multiple independent-fading paths. Since independent signal paths have a much lower probability of experiencing deep fades simultaneously, if the multiple received signal copies are combined appropriately, the effect of deep fading is reduced. This technique is called diversity, and it can drastically improve the performance over fading channels.

The effectiveness of a diversity technique can be quantified by the so-called diversity order, which is defined as [C2-7, Chapter 1], [C2-1, Chapter 3], [C2-8]:

$$G_d = -\lim_{\overline{\gamma}\to\infty} \frac{\log(P_e(\overline{\gamma}))}{\log(\overline{\gamma})}$$

where $P_e(\overline{\gamma})$ is the error probability obtained with the average received signal-to-noise ratio (SNR) of $\overline{\gamma}$. In essence, the diversity order indicates the *slope* of the average error probability curve in terms of the average received SNR in a logarithm to logarithm scale when the average received SNR tends to infinity. From the previous discussion, it follows that the maximum diversity order of any communication scheme is equal to the number of independent signal paths over which the information is received. When the diversity order equals to the maximum diversity order, the system is said to achieve the full diversity order [C2-8].

There are many ways to achieve independent signal paths in a wireless communications system. Three important techniques that have been extensively studied in the literature and applied in practical systems are [C2-1, C2-7]:

- *Time diversity*: In this technique, the signal is repeated over different time intervals.
- *Spatial diversity*: The signal is transmitted and/or received over different antennas.
- *Frequency diversity*: With this technique the signal is transmitted over different carrier frequencies.

In what follows, the spatial diversity technique is discussed in more detail since it is directly related to the cooperative diversity technique studied in this thesis.

In general, spatial diversity does not suffer from a loss in bandwidth efficiency since it uses multiple antennas to achieve diversity [C2-1], [C2-7]. Spatial diversity can be classified into three categories as illustrated in Fig. 2.14: receive diversity (single-input multiple-output, or SIMO channels), transmit diversity (multiple-input

single-output, or MISO channels), and transmit and receive diversity (multiple-input multiple-output, or MIMO channels). Receive diversity can be simply obtained by deploying multiple antennas at the receiving end to gather independently faded copies of the transmitted signals. Transmit diversity requires a more complex signal processing at the transmitter. In particular, the source information is first precoded and then spread across the multiple transmit antennas. Transmit and receive diversity is achieved by using multiple antennas at both transmitting and receiving ends.

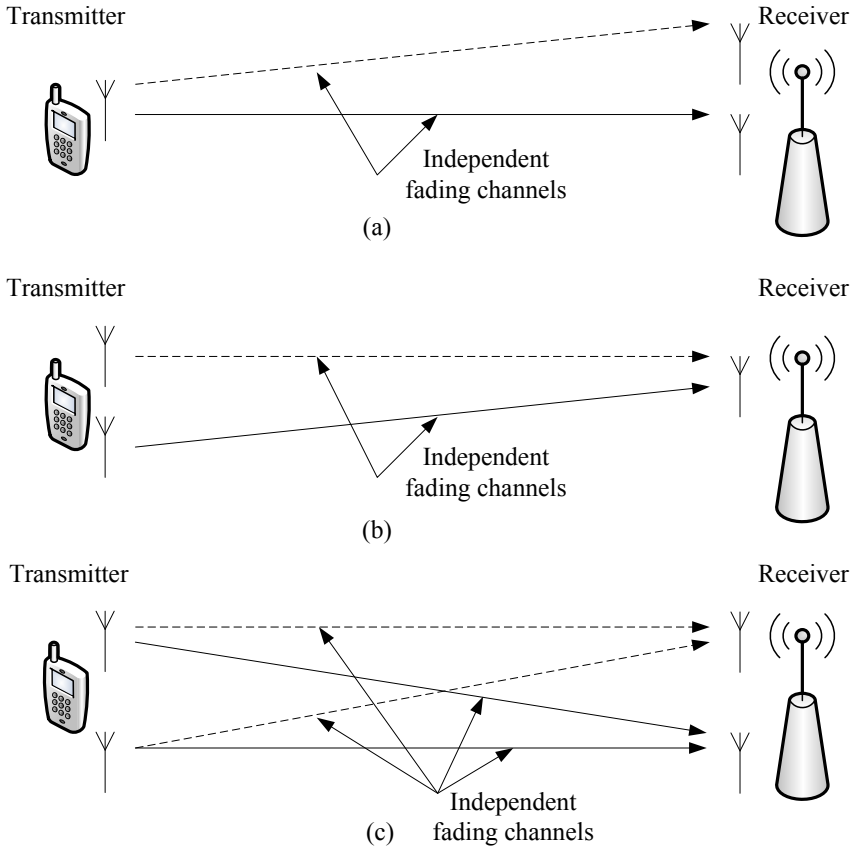

Figure 2.14 Illustration of spatial diversity techniques: (a) SIMO; (b) MISO; (c) MIMO.

2.3.1 Receive Diversity

Consider a wireless system with 1 transmit antenna and K receive antennas, i.e., there are K versions of the transmitted signal received through K independent channels at the destination. Let $x[n]$ be the transmitted signal. Then the K received

signals are

$$y_k[n] = h_k[n]x[n] + z_k[n], \quad k = 1, \ldots, N \tag{2.48}$$

where $h_k[n]$ is the channel fading coefficient between the transmit antenna and the kth receive antenna and $z_k[n]$ is the noise component at the kth receive antenna.

The K received signals need to be combined at the receiver to make a decision on the transmitted signal $x[n]$. There are two main combining techniques (see Fig. 2.15), namely the maximum ratio combining (MRC), and selection combining (SC) [31]. These combiners are further explained in the following.

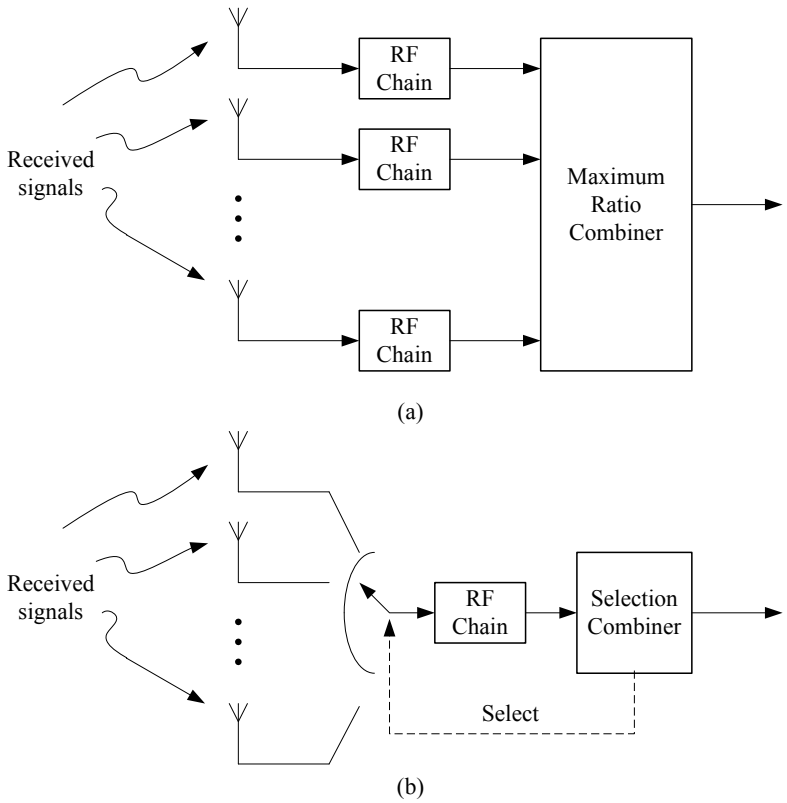

Figure 2.15 Block diagram of (a) Maximum ratio combining; (b) Selection combining.

Maximum Ratio Combining

In this combining technique, the knowledge of all fading channel coefficients is required at the destination. In practice, the fading channel coefficient can be estimated by sending known training (or pilot) signals. Given the fading channel coefficient,

each received signal is co-phased, weighted with its corresponding amplitude and then summed. It is an optimal combing scheme in the sense that it maximizes the combiner's SNR. In fact, the SNR of the combiner output is equal to the sum of all the instantaneous SNRs of the individual received signals, i.e.,

$$\gamma_{\text{MRC}} = \sum_{k=1}^{K} |h_k[n]|^2 \frac{E_s}{N_0} \tag{2.49}$$

where E_s is the average symbol energy of the transmitted signal and N_0 is the one-sided power spectral density of the noise $z_k[n]$.

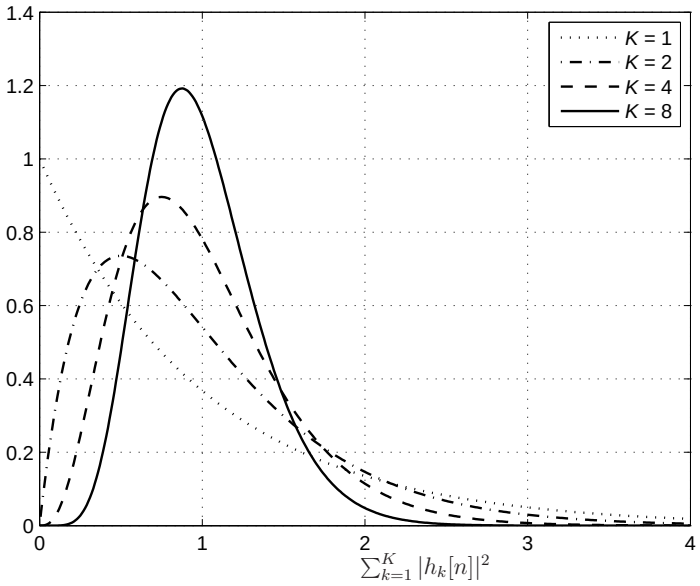

Figure 2.16 The pdf of $\sum_{k=1}^{K} |h_k[n]|^2$ for different values of K with maximum ratio combining.

Fig. 2.16 plots the distribution of $\sum_{k=1}^{K} |h_k[n]|^2$ for different values of K and when Ω_K is normalized to unity. Here Ω_K denotes the mean value of $\sum_{k=1}^{K} |h_k[n]|^2$. Under Rayleigh fading where each channel gain $h_k[n]$ is i.i.d. $\mathcal{CN}(0, \Omega)$, the sum $\sum_{k=1}^{K} |h_k[n]|^2$ is Chi-square distributed with $2K$ degrees of freedom since each term $|h_k[n]|^2$ is the sum of squares of the real and imaginary parts of $h_k[n]$. Clearly the tail of the distribution near zero becomes lighter for larger K, i.e., there is a low probability of having small instantaneous SNR for larger K. Therefore, increasing K can significantly decrease the error probability. This is confirmed by observing Fig.

2.17, which plots the error performance of the system with BPSK and different values of K. A higher value of K leads to a bigger improvement in the error performance.

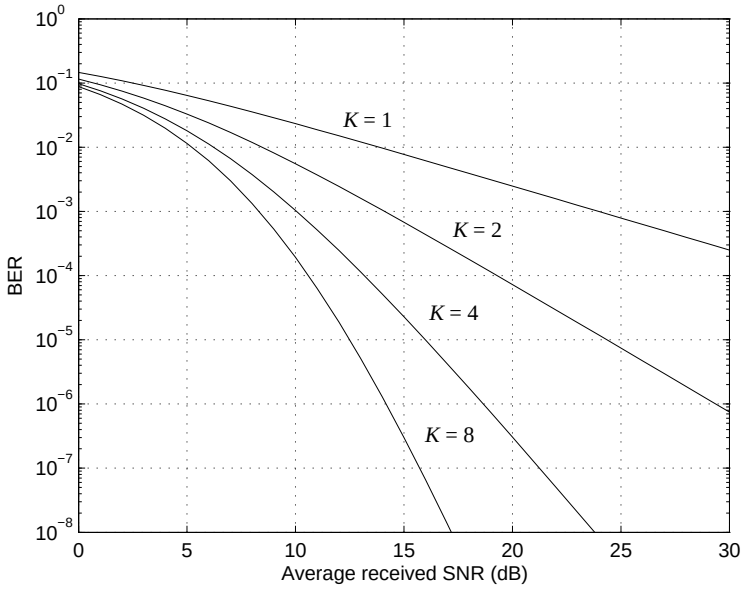

Figure 2.17 Error performance of coherent BPSK with MRC under Rayleigh fading channels.

Selection Combining

This combining technique processes only one of the received signals (see Fig. 2.15), i.e., only one radio frequency chain is required at the receiver to provide the baseband signal. Specifically, the destination chooses the received signal with the highest SNR for detection. The SNR at the output of the SC detector is simply determined as

$$\gamma_{\mathrm{SC}} = \left(\max_k |h_k[n]|^2 \right) \frac{E_s}{N_0} \tag{2.50}$$

Fig. 2.18 plots the pdf of $\max_k |h_k[n]|^2$ for different values of K. As can be seen, increasing K also results in the lighter tail of the pdf near zero, hence, the error performance can be improved. However, this technique still requires the estimation of the fading amplitudes of all the received signals and the fading phase of the selected signal. In practice, the received signal with the highest sum of signal and noise powers is often used for detection since it is more difficult to measure the instantaneous SNR of each receiving branch [C2-9].

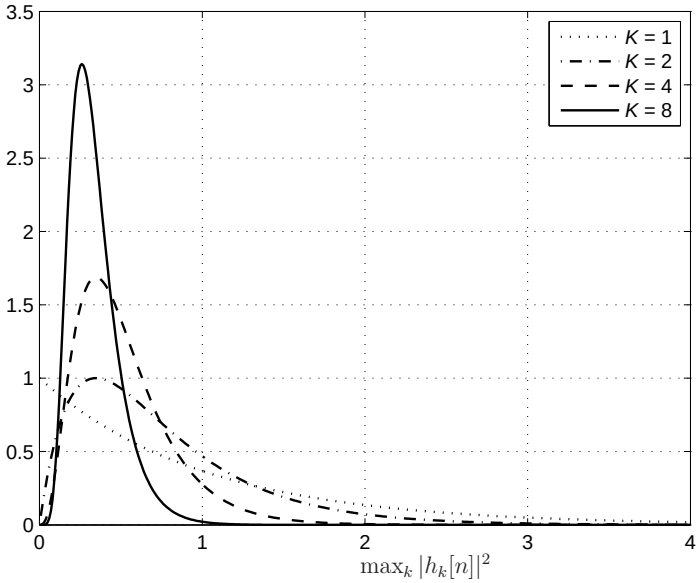

Figure 2.18 The pdf of $\max_k |h_k[n]|^2$ for different values of K with selection combining.

2.3.2 Transmit Diversity

When implementing multiple receive antennas to achieve receive diversity is not possible due to the constraints on complexity, power consumption, and cost at the receiver [C2-10, C2-11, C2-12, C2-9], transmit diversity is desirable since it can reduce the required signal processing efforts at the receiver. In addition, transmit diversity can further improve the system performance when incorporating with receive diversity.

To describe transmit diversity technique, consider a wireless system with K transmit antennas and 1 receive antenna. It is easy to have K independent replicas of a transmitted signal by simply transmitting the same symbol over the K different antennas during K symbol times. At any one time, only one antenna transmits and others remain silent. However, such an approach is clearly very inefficient. One would need to expand the bandwidth by K times to achieve the same data rate. A more intelligent approach, called *space-time coding*, realizes transmit diversity by spreading the transmitted signals over both spatial and temporal dimensions [C2-11, C2-12].

In what follows, we discuss a remarkably simple scheme to gain some insight into how a space-time coding system works. This scheme is the very well-known Alamouti scheme, originally designed for two transmit antennas without any loss of bandwidth [C2-10]. The scheme transmits two symbols over two time slots under the assumption that channel coefficients remain constant during that period, i.e., over n and $n+1$ time slots. Specifically, in the nth time slot, $x_1[n]$ is transmitted from the first antenna and $x_2[n]$ is transmitted from the second antenna simultaneously. In the $(n+1)$th time slot, the scheme transmits $-x_2^*[n]$ from the first antenna and $x_1^*[n]$ from the second antenna simultaneously. Here $(\cdot)^*$ represents complex conjugate operation. The received signals over the two time slots, denoted by $y[n]$ and $y[n+1]$, can be written as

$$y[n] = h_1[n]x_1[n] + h_2[n]x_2[n] + z[n] \tag{2.51}$$

$$y[n+1] = -h_1[n]x_2^*[n] + h_2[n]x_1^*[n] + z[n+1] \tag{2.52}$$

or

$$\underbrace{\begin{bmatrix} y[n] \\ y^*[n+1] \end{bmatrix}}_{\mathbf{y}[n]} = \underbrace{\begin{bmatrix} h_1[n] & h_2[n] \\ h_2^*[n] & -h_1^*[n] \end{bmatrix}}_{\mathbf{H}[n]} \underbrace{\begin{bmatrix} x_1[n] \\ x_2[n] \end{bmatrix}}_{\mathbf{x}[n]} + \underbrace{\begin{bmatrix} z[n] \\ z^*[n+1] \end{bmatrix}}_{\mathbf{z}[n]}, \tag{2.53}$$

where $h_1[n]$ and $h_2[n]$ denote the channel coefficients from the first and second antennas to the receiver, respectively, $z[n]$ is the AWGN sample at the receiver in the nth time slot.

It can be observed that the columns of the square matrix $\mathbf{H}[n]$ are orthogonal. In particular, $\mathbf{H}^H[n]\mathbf{H}[n] = (|h_1[n]|^2 + |h_2[n]|^2)\mathbf{I}_2$ where $(\cdot)^H$ represents conjugate transpose operation and $\mathbf{I}_n$ is an identity matrix of size n. Therefore, one can detect $x_1[n]$ and $x_2[n]$ as follows. First, obtain

$$\mathbf{r}[n] = \begin{bmatrix} r_1[n] \\ r_2[n] \end{bmatrix} = \mathbf{H}^H[n]\mathbf{y}[n] = \mathbf{H}^H[n]\mathbf{H}[n]\mathbf{x}[n] + \mathbf{H}^H\mathbf{z}[n]. \tag{2.54}$$

It follows that

$$r_1[n] = (|h_1[n]|^2 + |h_2[n]|^2)x_1[n] + \underbrace{h_1^*[n]z[n] + h_2[n]z^*[n+1]}_{\hat{z}_1[n]} \quad (2.55)$$

$$r_2[n] = (|h_1[n]|^2 + |h_2[n]|^2)x_2[n] + \underbrace{h_2^*[n]z[n] - h_1[n]z^*[n+1]}_{\hat{z}_2[n]} \quad (2.56)$$

It can be easily verified that $\hat{z}_i[n] \sim \mathcal{CN}(0, N_0)$ and $\hat{z}_1[n]$ and $\hat{z}_2[n]$ are independent. It can also be seen that each of the two transmitted symbols can be detected separately (i.e., symbol-wise decoding). Thus, the instantaneous received SNR for each transmitted symbol is given by

$$\gamma_i = \sum_{k=1}^{2} |h_k[n]|^2 \frac{E_s}{N_0}; \quad i = 1, 2$$

Furthermore, the received SNR for each transmitted symbol is the sum of the squares of the two independent channel magnitudes. It follows immediately from the discussion on MRC (see Eq. (2.49)) that the Alamouti scheme achieves the maximal diversity order of 2 for a system with two transmit antennas. In addition, two symbols are transmitted over two symbol intervals and hence there is no loss in bandwidth deficiency.

Alamouti's space-time coding concept can be generalized for $K > 2$ with all the desired properties, i.e., (i) full-diversity order, (ii) symbol-wise maximum likelihood decoding, if the constellations are real (such as ASK). Unfortunately, the construction is only possible with some special cases and a reduction in code rate is unavoidable if the constellations are complex (such as PSK and QAM).

2.4 Cooperative Wireless Networks

Although spatial diversity is a very powerful technique to improve transmission reliability over a fading channel, implementing multiple transmit and/or receive antennas to provide diversity might not be a feasible solution due to the size, cost, and hardware limitations. As mentioned before, the cooperative diversity method has recently been proposed to overcome the above limitations [C2-13, C2-14]. The

basic idea of cooperative diversity is that a source node transmits information data to the destination through multiple nodes (or relays). In this way, the destination can receive the transmitted data with multiple copies that are generally affected by different and statistically independent fading paths. In fact, a virtual multiple antenna system is formed by using antennas from other users (or nodes, relays) within the network. This section provides an introduction to some of the most important cooperative (relaying) protocols and signal processing methods at the relays.

2.4.1 Relaying Protocols

In the literature, there are three main approaches to achieve cooperative diversity. The first approach is based on repetition coding among participating nodes, i.e., the source and relays transmit the signal to the destination over orthogonal channels. The destination decodes the transmitted data based on the received signals from different nodes that experience independent channel fading, thereby obtains the full diversity order. However, the approach typically suffers a certain throughput loss since the number of required channels cannot be less than the number of relays [C2-15]. One way to overcome this disadvantage is implementing distributed space-time coding (DSTC) among participating nodes. In DSTC protocol, the source and/or all the relays collaborate to transmit a codeword to the destination. The protocol potentially achieves a better throughput than the repetition-based protocol. However, it requires symbol-level synchronization of collaborating relays and large overhead during the set-up phase. Also, finding codes for a network with more than one relay is still largely open [C2-16, C2-17, C2-18]. Another approach is to implement relay selection. Instead of retransmitting the data from all the relays, only one relay is selected to retransmit the data to the destination. As a result, the system throughput is significantly improved [C2-19, C2-20].

Three possible protocols, called Protocols A, B, and C, that can be used to assist the source-destination communication are summarized next.

- *Protocol A (repetition-based)*: In the first phase, the source broadcasts the signal to both the relays and destination. In the second phase, the relays communicate with the destination over orthogonal channels.

- *Protocol B (DSTC)*: In this protocol, the source communicates with the relays and destination during the first phase. Then the source and relays communicate with the destination in the second phase.

- *Protocol C (relay selection)*: The third protocol is identical to both Protocol I and Protocol II in the first phase. In the second phase, a single relay is selected based on some criteria to retransmit the signal to the destination.

2.4.2 Processing Methods at Relays

Depending on the signal processing performed at relays, cooperative protocols can be classified into three main groups: amplify-and-forward (AF), decode-and-forward (DF), and compress-and-forward (CF) [C2-16, C2-21]. The two processing methods considered in this thesis are AF and DF.

As illustrated in Fig. 2.19a, with DF, the relays decode the source's messages, re-encode and re-transmit to the destination. A major challenge with the DF method is that it is not simple to realize the cooperative diversity. This is due to possible re-transmission of erroneously decoded information by the relays in the DF method [C2-16, C2-15, C2-19, C2-22]. There are many ways to overcome such a challenge. For example, an error detection code can be added at the source. Based on the decoding result in the first phase, the relay can decide to retransmit or remain silent in the second phase [C2-23, C2-24]. Setting a threshold based on the link SNR is another practical approach to reduce error propagation. Specifically, when the source-relay SNR is larger than a threshold, the probability of decoding error at the relay is negligible and hence the relay retransmits the message [C2-16, C2-15, C2-19, C2-25, C2-22]. In [C2-26], a receiver has been designed to eliminate errors at the relay, which allows the relay to always forward the received data. In particular, a cooperative maximum-ratio-combining (C-MRC) detector was proposed at the destination to collect the full

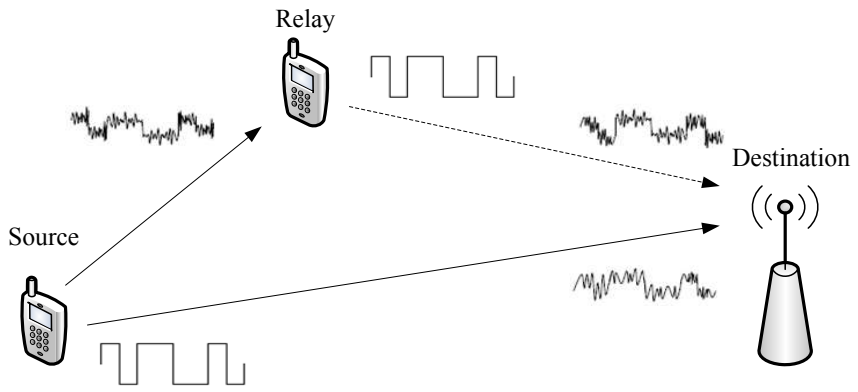

(a) Decode-and-Forward

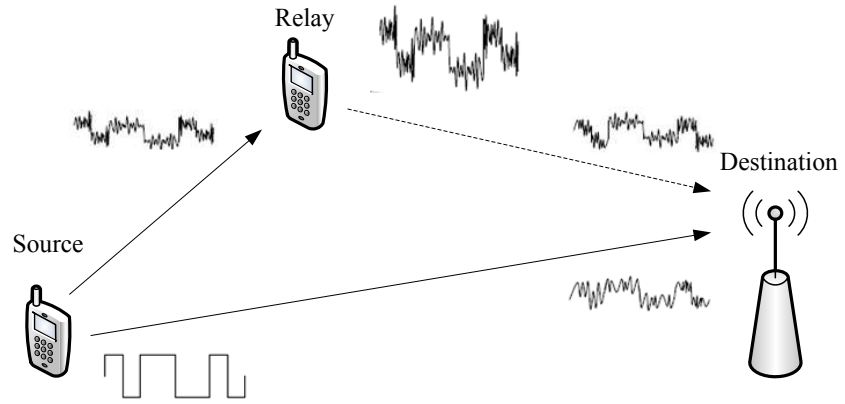

(b) Amplify-and-Forward

Figure 2.19 Illustration of Amplify-and-Forward and Decode-and-Forward signal processing methods.

diversity order by taking into consideration the instantaneous BER of the source-relay link. How to avoid error propagation by using adaptive techniques at the relays(s) in coherent/noncoherent DF cooperative networks is one of the main objectives of this thesis.

With AF, as depicted in Fig. 2.19b, the relays receive noisy versions of the source's messages, amplify and re-transmit to the destination. The AF method is further categorized as variable-gain or fixed-gain relaying based on the availability of CSI at the relays. The variable-gain AF relaying scheme requires the instantaneous CSI of the source-relay link at the corresponding relay to maintain a fixed transmit power at all time. On the other hand, the fixed-gain AF relaying scheme does not need

the instantaneous CSI, but the average signal-to-noise ratio of the source-relay link in order to maintain a fixed average transmit power at each relay [C2-15, C2-27, C2-28, C2-29]. Although the AF method does not suffer from the error propagation problem as the DF method, it presents another problem, that of noise accumulation at the relays. However, it is still attractive since it puts a less signal processing burden on the relays. With AF, the destination requires the perfect knowledge of CSI of all the transmission links propagated by its received signals in order to perform a coherent detection, e.g., employing MRC detection. This requirement implies a high cost for a network with multiple relays, especially in a fast fading environment. How to overcome this disadvantage is another objective of this thesis.

2.5 Noncoherent Communications

The fundamental concepts of cooperative communications are discussed in the previous section. This technique achieves spatial diversity without implementing multiple transmit and/or receive antennas. However, it also implies a high cost for a network with multiple relay transmission links if channel estimation needs to be carried out. To make the cooperative techniques less expensive, noncoherent communication can be used so that the need of channel estimation can be eliminated. In what follows, noncoherent communication techniques in point-to-point communications are discussed. Applying noncoherent communication techniques in cooperative networks will be investigated in this thesis.

In the literature, the two well-known noncoherent communication techniques are:

- Using differential modulation and demodulation schemes such as the differential phase-shift keying (DPSK).
- Employing noncoherent detection techniques such as the envelope or square law detection of appropriately signal sets, such as frequency shift-keying (FSK) signals.

The basic idea of the first technique is to use the phase of the previous channel sym-

bol as a reference for the phase of the current channel symbol, thus a coherent phase reference at the receiver is not necessary. With this technique, the phase differences between consecutive symbols carry the information. Specifically, in differential M-PSK modulation, each symbol is generated by the root of unity: $s_m = \exp\left(j2\pi\frac{(m-1)}{M}\right)$ where $m = 1, \ldots, M$. The discrete-time baseband equivalent input $x[n]$ in the nth symbol period in (2.12) is

$$x[n] = s_m x[n-1]. \tag{2.57}$$

where the differential modulation transmits $x[1] = +\sqrt{E_s}$ in the first symbol period. The quality E_s is the average transmitted symbol energy. The discrete-time baseband equivalent output in the nth symbol period can be written as

$$y[n] = h[n]x[n] + z[n], \tag{2.58}$$

where $h[n]$ and $z[n]$ are the fading channel coefficient and noise component, respectively.

By performing the following derivations, one can reveal the detection rule of differential modulation. From (2.58), one has

$$y[n-1] = h[n-1]x[n-1] + z[n-1]. \tag{2.59}$$

Assuming that the fading coefficients are constant over two symbol periods, i.e., $h[n] = h[n-1]$, Equation (2.58) can be rewritten as

$$\begin{aligned} y[n] = h[n]x[n] + z[n] &= h[n]s_m x[n-1] + z[n] \\ &= s_m y[n-1] + \underbrace{\left(z[n] - s_m z[n-1]\right)}_{\text{noise}}. \end{aligned} \tag{2.60}$$

Therefore, the transmitted information can be decoded as

$$\hat{s}_m = \arg \min_{m=1,\ldots,M} \left| y[n] - s_m y[n-1] \right|^2 \tag{2.61}$$

One can observe from (2.61) that the differential demodulation relies on two consecutive received signals, and it does not need the phase reference (or the fading coefficient).

With the second technique, due to the orthogonal property of the signal waveforms in FSK modulation, the detection of information is done by comparing the energy of the signal at each frequency. Specifically, the information bits are transmitted by one of M orthogonal carriers, i.e., the signal waveforms are represented as

$$\begin{aligned} x_{\mathrm{PB},m}(t) &= \mathcal{R}\left\{x_m(t)\exp\left(j2\pi f_c t\right)\right\} \\ &= \mathcal{R}\left\{\sqrt{\frac{2E_s}{T_s}}\exp\left(j\pi(2m-M-1)\Delta f t\right)\exp\left(j2\pi f_c t\right)\right\} \\ &= \sqrt{\frac{2E_s}{T_s}}\cos\Big(2\pi\big(\underbrace{f_c+\frac{(2m-M-1)\Delta f}{2}}_{f_m}\big)t\Big), \quad m=1,2,\ldots,M, \end{aligned} \tag{2.62}$$

where E_s is the energy in each signal and Δf represents the minimum frequency separation between adjacent carriers so that the signal waveforms are orthogonal over the interval $[0, T_s]$. When the signals are "noncoherently" orthogonal, $\Delta f = \frac{1}{T_s}$. When the signals are "coherently" orthogonal, $\Delta f = \frac{1}{2T_s}$ [C2-2]. The equivalent low-pass signal waveforms for "noncoherently" orthogonal signals are defined as

$$x_m(t) = \sqrt{\frac{2E_s}{T_s}}\exp\left(\frac{j\pi t}{T_s}(2m-M-1)\right), \quad m=1,\ldots,M \tag{2.63}$$

The signal $x_m(t)$ corresponds to frequency $f_m = f_c + \frac{2m-M-1}{2T_s}$. The equivalent base-band received signal over a Rayleigh fading channel can be expressed as

$$y(t) = hx_m(t) + z(t) \tag{2.64}$$

where h denotes the channel fading coefficient between the transmitter and receiver, which is assumed to be fixed over the symbol duration T_s, and $z(t)$ is zero-mean AWGN at the receiver whose two-sided power spectral density is $N_0/2$.

The destination correlates the received signal with the following vector of basis waveforms in M-FSK:

$$x(t) = \left[\begin{array}{cccc} \frac{x_1^*(t)}{\sqrt{E_s}} & \frac{x_2^*(t)}{\sqrt{E_s}} & \cdots & \frac{x_M^*(t)}{\sqrt{E_s}} \end{array}\right]^T. \tag{2.65}$$

Due to the orthogonal property of the signal waveforms, the outputs of the correlators

can be shown to be:

$$\mathbf{y} = \begin{bmatrix} y_1 \\ y_2 \\ \vdots \\ y_M \end{bmatrix} = h \begin{bmatrix} x_1 \\ x_2 \\ \vdots \\ x_M \end{bmatrix} + \begin{bmatrix} z_1 \\ z_2 \\ \vdots \\ z_M \end{bmatrix} = h\mathbf{x}_m + \mathbf{z}, \tag{2.66}$$

where the $M \times 1$ vector $\mathbf{x}_m$, $m = 1, \ldots, M$, represents the transmitted symbol. Note that $\mathbf{x}_m$ has $\sqrt{E_s}$ as its mth element and 0 as its other elements, i.e.,

$$\begin{array}{rcl} \mathbf{x}_1 & = & \begin{bmatrix} \sqrt{E_s} & 0 & 0 & \ldots & 0 & 0 \end{bmatrix} \\ \mathbf{x}_2 & = & \begin{bmatrix} 0 & \sqrt{E_s} & 0 & \ldots & 0 & 0 \end{bmatrix} \\ & \vdots & \\ \mathbf{x}_M & = & \begin{bmatrix} 0 & 0 & 0 & \ldots & 0 & \sqrt{E_s} \end{bmatrix} \end{array} \tag{2.67}$$

The elements of $M \times 1$ noise vector $\mathbf{z}$ are i.i.d. zero-mean random variables with variance N_0. Equation (2.66) is the equivalent discrete-time input/output model for M-FSK. In the following, we develop the optimum receiver for noncoherent M-FSK, i.e., when the fading channel coefficient h is unknown at the receiver.

Since y_k, z_k, $k = 1, \ldots, M$, and h are complex random variables, one can write $y_k = y_{k,R} + jy_{k,I}$, $z_k = z_{k,R} + jz_{k,I}$, $k = 1, \ldots, M$, and $h = h_R + jh_I$, where the subscripts R and I stand for the real and imaginary components, respectively. The $z_{k,R}$ and $z_{k,I}$ are i.i.d. zero-mean Gaussian random variables with variance $N_0/2$. As mentioned earlier, the fading components h_R and h_I are also i.i.d. zero-mean Gaussian random variables with variance $\Omega/2$. It can be verified that the pdfs of the correlator output are

$$p\left(y_{k,R}|\mathbf{x}_m\right) = \begin{cases} \frac{1}{\sqrt{\pi(E_s\Omega+N_0)}} \exp\left(-\frac{y_{k,R}^2}{E_s\Omega+N_0}\right), & \text{if } k = m, \\ \frac{1}{\sqrt{\pi N_0}} \exp\left(-\frac{y_{k,R}^2}{N_0}\right), & \text{if } k \neq m, \end{cases} \tag{2.68}$$

$$p\left(y_{k,I}|\mathbf{x}_m\right) = \begin{cases} \frac{1}{\sqrt{\pi(E_s\Omega+N_0)}} \exp\left(-\frac{y_{k,I}^2}{E_s\Omega+N_0}\right), & \text{if } k = m, \\ \frac{1}{\sqrt{\pi N_0}} \exp\left(-\frac{y_{k,I}^2}{N_0}\right), & \text{if } k \neq m \end{cases} \tag{2.69}$$

Therefore, given $\mathbf{x}_m$, the likelihood function can be computed as

$$p\left(y_{1,R}, y_{1,I}, \ldots, y_{M,R}, y_{M,I} \middle| \mathbf{x}_m\right) = \prod_{\substack{k=1 \\ k \neq m}}^{M} \left(\frac{1}{\pi N_0} \exp\left(-\frac{y_{k,R}^2 + y_{k,I}^2}{N_0}\right)\right) \frac{1}{\pi(E_s\Omega + N_0)} \exp\left(-\frac{y_{m,R}^2 + y_{m,I}^2}{E_s\Omega + N_0}\right) \quad (2.70)$$

The maximum-likelihood detection is expressed as follows

$$\begin{gathered} \text{choose } m \text{ if} \\ p\left(y_{1,R}, y_{1,I}, \ldots, y_{M,R}, y_{M,I} \middle| \mathbf{x}_m\right) > p\left(y_{1,R}, y_{1,I}, \ldots, y_{M,R}, y_{M,I} \middle| \mathbf{x}_k\right) \\ k = 1, 2, \ldots, M; \quad k \neq m \end{gathered} \quad (2.71)$$

Equivalently the decision rule can be simplified to

$$\begin{gathered} \text{choose } m \text{ if} \\ |y_m|^2 = \left|\sqrt{E_s}h + z_m\right|^2 > |y_k|^2 = \left|\sqrt{E_s}h + z_j\right|^2, \\ k = 1, 2, \ldots, M; \quad k \neq m \end{gathered} \quad (2.72)$$

The decision rule picks frequency f_m if the mth branch has the highest energy. Basically, (2.72) is energy detection or square-law detection (see Fig. 2.20). Such a detection rule is intuitively satisfying since both the amplitude and phase of the transmitted waveform are affected by fading channel which is unknown at the receiver. The difference among different hypotheses lies in the received power.

As mentioned before, our interest is to efficiently apply M-FSK modulation in cooperative networks. Specifically, we are interested in using energy-difference thresholds to improve the BER performances in DF cooperative networks in which FSK modulation is employed for noncoherent communications. In addition, how to decode the transmitted information in AF cooperative networks with M-FSK modulation is another topic of this thesis.

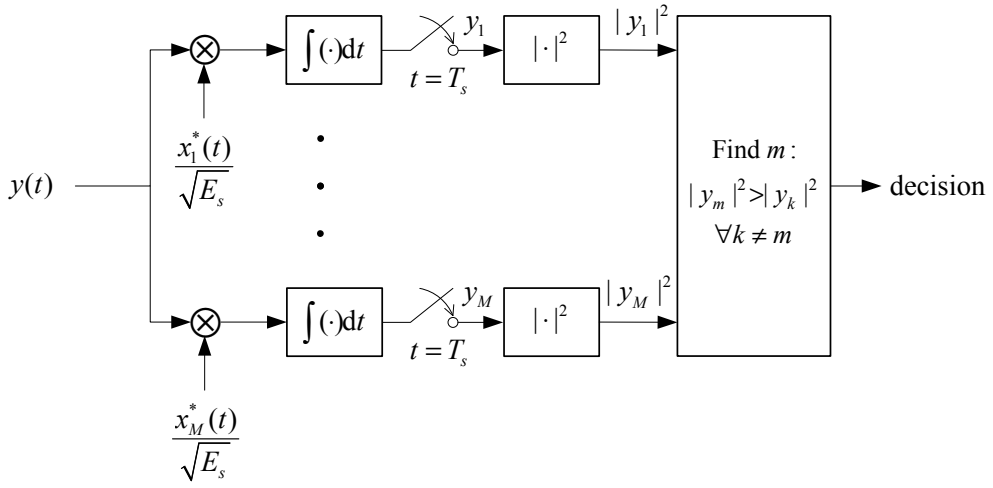

Figure 2.20 Noncoherent demodulator of M-FSK.

2.6 Summary

First, the fading effects experienced by wireless communications systems are explained. Different statistical models to describe a fading channel such as Rayleigh, Rician, and Nakagami-m fading have been discussed. Various diversity techniques to improve the performance over fading channels have been presented. In addition, different digital modulation methods such as M-ASK, M-PSK, M-QAM, and M-FSK have also been described and analyzed in this chapter. Unequal error protection, an important technique to protect the data according to the system requirements, has been described. This chapter reviews principal knowledge widely used in the thesis.

The next chapter includes the first paper which proposes and analyzes performance of a single-relay network in which a hierarchical 2/4-ASK constellation is employed to achieve unequal error protection.

References

[C2-1] D. Tse and P. Viswanath, *Fundamentals of Wireless Communications*. Cambridge University Press, 2005.

[C2-2] J. G. Proakis, *Digital Communications*. McGraw-Hill, 2000.

[C2-3] P. Vitthaladevuni and M.-S. Alouini, "Exact BER computation of generalized

hierarchical PSK constellations," *IEEE Trans. Commun.*, vol. 51, pp. 2030–2037, December 2003.

[C2-4] H. H. Nguyen and E. Shwedyk, *A First Course in Digital Communications*. Cambridge University Press, 2009.

[C2-5] I. S. Gradshteyn, I. M. Ryzhik, A. Jeffrey, and D. Zwillinger, *Table of Integrals, Series, and Products*. Academic Press, 2000.

[C2-6] M. K. Simon and M.-S. Alouini, *Digital Communication over Fading Channels*. Wiley, 2005.

[C2-7] H. Jafarkhani, *Space-Time Coding: Theory and Practice*. Cambridge University Press, 2005.

[C2-8] L. Zheng and D. N. C. Tse, "Diversity and multiplexing: A fundamental tradeoff in multiple antenna channels," *IEEE Trans. Inform. Theory*, vol. 49, pp. 1073–1096, 2002.

[C2-9] A. Goldsmith, *Wireless Communications*. Cambridge University Press, 2005.

[C2-10] S. Alamouti, "A simple transmit diversity technique for wireless communications," *IEEE J. Select. Areas in Commun.*, vol. 16, pp. 1451–1458, October 1998.

[C2-11] V. Tarokh, N. Seshadri, and A. Calderbank, "Space-time codes for high data rate wireless communication: Performance criterion and code construction," *IEEE Trans. Inform. Theory*, vol. 44, pp. 744 –765, March 1998.

[C2-12] V. Tarokh, H. Jafarkhani, and A. Calderbank, "Space-time block codes from orthogonal designs," *IEEE Trans. Inform. Theory*, vol. 45, pp. 1456–1467, July 1999.

[C2-13] A. Sendonaris, E. Erkip, and B. Aazhang, "User cooperation diversity, Part I: System description," *IEEE Trans. Commun.*, vol. 51, no. 11, pp. 1927–1938, November 2003.

[C2-14] A. Sendonaris, E. Erkip, and B. Aazhang, "User cooperation diversity, Part II: Implementation aspects and performance analysis," *IEEE Trans. Commun.*, vol. 51, no. 11, pp. 1939–1948, November 2003.

[C2-15] J. Laneman, D. Tse, and G. Wornell, "Cooperative diversity in wireless networks: Efficient protocols and outage behavior," *IEEE Trans. Inform. Theory*, vol. 50, pp. 3062–3080, December 2004.

[C2-16] J. Laneman and G. Wornell, "Distributed space-time-coded protocols for exploiting cooperative diversity in wireless networks," *IEEE Trans. Inform. Theory*, vol. 49, pp. 2415–2425, October 2003.

[C2-17] Y. Jing and B. Hassibi, "Distributed space-time coding in wireless relay networks," *IEEE Trans. Wireless Commun.*, vol. 5, no. 12, pp. 3524–3536, December 2006.

[C2-18] Y. Jing and H. Jafarkhani, "Using orthogonal and quasi-orthogonal designs in wireless relay networks," *IEEE Trans. Inform. Theory*, vol. 53, pp. 4106–4118, Nov. 2007.

[C2-19] A. Bletsas, A. Khisti, D. Reed, and A. Lippman, "A simple cooperative diversity method based on network path selection," *IEEE J. Select. Areas in Commun.*, vol. 24, pp. 659–672, March 2006.

[C2-20] Y. Zhao, R. Adve, and T. Lim, "Improving amplify-and-forward relay networks: Optimal power allocation versus selection," *IEEE Trans. Wireless Commun.*, vol. 6, pp. 3114–3123, August 2007.

[C2-21] J. Hi and R. Hu, "Slepian-Wolf cooperation: A practical and effcient compress-and-forward relay scheme," in *Allerton Conf. Commun. Contr. and Comp.*, November 2005.

[C2-22] A. Bletsas, H. Shin, and M. Win, "Cooperative communications with outage-optimal opportunistic relaying," *IEEE Trans. Wireless Commun.*, vol. 6, pp. 3450–3460, September 2007.

[C2-23] T. Hunter and A. Nosratinia, "Diversity through coded cooperation," *IEEE Trans. Wireless Commun.*, vol. 5, pp. 283–289, February 2006.

[C2-24] T. Hunter, S. Sanayei, and A. Nosratinia, "Outage analysis of coded cooperation," *IEEE Trans. Inform. Theory*, vol. 52, pp. 375–391, February 2006.

[C2-25] A. Bletsas, H. Shin, and M. Win, "Outage optimality of opportunistic amplify-and-forward relaying," *IEEE Commun. Letters*, vol. 11, pp. 261–263, March 2007.

[C2-26] T. Wang, A. Cano, G. Giannakis, and J. Laneman, "High-performance cooperative demodulation with decode-and-forward relays," *IEEE Trans. Commun.*, vol. 55, pp. 1427–1438, July 2007.

[C2-27] M. Hasna and M.-S. Alouini, "A performance study of dual-hop transmissions with fixed gain relays," *IEEE Trans. Wireless Commun.*, vol. 3, pp. 1963–1968, November 2004.

[C2-28] R. Nabar, H. Bolcskei, and F. Kneubuhler, "Fading relay channels: Performance limits and space-time signal design," *IEEE J. Select. Areas in Commun.*, vol. 22, pp. 1099–1109, August 2004.

[C2-29] D. Chen and J. Laneman, "Modulation and demodulation for cooperative diversity in wireless systems," *IEEE Trans. Wireless Commun.*, vol. 5, pp. 1785–1794, July 2006.

3. Signal Transmission with Unequal Error Protection in Wireless Relay Networks

Published as:

Ha X. Nguyen, Ha H. Nguyen and Tho Le-Ngoc, "Signal Transmission with Unequal Error Protection in Wireless Relay Networks", *IEEE Transactions on Vehicular Technology*, vol. 59, pp. 2166-2178, June 2010.

As mentioned in the previous chapter, for DF relaying method, if the relay makes any errors, the phenomenon of error propagation results in poor performance. This phenomenon is referred as error propagation. A simple way to mitigate error propagation is to implement adaptive relaying technique. In particular, the relay uses a threshold and decides to retransmit in the second phase only if the instantaneous source-relay SNR is larger than a threshold. Otherwise, it remains silent.

Given the importance of the UEP technique in providing different levels of error protection, the manuscript in this chapter studies a relaying technique in cooperative networks in which hierarchical modulation is employed to achieve UEP. To be more specific, the manuscript considers a cooperative network with one source, one relay, and one destination and there are two different protection classes at the source. A hierarchical 2/4-ASK constellation is employed to modulate the transmitted bits at the source. Based on the instantaneous received SNR at the relay, the relay decides to retransmit both classes by using a hierarchical 2/4- ASK constellation, or the more protection class by using a 2-ASK constellation, or remains silent. Based on the average BERs for two different protection classes, optimal thresholds are chosen to

minimize the BER for the less protection class while the BER of the more protection class satisfies a given requirement. To verify the analytical results, numerical simulations are presented. Performance comparison reveals that the optimal thresholds improve the error performance significantly.

Signal Transmission with Unequal Error Protection in Wireless Relay Networks

Ha X. Nguyen, *Student Member, IEEE*, Ha H. Nguyen, *Senior Member, IEEE*, and Tho Le-Ngoc, *Fellow, IEEE*

Abstract

This paper studies a relaying technique based on the signal-to-noise ratio (SNR) threshold in cooperative networks using hierarchical modulation. Hierarchical modulation is useful in applications that require different protection classes of the information. In particular, a cooperative network with one source, one relay, and one destination is considered. Two different protection classes are modulated by a hierarchical 2/4-amplitude shift keying (ASK) constellation at the source. Based on the instantaneous received SNR at the relay, the relay decides to retransmit both classes by using a hierarchical 2/4-ASK constellation, or the more protection class by using a 2-ASK constellation, or remains silent. Optimal thresholds are chosen to minimize the bit-error-rate (BER) of the less protection class while the BER of the more protection class meets a given requirement. Numerical and simulation results are provided to verify the analysis. The results show that the optimal thresholds improve the performance significantly.

Index terms

Cooperative diversity, cooperative communications, relay networks, fading channel, unequal error protection, hierarchical modulation.

Manuscript received May, 4, 2009; revised October 2, 2009 and December 29, 2009; accepted January 24, 2010. The review of this paper was coordinated by Prof. A. M. Tonello.

Ha X. Nguyen (*contact author) and Ha H. Nguyen are with the Department of Electrical and Computer Engineering, University of Saskatchewan, 57 Campus Drive, Saskatoon, Sask., Canada, S7N 5A9 (e-mails: hxn201@mail.usask.ca, ha.nguyen@usask.ca).

Tho Le-Ngoc is with the Department of Electrical and Computer Engineering, McGill University, 3480 University Street, Montreal, Quebec, Canada, H3A 2A7 (e-mail: tho@ece.mcgill.ca).

3.1 Introduction

In cooperative systems, the transmission from a source to a destination is assisted by relay(s). Research on cooperative communication systems started with the introduction of the relay channel in [C3-1]. Fundamental theorems on the bound of the capacity of relay networks were then established in [C3-2, C3-3]. Recently, cooperative (or relay) diversity has also been actively studied as a technique to combat fading experienced in wireless transmission [C3-4, C3-5, C3-6, C3-7, C3-8]. In particular, the end-to-end (e2e) bit-error-rate (BER) performance in a wireless network can be improved by having nodes (users) in the network cooperate with each other. The basic idea is that a source node cooperates with other nodes (or relays) in the network to form a virtual multiple antenna system [C3-4, C3-5, C3-6, C3-7, C3-8], hence providing spatial diversity. In a relay network, it is common to consider the amplify-and-forward (AF), decode-and-forward (DF), or compress-and-forward (CF) protocol at the relays. With AF, relays receive noisy versions of the source's messages, amplify and re-transmit to the destination. With DF, relays decode the source's messages, re-encode and re-transmit to the destination. On the other hand, the relays in CF protocol forward the quantized/compressed/estimated version of its received signals [C3-2, C3-9]. A major drawback of the DF protocol is that cooperation does not achieve the full diversity if the relays always re-transmit the decoded message. This is due to possible retransmission of erroneously decoded bits of the message by the relays. With an adaptive version of the DF protocol, the full diversity can be achieved since only the relay(s) that successfully decodes the message from the source re-encodes and retransmits the message to the destination [C3-7, C3-10, C3-11, C3-12, C3-13].

Consider a simple network with only one source-destination pair and a single relay. When the link between the source and relay is error-free, it is possible for the destination to combine two signals received from the source and relay to achieve a diversity order of two. However, it is impractical to have error-free source-relay link. As mentioned before, there is no performance improvement when the relay retransmits the erroneous bits. Hence, dealing with detection (or decoding) errors at the relay

becomes crucial. For example, an error detection code can be added at the source. Based on the decoding result in the first phase, the relay can decide to retransmit or remain silent in the second phase [C3-14, C3-15]. Another approach is based on the instantaneous SNR of the source-relay link. When the source-relay SNR is larger than a threshold, the probability of decoding error at the relay can be negligible and hence the relay retransmits the message [C3-7, C3-10, C3-11, C3-12, C3-13]. In [C3-16], a receiver has been designed to eliminate errors at the relay, which allows the relay to always forward the received data. In particular, a cooperative maximum-ratio-combining (C-MRC) detector was proposed at the destination to collect the full diversity order by taking into consideration the instantaneous BER of the source-relay link.

However, the use of error detection codes increases the processing complexity of the relay as well as the delay of the network. Using C-MRC detector is also complicated because the destination requires to know the instantaneous BER values of the source-relay link. Setting a threshold at the relay is clearly more practical. For this approach, references [C3-17, C3-18] derive the optimal threshold value for BPSK modulation to minimize the e2e BER. It was demonstrated that the e2e BER can be reduced significantly with the optimal threshold value.

An important consideration in many communication systems is the quality of services under a wide range of channel conditions. Typically, data can be divided into different important classes, which require different degrees of protection. In poor channel conditions, the receiver can recover the more important classes (known as basic or coarse data) with an acceptable BER while the less important classes (known as refinement or enhancement data) are only recovered in better channel conditions [C3-19, C3-20]. For example, multimedia data such as audio, images and video exhibit unequal sensitivity for different bits. It is wasteful if all of the bits are protected equally. In contrast, the unequal error protection (UEP) scheme protects the data according to the system requirements. The bit stream of the source data is divided into two or more groups and different protection levels are applied to these

groups.

A simple and practical way to achieve UEP is by using hierarchical modulations. Basically hierarchical modulations are those constellations with nonuniformly spaced signal points [C3-19, C3-20, C3-21, C3-22]. The basic idea in using hierarchical modulations is that the information bits are mapped onto nonuniform constellation points according to their importance. With such modulations, the more important bits are decoded with fewer errors than the less important bits. As a result, hierarchical modulations can offer variable degrees of error protection for the information bits. In the literature, although a large amount of research work related to UEP in point-to-point communications exists [C3-23, C3-24, C3-19, C3-20], only a few studies were devoted to UEP in cooperative networks. In particular, a relay communication system employing distributed turbo coding together with hierarchical modulation is studied in [C3-25]. The relay adjusts the modulation order based on the cyclic redundancy check (CRC) indication of the decoding result over the source-relay link. However, how to systematically choose the channel code, modulation, and allocate power between the source and relay are not discussed. Hierarchical modulation is also adopted in [C3-26] to broadcast the signals to multiple destinations. Higher destinations work as relays to lower destinations[1]. C-MRC is applied at each destination, which also means that each destination requires to know the BERs of all previous destinations. In [C3-27], the optimal distance parameters of the constellation are analyzed to minimize the BERs. The technique in [C3-26] is complicated. Moreover, the relay always reduces the size of the hierarchical constellation, which implies that the destination cannot exploit the full diversity for the less important class even though it can be correctly decoded at the relay. Regarding the approach in [C3-27], since the relay always retransmits the decoded bits, error propagation to the destination can happen as discussed before.

This work is also concerned with a cooperative network with hierarchical modula-

[1]A higher destination means a destination with a higher reception capability, i.e., the destination is able to reliably detect most of the transmitted bits.

tion for unequal error protection of information data. Two information classes with different levels of protection are transmitted from the source. The adaptive transmission protocol proposed at the relay is based on two thresholds as follows. After receiving the signal in the first phase from the source, the relay compares the instantaneous received SNR with the two thresholds to decide whether to retransmit both classes, or the more important class, or remain silent in the second phase. As such, the key difference of the protocol in this paper as compared to those in [C3-26, C3-27] is in the adaptive transmission at the relay in the second phase. In particular, how many and which bits are transmitted in the second phase in our protocol are determined by the channel quality of the source-relay links in the first phase. In contrast the relays always retransmit a predefined number of bits in [C3-26, C3-27].

For simplicity, we concentrate on the use of a hierarchical 2/4-ASK constellation at the source. At the relay, depending on the received instantaneous SNR, a hierarchical 2/4-ASK or 2-ASK constellation is employed. The BER for each information class is derived first. The use of optimal thresholds at the relay is then discussed to minimize the BER of the less protection class while the BER of the more protection class satisfies a given requirement[2]. It should be pointed out that the framework proposed here can be extended to a general hierarchical modulation (such as QAM) with many different classes. As an example, Appendix 3.C discusses the analysis with generalized hierarchical 4/16-QAM constellations[3]. It should also be mentioned that, although our system and analysis do not consider explicit channel coding, the developed framework and results could be applied to the coded bits corresponding to each information class (i.e., the error probability of the coded bits is considered

[2]It might also be of interest and straightforward to minimize the BER of the more protection class under some constraint on the BER of the less protection class. It should also be pointed out that our system model and analysis do not consider channel coding. If the channel coding is employed, the BER expressions will be different and deserve a further study.

[3]The analysis extension to a non-symmetric hierarchical modulation (such as the non-regular QAM used in ADSL and HDSL) is more tedious since the BER computation is much more complicated and no general expressions exist for an arbitrary modulation order.

instead of the error probability of the information bits).

The remainder of this paper is organized as follows. Section 3.2 describes the system model and presents the BER analysis for two information classes. Approximations of the BERs are presented in Section 3.3, which are used to conveniently optimize the threshold values in Section 3.4. Numerical and simulation results are presented in Section 3.5. Finally, Section 3.6 concludes the paper.

Notations: $\mathbb{E}_\gamma\{x\}$ is the expectation of $x(\gamma)$ with respect to the random variable γ. The conditional probability distribution function (pdf) of γ given Θ is denoted by $f_{\gamma|\Theta}(\gamma)$. $\mathcal{CN}(0,\sigma^2)$ denotes a circularly symmetric complex Gaussian random variable with variance σ^2. $P(\cdot)$ denotes the probability measure of some probability space $(\Omega,\mathcal{B})$ where Ω is the finite set and $\mathcal{B}$ is the sigma algebra generated by this set. The Q function is defined as $Q(x)=\int_x^\infty \frac{1}{\sqrt{2\pi}}\mathrm{e}^{-t^2/2}\mathrm{d}t$.

3.2 System Model and BER Analysis

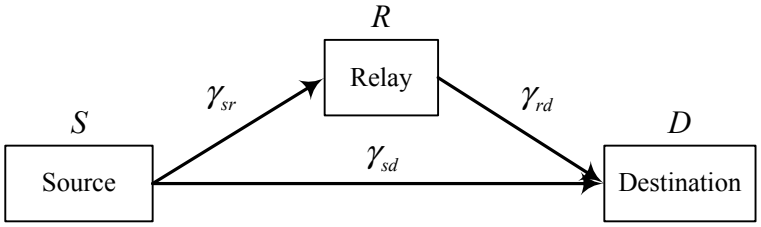

Figure 3.1 A simple wireless relay network.

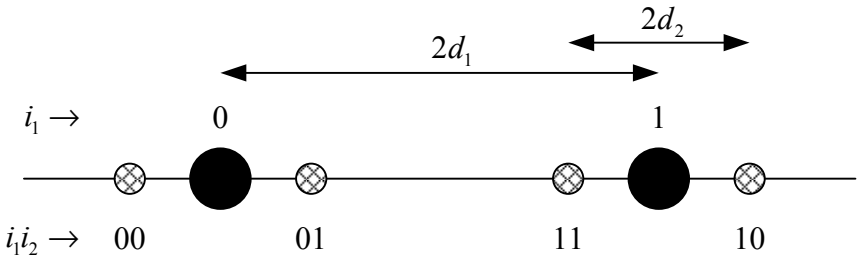

Figure 3.2 Generalized hierarchical 2/4-ASK constellation.

Fig. 3.1 illustrates a simple relay network with 3 nodes, in which a source node S sends information to a destination node D with the assistance of a relay node R. The information bits at S are modulated to symbol x_s by a hierarchical 2/4-ASK

constellation as shown in Fig. 3.2, where bit i_1 is more protected than bit i_2. The received signals at the relay and destination in the first phase can be written as

$$y_{\rm sr} = \sqrt{E_{\rm s}} h_{\rm sr} x_{\rm s} + n_{\rm sr} \tag{3.1}$$

$$y_{\rm sd} = \sqrt{E_{\rm s}} h_{\rm sd} x_{\rm s} + n_{\rm sd} \tag{3.2}$$

where $E_{\rm s}$ is the average symbol energy at the source, h_{ij} is the fading channel coefficient between node i and node j, where $i, j \in \{{\rm s}, {\rm r}, {\rm d}\}$. In this paper, we assume that the channel between any two nodes is Rayleigh flat fading, modeled as $\mathcal{CN}(0, \sigma_{ij}^2)$, where i, j refer to transmit and receive nodes, respectively. The noise components $(n_{\rm sr}, n_{\rm sd})$ at both the relay and destination are modeled as i.i.d. $\mathcal{CN}(0, N_0)$ random variables. Therefore the instantaneous received SNR for the transmission from node i to node j, denoted by γ_{ij}, is given as $\gamma_{ij} = E_i |h_{i,j}|^2 / N_0$. With Rayleigh fading, the pdf of γ_{ij} is exponential and given by $f_{ij}(\gamma_{ij}) = \frac{1}{\sigma_{ij}^2} {\rm e}^{-\gamma_{ij}/\sigma_{ij}^2}$, where σ_{ij}^2 is the average SNR of the i-j link.

Let the two thresholds employed at R be denoted by $\gamma_1^{\rm th}$ and $\gamma_2^{\rm th}$ where $\gamma_1^{\rm th} < \gamma_2^{\rm th}$. In the second phase, if the instantaneous received SNR at R satisfies $\gamma_{\rm sr} > \gamma_2^{\rm th}$, R decodes both bits and remodulates to $x_{\rm r}$ by the same hierarchical 2/4-ASK constellation as used in the source S. If $\gamma_1^{\rm th} < \gamma_{\rm sr} < \gamma_2^{\rm th}$, R decodes the important bit and remodulates to symbol $x_{\rm r}$ with a 2-ASK constellation. If $\gamma_{\rm sr} < \gamma_1^{\rm th}$, R remains silent. If the relay transmits, the received signal at the destination is given by

$$y_{\rm rd} = \sqrt{E_{\rm r}} h_{\rm rd} x_{\rm r} + n_{\rm rd}, \tag{3.3}$$

where $E_{\rm r}$ is the average energy per symbol sent by R, $h_{\rm rd}$ is the fading channel coefficient between R and D, and $n_{\rm rd}$ is the noise component at D in the second phase, also modeled as $\mathcal{CN}(0, N_0)$. Depending on what R transmits in the second phase, D combines the received signals in two phases and decodes.

It is assumed that the relay utilizes the CSI information of $\{\gamma_{\rm sr}, \sigma_{\rm rd}^2, \sigma_{\rm sd}^2\}$ to make the decision. Furthermore the destination knows exactly the behavior of the relay. In practice this can be done by having the relay send one flag bit to the destination

whenever there is a change in the reliability status of detection at the relay. It should be noted that the SNR-based selective relaying [C3-17, C3-18] also needs one bit to inform the state of the relay to the destination. As a result, the efficiency of our proposed scheme is similar to the SNR-based selective relaying (referred to as the one-threshold method in the discussion and comparison with our scheme in Section V). In general, the rate at which the relay needs to inform the destination about its new detection status depends on the fading rate of the source-relay channel.

To compute the average BERs of both bits i_1 (more protected bit) and i_2 (less protected bit), we first classify all different cases that result in different conditional BERs at the destination. The average BER of each information bit is then obtained by a corresponding weighted sum of these conditional BERs. Three major cases can be classified and parameterized by variable Θ as follows. The first case, $\Theta = 1$, is when $\gamma_{\rm sr} < \gamma_1^{\rm th}$. In this case the destination simply uses the received signal in the first phase to decode both bits i_1 and i_2. The second case, parameterized by $\Theta = 2$, corresponds to $\gamma_1^{\rm th} < \gamma_{\rm sr} < \gamma_2^{\rm th}$. In this case the destination combines two received signals in two phases to decode bit i_1 and uses the received signal in the first phase to decode bit i_2. Two different sub-cases, parameterized by $\Phi = \{1, 2\}$, can be further classified under $\Theta = 2$ depending on the correctness of the decoded bit i_1 at the relay. Lastly, the third case, $\Theta = 3$, happens if $\gamma_{\rm sr} > \gamma_2^{\rm th}$. Under $\Theta = 3$ the destination combines two received signals in two phases to decode both bits i_1 and i_2. Since the relay may decode either i_1 or i_2 incorrectly, four different sub-cases, parameterized by $\Phi = \{1, 2, 3, 4\}$, can be further separated under $\Theta = 3$. All seven different cases resulting from the above three major cases are summarized in Fig. 3.3.

Let[4] $P(\varepsilon_w, i_k, \Theta = j, \Phi = l)$ denote the BER of bit i_k at node w under case $\Theta = j$ and sub-case $\Phi = l$. With two given thresholds $\gamma_1^{\rm th}$ and $\gamma_2^{\rm th}$, the average BER for bit

[4]When a sub-case does not exist under $\Theta = 1$, $\Phi = l$ does not appear in the notation.

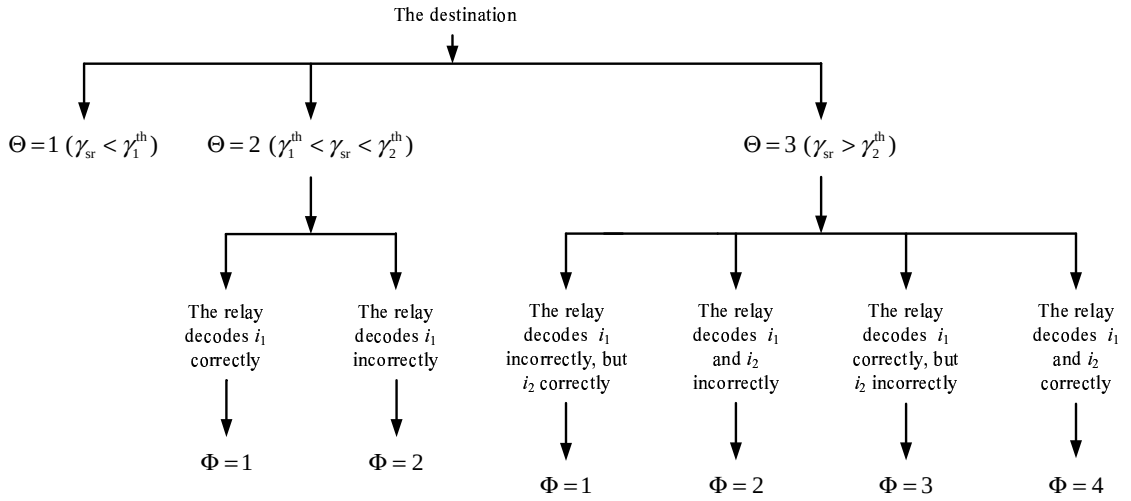

Figure 3.3 Seven different possible cases that result in different BERs at the destination.

i_k, where $k = 1, 2$, can be written as

$$\begin{aligned}
\mathrm{BER}(\gamma_1^{\mathrm{th}}, \gamma_2^{\mathrm{th}}, i_k) &= P(\varepsilon_{\mathrm{d}}, i_k, \Theta = 1) + \\
&\sum_{l=1}^{2} P(\varepsilon_{\mathrm{d}}, i_k, \Theta = 2, \Phi = l) + \sum_{l=1}^{4} P(\varepsilon_{\mathrm{d}}, i_k, \Theta = 3, \Phi = l) \\
&= P(\varepsilon_{\mathrm{d}}, i_k | \Theta = 1) P(\Theta = 1) + \\
&\sum_{l=1}^{2} P(\varepsilon_{\mathrm{d}}, i_k | \Theta = 2, \Phi = l) P(\Theta = 2 | \Phi = l) P(\Phi = l) + \\
&\sum_{l=1}^{4} P(\varepsilon_{\mathrm{d}}, i_k | \Theta = 3, \Phi = l) P(\Theta = 3 | \Phi = l) P(\Phi = l). \qquad (3.4)
\end{aligned}$$

All the terms in (3.4) are computed as follows.

3.2.1 Case 1 ($\Theta = 1$): $\gamma_{\mathrm{sr}} < \gamma_1^{\mathrm{th}}$

In this case, the instantaneous SNR of the S-R link is smaller than the threshold γ_1^{th}. Hence R remains silent in the second phase. D uses only the received signal in the first phase to decode both bits. Using the results in [C3-20, C3-26], the BERs conditioned on γ_{sd} for i_1 and i_2 are given, respectively, by

$$P(\varepsilon_{\mathrm{d}}, i_1 | \Theta = 1, \gamma_{\mathrm{sd}}) = \frac{1}{2} \left[Q\left(\frac{(\alpha + 1)\sqrt{2\gamma_{\mathrm{sd}}}}{\sqrt{\alpha^2 + 1}} \right) + Q\left(\frac{(\alpha - 1)\sqrt{2\gamma_{\mathrm{sd}}}}{\sqrt{\alpha^2 + 1}} \right) \right] \qquad (3.5)$$

$$P(\varepsilon_{\rm d}, i_2|\Theta=1,\gamma_{\rm sd}) = \frac{1}{2}\left[2Q\left(\frac{\sqrt{2\gamma_{\rm sd}}}{\sqrt{\alpha^2+1}}\right) - Q\left(\frac{(2\alpha+1)\sqrt{2\gamma_{\rm sd}}}{\sqrt{\alpha^2+1}}\right) + Q\left(\frac{(2\alpha-1)\sqrt{2\gamma_{\rm sd}}}{\sqrt{\alpha^2+1}}\right)\right]. \quad (3.6)$$

where $\alpha = \frac{d_1}{d_2}$, d_1 and d_2 are the two distance parameters of the hierarchical 2/4-ASK constellation as shown in Fig. 3.2.

The average BERs for i_1 and i_2 can be calculated by averaging the conditional BERs over $\gamma_{\rm sd}$. They are found to be [C3-20, C3-26]

$$\begin{aligned} P(\varepsilon_{\rm d}, i_1|\Theta=1) &= \mathbb{E}_{\gamma_{\rm sd}}\{P(\varepsilon_{\rm d}, i_1|\Theta=1,\gamma_{\rm sd})\} \\ &= \frac{1}{4}\left[2 - \sqrt{\frac{\frac{(\alpha+1)^2}{\alpha^2+1}\sigma_{\rm sd}^2}{1+\frac{(\alpha+1)^2}{\alpha^2+1}\sigma_{\rm sd}^2}} - \sqrt{\frac{\frac{(\alpha-1)^2}{\alpha^2+1}\sigma_{\rm sd}^2}{1+\frac{(\alpha-1)^2}{\alpha^2+1}\sigma_{\rm sd}^2}}\right] \end{aligned} \quad (3.7)$$

$$\begin{aligned} P(\varepsilon_{\rm d}, i_2|\Theta=1) &= \mathbb{E}_{\gamma_{\rm sd}}\{P(\varepsilon_{\rm d}, i_2|\Theta=1,\gamma_{\rm sd})\} \\ &= \frac{1}{4}\left[2 - 2\sqrt{\frac{\frac{1}{\alpha^2+1}\sigma_{\rm sd}^2}{1+\frac{1}{\alpha^2+1}\sigma_{\rm sd}^2}} + \sqrt{\frac{\frac{(2\alpha+1)^2}{\alpha^2+1}\sigma_{\rm sd}^2}{1+\frac{(2\alpha+1)^2}{\alpha^2+1}\sigma_{\rm sd}^2}} - \sqrt{\frac{\frac{(2\alpha-1)^2}{\alpha^2+1}\sigma_{\rm sd}^2}{1+\frac{(2\alpha-1)^2}{\alpha^2+1}\sigma_{\rm sd}^2}}\right] \end{aligned} \quad (3.8)$$

3.2.2 Case 2 ($\Theta = 2$): $\gamma_1^{\rm th} < \gamma_{\rm sr} < \gamma_2^{\rm th}$

In this case, since the instantaneous SNR of the S-R link is between thresholds $\gamma_1^{\rm th}$ and $\gamma_2^{\rm th}$, the relay decodes the first bit and remodulates the decoded bit as a 2-ASK signal. This is based on the expectation that the relay is likely to decode the first bit correctly, but the second bit incorrectly and hence only the first bit should be remodulated and sent to the destination. Note that there is still a probability of error in decoding the first bit at the relay. MRC method[5] is used at D to decode bit i_1. Meanwhile, only the signal received in the first phase at D is used to decode bit i_2.

[5]It should be pointed out that instead of MRC, equal-gain combining (EGC) or selection combining (SC) can also be employed. The comparison of MRC, EGC and SC methods is beyond the scope of this paper and the interested reader is referred to [C3-28] for a similar framework and analysis with SC.

When the first bit is correctly decoded at the relay, i.e., $\Phi = 1$, the BERs of i_1 and i_2 at the destination can be calculated as (see Appendix 3.A):

$$P(\varepsilon_{\rm d}, i_1|\Theta = 2, \Phi = 1) = \frac{1}{2}\left[J_1\left(\frac{\alpha+1}{\sqrt{\alpha^2+1}}, 1\right) + J_1\left(\frac{\alpha-1}{\sqrt{\alpha^2+1}}, 1\right)\right], \tag{3.9}$$

where

$$J_1(\mu,\nu) = \int_0^\infty \int_0^\infty Q\left(\frac{\mu\gamma_{\rm sd} + \nu\gamma_{\rm rd}}{\sqrt{(\gamma_{\rm sd}+\gamma_{\rm rd})/2}}\right) \frac{1}{\sigma_{\rm sd}^2\sigma_{\rm rd}^2} {\rm e}^{-\gamma_{\rm sd}/\sigma_{\rm sd}^2} {\rm e}^{-\gamma_{\rm rd}/\sigma_{\rm rd}^2} {\rm d}\gamma_{\rm sd}{\rm d}\gamma_{\rm rd} \tag{3.10}$$

and

$$P(\varepsilon_{\rm d}, i_2|\Theta = 2, \Phi = 1) = \frac{1}{4}\left\{2 - 2\sqrt{\frac{\frac{1}{\alpha^2+1}\sigma_{\rm sd}^2}{1+\frac{1}{\alpha^2+1}\sigma_{\rm sd}^2}} + \sqrt{\frac{\frac{(2\alpha+1)^2}{\alpha^2+1}\sigma_{\rm sd}^2}{1+\frac{(2\alpha+1)^2}{\alpha^2+1}\sigma_{\rm sd}^2}} - \sqrt{\frac{\frac{(2\alpha-1)^2}{\alpha^2+1}\sigma_{\rm sd}^2}{1+\frac{(2\alpha-1)^2}{\alpha^2+1}\sigma_{\rm sd}^2}}\right\} \tag{3.11}$$

When the first bit is wrongly decoded at the relay, i.e., $\Phi = 2$, the BER of i_1 is given by (see Appendix 3.A)

$$P(\varepsilon_{\rm d}, i_1|\Theta = 2, \Phi = 2) = \frac{1}{2}\left[J_2\left(\frac{\alpha+1}{\sqrt{\alpha^2+1}}, 1\right) + J_2\left(\frac{\alpha-1}{\sqrt{\alpha^2+1}}, 1\right)\right], \tag{3.12}$$

where

$$J_2(\mu,\nu) = \int_0^\infty \int_0^\infty Q\left(\frac{\mu\gamma_{\rm sd} - \nu\gamma_{\rm rd}}{\sqrt{(\gamma_{\rm sd}+\gamma_{\rm rd})/2}}\right) \frac{1}{\sigma_{\rm sd}^2\sigma_{\rm rd}^2} {\rm e}^{-\gamma_{\rm sd}/\sigma_{\rm sd}^2} {\rm e}^{-\gamma_{\rm rd}/\sigma_{\rm rd}^2} {\rm d}\gamma_{\rm sd}{\rm d}\gamma_{\rm rd}. \tag{3.13}$$

The BER of i_2 does not change in this case, i.e.,

$$P(\varepsilon_{\rm d}, i_2|\Theta = 2, \Phi = 1) = P(\varepsilon_{\rm d}, i_2|\Theta = 2, \Phi = 2) = P(\varepsilon_{\rm d}, i_2|\Theta = 1) \tag{3.14}$$

3.2.3 Case 3 ($\Theta = 3$): $\gamma_{\rm sr} > \gamma_2^{\rm th}$

In this case, the instantaneous SNR of the S-R link is larger than a threshold $\gamma_2^{\rm th}$. The relay decodes both bits and remodulates by using a hierarchical 2/4-ASK constellation as done in the source. Since $\gamma_{\rm sr} > \gamma_2^{\rm th}$, it is likely that both bits are decoded correctly. However, errors can still happen. All sub-cases are considered as follows.

In the first sub-case ($\Phi = 1$), the relay decodes the first bit incorrectly, but correctly decodes the second bit, the BERs of i_1 and i_2 are given, respectively, by (see Appendix 3.B)

$$P(\varepsilon_{\mathrm{d}}, i_1|\Theta = 3, \Phi = 1) = \frac{1}{2}\left[J_2\left(\frac{\alpha+1}{\sqrt{\alpha^2+1}}, \frac{\alpha+1}{\sqrt{\alpha^2+1}}\right) + J_2\left(\frac{\alpha-1}{\sqrt{\alpha^2+1}}, \frac{\alpha-1}{\sqrt{\alpha^2+1}}\right)\right], \tag{3.15}$$

$$P(\varepsilon_{\mathrm{d}}, i_2|\Theta = 3, \Phi = 1) = \frac{1}{2}\left[J_2\left(\frac{1}{\sqrt{\alpha^2+1}}, \frac{2\alpha+1}{\sqrt{\alpha^2+1}}\right) - J_2\left(\frac{2\alpha+1}{\sqrt{\alpha^2+1}}, \frac{1}{\sqrt{\alpha^2+1}}\right) + J_1\left(\frac{1}{\sqrt{\alpha^2+1}}, \frac{2\alpha-1}{\sqrt{\alpha^2+1}}\right) + J_1\left(\frac{2\alpha-1}{\sqrt{\alpha^2+1}}, \frac{1}{\sqrt{\alpha^2+1}}\right)\right]. \tag{3.16}$$

In the second sub-case ($\Phi = 2$), the relay decodes incorrectly both bits, the BERs of i_1 and i_2 are

$$P(\varepsilon_{\mathrm{d}}, i_1|\Theta = 3, \Phi = 2) = \frac{1}{2}\left[J_2\left(\frac{\alpha+1}{\sqrt{\alpha^2+1}}, \frac{\alpha-1}{\sqrt{\alpha^2+1}}\right) + J_2\left(\frac{\alpha-1}{\sqrt{\alpha^2+1}}, \frac{\alpha+1}{\sqrt{\alpha^2+1}}\right)\right], \tag{3.17}$$

$$P(\varepsilon_{\mathrm{d}}, i_2|\Theta = 3, \Phi = 2) = \frac{1}{2}\left[J_2\left(\frac{1}{\sqrt{\alpha^2+1}}, \frac{2\alpha-1}{\sqrt{\alpha^2+1}}\right) - J_1\left(\frac{2\alpha+1}{\sqrt{\alpha^2+1}}, \frac{1}{\sqrt{\alpha^2+1}}\right) + J_1\left(\frac{1}{\sqrt{\alpha^2+1}}, \frac{2\alpha+1}{\sqrt{\alpha^2+1}}\right) + J_2\left(\frac{2\alpha-1}{\sqrt{\alpha^2+1}}, \frac{1}{\sqrt{\alpha^2+1}}\right)\right] \tag{3.18}$$

In the third sub-case ($\Phi = 3$), the relay decodes the first bit correctly, but the second bit incorrectly, the BERs of i_1 and i_2 are

$$P(\varepsilon_{\mathrm{d}}, i_1|\Theta = 3, \Phi = 3) = \frac{1}{2}\left[J_1\left(\frac{\alpha+1}{\sqrt{\alpha^2+1}}, \frac{\alpha-1}{\sqrt{\alpha^2+1}}\right) + J_1\left(\frac{\alpha-1}{\sqrt{\alpha^2+1}}, \frac{\alpha+1}{\sqrt{\alpha^2+1}}\right)\right], \tag{3.19}$$

$$P(\varepsilon_{\mathrm{d}}, i_2|\Theta = 3, \Phi = 3) = \frac{1}{2}\left[2J_2\left(\frac{1}{\sqrt{\alpha^2+1}}, \frac{1}{\sqrt{\alpha^2+1}}\right) + J_1\left(\frac{2\alpha+1}{\sqrt{\alpha^2+1}}, \frac{2\alpha-1}{\sqrt{\alpha^2+1}}\right) + J_1\left(\frac{2\alpha-1}{\sqrt{\alpha^2+1}}, \frac{2\alpha+1}{\sqrt{\alpha^2+1}}\right)\right]. \tag{3.20}$$

Finally, in the fourth sub-case ($\Phi = 4$), both bits are correctly decoded at the relay, the BERs of i_1 and i_2 are

$$P(\varepsilon_{\rm d}, i_1|\Theta = 3, \Phi = 4) = \frac{1}{2}\left[J_1\left(\frac{\alpha+1}{\sqrt{\alpha^2+1}}, \frac{\alpha+1}{\sqrt{\alpha^2+1}}\right) + J_1\left(\frac{\alpha-1}{\sqrt{\alpha^2+1}}, \frac{\alpha-1}{\sqrt{\alpha^2+1}}\right)\right], \quad (3.21)$$

$$P(\varepsilon_{\rm d}, i_2|\Theta = 3, \Phi = 4) = \frac{1}{2}\left[2J_2\left(\frac{1}{\sqrt{\alpha^2+1}}, \frac{1}{\sqrt{\alpha^2+1}}\right) + J_1\left(\frac{2\alpha+1}{\sqrt{\alpha^2+1}}, \frac{2\alpha+1}{\sqrt{\alpha^2+1}}\right) + J_1\left(\frac{2\alpha-1}{\sqrt{\alpha^2+1}}, \frac{2\alpha-1}{\sqrt{\alpha^2+1}}\right)\right] \quad (3.22)$$

Furthermore, the expectations over random variables $\gamma_{\rm sd}$ and $\gamma_{\rm rd}$ in (3.21) and (3.22) can be evaluated explicitly (see (3.66) of Appendix 3.B).

3.2.4 Other Computations

Since the channel between S and R is Rayleigh flat fading, $\gamma_{\rm sr}$ is an exponential random variable with mean $\sigma_{\rm sr}^2$. One has

$$P(\Theta = 1) = P(\gamma_{\rm sr} \le \gamma_1^{\rm th}) = 1 - {\rm e}^{-\gamma_1^{\rm th}/\sigma_{\rm sr}^2} \quad (3.23)$$

$$P(\Theta = 2) = P(\gamma_1^{\rm th} < \gamma_{\rm sr} \le \gamma_2^{\rm th}) = {\rm e}^{-\gamma_1^{\rm th}/\sigma_{\rm sr}^2} - {\rm e}^{-\gamma_2^{\rm th}/\sigma_{\rm sr}^2} \quad (3.24)$$

$$P(\Theta = 3) = P(\gamma_{\rm sr} > \gamma_2^{\rm th}) = {\rm e}^{-\gamma_2^{\rm th}/\sigma_{\rm sr}^2} \quad (3.25)$$

To compute (3.4), we also need to calculate the BERs of i_1 and i_2 at the relay. It can be verified that

$$f_{\gamma_{\rm sr}|\Theta=1}(\gamma_{\rm sr}) = \frac{1}{1 - {\rm e}^{-\gamma_1^{\rm th}/\sigma_{\rm sr}^2}} \frac{{\rm e}^{-\gamma_{\rm sr}/\sigma_{\rm sr}^2}}{\sigma_{\rm sr}^2} \quad (3.26)$$

$$f_{\gamma_{\rm sr}|\Theta=2}(\gamma_{\rm sr}) = \frac{1}{{\rm e}^{-\gamma_1^{\rm th}/\sigma_{\rm sr}^2} - {\rm e}^{-\gamma_2^{\rm th}/\sigma_{\rm sr}^2}} \frac{{\rm e}^{-\gamma_{\rm sr}/\sigma_{\rm sr}^2}}{\sigma_{\rm sr}^2} \quad (3.27)$$

$$f_{\gamma_{\rm sr}|\Theta=3}(\gamma_{\rm sr}) = \frac{1}{\sigma_{\rm sr}^2} {\rm e}^{\gamma_2^{\rm th}/\sigma_{\rm sr}^2} {\rm e}^{-\gamma_{\rm sr}/\sigma_{\rm sr}^2} \quad (3.28)$$

Using [C3-29], [C3-30, Eq. 3.361.1][6], the average BERs of i_1 at the relay when $\Theta = 2$ can be found as follows:

$$P(\varepsilon_{\rm r}, i_1|\Theta = 2) = \frac{1}{{\rm e}^{-\gamma_1^{\rm th}/\sigma_{\rm sr}^2} - {\rm e}^{-\gamma_2^{\rm th}/\sigma_{\rm sr}^2}} \frac{1}{2\sigma_{\rm sr}^2} \times \int_{\gamma_1^{\rm th}}^{\gamma_2^{\rm th}} \left\{ Q\left(\frac{(\alpha+1)\sqrt{2\gamma_{\rm sr}}}{\sqrt{\alpha^2+1}} \right) + Q\left(\frac{(\alpha-1)\sqrt{2\gamma_{\rm sr}}}{\sqrt{\alpha^2+1}} \right) \right\} \times {\rm e}^{-\gamma_{\rm sr}/\sigma_{\rm sr}^2} {\rm d}\gamma_{\rm sr} = \frac{1}{2} \frac{1}{{\rm e}^{-\gamma_1^{\rm th}/\sigma_{\rm sr}^2} - {\rm e}^{-\gamma_2^{\rm th}/\sigma_{\rm sr}^2}} \times \left\{ I\left(\frac{2(\alpha+1)^2}{\alpha^2+1}, \sigma_{\rm sr}^2, \gamma_1^{\rm th} \right) - I\left(\frac{2(\alpha-1)^2}{\alpha^2+1}, \sigma_{\rm sr}^2, \gamma_2^{\rm th} \right) + I\left(\frac{2(\alpha+1)^2}{\alpha^2+1}, \sigma_{\rm sr}^2, \gamma_1^{\rm th} \right) - I\left(\frac{2(\alpha-1)^2}{\alpha^2+1}, \sigma_{\rm sr}^2, \gamma_2^{\rm th} \right) \right\}, \quad (3.29)$$

where

$$I(a, \sigma^2, x) = \int_x^\infty Q(\sqrt{at}) \frac{{\rm e}^{-t/\sigma^2}}{\sigma^2} {\rm d}t = {\rm e}^{-x/\sigma^2} Q\left(\sqrt{ax}\right) - \sqrt{\frac{a}{\frac{2}{\sigma^2}+a}} Q\left(\sqrt{x\left(\frac{2}{\sigma^2}+a\right)} \right). \quad (3.30)$$

Similarly, the average BERs of i_1 and i_2 at the relay when $\Theta = 3$ can be found as

$$P(\varepsilon_{\rm r}, i_1|\Theta = 3) = \frac{{\rm e}^{\gamma_2^{\rm th}/\sigma_{\rm sr}^2}}{2\sigma_{\rm sr}^2} \int_{\gamma_2^{\rm th}}^\infty \left\{ Q\left(\frac{(\alpha+1)\sqrt{2\gamma_{\rm sr}}}{\sqrt{\alpha^2+1}} \right) + Q\left(\frac{(\alpha-1)\sqrt{2\gamma_{\rm sr}}}{\sqrt{\alpha^2+1}} \right) \right\} {\rm e}^{-\gamma_{\rm sr}/\sigma_{\rm sr}^2} {\rm d}\gamma_{\rm sr} = \frac{{\rm e}^{\gamma_2^{\rm th}/\sigma_{\rm sr}^2}}{2} \times \left\{ I\left(\frac{2(\alpha+1)^2}{\alpha^2+1}, \sigma_{\rm sr}^2, \gamma_2^{\rm th} \right) - I\left(\frac{2(\alpha-1)^2}{\alpha^2+1}, \sigma_{\rm sr}^2, \gamma_2^{\rm th} \right) \right\}, \quad (3.31)$$

$$P(\varepsilon_{\rm r}, i_2|\Theta = 3) = \frac{{\rm e}^{\gamma_2^{\rm th}/\sigma_{\rm sr}^2}}{4\sigma_{\rm sr}^2} \int_{\gamma_2^{\rm th}}^\infty \left\{ 4Q\left(\frac{\sqrt{2\gamma_{\rm sd}}}{\sqrt{\alpha^2+1}} \right) - 2Q\left(\frac{(2\alpha+1)\sqrt{2\gamma_{\rm sd}}}{\sqrt{\alpha^2+1}} \right) + 2Q\left(\frac{(2\alpha-1)\sqrt{2\gamma_{\rm sd}}}{\sqrt{\alpha^2+1}} \right) \right\} \times {\rm e}^{-\gamma_{\rm sr}/\sigma_{\rm sr}^2} {\rm d}\gamma_{\rm sr} = \frac{{\rm e}^{\gamma_2^{\rm th}/\sigma_{\rm sr}^2}}{2} \left\{ 2I\left(\frac{2}{\alpha^2+1}, \sigma_{\rm sr}^2, \gamma_2^{\rm th} \right) - I\left(\frac{2(2\alpha+1)^2}{\alpha^2+1}, \sigma_{\rm sr}^2, \gamma_2^{\rm th} \right) + I\left(\frac{2(2\alpha-1)^2}{\alpha^2+1}, \sigma_{\rm sr}^2, \gamma_2^{\rm th} \right) \right\}. \quad (3.32)$$

[6]We should mention here that the average BERs of i_1 and i_2 at the relay given $\Theta = 1$ do not need to be calculated.

Finally, the remaining computations required in (3.4) are as follows:

$$P(\Phi = 1|\Theta = 2) = 1 - P(\varepsilon_{\mathrm{r}}, i_1|\Theta = 2) \tag{3.33}$$

$$P(\Phi = 2|\Theta = 2) = P(\varepsilon_{\mathrm{r}}, i_1|\Theta = 2) \tag{3.34}$$

$$P(\Phi = 1|\Theta = 3) = P(\varepsilon_{\mathrm{r}}, i_1|\Theta = 3)\left[1 - P(\varepsilon_{\mathrm{r}}, i_2|\Theta = 3)\right] \tag{3.35}$$

$$P(\Phi = 2|\Theta = 3) = P(\varepsilon_{\mathrm{r}}, i_1|\Theta = 3)P(\varepsilon_{\mathrm{r}}, i_2|\Theta = 3) \tag{3.36}$$

$$P(\Phi = 3|\Theta = 3) = \left[1 - P(\varepsilon_{\mathrm{r}}, i_1|\Theta = 3)\right]P(\varepsilon_{\mathrm{r}}, i_2|\Theta = 3) \tag{3.37}$$

$$P(\Phi = 4|\Theta = 3) = \left[1 - P(\varepsilon_{\mathrm{r}}, i_1|\Theta = 3)\right]\left[1 - P(\varepsilon_{\mathrm{r}}, i_2|\Theta = 3)\right] \tag{3.38}$$

where $P(\Phi = l|\Theta = k)$ denotes the probability of occurrence of sub-case $\Phi = l$ given the case $\Theta = k$.

To summarize, the final expressions of the average e2e BERs of two information classes have been formulated in (3.4). These expressions can be computed by substituting in Equations (3.7)–(3.25), (3.29)–(3.38). Note that all the expressions can be calculated analytically, except the integrals in (3.15) to (3.20), which need to be numerically evaluated. Based on the average e2e BERs, the optimal threshold values shall be chosen to minimize the average e2e BER of the second class while making sure that the average e2e BER of the first class meets a given requirement. The optimization problem can be extended to include the distance parameters and this is illustrated in Section 3.4. While the above-mentioned optimization problems are interesting and appealing, finding the solutions is challenging due to the complicated expressions of the e2e BERs. To overcome this difficulty, we propose to work with the asymptotic approximations of the BERs as presented in the next section.

3.3 Approximations of Asymptotic BERs

The approximate expressions are given to calculate the probability of errors given in (3.9), (3.12) and from (3.15) to (3.20). First, we deal with the two expressions $J_1(\mu, \nu)$ and $J_2(\mu, \nu)$ in (3.10) and (3.13), respectively, where $\mu > 0$ and $\nu > 0$. The expression in (3.10) is invoked when the relay forwards a correctly decoded bit to the

destination. The destination combines two signals using MRC and decodes. There is no error propagation in this case. With high SNR, it is expected that the destination decodes the bit with a very small probability of error. The second expression in (3.13) applies when the relay forwards an incorrect bit to the destination. Normally, the *R-D* link has a stronger impact on the decision at the destination than the *S-D* link. Therefore, one can approximate the error probability in (3.13) by the probability of $(\mu\gamma_{\rm sd} - \nu\gamma_{\rm rd}) < 0$ [C3-17]. Since $\gamma_{\rm sd}$ and $\gamma_{\rm rd}$ are independent, one has

$$J_2(\mu,\nu) \approx \int_0^{\infty}\int_0^{\frac{\nu}{\mu}\gamma_{\rm rd}} \frac{1}{\sigma_{\rm sd}^2\sigma_{\rm rd}^2} \mathrm{e}^{-\gamma_{\rm sd}/\sigma_{\rm sd}^2}\mathrm{e}^{-\gamma_{\rm rd}/\sigma_{\rm rd}^2}\mathrm{d}\gamma_{\rm sd}\mathrm{d}\gamma_{\rm rd} = \frac{\nu\sigma_{\rm rd}^2}{\mu\sigma_{\rm sd}^2 + \nu\sigma_{\rm rd}^2}. \tag{3.39}$$

On the other hand, Equation (3.12) can be approximated as:

$$\begin{aligned} P(\varepsilon_{\rm d}, i_1|\Theta=2,\Phi=2) &= \frac{1}{2}\left[J_2\left(\frac{\alpha+1}{\sqrt{\alpha^2+1}},1\right) + J_2\left(\frac{\alpha-1}{\sqrt{\alpha^2+1}},1\right)\right] \\ &\approx \frac{1}{2}\left(\frac{\sigma_{\rm rd}^2}{\frac{\alpha+1}{\sqrt{\alpha^2+1}}\sigma_{\rm sd}^2+\sigma_{\rm rd}^2} + \frac{\sigma_{\rm rd}^2}{\frac{\alpha-1}{\sqrt{\alpha^2+1}}\sigma_{\rm sd}^2+\sigma_{\rm rd}^2}\right). \end{aligned} \tag{3.40}$$

Similarly, since $J_1(\mu,\nu)$ is very small compared to $J_2(\mu,\nu)$ and can be neglected, other BER expressions of i_1 and i_2 can be approximated as follows:

$$P(\varepsilon_{\rm d}, i_1|\Theta=3,\Phi=1) \approx \frac{\sigma_{\rm rd}^2}{\sigma_{\rm sd}^2+\sigma_{\rm rd}^2} \tag{3.41}$$

$$P(\varepsilon_{\rm d}, i_2|\Theta=3,\Phi=1) \approx \frac{1}{2}\left[\frac{(2\alpha+1)\sigma_{\rm rd}^2}{\sigma_{\rm sd}^2+(2\alpha+1)\sigma_{\rm rd}^2} - \frac{\sigma_{\rm rd}^2}{(2\alpha+1)\sigma_{\rm sd}^2+\sigma_{\rm rd}^2}\right] \tag{3.42}$$

$$\begin{aligned} P(\varepsilon_{\rm d}, i_1|\Theta=3,\Phi=2) \approx \frac{1}{2}\Bigg[&\frac{(\alpha-1)\sigma_{\rm rd}^2}{(\alpha+1)\sigma_{\rm sd}^2+(\alpha-1)\sigma_{\rm rd}^2} \\ &+\frac{(\alpha+1)\sigma_{\rm rd}^2}{(\alpha-1)\sigma_{\rm sd}^2+(\alpha+1)\sigma_{\rm rd}^2}\Bigg] \end{aligned} \tag{3.43}$$

$$P(\varepsilon_{\rm d}, i_2|\Theta=3,\Phi=2) \approx \frac{1}{2}\left[\frac{(2\alpha-1)\sigma_{\rm rd}^2}{\sigma_{\rm sd}^2+(2\alpha-1)\sigma_{\rm rd}^2} + \frac{\sigma_{\rm rd}^2}{(2\alpha-1)\sigma_{\rm sd}^2+\sigma_{\rm rd}^2}\right] \tag{3.44}$$

$$P(\varepsilon_{\rm d}, i_2|\Theta=3,\Phi=3) \approx \frac{\sigma_{\rm rd}^2}{\sigma_{\rm sd}^2+\sigma_{\rm rd}^2} \tag{3.45}$$

Next, we shall approximate $P(\varepsilon_{\rm d}, i_1|\Theta=2,\Phi=1)$ and $P(\varepsilon_{\rm d}, i_1|\Theta=3,\Phi=3)$ in order to compute the average BER of i_1 in (3.4). Consider the following terms

corresponding to the BER expression of i_1 in (3.4):

$$K_2 = \sum_{l=1}^{2} P(\Theta = 2)P(\Phi = l|\Theta = 2)P(\varepsilon_{\rm d}, i_1|\Theta = 2, \Phi = k), \tag{3.46}$$

and

$$K_3 = \sum_{l=1}^{4} P(\Theta = 3)P(\Phi = l|\Theta = 3)P(\varepsilon_{\rm d}, i_1|\Theta = 3, \Phi = k) \tag{3.47}$$

For K_2, with a sufficient high SNR, it can be seen that[7] $P(\varepsilon_{\rm d}, i_1|\Theta = 2, \Phi = 1) = O(\text{SNR}^{-2})$, $P(\Phi = 2|\Theta = 2) = O(\text{SNR}^{-1})$, while $P(\varepsilon_{\rm d}, i_1|\Theta = 2, \Phi = 2)$ is given as in (3.40). Therefore, the dominant component in K_2 is $P(\Theta = 2)P(\Phi = 2|\Theta = 2)P(\varepsilon_{\rm d}, i_1|\Theta = 2, \Phi = 2)$ and we can ignore $P(\varepsilon_{\rm d}, i_1|\Theta = 2, \Phi = 1)$. Similarly, for the computation of K_3, one can approximate $P(\varepsilon_{\rm d}, i_1|\Theta = 3, \Phi = 3) \approx 0$.

The accuracy of the above approximations shall be verified in Section 3.5 by comparing them with the exact expressions obtained in Section 3.2.

3.4 Optimum SNR Thresholds

As mentioned before, with the approximate expressions of the average e2e BERs of two bits i_1 and i_2, one can choose the optimal thresholds to minimize the BER of the less protected bit i_2 when the BER of the more protected bit i_1 meets a given requirement. This type of UEP design is considered in different broadcasting and multimedia applications [C3-22, C3-24, C3-27]. The optimization problem can be set up as follows:

$$(\widehat{\gamma}_1^{\rm th}, \widehat{\gamma}_2^{\rm th}) = \arg \min_{(\gamma_1^{\rm th}, \gamma_2^{\rm th})} \text{BER}(\gamma_1^{\rm th}, \gamma_2^{\rm th}, i_2)$$
$$\text{subject to } \begin{cases} \text{BER}(\gamma_1^{\rm th}, \gamma_2^{\rm th}, i_1) \le \text{BER}_1 \\ 0 \le \gamma_1^{\rm th} \le \gamma_2^{\rm th} \end{cases} \tag{3.48}$$

where BER_1 is the BER requirement of the more protected information class.

The distance parameters can also be considered jointly with the thresholds in the

[7] With two positive real functions $f(x)$ and $g(x)$, we say $f(x) = O(g(x))$ if $\limsup_{x\to\infty} \frac{f(x)}{g(x)} < \infty$.

optimization problem. In this case, the optimization problem can be stated as follows:

$$(\widehat{\gamma}_1^{\text{th}}, \widehat{\gamma}_2^{\text{th}}, \widehat{\alpha}) = \arg \min_{(\gamma_1^{\text{th}}, \gamma_2^{\text{th}}, \alpha)} \text{BER}(\gamma_1^{\text{th}}, \gamma_2^{\text{th}}, \alpha, i_2)$$
$$\text{subject to } \begin{cases} \text{BER}(\gamma_1^{\text{th}}, \gamma_2^{\text{th}}, \alpha, i_1) \leq \text{BER}_1, \\ 0 \leq \gamma_1^{\text{th}} \leq \gamma_2^{\text{th}}. \end{cases} \tag{3.49}$$

The above problems can be solved by some optimization techniques such as the augmented Lagrange method [C3-31] since the average e2e BER formulas of two bits i_1 and i_2 have been set up. Here the optimization problems in (3.48) and (3.49) are solved by using the MATLAB Optimization Toolbox[8]. Since it is difficult to prove the cost functions to be convex or not[9], to have a good confidence in the numerical results, the optimization problems are solved with many initial conditions and the best value is retained. Furthermore, it should be noted that the average BERs formulated in (3.4) only require information on the average SNRs of the source-destination, source-relay, and relay-destination links. The optimization problems can therefore be solved off-line for typical sets of average SNRs and the obtained optimal thresholds and/or distance parameters are stored in a look-up table.

3.5 Simulation Results

This section presents analytical and simulation results to confirm the analysis of the average e2e BERs of two different classes. Moreover, the BER performances with approximations are provided to illustrate the accuracy of the approximations made. In all simulations, transmitted powers are set to be the same for the source and the relay (i.e., $E_{\text{s}} = E_{\text{r}}$). The noise components at both the source and relay are modeled

[8]Specifically, we have used the routine "fmincon", which is designed to find the minimum of a given constrained nonlinear multivariate function. The exact complexity analysis of this routine requires expressions of the gradients and Hessian of the objective function, which are unfortunately not available. However, in general, the complexity would be $O(n^3)$, where n is the number of variables. Since our optimization problems involve only small numbers of variables, the complexity of the numerical optimization procedure is low.

[9]It is expected that the cost functions are convex.

as i.i.d. $\mathcal{CN}(0,1)$ random variables. The average SNR of link i-j is represented by $\sigma_{ij}^2 = \lambda_{ij} E_i / N_0$ where λ_{ij} is a scaling factor to reflect different distances among nodes. We also use the *normalized* thresholds λ_1^{th} and λ_2^{th} to represent the actual thresholds as $\gamma_1^{\text{th}} = \lambda_1^{\text{th}} E_{\text{s}} / N_0$ and $\gamma_2^{\text{th}} = \lambda_2^{\text{th}} E_{\text{s}} / N_0$. Unless stated otherwise, we simply refer to *normalized* thresholds as thresholds in the following discussion.

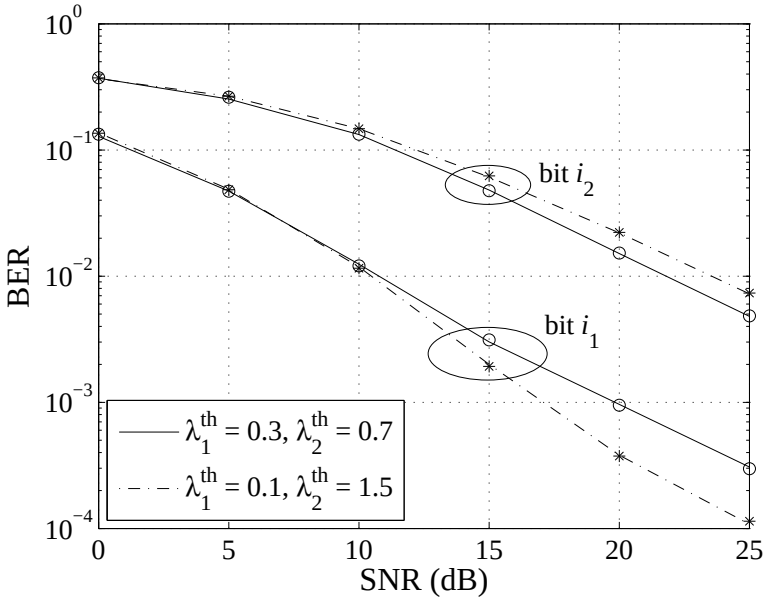

Figure 3.4 BERs of i_1 and i_2 when $\lambda_{\text{sr}} = \lambda_{\text{rd}} = \lambda_{\text{sd}} = 1$. Simulation results are shown in lines and exact analytical values are shown as marker symbols.

Figs. 3.4 and 3.5 plot the BERs of i_1 and i_2 at the destination for different values of thresholds λ_1^{th} and λ_2^{th}. Here $\alpha = 1/0.3$, $\lambda_{\text{sr}} = \lambda_{\text{rd}} = \lambda_{\text{sd}} = 1$ for Fig. 3.4, and $\lambda_{\text{sr}} = \lambda_{\text{rd}} = 10\lambda_{\text{sd}} = 1$ for Fig. 3.5. The figures show that the exact analytical and simulation results are basically the same. The exact analytical results are obtained with numerical integrations of (3.9), (3.12), and (3.15)−(3.20). Similarly, Fig. 3.6 compares the BER performances at various channel conditions with approximate analytical and simulation results. Observe that over the whole SNR range, the approximations are very accurate. Therefore the approximations provide a useful tool in calculating the e2e BERs for both bits as well as to optimize the relaying thresholds and distance parameters.

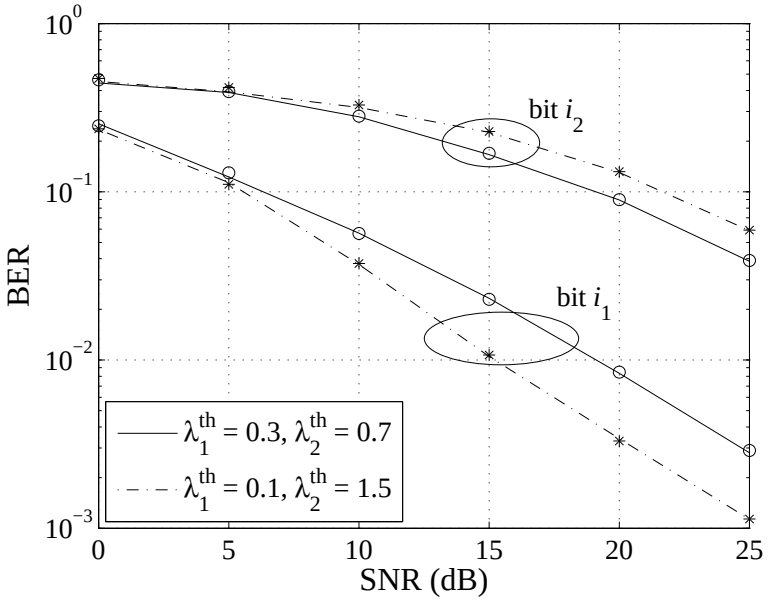

Figure 3.5 BERs of i_1 and i_2 when $\lambda_{\rm sr} = \lambda_{\rm rd} = 10\lambda_{\rm sd} = 1$. Simulation results are shown in lines and exact analytical values are shown as marker symbols.

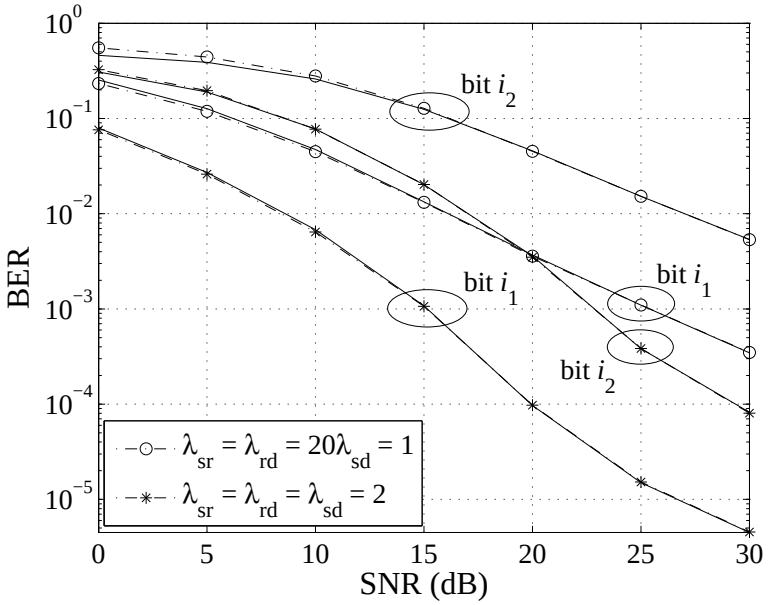

Figure 3.6 BERs of i_1 and i_2 when $\lambda_1^{\rm th} = 0.05$, $\lambda_2^{\rm th} = 0.1$ and $\alpha = 1/0.3$. Simulation results are shown in solid lines and approximate analytical values are shown in dashed lines.

Next, Fig. 3.7 shows the BERs of i_1 and i_2 obtained by simulation for one-

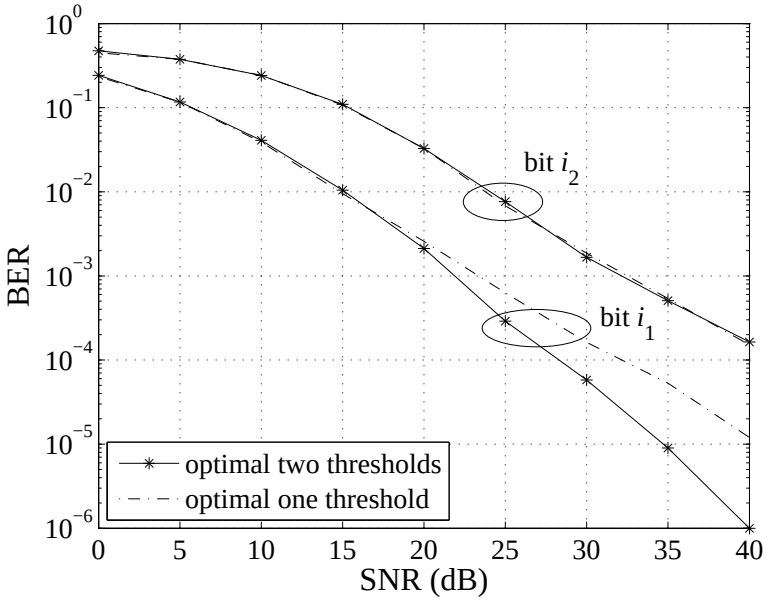

Figure 3.7 BERs of i_1 and i_2 for optimal one-threshold ($\{\lambda_1^{\text{th}} = \lambda_2^{\text{th}} = 0.055\}$) and two-threshold ($\{\lambda_1^{\text{th}} = 0.009, \lambda_2^{\text{th}} = 0.055\}$) methods when $\lambda_{\text{sr}} = \lambda_{\text{rd}} = 10\lambda_{\text{sd}} = 1$ and $\alpha = 1/0.3$.

threshold and two-threshold methods. With the one-threshold method, the relay retransmits both bits received in the first phase during the second phase when the instantaneous received SNR at the relay is larger than a threshold value. Otherwise, the relay remains silent. Matlab Optimization Toolbox is also used to obtain the optimal threshold for this method. The obtained optimal threshold values are $\{\lambda_1^{\text{th}} = \lambda_2^{\text{th}} = 0.055\}$ and $\{\lambda_1^{\text{th}} = 0.009, \lambda_2^{\text{th}} = 0.055\}$ for the one-threshold and two-threshold methods, respectively. The figure clearly shows that, while the BERs of i_2 in both methods are the same, the BER of i_1 obtained with the two-threshold method is significantly better than the BER obtained with the one-threshold method. In particular, a SNR gain of about 5 dB is observed at the BER level of 10^{-5} for bit i_1.

Fig. 3.8 shows performance improvement (also obtained with simulation) of the less protected bit when we set BER_1 in (3.48) to be 4×10^{-4} at SNR = 20 (dB). The scaling factors of Rayleigh fading channels are set to be identical with $\lambda_{\text{sr}} = \lambda_{\text{rd}} = \lambda_{\text{sd}} = 1$. With two other sets of threshold values, namely $\{\lambda_1^{\text{th}} = 0.1, \lambda_2^{\text{th}} = 1.5\}$

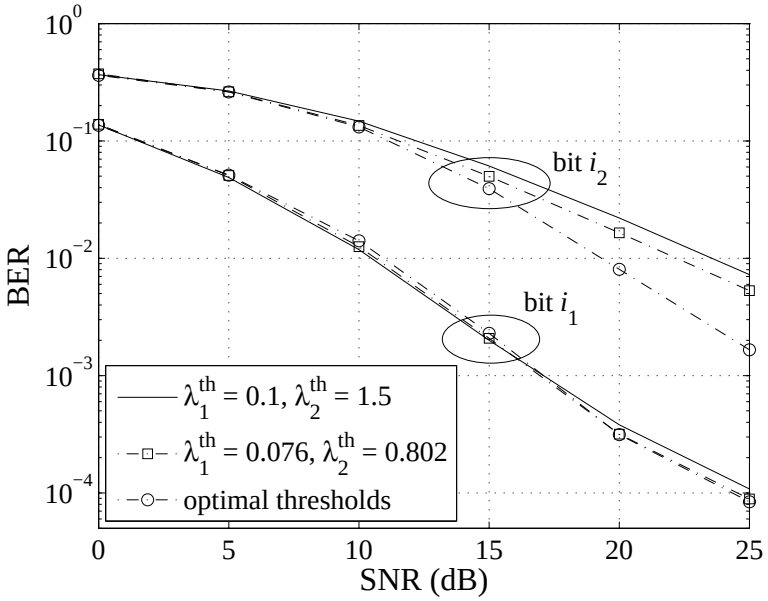

Figure 3.8 BER comparison of i_1 and i_2 when $\lambda_{sr} = \lambda_{rd} = \lambda_{sd} = 1$. The optimal thresholds are $\{\lambda_1^{th} = 0.071, \lambda_2^{th} = 0.161\}$.

Table 3.1 BER Constraint, Optimal Thresholds and Distance Parameter

Fig. 3.9	Optimal thresholds and α (exact)						Optimal thresholds and α (appr.)					
SNR (dB)	0	5	10	15	20	25	0	5	10	15	20	25
BER_1	0.250	0.150	0.040	0.010	0.003	0.001	0.250	0.150	0.040	0.010	0.003	0.001
λ_1^{th}	0.099	0.075	0.060	0.045	0.035	0.026	0.047	0.06	0.057	0.045	0.035	0.026
λ_2^{th}	0.151	0.113	0.083	0.107	0.054	0.028	1.145	0.847	0.509	0.107	0.054	0.028
α	2.192	2.457	2.423	2.902	2.404	1.554	1.675	2.438	3.251	2.902	2.404	1.554

and $\{\lambda_1^{th} = 0.076, \lambda_2^{th} = 0.802\}$, the BER of the more protected bit also satisfies the requirement. However, with the optimal thresholds, namely $\{\lambda_1^{th} = 0.071, \lambda_2^{th} = 0.161\}$, the BER of the less protected bit is significantly better than that provided by the other threshold values. Note also that, although the optimality of the obtained thresholds is only guaranteed and can be confirmed at SNR = 20 (dB), Fig. 3.8 shows that such a set of thresholds also works very well at other SNR values.

Finally, Fig. 3.9 illustrates the usefulness of jointly optimizing relaying thresholds and distance parameters. Note that, for the case of hierarchical 2/4-ASK constellation under consideration, the distance parameters can be optimized with a single variable $\alpha = \frac{d_1}{d_2}$. For each SNR value in Fig. 3.9 the optimal thresholds and distance

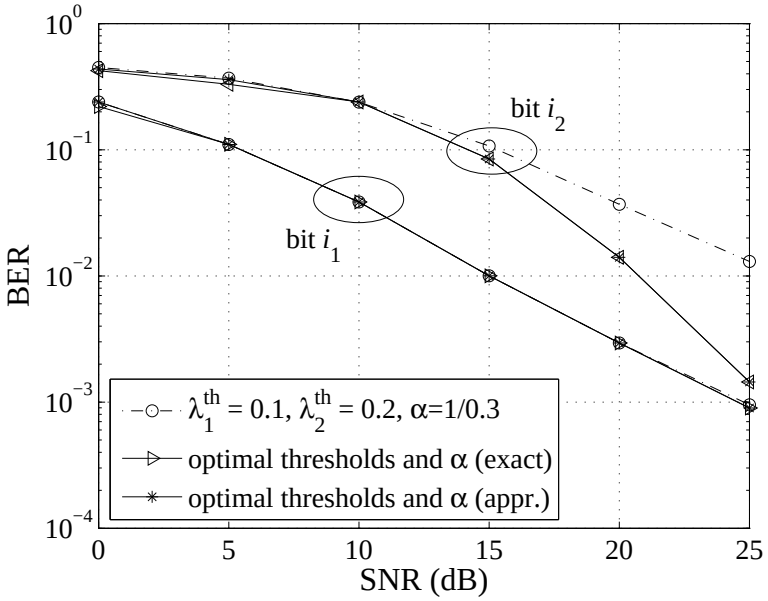

Figure 3.9 BER comparison of i_1 and i_2 when $\lambda_{\rm sr} = \lambda_{\rm rd} = 8\lambda_{\rm sd} = 1$. The jointly optimal thresholds and distance parameter are provided in Table 3.1.

parameters, obtained by both exact and approximated BER expressions, are provided in Table 3.1. Note that the constraint on BER_1 at each SNR is also listed in Table 3.1 and we set $\lambda_{\rm sr} = \lambda_{\rm rd} = 8\lambda_{\rm sd} = 1$. The first observation from Fig. 3.9 is that the results obtained with approximated and exact BER expressions are very close (the curves are not clearly distinguishable). More importantly it is seen from Fig. 3.9 that the jointly optimal thresholds and distance parameters yield a much better BER performance as compared to other arbitrarily values of the thresholds and distance parameter.

3.6 Conclusion

In this paper, we have obtained the average e2e BERs for two different protection classes in data transmission over a cooperative network which consists of a source, a relay, and a destination. Each node is equipped with a single antenna and the channels are Rayleigh fading. The two classes are modulated by a hierarchical 2/4-ASK constellation at the source. At the relay, based on the instantaneous received SNR and two threshold values, these classes can be modulated with a hierarchical

2/4-ASK constellation, or a 2-ASK constellation or are not transmitted to the destination. Moreover, optimal thresholds are chosen to minimize the BER for the less protection class while the BER of the more protection class satisfies a given requirement. Numerical and simulation results were presented to corroborate the analysis. Performance comparison reveals that the optimal thresholds improve the error performance significantly.

Acknowledgement

The authors would like to thank the anonymous reviewers for their helpful comments which have greatly improved the presentation of the paper.

3.A BERs for Case 2 ($\Theta = 2$)

3.A.1 The sub-case $\Phi = 1$

In this sub-case, the relay decodes i_1 correctly. The received signals at the destination in the first and second phases are written, respectively, as:

$$y_{\rm sd} = \sqrt{E_{\rm s}} h_{\rm sd}(\alpha s_1 + s_2) + n_{\rm sd} \quad (3.50)$$

$$y_{\rm rd} = \sqrt{E_{\rm r}} h_{\rm rd}(\widehat{s}_1) + n_{\rm rd} \quad (3.51)$$

where s_m is the symbol corresponding to bit i_m at the source, $m = 1, 2$, $\widehat{s}_1$ is the symbol corresponding to bit i_1 at the relay. In this sub-case, one has $s_1, s_2 = \pm d_2 = \pm\frac{1}{\sqrt{\alpha^2+1}}$, $\widehat{s}_1 = \frac{1}{d_2} s_1$.

The destination combines two received signals using MRC and produces the following sufficient statistic:

$$\begin{aligned} y_{\rm d} &= \sqrt{E_{\rm s}}|h_{\rm sd}|^2(\alpha s_1 + s_2) + \sqrt{E_{\rm r}}|h_{\rm rd}|^2 \widehat{s}_1 + h_{\rm sd}^* n_{\rm sd} + h_{\rm rd}^* n_{\rm rd} \\ &= \left(\alpha|h_{\rm sd}|^2\sqrt{E_{\rm s}} + \sqrt{\alpha^2+1}|h_{\rm rd}|^2\sqrt{E_{\rm r}}\right) s_1 + |h_{\rm sd}|^2\sqrt{E_{\rm s}} s_2 + h_{\rm sd}^* n_{\rm sd} + h_{\rm rd}^* n_{\rm rd}. \quad (3.52) \end{aligned}$$

The BER for the first bit i_1 in this sub-case is given by[10]

$$\begin{aligned}
&P(\varepsilon_{\rm d}, i_1|\Theta=2,\Phi=1) = \\
&\quad \frac{1}{4}\left\{P(\varepsilon_{\rm d}, i_1|\Theta=2,\Phi=1,00 \text{ sent}) + P(\varepsilon_{\rm d}, i_1|\Theta=2,\Phi=1,01 \text{ sent})\right. \\
&\quad \left. + P(\varepsilon_{\rm d}, i_1|\Theta=2,\Phi=1,10 \text{ sent}) + P(\varepsilon_{\rm d}, i_1|\Theta=2,\Phi=1,11 \text{ sent})\right\} \\
&\quad = \mathbb{E}_{\gamma_{\rm sd},\gamma_{\rm rd}}\left\{\frac{1}{2}\left\{Q\left(\frac{\frac{\alpha+1}{\sqrt{\alpha 2+1}}\gamma_{\rm sd}+\gamma_{\rm rd}}{\sqrt{(\gamma_{\rm sd}+\gamma_{\rm rd})/2}}\right) + Q\left(\frac{\frac{\alpha-1}{\sqrt{\alpha 2+1}}\gamma_{\rm sd}+\gamma_{\rm rd}}{\sqrt{(\gamma_{\rm sd}+\gamma_{\rm rd})/2}}\right)\right\}\right\}. \qquad (3.53)
\end{aligned}$$

For the second bit i_2, only the signal received in the first phase is used to decode. The average BER of i_2 is

$$\begin{aligned}
P(\varepsilon_{\rm d}, i_2|\Theta=2,\Phi=1) = \frac{1}{4}\left\{2 - 2\sqrt{\frac{\frac{1}{\alpha^2+1}\sigma_{\rm sd}^2}{1+\frac{1}{\alpha^2+1}\sigma_{\rm sd}^2}}\right. \\
\left. + \sqrt{\frac{\frac{(2\alpha+1)^2}{\alpha^2+1}\sigma_{\rm sd}^2}{1+\frac{(2\alpha+1)^2}{\alpha^2+1}\sigma_{\rm sd}^2}} - \sqrt{\frac{\frac{(2\alpha-1)^2}{\alpha^2+1}\sigma_{\rm sd}^2}{1+\frac{(2\alpha-1)^2}{\alpha^2+1}\sigma_{\rm sd}^2}}\right\}. \qquad (3.54)
\end{aligned}$$

3.A.2 The sub-case $\Phi = 2$

In this sub-case, the relay decodes i_1 incorrectly. The received signals at the destination in two phases are similar to (3.50) and (3.51). However, $\widehat{s}_1 = -\frac{1}{d_2}s_1$. The sufficient statistic after combining two received signals using MRC is:

$$y_{\rm d} = \left(\alpha|h_{\rm sd}|^2\sqrt{E_{\rm s}} - \sqrt{\alpha^2+1}|h_{\rm rd}|^2\sqrt{E_{\rm r}}\right)s_1 + |h_{\rm sd}|^2\sqrt{E_{\rm s}}s_2 + h_{\rm sd}^* n_{\rm sd} + h_{\rm rd}^* n_{\rm rd}. \quad (3.55)$$

Similar to the cooperation error, the BER of i_1 is as follows:

$$\begin{aligned}
&P(\varepsilon_{\rm d}, i_1|\Theta=2,\Phi=2) = \\
&\quad \mathbb{E}_{\gamma_{\rm sd},\gamma_{\rm rd}}\left\{\frac{1}{2}\left\{Q\left(\frac{\frac{\alpha-1}{\sqrt{\alpha^2+1}}\gamma_{\rm sd}-\gamma_{\rm rd}}{\sqrt{(\gamma_{\rm sd}+\gamma_{\rm rd})/2}}\right) + Q\left(\frac{\frac{\alpha+1}{\sqrt{\alpha^2+1}}\gamma_{\rm sd}-\gamma_{\rm rd}}{\sqrt{(\gamma_{\rm sd}+\gamma_{\rm rd})/2}}\right)\right\}\right\}. \qquad (3.56)
\end{aligned}$$

[10]The proposed combining scheme in (3.52) is optimal in the sense that it maximizes the combiner's SNR if the relay decodes i_1 correctly. The destination decodes s_1 by considering both s_1 and s_2 as follows: $(s_1^*, s_2^*) = \arg\min x_{(s_1,s_2=\pm 1/\sqrt{\alpha^2+1})}\left|y_{\rm d} - \left(\left(\alpha|h_{\rm sd}|^2\sqrt{E_{\rm s}} + \sqrt{\alpha^2+1}|h_{\rm rd}|^2\sqrt{E_{\rm r}}\right)s_1 + |h_{\rm sd}|^2\sqrt{E_{\rm s}}s_2\right)\right|$. After s_1 is decoded, the decision for s_2 is implemented by canceling the "interference" component due to s_1 in the signal received at the destination in the first phase. *Remark:* This footnote is added to address the external examiner's comment. It is not in the original paper.

3.B BERs for Case 3 ($\Theta = 3$)

3.B.1 The sub-cases $\Phi = 1, 2, 3$

In these sub-cases, the received signals at the destination in two phases are:

$$y_{\rm sd} = \sqrt{E_{\rm s}} h_{\rm sd}(\alpha s_1 + s_2) + n_{\rm sd} \tag{3.57}$$

$$y_{\rm rd} = \sqrt{E_{\rm r}} h_{\rm rd}(\alpha \widehat{s}_1 + \widehat{s}_2) + n_{\rm rd} \tag{3.58}$$

where s_m and $\widehat{s}_m$ are the symbols corresponding to bit i_m, $m = 1, 2$ at the source and relay, respectively, i.e., $s_1, s_2 = \pm d_2 = \pm\frac{1}{\sqrt{\alpha^2+1}}$, $\widehat{s}_1 = \pm s_1$ and $\widehat{s}_2 = \pm s_2$. Using MRC to combine both signals gives:

$$\begin{aligned} y_{\rm d} &= \sqrt{E_{\rm s}}|h_{\rm sd}|^2(\alpha s_1 + s_2) + \sqrt{E_{\rm r}}|h_{\rm rd}|^2(\alpha \widehat{s}_1 + \widehat{s}_2) + h_{\rm sd}^* n_{\rm sd} + h_{\rm rd}^* n_{\rm rd} \\ &= \alpha\left(\sqrt{E_{\rm s}}|h_{\rm sd}|^2 s_1 + \sqrt{E_{\rm r}}|h_{\rm rd}|^2 \widehat{s}_1\right) + \left(\sqrt{E_{\rm s}}|h_{\rm sd}|^2 s_2 + \sqrt{E_{\rm r}}|h_{\rm rd}|^2 \widehat{s}_2\right) \\ &\qquad + h_{\rm sd}^* n_{\rm sd} + h_{\rm rd}^* n_{\rm rd} \end{aligned} \tag{3.59}$$

With the first sub-case ($\Phi = 1$), the first bit is wrongly decoded at the relay, however, the second bit is correctly decoded, i.e., $\widehat{s}_1 = -s_1$ and $\widehat{s}_2 = s_2$, (3.59) becomes

$$\begin{aligned} y_{\rm d} &= \alpha\left(\sqrt{E_{\rm s}}|h_{\rm sd}|^2 - \sqrt{E_{\rm r}}|h_{\rm rd}|^2\right) s_1 + \left(\sqrt{E_{\rm s}}|h_{\rm sd}|^2 + \sqrt{E_{\rm r}}|h_{\rm rd}|^2\right) s_2 \\ &\qquad + h_{\rm sd}^* n_{\rm sd} + h_{\rm rd}^* n_{\rm rd} \end{aligned} \tag{3.60}$$

The average BERs of i_1 and i_2 can be calculated as

$$\begin{aligned} &P(\varepsilon_{\rm d}, i_1|\Theta = 3, \Phi = 1) = \\ &\quad \frac{1}{4}\{P(\varepsilon_{\rm d}, i_1|\Theta = 3, \Phi = 1, 00 \text{ sent}) + P(\varepsilon_{\rm d}, i_1|\Theta = 3, \Phi = 1, 01 \text{ sent}) \\ &\quad + P(\varepsilon_{\rm d}, i_1|\Theta = 3, \Phi = 1, 10 \text{ sent}) + P(\varepsilon_{\rm d}, i_1|\Theta = 3, \Phi = 1, 11 \text{ sent})\} \\ &\qquad = \mathbb{E}_{\gamma_{\rm sd}, \gamma_{\rm rd}}\left\{\frac{1}{2}\left\{Q\left(\frac{\frac{\alpha+1}{\sqrt{\alpha^2+1}}\gamma_{\rm sd} - \frac{\alpha+1}{\sqrt{\alpha^2+1}}\gamma_{\rm rd}}{\sqrt{(\gamma_{\rm sd}+\gamma_{\rm rd})/2}}\right)\right.\right. \\ &\qquad\qquad \left.\left. + Q\left(\frac{\frac{\alpha-1}{\sqrt{\alpha^2+1}}\gamma_{\rm sd} - \frac{\alpha-1}{\sqrt{\alpha^2+1}}\gamma_{\rm rd}}{\sqrt{(\gamma_{\rm sd}+\gamma_{\rm rd})/2}}\right)\right\}\right\} \end{aligned} \tag{3.61}$$

$$P(\varepsilon_{\rm d}, i_2|\Theta=3,\Phi=1) = \mathbb{E}_{\gamma_{\rm sd},\gamma_{\rm rd}}\left\{\frac{1}{2}\left\{Q\left(\frac{\frac{1}{\sqrt{\alpha^2+1}}\gamma_{\rm sd}-\frac{2\alpha+1}{\sqrt{\alpha^2+1}}\gamma_{\rm rd}}{\sqrt{(\gamma_{\rm sd}+\gamma_{\rm rd})/2}}\right) - Q\left(\frac{\frac{2\alpha+1}{\sqrt{\alpha^2+1}}\gamma_{\rm sd}-\frac{1}{\sqrt{\alpha^2+1}}\gamma_{\rm rd}}{\sqrt{(\gamma_{\rm sd}+\gamma_{\rm rd})/2}}\right)\right.\right.$$
$$\left.\left. + Q\left(\frac{\frac{1}{\sqrt{\alpha^2+1}}\gamma_{\rm sd}+\frac{2\alpha-1}{\sqrt{\alpha^2+1}}\gamma_{\rm rd}}{\sqrt{(\gamma_{\rm sd}+\gamma_{\rm rd})/2}}\right) + Q\left(\frac{\frac{2\alpha-1}{\sqrt{\alpha^2+1}}\gamma_{\rm sd}+\frac{1}{\sqrt{\alpha^2+1}}\gamma_{\rm rd}}{\sqrt{(\gamma_{\rm sd}+\gamma_{\rm rd})/2}}\right)\right\}\right\} \quad (3.62)$$

Similar to the first sub-case, one can verify the BERs for the second and third cases as given in (3.17) to (3.20).

3.B.2 The sub-case $\Phi = 4$

Similar to the previous sub-cases, the combination of two received signals by using MRC is

$$\begin{aligned} y_{\rm d} &= \sqrt{E_{\rm s}}|h_{\rm sd}|^2(\alpha s_1 + s_2) + \sqrt{E_{\rm r}}|h_{\rm rd}|^2(\alpha\widehat{s}_1 + \widehat{s}_2) + h_{\rm sd}^* n_{\rm sd} + h_{\rm rd}^* n_{\rm rd} \\ &= \alpha\left(\sqrt{E_{\rm s}}|h_{\rm sd}|^2 + \sqrt{E_{\rm r}}|h_{\rm rd}|^2\right)s_1 + \left(\sqrt{E_{\rm s}}|h_{\rm sd}|^2 + \sqrt{E_{\rm r}}|h_{\rm rd}|^2\right)s_2 \\ &\qquad + h_{\rm sd}^* n_{\rm sd} + h_{\rm rd}^* n_{\rm rd}. \end{aligned} \quad (3.63)$$

where $s_1, s_2 = \pm d_2 = \pm\frac{1}{\sqrt{\alpha^2+1}}$.

The probability of error of the sub-case $\Phi = 4$ of i_1 and i_2 are given, respectively, as

$$P(\varepsilon_{\rm d}, i_1|\Theta=3,\Phi=4) = \mathbb{E}_{\gamma_{\rm sd},\gamma_{\rm rd}}\left\{\frac{1}{2}\left\{Q\left(\frac{(\alpha+1)\sqrt{2(\gamma_{\rm sd}+\gamma_{\rm rd})}}{\sqrt{\alpha^2+1}}\right)\right.\right.$$
$$\left.\left. + Q\left(\frac{(\alpha-1)\sqrt{2(\gamma_{\rm sd}+\gamma_{\rm rd})}}{\sqrt{\alpha^2+1}}\right)\right\}\right\} \quad (3.64)$$

$$P(\varepsilon_{\rm d}, i_2|\Theta=3,\Phi=4) = \mathbb{E}_{\gamma_{\rm sd},\gamma_{\rm rd}}\left\{\frac{1}{4}\left\{4Q\left(\frac{\sqrt{2(\gamma_{\rm sd}+\gamma_{\rm rd})}}{\sqrt{\alpha^2+1}}\right)\right.\right.$$
$$\left.\left. - 2Q\left(\frac{(2\alpha+1)\sqrt{2(\gamma_{\rm sd}+\gamma_{\rm rd})}}{\sqrt{\alpha^2+1}}\right) + 2Q\left(\frac{(2\alpha-1)\sqrt{2(\gamma_{\rm sd}+\gamma_{\rm rd})}}{\sqrt{\alpha^2+1}}\right)\right\}\right\} \quad (3.65)$$

Based on [C3-32], it can be verified that:

$$\mathbb{E}_{\gamma_{\rm sd},\gamma_{\rm rd}}\left\{Q\left[\sqrt{2\beta(\gamma_{\rm sd}+\gamma_{\rm rd})}\right]\right\} = \begin{cases} \frac{1}{2}\left(1-\sqrt{\frac{\beta\sigma_{\rm rd}^2}{1+\beta\sigma_{\rm rd}^2}}\right)^2\left(1+\frac{1}{2}\sqrt{\frac{\beta\sigma_{\rm rd}^2}{1+\beta\sigma_{\rm rd}^2}}\right), & \text{if } \sigma_{\rm rd}^2=\sigma_{\rm sd}^2; \\ \frac{1}{2}\left(1-\frac{\sigma_{\rm sd}^2\sqrt{\frac{\beta\sigma_{\rm sd}^2}{1+\beta\sigma_{\rm sd}^2}}-\sigma_{\rm rd}^2\sqrt{\frac{\beta\sigma_{\rm rd}^2}{1+\beta\sigma_{\rm rd}^2}}}{\sigma_{\rm sd}^2-\sigma_{\rm rd}^2}\right), & \text{if } \sigma_{\rm rd}^2\neq\sigma_{\rm sd}^2; \end{cases} \tag{3.66}$$

Therefore, the BERs of i_1 and i_2 in (3.64) and (3.65) can be calculated analytically.

3.C The e2e BERs for Generalized Hierarchical 4/16-QAM Constellations

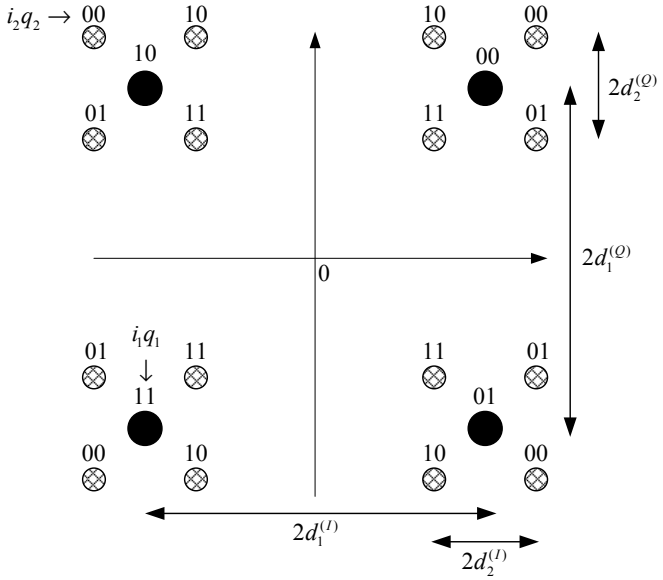

Figure 3.10 Generalized hierarchical 4/16-QAM constellation.

In this Appendix, we consider the case that the source and relay use a hierarchical 4/16-QAM rectangular constellation as illustrated in Fig. 3.10 [C3-20]. It means that there are also two classes and each class contains two bits. Two bits from the first class are assigned to the most significant bits in the in-phase (I) and quadrature (Q) channels. Similarly, two bits from the second class are assigned to the least significant bits in the I and Q channels. We have two distance vectors $\mathbf{d}^{(I)} = [d_1^{(I)}, d_2^{(I)}]$ and

$\mathbf{d}^{(Q)} = [d_1^{(Q)}, d_2^{(Q)}]$. As shown in [C3-20], [C3-33], the average BER of the first class is

$$\mathrm{BER}^{(1)}(\gamma_1^{\mathrm{th}}, \gamma_2^{\mathrm{th}}) = \frac{\mathrm{BER}(\gamma_1^{\mathrm{th}}, \gamma_2^{\mathrm{th}}, i_1) + \mathrm{BER}(\gamma_1^{\mathrm{th}}, \gamma_2^{\mathrm{th}}, q_1)}{2} \tag{3.67}$$

where $\mathrm{BER}(\gamma_1^{\mathrm{th}}, \gamma_2^{\mathrm{th}}, i_1)$, $\mathrm{BER}(\gamma_1^{\mathrm{th}}, \gamma_2^{\mathrm{th}}, q_1)$ are the BERs of more protected bits of the in-phase and quadrature channels, respectively.

Likewise, the average BER of the second class is

$$\mathrm{BER}^{(2)}(\gamma_1^{\mathrm{th}}, \gamma_2^{\mathrm{th}}) = \frac{\mathrm{BER}(\gamma_1^{\mathrm{th}}, \gamma_2^{\mathrm{th}}, i_2) + \mathrm{BER}(\gamma_1^{\mathrm{th}}, \gamma_2^{\mathrm{th}}, q_2)}{2} \tag{3.68}$$

where $\mathrm{BER}(\gamma_1^{\mathrm{th}}, \gamma_2^{\mathrm{th}}, i_1)$, $\mathrm{BER}(\gamma_1^{\mathrm{th}}, \gamma_2^{\mathrm{th}}, q_1)$ are the BERs of less protected bits of the in-phase and quadrature channels, respectively.

With rectangular constellations, the average BER computation of the first and second classes reduces to finding the BER of the in-phase bits only. The average e2e BERs for the in-phase bits i_1 and i_2 are similar to (3.4). The only differences are scaling factors. Similarly, we can find the average e2e BERs for the quadrature bits q_1 and q_2. Therefore, the average e2e BERs of the first and second classes of a hierarchical 4/16-QAM constellation can be formulated. Based on such a formulation, the two optimum thresholds can be found numerically.

References

[C3-1] E. C. van der Meulen, "Three-terminal communication channels," *Adv. Appl. Probab.*, vol. 3, pp. 120–154, 1971.

[C3-2] T. Cover and A. E. Gamal, "Capacity theorems for the relay channel," *IEEE Trans. Inform. Theory*, vol. 25, pp. 572–584, September 1979.

[C3-3] G. Kramer, M. Gastpar, and P. Gupta, "Cooperative strategies and capacity theorems for relay networks," *IEEE Trans. Inform. Theory*, vol. 51, pp. 3037–3063, September 2005.

[C3-4] A. Sendonaris, E. Erkip, and B. Aazhang, "User cooperation diversity, Part I: System description," *IEEE Trans. Commun.*, vol. 51, no. 11, pp. 1927–1938, November 2003.

[C3-5] A. Sendonaris, E. Erkip, and B. Aazhang, "User cooperation diversity, Part II: Implementation aspects and performance analysis," *IEEE Trans. Commun.*, vol. 51, no. 11, pp. 1939–1948, November 2003.

[C3-6] Y. Jing and B. Hassibi, "Distributed space-time coding in wireless relay networks," *IEEE Trans. Wireless Commun.*, vol. 5, no. 12, pp. 3524–3536, December 2006.

[C3-7] J. Laneman and G. Wornell, "Distributed space-time-coded protocols for exploiting cooperative diversity in wireless networks," *IEEE Trans. Inform. Theory*, vol. 49, pp. 2415–2425, October 2003.

[C3-8] A. Ribeiro, X. Cai, and G. Giannakis, "Symbol error probabilities for general cooperative links," *IEEE Trans. Wireless Commun.*, vol. 4, pp. 1264–1273, May 2005.

[C3-9] J. Hi and R. Hu, "Slepian-Wolf cooperation: A practical and effcient compress-and-forward relay scheme," in *Allerton Conf. Commun. Contr. and Comp.*, November 2005.

[C3-10] J. Laneman, D. Tse, and G. Wornell, "Cooperative diversity in wireless networks: Efficient protocols and outage behavior," *IEEE Trans. Inform. Theory*, vol. 50, pp. 3062–3080, December 2004.

[C3-11] A. Bletsas, A. Khisti, D. Reed, and A. Lippman, "A simple cooperative diversity method based on network path selection," *IEEE J. Select. Areas in Commun.*, vol. 24, pp. 659–672, March 2006.

[C3-12] A. Bletsas, H. Shin, and M. Win, "Outage optimality of opportunistic amplify-and-forward relaying," *IEEE Commun. Letters*, vol. 11, pp. 261–263, March 2007.

[C3-13] A. Bletsas, H. Shin, and M. Win, "Cooperative communications with outage-optimal opportunistic relaying," *IEEE Trans. Wireless Commun.*, vol. 6, pp. 3450–3460, September 2007.

[C3-14] T. Hunter and A. Nosratinia, "Diversity through coded cooperation," *IEEE Trans. Wireless Commun.*, vol. 5, pp. 283–289, February 2006.

[C3-15] T. Hunter, S. Sanayei, and A. Nosratinia, "Outage analysis of coded cooperation," *IEEE Trans. Inform. Theory*, vol. 52, pp. 375–391, February 2006.

[C3-16] T. Wang, A. Cano, G. Giannakis, and J. N. Laneman, "High-performance cooperative demodulation with decode-and-forward relays," *IEEE Trans. Commun.*, vol. 55, pp. 830–830, April 2007.

[C3-17] F. Onat, A. Adinoyi, Y. Fan, H. Yanikomeroglu, J. Thompson, and I. Marsland, "Threshold selection for SNR-based selective digital relaying in cooperative wireless networks," *IEEE Trans. Wireless Commun.*, vol. 7, pp. 4226–4237, November 2008.

[C3-18] F. Onat, Y. Fan, H. Yanikomeroglu, and J. Thompson, "Asymptotic BER analysis of threshold digital relaying schemes in cooperative wireless systems," *IEEE Trans. Wireless Commun.*, vol. 7, pp. 4938–4947, December 2008.

[C3-19] P. Vitthaladevuni and M.-S. Alouini, "Exact BER computation of generalized hierarchical PSK constellations," *IEEE Trans. Commun.*, vol. 51, pp. 2030–2037, December 2003.

[C3-20] P. Vitthaladevuni and M.-S. Alouini, "A recursive algorithm for the exact BER computation of generalized hierarchical QAM constellations," *IEEE Trans. Inform. Theory*, vol. 49, pp. 297–307, January 2003.

[C3-21] A. Calderbank and N. Seshadri, "Multilevel codes for unequal error protection," *IEEE Trans. Inform. Theory*, vol. 39, pp. 1234–1248, July 1993.

[C3-22] M. Pursley and J. Shea, "Nonuniform phase-shift-key modulation for multimedia multicast transmission in mobile wireless networks," *IEEE J. Select. Areas in Commun.*, vol. 17, pp. 774–783, May 1999.

[C3-23] M. Aydinlik and M. Salehi, "Turbo coded modulation for unequal error protection," *IEEE Trans. Commun.*, vol. 56, pp. 555–564, April 2008.

[C3-24] M. Hossain, P. Vitthaladevuni, M.-S. Alouini, V. Bhargava, and A. Goldsmith, "Adaptive hierarchical modulation for simultaneous voice and multiclass data transmission over fading channels," *IEEE Trans. Veh. Technol.*, vol. 55, pp. 1181–1194, July 2006.

[C3-25] C. Hausl and J. Hagenauer, "Relay communication with hierarchical modulation," *IEEE Commun. Letters*, vol. 11, pp. 64–66, January 2007.

[C3-26] T. Wang, A. Cano, G. Giannakis, and J. Ramos, "Multi-tier cooperative broadcasting with hierarchical modulations," *IEEE Trans. Wireless Commun.*, vol. 6, pp. 3047–3057, August 2007.

[C3-27] M.-K. Chang and S.-Y. Lee, "Performance analysis of cooperative communication system with hierarchical modulation over Rayleigh fading channel," *IEEE Trans. Wireless Commun.*, vol. 8, pp. 2848–2852, June 2009.

[C3-28] H. X. Nguyen, H. H. Nguyen, and T. Le-Ngoc, "Signal transmission with unequal error protection in relay selection networks," *to appear in Proc. IEEE Int. Conf. Commun.*, May 2010.

[C3-29] P. Herhold, E. Zimmermann, and G. Fettweis, "A simple cooperative extension to wireless relaying," *International Zurich Seminar on Communications*, pp. 36–39, 2004.

[C3-30] I. S. Gradshteyn, I. M. Ryzhik, A. Jeffrey, and D. Zwillinger, *Table of Integrals, Series, and Products*. Academic Press, 2000.

[C3-31] D. P. Bertsekas, *Constrained Optimization and Lagrange Multiplier Methods*. Athena Scientific, 1996.

[C3-32] J. G. Proakis, *Digital Communications*. McGraw-Hill, 2000.

[C3-33] P. Vitthaladevuni and M.-S. Alouini, "BER computation of $4/M$-QAM hierarchical constellations," *IEEE International Symposium on Personal, Indoor and Mobile Radio Communications*, vol. 1, pp. B–85–B–89, September 2001.

4. Signal Transmission with Unequal Error Protection in Relay Selection Networks

Published as:

Ha X. Nguyen, Ha H. Nguyen and Tho Le-Ngoc, "Signal Transmission with Unequal Error Protection in Relay Selection Networks", *IET Communications*, vol. 4, pp. 1624-1635, September 2010.

The manuscript included in Chapter 3 studies a relaying technique in cooperative networks having a single relay. As discussed in Chapter 2, multiple relays can offer higher diversity gains, i.e., better error performance. Therefore, the manuscript in this chapter is concerned with a multiple-relay network in which hierarchical modulation is employed for unequal error protection. It is a further development of the manuscript in Chapter 3. However, as mentioned earlier in Chapter 2, it is important to recognize that a cooperative diversity system suffers a certain loss in throughput since the number of required channels cannot be less than the number of relays. To overcome this disadvantage, a single relay selection scheme is employed to select the "best" relay to cooperate with the source in the second phase. Therefore, the goal of the manuscript in this chapter is to further improve the error performance of two different classes without sacrificing a throughput loss in cooperative networks with multiple relays.

After receiving the signal in the first phase from the source, all relays are classified into three different subsets with different reliability indicators based on the instantaneous received SNRs of the source-relay links. A single relay is selected from the most

reliable subset which yields the highest SNR of relay-destination link to retransmit. Based on the subset that the selected relay is in, the selected relay might retransmit both classes, the more important class, or remains silent in the second phase. The approximated BER of each information class is derived. The simulation results are presented to show that the optimal thresholds can improve the error performance significantly.

Signal Transmission with Unequal Error Protection in Relay Selection Networks

Ha X. Nguyen, Ha H. Nguyen, and Tho Le-Ngoc

Abstract

A relaying technique based on single relay selection is studied for multiple-relay networks when hierarchical modulation is employed for unequal error protection. A single relay selection scheme achieves a higher bandwidth efficiency while maintaining the same diversity order as when all the relays are selected in a multiple-relay network. Specifically, a cooperative network with one source, K relays, and one destination is considered in which two different protection information classes are modulated by a hierarchical 2/4-amplitude shift keying (ASK) constellation at the source. After selecting a relay to cooperate with the source, based on the instantaneous received SNR, the selected relay decides to retransmit both classes by using a hierarchical 2/4-ASK constellation, or the more protection class by using a 2-ASK constellation, or remains silent. The approximated bit error rate (BER) of each information class is derived. Optimal thresholds are chosen to minimize the BER of one class while the BER of the other class satisfies a requirement. Numerical and simulation results are provided to validate the analysis. The results also show that the optimal thresholds can improve the error performance significantly.

Index terms

Cooperative diversity, relay selection, fading channel, unequal error protection, hierarchical modulation.

Manuscript received August, 14, 2009; revised February 18, 2010; accepted March 3, 2010.

Ha X. Nguyen (*contact author) and Ha H. Nguyen are with the Department of Electrical and Computer Engineering, University of Saskatchewan, 57 Campus Drive, Saskatoon, Sask., Canada, S7N 5A9 (e-mails: hxn201@mail.usask.ca, ha.nguyen@usask.ca).

Tho Le-Ngoc is with the Department of Electrical and Computer Engineering, McGill University, 3480 University Street, Montreal, Quebec, Canada, H3A 2A7 (e-mail: tho@ece.mcgill.ca).

4.1 Introduction

In wireless communications, implementing multiple transmit and/or receive antennas to provide spatial diversity might not be possible due to the size and cost limitations. Cooperative (or relay) diversity has emerged as a promising technique to overcome such limitations. The basic idea is that the source cooperates with other nodes (or relays) in the network to form a virtual multiple antenna system [C4-1, C4-2,C4-3,C4-4,C4-5]. However, with the decode-and-forward (DF) protocol, cooperative communication does not achieve a full diversity order if the relays always re-transmit the decoded messages. This is due to possible retransmission of erroneously decoded bits of the message from the relays. Moreover, transmissions from relays to the destination are usually carried out in mutually orthogonal channels, which reduces bandwidth efficiency. To overcome these disadvantages, selection relaying has been proposed for cooperative systems. The operation is based on the selection of the best relay that yields the maximum instantaneous signal-to-noise ratio (SNR) of the relay-destination link in a set of "reliable" relays. In general, a relay is in the set of reliable relays if the instantaneous SNR of the source-relay link is larger than a predefined threshold. The single relay selection scheme achieves a higher bandwidth efficiency while maintaining the same diversity order as the conventional cooperative scheme[1] [C4-6, C4-7, C4-8].

Unequal error protection (UEP) is an important consideration in wireless communication systems. In particular, this technique protects data according to the system requirements. In poor channel conditions, the receiver recovers the more important classes (known as basic or coarse data) while the less important classes (known as refinement or enhancement data) are recovered from better channel conditions. In the literature, a large amount of research work related to unequal error protection in point-to-point communications exists [C4-9, C4-10, C4-11, C4-12, C4-13, C4-14, C4-15, C4-16, C4-17]. However, only a few studies were concentrated on

[1]For convenience, the scheme in which all the relays are selected to transmit to the destination over orthogonal channels shall be referred to as a conventional cooperative scheme.

UEP in cooperative networks. For example, in [C4-18], the source broadcasts the signals to multiple destinations by employing hierarchical modulation. Cooperation maximum ratio combining (C-MRC) is applied at each destination to decode the signals. However, the system has a high complexity since each destination is required to know the instantaneous BERs of all previous destinations. The work in [C4-19] considers a three-node cooperative network and the relay always retransmits the decoded message to the destination. The distance parameters of the constellation are optimized to minimize the BERs. However, the continuous retransmission of the relay can cause error propagation, which limits the BER performance of the system. Reference [C4-20] proposes a two-threshold method in a *single relay* network using hierarchical modulation. Based on the instantaneous received SNR at the relay, the relay retransmits both classes, or the more protection class, or remains silent in the second phase. The results in [C4-20] show that the two-threshold method improves the performance significantly compared to the conventional one-threshold method.

This work is a further development of [C4-20]. It is concerned with a *multiple-relay* network employing hierarchical modulation for unequal error protection of two different information classes at the source. A single relay selection scheme is employed to select the "best" relay to cooperate with the source. In particular, after receiving the signal in the first phase from the source, all relays form three different subsets with different reliability indicators based on the instantaneous received SNRs of the source-relay links. A single relay is selected from the most reliable subset which yields the highest SNR of relay-destination link. Based on the subset that the selected relay is in, the selected relay might retransmit both classes, the more important class, or remains silent in the second phase. To simplify our derivations, we assume that a hierarchical 2/4-ASK constellation is used at the source. At the selected relay, depending on the instantaneous received SNR, a hierarchical 2/4-ASK or 2-ASK constellation is employed[2]. The approximated BER formulation for each information class is derived

[2]It should be noted that the use of hierarchical 2/4-ASK modulation is for simplicity of presentation. Our framework can be extended to a general hierarchical QAM modulation with many different classes.

and shown to be very tight. Based on the tight BER approximation, the use of the optimal thresholds at the relays is discussed to minimize the BER of one information class while the BER of the other information class satisfies a requirement.

The remainder of this paper is organized as follows. Section 4.2 describes the system model. Section 4.3 presents BER computations and discusses the use of optimal thresholds. Numerical and simulation results are presented in Section 4.4. Finally, Section 4.5 concludes the paper.

Notations: $\mathbb{E}\{x\}$ is the expectation of x and $\mathcal{CN}(0, \sigma^2)$ denotes a circularly symmetric complex Gaussian random variable with variance σ^2. $|\Omega|$ denotes the cardinality of the set Ω. The Q-function is defined as $Q(x) = \int_x^\infty \frac{1}{\sqrt{2\pi}} \mathrm{e}^{-t^2/2} \mathrm{d}t$.

4.2 System Model

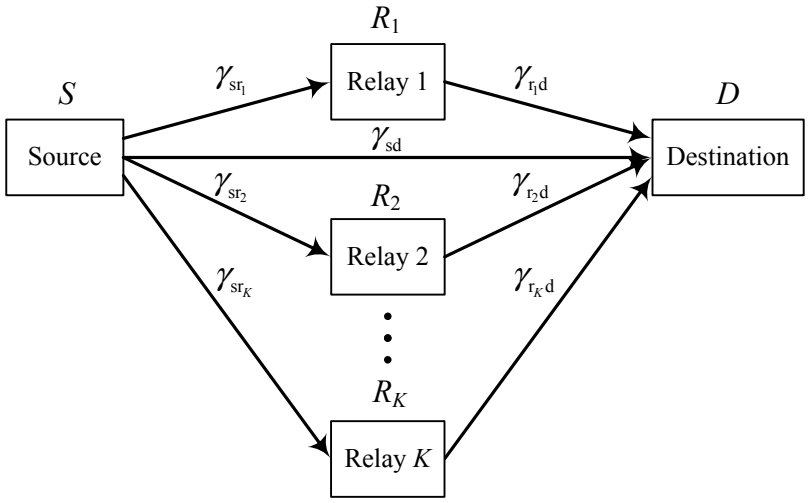

Figure 4.1 A wireless relay network.

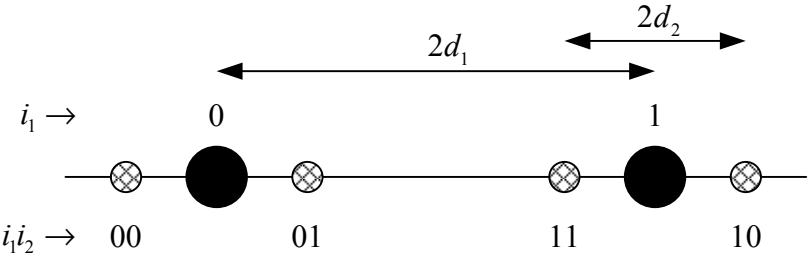

Figure 4.2 Generalized hierarchical 2/4-ASK constellation.

Consider a wireless network with $K+2$ nodes as illustrated in Fig. 4.1. There are one source node, K relay nodes, and one destination node. Every node has only one antenna. A source node S sends its message to a destination node D with the assistance of K relay nodes, denoted by R_k, $k = 1, 2, \ldots, K$. Assume that all nodes operate in a half-duplex mode, i.e., a node cannot transmit and receive simultaneously and DF protocol is employed at the relays. The symbols at the source node S are modulated to $x_{\rm s}$ by a hierarchical 2/4-ASK constellation as shown in Fig. 4.2, where bit i_1 is more protected than bit i_2. In the first phase, S transmits signals, K relays and D receive. The received signals at R_k and D can be written, respectively, as

$$y_{{\rm sr}_k} = \sqrt{E_{\rm s}} h_{{\rm sr}_k} x_{\rm s} + n_{{\rm sr}_k}, \tag{4.1}$$

$$y_{\rm sd} = \sqrt{E_{\rm s}} h_{\rm sd} x_{\rm s} + n_{\rm sd}, \tag{4.2}$$

where $E_{\rm s}$ is the average symbol energy at S, $h_{{\rm sr}_k}, h_{\rm sd}$ are the channel fading coefficients between S and R_k, S and D, respectively, and $n_{{\rm sr}_k}, n_{\rm sd}$ are the noise components at R_k and D, respectively.

In order to avoid error propagation with the DF protocol, two different SNR thresholds shall be employed at each relay. They are denoted by $\gamma_1^{\rm th}$ and $\gamma_2^{\rm th}$, where $\gamma_1^{\rm th} < \gamma_2^{\rm th}$ [C4-20]. When the instantaneous SNR of the S-R_k link, denoted by $\gamma_{{\rm sr}_k}$, is larger than $\gamma_2^{\rm th}$, R_k likely decodes both bits correctly. When it is between $\gamma_1^{\rm th}$ and $\gamma_2^{\rm th}$, only the more important bit is likely to be decoded correctly. If it is less than $\gamma_1^{\rm th}$, R_k likely decodes both bits incorrectly. Mathematically, three subsets with different reliability can be defined as $\Omega_1 \triangleq \left\{k \in \mathcal{S}_{\rm relay} : \gamma_{{\rm sr}_k} < \gamma_1^{\rm th}\right\}$, $\Omega_2 \triangleq \left\{k \in \mathcal{S}_{\rm relay} : \gamma_1^{\rm th} < \gamma_{{\rm sr}_k} < \gamma_2^{\rm th}\right\}$, $\Omega_3 \triangleq \left\{k \in \mathcal{S}_{\rm relay} : \gamma_{{\rm sr}_k} > \gamma_2^{\rm th}\right\}$ where $\mathcal{S}_{\rm relay} = \{1, 2, \ldots, K\}$. Only the best relay[3] in the most reliable nonempty subset is selected to transmit the decoded symbol to the destination in the second phase. Specifically, if $\{\Omega_3 \neq \emptyset\}$, only the relay that yields the highest SNR among the relay-destination links transmits both classes with a 2/4-ASK constellation to the destination. If

[3]It is important to emphasize that we define the best relay as the one that yields the highest SNR over the *relay-destination* links, not over the source-relay links. *Remark:* This footnote is added to address the external examiner's comment. It is not in the original paper.

$\{\Omega_3 = \emptyset\}$ and $\{\Omega_2 \neq \emptyset\}$, only the "best" relay transmits the more important class with a 2-ASK constellation to the destination. Otherwise, all the relays remain silent in the second phase.

If relay R_k is selected to transmit in the second phase, the received signal at the destination is given by

$$y_{\mathrm{r}_k\mathrm{d}} = \sqrt{E_{\mathrm{r}_k}} h_{\mathrm{r}_k\mathrm{d}} x_{\mathrm{r}_k} + n_{\mathrm{r}_k\mathrm{d}}, \tag{4.3}$$

where x_{r_k} and E_{r_k} are the symbol and the average symbol energy sent by R_k, respectively, $h_{\mathrm{r}_k\mathrm{d}}$ is the channel fading coefficient between R_k and D, and $n_{\mathrm{r}_k\mathrm{d}}$ is the noise component at D in the second phase.

Depending on what the selected relay transmits in the second phase, D combines the signals in the first and second phases and decodes. The maximum ratio combiner (MRC) shall be used at the destination to decode the message.

In this paper, we assume that the channel between any two nodes is Rayleigh flat fading, modeled as $\mathcal{CN}(0, \sigma_{ij}^2)$, where i, j refers to transmit and receive nodes, respectively. The noise components at the relays and the destination are modeled as i.i.d. $\mathcal{CN}(0, N_0)$ random variables. The instantaneous received SNR for the transmission from node i to node j is denoted by γ_{ij} and computed as $\gamma_{ij} = E_i|h_{ij}|^2/N_0$. With Rayleigh fading, the probability distribution function (pdf) of γ_{ij} is an exponential random variable. It is given by $f_{ij}(\gamma_{ij}) = \frac{1}{\sigma_{ij}^2}\mathrm{e}^{-\gamma_{ij}/\sigma_{ij}^2}$, where σ_{ij}^2 is the average SNR of the i-j link.

To simplify our derivation, we assume that all the source-relays and relays-destination links have the same average channel quality, i.e., $\sigma_{\mathrm{sr}_i}^2 = \sigma_{\mathrm{sr}}^2$ and $\sigma_{\mathrm{r}_i\mathrm{d}}^2 = \sigma_{\mathrm{rd}}^2$ where $i = 1, \ldots, K$. However, the analysis can be straightforwardly extended to arbitrary average channel qualities.

4.3 BER Computations and Optimal Thresholds

In this section, the BER analysis for the proposed relaying scheme is first carried out. Then simpler BER approximations for both information classes are obtained.

Finally, the optimal thresholds are chosen to minimize the average BER of one information class while the average BER of another information class satisfies a given constraint.

4.3.1 BER Computations

We first classify all different cases that result in different conditioned BERs at the destination. Then the average BERs of two different information bits are obtained as weighted summations of these conditioned BERs. Recall that, if the instantaneous SNR of the S-R_k link where R_k is the selected relay is larger than the threshold γ_2^{th}, the selected relay transmits both information bits. If it is between the thresholds γ_1^{th} and γ_2^{th}, the selected relay transmits the more important bit. Otherwise, the selected relay remains silent. Therefore, three major groups can be classified. In the case that $\gamma_{\text{sr}_k} < \gamma_1^{\text{th}}$, the destination simply uses the received signal in the first phase to decode both bits i_1 (more protected bit) and i_2 (less protected bit). In the case that $\gamma_1^{\text{th}} < \gamma_{\text{sr}_k} < \gamma_2^{\text{th}}$, the destination combines two received signals in two phases to decode bit i_1 and uses the received signal in the first phase to decode bit i_2. Two different cases can be further classified depending on the correctness of the decoded bit i_1 at the selected relay. On the other hand, if $\gamma_{\text{sr}_k} > \gamma_2^{\text{th}}$, the destination combines two received signals in two phases to decode both bits i_1 and i_2. Since the selected relay may decode either i_1 or i_2 incorrectly, four different cases can be further separated. All of seven different cases are summarized in Fig. 4.3 and denoted by Φ_j, $j = 1, \ldots, 7$.

Let $P(\varepsilon_w, i_m, \Phi_j)$ denote the conditional BER of bit i_m at node w corresponding case Φ_j. With two given thresholds γ_1^{th} and γ_2^{th}, the average BERs for bits i_1 and i_2 can be written as

$$\text{BER}(\gamma_1^{\text{th}}, \gamma_2^{\text{th}}, i_m) = \sum_{j=1}^{7} P(\varepsilon_{\text{d}}, i_m, \Phi_j) \tag{4.4}$$

where $m = 1, 2$. In the following, the approximated expressions for seven cases in (4.4) are determined[4].

[4]For tractability of the analysis, we resort to approximated BERs. As we will show later, the

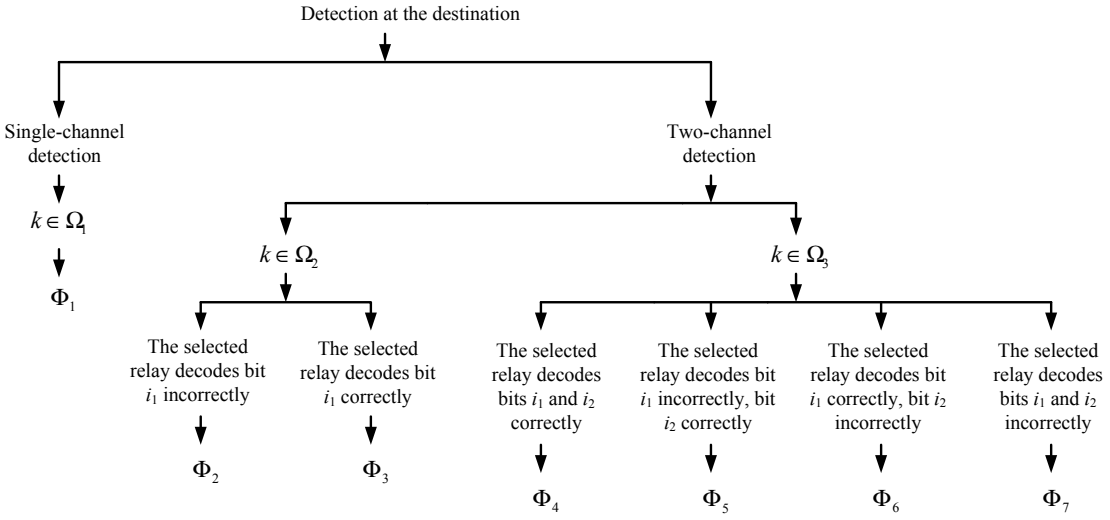

Figure 4.3 Seven different possible cases that result in different conditional BERs at the destination.

The first case, Φ_1, occurs when the instantaneous SNRs of all the S-R_k links, $k = 1, \ldots, K$, are smaller than the threshold γ_1^{th}. It follows that $|\Omega_1| = K$ and $|\Omega_2| = |\Omega_3| = 0$. The BERs of i_m, $m = 1, 2$, can be calculated as

$$P(\varepsilon_{\text{d}}, i_m, \Phi_1) = P(\varepsilon_{\text{d}}, i_m \Big| |\Omega_1| = K) P(|\Omega_1| = K). \tag{4.5}$$

The destination uses the received signal in the first phase to decode both bits i_1 and i_2. Since γ_{sd} is an exponential random variable with mean σ_{sd}^2, the average BERs of i_1 and i_2 given $|\Omega_1| = K$ can be found to be [C4-14, C4-18, C4-20]

$$\begin{aligned} P(\varepsilon_{\text{d}}, i_1 \Big| |\Omega_1| = K) &= \mathbb{E}_{\gamma_{\text{sd}}} \{ P(\varepsilon_{\text{d}}, i_1 \Big| |\Omega_1| = K, \gamma_{\text{sd}}) \} \\ &= \frac{1}{4} \left[2 - \sqrt{\frac{\frac{(\alpha+1)^2}{\alpha^2+1}\sigma_{\text{sd}}^2}{1 + \frac{(\alpha+1)^2}{\alpha^2+1}\sigma_{\text{sd}}^2}} - \sqrt{\frac{\frac{(\alpha-1)^2}{\alpha^2+1}\sigma_{\text{sd}}^2}{1 + \frac{(\alpha-1)^2}{\alpha^2+1}\sigma_{\text{sd}}^2}} \right], \end{aligned} \tag{4.6}$$

$$\begin{aligned} P(\varepsilon_{\text{d}}, i_2 \Big| |\Omega_1| = K) &= \mathbb{E}_{\gamma_{\text{sd}}} \{ P(\varepsilon_{\text{d}}, i_2 \Big| |\Omega_1| = K, \gamma_{\text{sd}}) \} \\ &= \frac{1}{4} \left[2 - 2\sqrt{\frac{\frac{1}{\alpha^2+1}\sigma_{\text{sd}}^2}{1 + \frac{1}{\alpha^2+1}\sigma_{\text{sd}}^2}} + \sqrt{\frac{\frac{(2\alpha+1)^2}{\alpha^2+1}\sigma_{\text{sd}}^2}{1 + \frac{(2\alpha+1)^2}{\alpha^2+1}\sigma_{\text{sd}}^2}} - \sqrt{\frac{\frac{(2\alpha-1)^2}{\alpha^2+1}\sigma_{\text{sd}}^2}{1 + \frac{(2\alpha-1)^2}{\alpha^2+1}\sigma_{\text{sd}}^2}} \right], \end{aligned} \tag{4.7}$$

analytical BERs obtained from the approximations are very close to the simulation results.

where $\alpha = d_1/d_2$, d_1 and d_2 are two distance parameters of the hierarchical 2/4-ASK constellation as illustrated in Fig. 4.2. On the other hand, the probability of Φ_1 occurring is

$$P(\Phi_1) = P(|\Omega_1| = K) = \left[1 - \exp\left(-\frac{\gamma_1^{\text{th}}}{\sigma_{\text{sr}}^2}\right)\right]^K \tag{4.8}$$

The two cases Φ_2 and Φ_3 are related to the scenario that the instantaneous SNR of the S-R_k (where R_k is the selected relay) is between the two thresholds γ_1^{th} and γ_2^{th}, i.e., $\gamma_1^{\text{th}} < \gamma_{\text{sr}_k} < \gamma_2^{\text{th}}$. Consider the case Φ_2, i.e., $|\Omega_2| > 0$, $|\Omega_3| = 0$ and the selected relay decodes i_1 incorrectly. The BER of i_1 is computed as[5]

$$\begin{aligned} P(\varepsilon_{\text{d}}, i_1, \Phi_2) = &\sum_{l=1}^{K} P(\varepsilon_{\text{r}}, i_1 \Big| \gamma_1^{\text{th}} < \gamma_{\text{sr}} < \gamma_2^{\text{th}}) \\ &\times P_{\Phi_2}(\varepsilon_{\text{d}}, i_1 \Big| |\Omega_2| = l, |\Omega_3| = 0) P(|\Omega_2| = l, |\Omega_3| = 0) \end{aligned} \tag{4.9}$$

where $P_{\Phi_2}(\varepsilon_{\text{d}}, i_1 \Big| |\Omega_2| = l, |\Omega_3| = 0)$ is the BER of i_1 given $|\Omega_2| = l$, $|\Omega_3| = 0$ and the selected relay transmits an incorrect bit i_1 and $P(|\Omega_2| = l, |\Omega_3| = 0)$ is the probability of $\{|\Omega_2| = l, |\Omega_3| = 0\}$ occurring. They can be approximated as (see Appendix 4.A)

$$\begin{aligned} &P_{\Phi_2}(\varepsilon_{\text{d}}, i_1 \Big| |\Omega_2| = l, |\Omega_3| = 0) \approx \\ &\quad \frac{l}{2} \sum_{j=0}^{l-1} \binom{l-1}{j} \frac{(-1)^j}{(j+1)^2} \left(\frac{\sigma_{\text{rd}}^2}{\frac{\alpha+1}{\sqrt{\alpha^2+1}}\sigma_{\text{sd}}^2 + \frac{\sigma_{\text{rd}}^2}{j+1}} + \frac{\sigma_{\text{rd}}^2}{\frac{\alpha-1}{\sqrt{\alpha^2+1}}\sigma_{\text{sd}}^2 + \frac{\sigma_{\text{rd}}^2}{j+1}} \right), \end{aligned} \tag{4.10}$$

$$P(|\Omega_2| = l, |\Omega_3| = 0) = \binom{K}{l} \left[\exp\left(-\frac{\gamma_1^{\text{th}}}{\sigma_{\text{sr}}^2}\right) - \exp\left(-\frac{\gamma_2^{\text{th}}}{\sigma_{\text{sr}}^2}\right)\right]^l \left[1 - \exp\left(-\frac{\gamma_1^{\text{th}}}{\sigma_{\text{sr}}^2}\right)\right]^{K-l}. \tag{4.11}$$

Next, $P(\varepsilon_{\text{r}}, i_1 \Big| \gamma_1^{\text{th}} < \gamma_{\text{sr}} < \gamma_2^{\text{th}})$, the BER of i_1 at the selected relay given $\gamma_1^{\text{th}} < \gamma_{\text{sr}} < \gamma_2^{\text{th}}$, needs to be computed to complete the calculation in (4.9). One can verify that the conditional pdf of γ_{sr}, conditioned on $\gamma_1^{\text{th}} < \gamma_{\text{sr}} < \gamma_2^{\text{th}}$, is

$$f_{\gamma_{\text{sr}}|\gamma_1^{\text{th}} < \gamma_{\text{sr}} < \gamma_2^{\text{th}}}(\gamma_{\text{sr}}) = \frac{\text{e}^{-\gamma_{\text{sr}}/\sigma_{\text{sr}}^2}}{\sigma_{\text{sr}}^2 \left(\text{e}^{-\gamma_1^{\text{th}}/\sigma_{\text{sr}}^2} - \text{e}^{-\gamma_2^{\text{th}}/\sigma_{\text{sr}}^2}\right)} \tag{4.12}$$

[5]It should be mentioned here that because the average SNRs of the channel links from the source to all the relays are the same, the average BERs for i_1 and i_2 at any relays are the same. To simplify our notation, the relay index can be dropped, i.e., ε_{r} and γ_{sr} are used.

Using [C4-21], [C4-22, Eq. 3.361.1], the average BER of i_1 at the selected relay given $\gamma_1^{\rm th} < \gamma_{\rm sr} < \gamma_2^{\rm th}$ can be found as follows:

$$\begin{aligned} P(\varepsilon_{\rm r}, i_1 \Big| \gamma_1^{\rm th} < \gamma_{\rm sr} < \gamma_2^{\rm th}) &= \frac{1}{{\rm e}^{-\gamma_1^{\rm th}/\sigma_{\rm sr}^2} - {\rm e}^{-\gamma_2^{\rm th}/\sigma_{\rm sr}^2}} \frac{1}{2\sigma_{\rm sr}^2} \int_{\gamma_1^{\rm th}}^{\gamma_2^{\rm th}} \left[Q\left(\frac{(\alpha+1)\sqrt{2\gamma_{\rm sr}}}{\sqrt{\alpha^2+1}} \right) \right. \\ &\quad \left. + Q\left(\frac{(\alpha-1)\sqrt{2\gamma_{\rm sr}}}{\sqrt{\alpha^2+1}} \right) \right] {\rm e}^{-\gamma_{\rm sr}/\sigma_{\rm sr}^2} {\rm d}\gamma_{\rm sr} \\ &= \frac{1}{2({\rm e}^{-\gamma_1^{\rm th}/\sigma_{\rm sr}^2} - {\rm e}^{-\gamma_2^{\rm th}/\sigma_{\rm sr}^2})} \left[I_1\left(\frac{2(\alpha+1)^2}{\alpha^2+1}, \sigma_{\rm sr}^2, \gamma_1^{\rm th} \right) - I_1\left(\frac{2(\alpha+1)^2}{\alpha^2+1}, \sigma_{\rm sr}^2, \gamma_2^{\rm th} \right) \right. \\ &\quad \left. + I_1\left(\frac{2(\alpha-1)^2}{\alpha^2+1}, \sigma_{\rm sr}^2, \gamma_1^{\rm th} \right) - I_1\left(\frac{2(\alpha-1)^2}{\alpha^2+1}, \sigma_{\rm sr}^2, \gamma_2^{\rm th} \right) \right] \end{aligned} \quad (4.13)$$

where

$$I_1(a, \sigma^2, x) = \int_x^\infty Q(\sqrt{at}) \frac{{\rm e}^{-t/\sigma^2}}{\sigma^2} {\rm d}t = {\rm e}^{-x/\sigma^2} Q\left(\sqrt{ax}\right) - \sqrt{\frac{a}{\frac{2}{\sigma^2}+a}} Q\left(\sqrt{x\left(\frac{2}{\sigma^2}+a\right)} \right). \quad (4.14)$$

By substituting (4.10), (4.11) and (4.13) into (4.9), one can compute the BER of i_1 for the case Φ_2.

Similarly, consider the case Φ_3, i.e., $|\Omega_2| > 0$, $|\Omega_3| = 0$ and the selected relay decodes i_1 correctly. The BER of i_1 under Φ_3 can be found as

$$\begin{aligned} P(\varepsilon_{\rm d}, i_1, \Phi_3) &= \sum_{l=1}^{K} \left[1 - P(\varepsilon_{\rm r}, i_1 \Big| \gamma_1^{\rm th} < \gamma_{\rm sr} < \gamma_2^{\rm th}) \right] \\ &\quad \times P_{\Phi_3}(\varepsilon_{\rm d}, i_1 \Big| |\Omega_2| = l, |\Omega_3| = 0) P(|\Omega_2| = l, |\Omega_3| = 0). \end{aligned} \quad (4.15)$$

With sufficiently high SNR[6], $P(\varepsilon_{\rm r}, i_1 \Big| \gamma_1^{\rm th} < \gamma_{\rm sr} < \gamma_2^{\rm th}) = O(1/{\rm SNR})$, $P_{\Phi_2}(\varepsilon_{\rm d}, i_1 \Big| |\Omega_2| = l, |\Omega_3| = 0)$ is given as in (4.10), and $P_{\Phi_3}(\varepsilon_{\rm d}, i_1 \Big| |\Omega_2| = l, |\Omega_3| = 0) < O(1/{\rm SNR}^2)$ (see Appendix 4.A). Therefore, $P(\varepsilon_{\rm d}, i_1, \Phi_3) \ll P(\varepsilon_{\rm d}, i_1, \Phi_2)$ and we can approximate $P(\varepsilon_{\rm d}, i_1, \Phi_3) \approx 0$.

Under both Φ_2 and Φ_3 cases, the destination uses the received signal in the first phase to decode i_2. The BERs of i_2 in both cases Φ_2 and Φ_3 are equal and calculated as

$$P(\varepsilon_{\rm d}, i_2, \Phi_2) = P(\varepsilon_{\rm d}, i_2, \Phi_3) = \sum_{l=1}^{K} P(\varepsilon_{\rm d}, i_2 \Big| |\Omega_1| = K) P(|\Omega_2| = l, |\Omega_3| = 0). \quad (4.16)$$

[6]With two positive real functions $f(x)$ and $g(x)$, we say $f(x) = O(g(x))$ if $\limsup_{x\to\infty} \frac{f(x)}{g(x)} < \infty$.

The remaining cases, namely Φ_4 to Φ_7, are related to the scenario that the instantaneous SNR of the S-R_k link (where R_k is the selected relay) is larger than the threshold $\gamma_2^{\rm th}$, i.e., $|\Omega_3| > 0$. The difference between these cases is the correctness of the decoded bits i_1 and i_2 at the selected relay. When Φ_4 occurs, the BER of i_m, $m = 1, 2$, can be found as

$$\begin{aligned} P(\varepsilon_{\rm d}, i_m, \Phi_4) = &\sum_{l=1}^{K} \left[1 - P(\varepsilon_{\rm r}, i_1 | \gamma_{\rm sr} > \gamma_2^{\rm th})\right] \\ &\times \left[1 - P(\varepsilon_{\rm r}, i_2 | \gamma_{\rm sr} > \gamma_2^{\rm th})\right] P_{\Phi_4}(\varepsilon_{\rm d}, i_m \Big| |\Omega_3| = l) P(|\Omega_3| = l) \end{aligned} \tag{4.17}$$

where $P_{\Phi_4}(\varepsilon_{\rm d}, i_m \Big| |\Omega_3| = l)$ is the BER of i_m given $|\Omega_3| = l$ and $P(|\Omega_3| = l)$ is the probability of $|\Omega_3| = l$ occurring. They can be written as (see Appendix 4.B):

$$\begin{aligned} &P_{\Phi_4}(\varepsilon_{\rm d}, i_1 \Big| |\Omega_3| = l) \\ &\quad = \sum_{j=0}^{l-1} \binom{l-1}{j} \frac{(-1)^j}{2(j+1)} \left[I_2\left(\sigma_{\rm sr}^2, \frac{\sigma_{\rm rd}^2}{j+1}, \frac{(\alpha+1)^2}{\alpha^2+1}\right) + I_2\left(\sigma_{\rm sr}^2, \frac{\sigma_{\rm rd}^2}{j+1}, \frac{(\alpha-1)^2}{\alpha^2+1}\right)\right], \end{aligned} \tag{4.18}$$

$$\begin{aligned} P_{\Phi_4}(\varepsilon_{\rm d}, i_2 \Big| |\Omega_3| = l) = &\sum_{j=0}^{l-1} \binom{l-1}{j} \frac{(-1)^j}{2(j+1)} \left[I_2\left(\sigma_{\rm sr}^2, \frac{\sigma_{\rm rd}^2}{j+1}, \frac{1}{\alpha^2+1}\right)\right. \\ &\left. - I_2\left(\sigma_{\rm sr}^2, \frac{\sigma_{\rm rd}^2}{j+1}, \frac{(2\alpha+1)^2}{\alpha^2+1}\right) + I_2\left(\sigma_{\rm sr}^2, \frac{\sigma_{\rm rd}^2}{j+1}, \frac{(2\alpha-1)^2}{\alpha^2+1}\right)\right], \end{aligned} \tag{4.19}$$

$$P(|\Omega_3| = l) = \binom{K}{l} \left[\exp\left(-\frac{\gamma_2^{\rm th}}{\sigma_{\rm sr}^2}\right)\right]^l \left[1 - \exp\left(-\frac{\gamma_2^{\rm th}}{\sigma_{\rm sr}^2}\right)\right]^{K-l}, \tag{4.20}$$

where $I_2(\cdot)$ is as (4.49) in Appendix 4.B.

Furthermore, $P(\varepsilon_{\rm r}, i_m \Big| \gamma_{\rm sr} > \gamma_2^{\rm th})$, the average BERs of i_m at the selected relay given $\gamma_{\rm sr} > \gamma_2^{\rm th}$, can be found as [C4-20]

$$\begin{aligned} P(\varepsilon_{\rm r}, i_1 \Big| \gamma_{\rm sr}^{\rm th} > \gamma_2^{\rm th}) &= \frac{{\rm e}^{\gamma_2^{\rm th}/\sigma_{\rm sr}^2}}{2\sigma_{\rm sr}^2} \int_{\gamma_2^{\rm th}}^{\infty} \left[Q\left(\frac{(\alpha+1)\sqrt{2\gamma_{\rm sr}}}{\sqrt{\alpha^2+1}}\right) + Q\left(\frac{(\alpha-1)\sqrt{2\gamma_{\rm sr}}}{\sqrt{\alpha^2+1}}\right)\right] {\rm e}^{-\gamma_{\rm sr}/\sigma_{\rm sr}^2} {\rm d}\gamma_{\rm sr} \\ &= \frac{{\rm e}^{\gamma_2^{\rm th}/\sigma_{\rm sr}^2}}{2} \left[I_1\left(\frac{2(\alpha+1)^2}{\alpha^2+1}, \sigma_{\rm sr}^2, \gamma_2^{\rm th}\right) + I_1\left(\frac{2(\alpha-1)^2}{\alpha^2+1}, \sigma_{\rm sr}^2, \gamma_2^{\rm th}\right)\right] \end{aligned} \tag{4.21}$$

$$P(\varepsilon_{\rm r}, i_2|\gamma_{\rm sr}^{\rm th} > \gamma_2^{\rm th}) = \frac{{\rm e}^{\gamma_2^{\rm th}/\sigma_{\rm sr}^2}}{4\sigma_{\rm sr}^2}\int_{\gamma_2^{\rm th}}^{\infty}\left[4Q\left(\frac{\sqrt{2\gamma_{sd}}}{\sqrt{\alpha^2+1}}\right)\right.$$
$$\left. - 2Q\left(\frac{(2\alpha+1)\sqrt{2\gamma_{sd}}}{\sqrt{\alpha^2+1}}\right) + 2Q\left(\frac{(2\alpha-1)\sqrt{2\gamma_{sd}}}{\sqrt{\alpha^2+1}}\right)\right]{\rm e}^{-\gamma_{\rm sr}/\sigma_{\rm sr}^2}{\rm d}\gamma_{\rm sr}$$
$$= \frac{{\rm e}^{\gamma_2^{\rm th}/\sigma_{\rm sr}^2}}{2}\left[2I_1\left(\frac{2}{\alpha^2+1}, \sigma_{\rm sr}^2, \gamma_2^{\rm th}\right) - I_1\left(\frac{2(2\alpha+1)^2}{\alpha^2+1}, \sigma_{\rm sr}^2, \gamma_2^{\rm th}\right)\right.$$
$$\left. + I_1\left(\frac{2(2\alpha-1)^2}{\alpha^2+1}, \sigma_{\rm sr}^2, \gamma_2^{\rm th}\right)\right] \quad (4.22)$$

By substituting (4.18)–(4.22) into (4.17), the average BERs of i_1 and i_2 for the case Φ_4 can be computed analytically. Similarly, the BERs of i_m, $m = 1, 2$, under the cases Φ_5 to Φ_7, can be found, respectively, as

$$P(\varepsilon_{\rm d}, i_m, \Phi_5) = \sum_{l=1}^{K} P(\varepsilon_{\rm r}, i_1\Big|\gamma_{\rm sr} > \gamma_2^{\rm th})$$
$$\times\left[1 - P(\varepsilon_{\rm r}, i_2\Big|\gamma_{\rm sr} > \gamma_2^{\rm th})\right] P_{\Phi_5}(\varepsilon_{\rm d}, i_m\Big||\Omega_3| = l)P(|\Omega_3| = l) \quad (4.23)$$

$$P(\varepsilon_{\rm d}, i_m, \Phi_6) = \sum_{l=1}^{K}\left[1 - P(\varepsilon_{\rm r}, i_1\Big|\gamma_{\rm sr} > \gamma_2^{\rm th})\right]$$
$$\times P(\varepsilon_{\rm r}, i_2\Big|\gamma_{\rm sr} > \gamma_2^{\rm th})P_{\Phi_6}(\varepsilon_{\rm d}, i_m\Big||\Omega_3| = l)P(|\Omega_3| = l) \quad (4.24)$$

$$P(\varepsilon_{\rm d}, i_m, \Phi_7) = \sum_{l=1}^{K} P(\varepsilon_{\rm r}, i_1\Big|\gamma_{\rm sr} > \gamma_2^{\rm th})$$
$$\times P(\varepsilon_{\rm r}, i_2\Big|\gamma_{\rm sr} > \gamma_2^{\rm th})P_{\Phi_7}(\varepsilon_{\rm d}, i_m\Big||\Omega_3| = l)P(|\Omega_3| = l) \quad (4.25)$$

where (see Appendix 4.B)

$$P_{\Phi_5}(\varepsilon_{\rm d}, i_1\Big||\Omega_3| = l) \approx \frac{l}{2}\sum_{j=0}^{l-1}\binom{l-1}{j}\frac{(-1)^j}{(j+1)^2}\left(\frac{\sigma_{\rm rd}^2}{\sigma_{\rm sd}^2 + \frac{\sigma_{\rm rd}^2}{j+1}} + \frac{\sigma_{\rm rd}^2}{\sigma_{\rm sd}^2 + \frac{\sigma_{\rm rd}^2}{j+1}}\right) \quad (4.26)$$

$$P_{\Phi_7}(\varepsilon_{\rm d}, i_1\Big||\Omega_3| = l)$$
$$\approx \frac{l}{2}\sum_{j=0}^{l-1}\binom{l-1}{j}\frac{(-1)^j}{(j+1)^2}\left[\frac{(\alpha-1)\sigma_{\rm rd}^2}{(\alpha+1)\sigma_{\rm sd}^2 + \frac{\alpha-1}{j+1}\sigma_{\rm rd}^2} + \frac{(\alpha+1)\sigma_{\rm rd}^2}{(\alpha+1)\sigma_{\rm sd}^2 + \frac{\alpha+1}{j+1}\sigma_{\rm rd}^2}\right] \quad (4.27)$$

$$P_{\Phi_5}(\varepsilon_{\rm d}, i_2 \Big| |\Omega_3| = l) \approx$$
$$\frac{l}{2}\sum_{j=0}^{l-1}\binom{l-1}{j}\frac{(-1)^j}{(j+1)^2}\left(\frac{(2\alpha+1)\sigma_{\rm rd}^2}{\sigma_{\rm sd}^2+\frac{2\alpha+1}{j+1}\sigma_{\rm rd}^2}-\frac{\sigma_{\rm rd}^2}{(2\alpha+1)\sigma_{\rm sd}^2+\frac{\sigma_{\rm rd}^2}{j+1}}\right) \tag{4.28}$$

$$P_{\Phi_6}(\varepsilon_{\rm d}, i_2 \Big| |\Omega_3| = l) \approx \frac{l}{2}\sum_{j=0}^{l-1}\binom{l-1}{j}\frac{(-1)^j}{j+1}\frac{2\sigma_{\rm rd}^2}{\sigma_{\rm sd}^2+(j+1)\sigma_{\rm rd}^2} \tag{4.29}$$

$$P_{\Phi_7}(\varepsilon_{\rm d}, i_2 \Big| |\Omega_3| = l) \approx$$
$$\frac{l}{2}\sum_{j=0}^{l-1}\binom{l-1}{j}\frac{(-1)^j}{(j+1)^2}\left(\frac{(2\alpha-1)\sigma_{\rm rd}^2}{\sigma_{\rm sd}^2+\frac{2\alpha-1}{j+1}\sigma_{\rm rd}^2}+\frac{\sigma_{\rm rd}^2}{(2\alpha-1)\sigma_{\rm sd}^2+\frac{\sigma_{\rm rd}^2}{j+1}}\right). \tag{4.30}$$

With a similar argument for the case $|\Omega_3| = 0$, one can verify that $P(\varepsilon_{\rm d}, i_1, \Phi_6) \ll P(\varepsilon_{\rm d}, i_1, \Phi_5)$. Therefore, we can also approximate $P(\varepsilon_{\rm d}, i_1, \Phi_6) \approx 0$.

By substituting all the related expressions into the final formulas of average BERs of two classes in (4.4), the closed-form expressions result and can be evaluated analytically. Comparison to simulation results in Section 4.4 shows that the BER approximations are very accurate. Based on the obtained average BERs, the optimal thresholds can be chosen to minimize the average BER of one class while the average BER of another class satisfies a given constraint. This is further discussed next.

4.3.2 Optimal SNR Thresholds

Given the average BERs of two different bits i_1 and i_2 expressed in (4.4), one can choose the thresholds to minimize the BER of the more protected bit i_1 when the BER of the less protected bit i_2 satisfies a constraint[7]. The optimization problem can be set up as follows:

$$(\widehat{\gamma}_1^{\rm th}, \widehat{\gamma}_2^{\rm th}) = \arg\min_{(\gamma_1^{\rm th}, \gamma_2^{\rm th})} {\rm BER}(\gamma_1^{\rm th}, \gamma_2^{\rm th}, i_1) \text{ subject to } \begin{cases} {\rm BER}(\gamma_1^{\rm th}, \gamma_2^{\rm th}, i_2) \le {\rm BER}_2 \\ 0 \le \gamma_1^{\rm th} \le \gamma_2^{\rm th} \end{cases} \tag{4.31}$$

[7]Of course one can also minimize the BER of the less protected bit i_2 when the BER of the more protected bit i_1 satisfies a constraint.

where BER_2 is the BER constraint of the less protected bit.

The above problem can be solved by some optimization techniques such as the augmented Lagrange method [C4-23] since the average BER formulas of two bits i_1 and i_2 have been set up. Here the optimization problem in (4.31) is solved by relying on the MATLAB Optimization Toolbox.

4.4 Simulation Results

This section presents analytical and simulation results to confirm the analysis of the average BERs of two different information classes presented in Section 4.3.1. In all simulations, transmission powers are set to be the same for the source and the relays. The noise components at the source and the relays are modeled as i.i.d. $\mathcal{CN}(0,1)$ random variables. The average SNR of a link i-j is represented by $\sigma_{ij}^2 = \lambda_{ij}E_i/N_0$ where λ_{ij} is a scaling factor to reflect different distances among nodes. We also use λ_1^{th} and λ_2^{th} to represent $\gamma_1^{\mathrm{th}} = \lambda_1^{\mathrm{th}}E_{\mathrm{s}}/N_0$ and $\gamma_2^{\mathrm{th}} = \lambda_2^{\mathrm{th}}E_{\mathrm{s}}/N_0$.

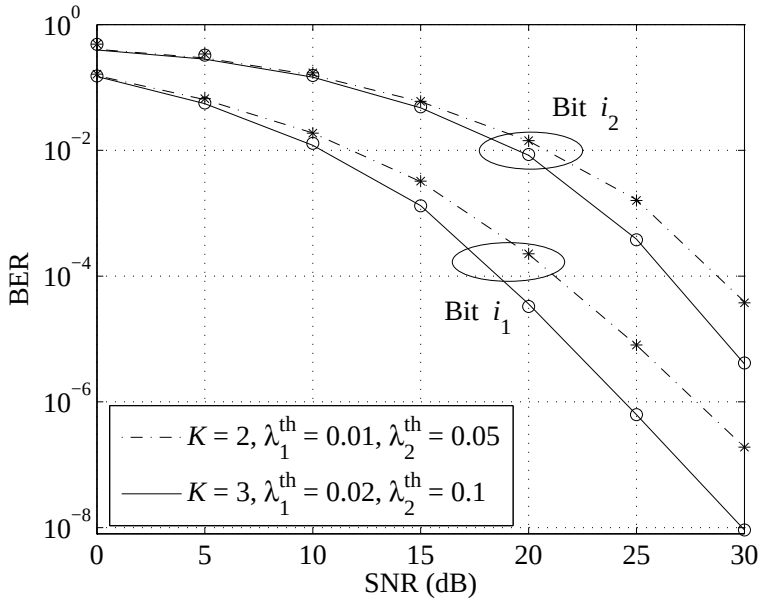

Figure 4.4 BERs of i_1 and i_2 when $\lambda_{\mathrm{sr}} = 0.5\lambda_{\mathrm{rd}} = 2\lambda_{\mathrm{sd}} = 1$. Exact analytical values are shown in lines and simulation results are shown as marker symbols.

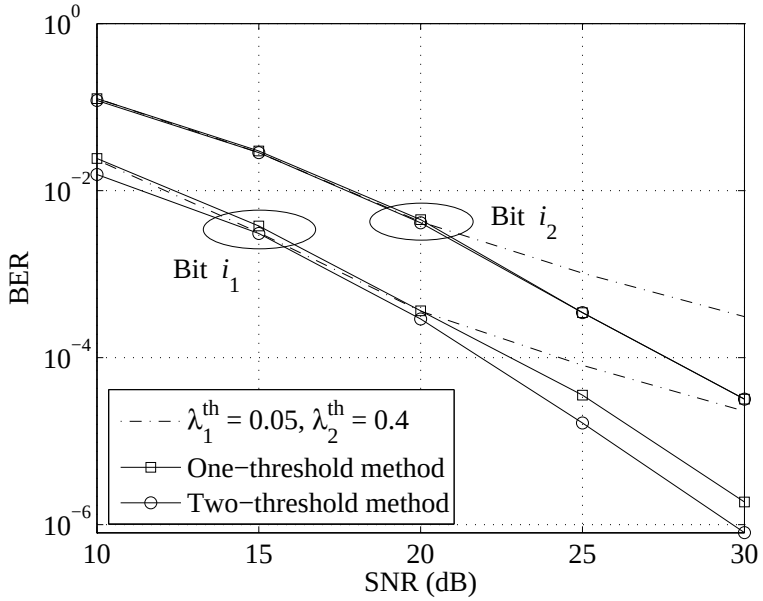

Figure 4.5 BERs of i_1 and i_2 when $\lambda_{\rm sr} = \lambda_{\rm rd} = 5\lambda_{\rm sd} = 1$, $K = 2$ and $\alpha = \frac{1}{0.4}$.

Fig. 4.4 shows the BERs of i_1 and i_2 at the destination for different values of thresholds $\lambda_1^{\rm th}$ and $\lambda_2^{\rm th}$ at various channel conditions and number of relays. Here $\alpha = d_1/d_2 = 1/0.3$ and the network is configured with 2 or 3 relays. The figure shows that the BER approximations are very accurate. Therefore the approximations are useful tool in calculating the BERs for two classes of information bits as well as to find the optimal relaying thresholds.

Then Fig. 4.5 shows the BERs of i_1 and i_2 for one-threshold and two-threshold methods with similar channel conditions of $\lambda_{\rm sr} = \lambda_{\rm rd} = 5\lambda_{\rm sd} = 1$. Here $\alpha = 1/0.4$ and $K = 2$. The thresholds for both methods are optimized and presented in Table 4.1. Observe from the figure, the BER of i_1 for two-threshold method improves compared to that for one-threshold method while the BERs of i_2 for both methods are identical. With another set of threshold values selected randomly, namely $\{\lambda_1^{\rm th} = 0.05, \lambda_2^{\rm th} = 0.4\}$, the BERs of both protected bits are significantly worse compared to that of the two-threshold method.

Finally, Fig. 4.6 shows the improvement of the more protected bit when we set BER_2 in (4.31) as in Table 4.1. The network is with 3 relays and $\alpha = 1/0.4$. The

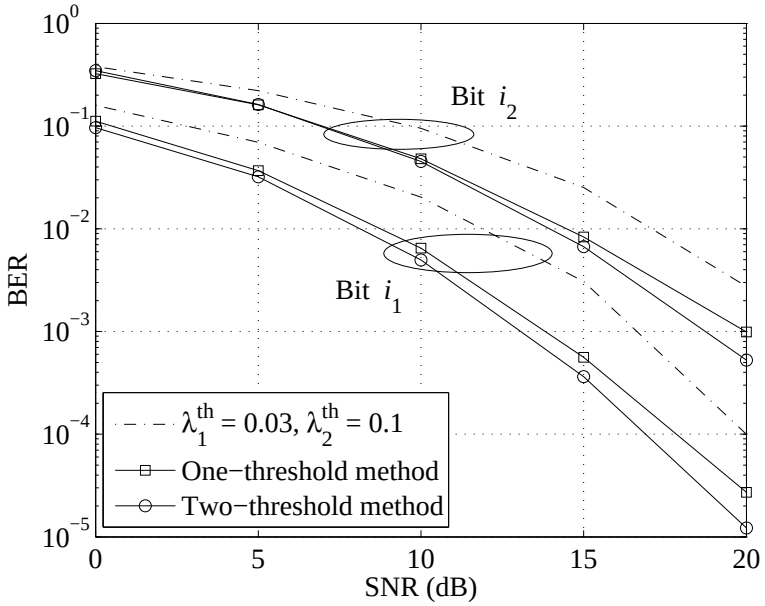

Figure 4.6 BERs of i_1 and i_2 when $\lambda_{\rm sr} = \lambda_{\rm sd} = 0.2\lambda_{\rm rd} = 1$, $K = 3$ and $\alpha = \frac{1}{0.4}$.

scaling factors of Rayleigh fading channels are set to be $\lambda_{\rm sr} = \lambda_{\rm sd} = 0.2\lambda_{\rm rd} = 1$. With the two optimal thresholds, the BER of the more protected bit is significantly improved compared to that of the arbitrary-threshold and one-threshold methods.

4.5 Conclusion

In this paper, we have obtained the average BERs for two different information classes in single relay selection networks which includes a source, K relays, and a destination. Each node is equipped with a single antenna and the channels are Rayleigh fading. A single relay is selected to cooperate with the source in transmission to the destination. The two information classes are modulated by a hierarchical 2/4-ASK constellation at the source. Based on the reliability of the set that the selected relay belongs to, the information classes can be modulated by using a hierarchical 2/4-ASK constellation, or a 2-ASK constellation, or are not transmitted to the destination. Moreover, optimal thresholds are chosen to minimize the BER for one class while the other class satisfies a given requirement. Simulation results were presented to corroborate the analytical results. Performance comparison reveals that the optimal

Table 4.1 Optimal Threshold Values.

Figures	SNR (dB)	BER_2	One-threshold method	Two-threshold method	
			$\lambda_1^{\text{th}} = \lambda_2^{\text{th}}$	λ_1^{th}	λ_2^{th}
Fig. 4.5	10	$10^{-0.5}$	0.214	0.247	10
	15	$10^{-1.5}$	0.155	0.093	0.244
	20	10^{-2}	0.090	0.054	0.192
	25	$10^{-3.5}$	0.073	0.028	0.072
	30	10^{-4}	0.143	0.071	0.143
Fig. 4.6	0	$10^{-0.3}$	0.827	0.854	10.020
	5	$10^{-0.5}$	0.700	0.566	1.298
	10	10^{-1}	0.536	0.393	0.832
	15	10^{-2}	0.325	0.247	0.597
	20	10^{-3}	0.168	0.107	0.227

thresholds improve the error performance significantly.

4.A BER Calculations when $k \in \Omega_2$

4.A.1 Case Φ_2

In this case, the selected relay R_k decodes i_1 incorrectly. The received signals at the destination in the first and second phases are written, respectively, as[8]:

$$y_{\text{sd}} = \sqrt{E_{\text{s}}} h_{\text{sd}} (\alpha s_1 + s_2) + n_{\text{sd}} \tag{4.32}$$

$$y_{\text{rd}} = \sqrt{E_{\text{r}}} h_{\text{rd}} \widehat{s}_1 + n_{\text{rd}} \tag{4.33}$$

where s_m is the symbol corresponding to bit i_m at the source, $m = 1, 2$, $\hat{s}_1$ is the symbol corresponding to bit i_1 at the selected relay. One has $s_1, s_2 = \pm d_2 = \pm \frac{1}{\sqrt{\alpha^2+1}}$, $\widehat{s}_1 = -\frac{1}{d_2} s_1$.

[8]Again, we drop the index of the selected relay for notational simplicity.

The sufficient statistic after combining two received signals using MRC is:

$$y_{\rm d} = \left(\alpha|h_{\rm sd}|^2\sqrt{E_{\rm s}} - \sqrt{\alpha^2+1}|h_{\rm rd}|^2\sqrt{E_{\rm r}}\right)s_1 + |h_{\rm sd}|^2\sqrt{E_{\rm s}}s_2 + h_{\rm sd}^* n_{\rm sd} + h_{\rm rd}^* n_{\rm rd}. \quad (4.34)$$

The average BER of the first bit i_1 in this case can be computed as

$$\begin{aligned} P_{\Phi_2}\left(\varepsilon_{\rm d}, i_1 \middle| |\Omega_2| = l, |\Omega_3| = 0\right) &= \frac{1}{4}\Big\{P_{\Phi_2}(\varepsilon_{\rm d}, i_1 \big| |\Omega_2| = l, |\Omega_3| = 0, 00 \text{ sent}) \\ &+ P_{\Phi_2}(\varepsilon_{\rm d}, i_1 \big| |\Omega_2| = l, |\Omega_3| = 0, 01 \text{ sent}) + P_{\Phi_2}(\varepsilon_{\rm d}, i_1 \big| |\Omega_2| = l, |\Omega_3| = 0, 10 \text{ sent}) \\ &+ P_{\Phi_2}(\varepsilon_{\rm d}, i_1 \big| |\Omega_2| = l, |\Omega_3| = 0, 11 \text{ sent})\Big\} \\ &= \mathbb{E}_{\gamma_{\rm sd},\gamma_{\rm rd}}\left\{\frac{1}{2}Q\left(\frac{\frac{(\alpha-1)}{\sqrt{\alpha^2+1}}\gamma_{\rm sd} - \gamma_{\rm rd}}{\sqrt{(\gamma_{\rm sd}+\gamma_{\rm rd})/2}}\right) + \frac{1}{2}Q\left(\frac{\frac{(\alpha+1)}{\sqrt{\alpha^2+1}}\gamma_{\rm sd} - \gamma_{\rm rd}}{\sqrt{(\gamma_{\rm sd}+\gamma_{\rm rd})/2}}\right)\right\} \quad (4.35) \end{aligned}$$

One can verify that the pdf of $\gamma_{\rm rd}$ given $\{|\Omega_2| = l, |\Omega_3| = 0\}$ is

$$f_{\gamma_{\rm rd}\left||\Omega_2|=l,|\Omega_3|=0\right.}(\gamma_{\rm rd}) = \frac{l}{\sigma_{\rm rd}^2}\sum_{j=0}^{l-1}\binom{l-1}{j}(-1)^j \exp\left(-(j+1)\frac{\gamma_{\rm rd}}{\sigma_{\rm rd}^2}\right). \quad (4.36)$$

Normally, the R_k-D link has a stronger impact on the decision at the destination than the S-D link. Therefore, we can approximate each component in (4.35) under the condition of $\{\mu\gamma_{\rm sd} - \nu\gamma_{\rm rd} < 0\}$ [C4-24] where $\mu > 0, \nu > 0$ are two parameters in $Q\left(\frac{\mu\gamma_{\rm sd}-\nu\gamma_{\rm rd}}{\sqrt{(\gamma_{\rm sd}+\gamma_{\rm rd})/2}}\right)$, i.e.,

$$\int_0^\infty\int_0^\infty Q\left(\frac{\mu\gamma_{\rm sd} - \nu\gamma_{\rm rd}}{\sqrt{(\gamma_{\rm sd}+\gamma_{\rm rd})/2}}\right)\frac{1}{\sigma_{\rm sd}^2\sigma_{\rm rd}^2}{\rm e}^{-\gamma_{\rm sd}/\sigma_{\rm sd}^2}{\rm e}^{-\gamma_{\rm rd}/\sigma_{\rm rd}^2}{\rm d}\gamma_{\rm sd}{\rm d}\gamma_{\rm rd} \approx \frac{\nu\sigma_{\rm rd}^2}{\mu\sigma_{\rm sd}^2 + \nu\sigma_{\rm rd}^2} \quad (4.37)$$

Since $\gamma_{\rm sd}$ and $\gamma_{\rm rd}$ are independent, (4.35) can be approximated as

$$\begin{aligned} &P_{\Phi_2}(\varepsilon_{\rm d}, i_1 \big| |\Omega_2| = l, |\Omega_3| = 0) \\ &\qquad \approx \frac{l}{2}\sum_{j=0}^{l-1}\binom{l-1}{j}\frac{(-1)^j}{(j+1)^2}\left(\frac{\sigma_{\rm rd}^2}{\frac{\alpha+1}{\sqrt{\alpha^2+1}}\sigma_{\rm sd}^2 + \frac{\sigma_{\rm rd}^2}{j+1}} + \frac{\sigma_{\rm rd}^2}{\frac{\alpha-1}{\sqrt{\alpha^2+1}}\sigma_{\rm sd}^2 + \frac{\sigma_{\rm rd}^2}{j+1}}\right) \quad (4.38) \end{aligned}$$

4.A.2 Case Φ_3

In this case, the selected relay R_k decodes i_1 correctly. The received signals at the destination in two phases are similar to (4.32) and (4.33). However, $\widehat{s}_1 = \frac{1}{d_2}s_1$.

The destination combines two received signals using MRC and produces the following sufficient statistic:

$$\begin{aligned} y_{\mathrm{d}} &= \sqrt{E_{\mathrm{s}}}|h_{\mathrm{sd}}|^2(\alpha s_1 + s_2) + \sqrt{E_{\mathrm{r}}}|h_{\mathrm{rd}}|^2\widehat{s}_1 + h_{\mathrm{sd}}^* n_{\mathrm{sd}} + h_{\mathrm{rd}}^* n_{\mathrm{rd}} \\ &= \left(\alpha|h_{\mathrm{sd}}|^2\sqrt{E_{\mathrm{s}}} + \sqrt{\alpha^2+1}|h_{\mathrm{rd}}|^2\sqrt{E_{\mathrm{r}}}\right)s_1 + |h_{\mathrm{sd}}|^2\sqrt{E_{\mathrm{s}}}s_2 + h_{\mathrm{sd}}^* n_{\mathrm{sd}} + h_{\mathrm{rd}}^* n_{\mathrm{rd}}. \quad (4.39) \end{aligned}$$

Similar to the case Φ_2, the BER of i_1 is as follows:

$$\begin{aligned} P_{\Phi_3}(\varepsilon_{\mathrm{d}}, i_1\Big||\Omega_2| = l, |\Omega_3| = 0) &= \frac{1}{4}\Big\{P_{\Phi_3}(\varepsilon_{\mathrm{d}}, i_1\Big||\Omega_2| = l, |\Omega_3| = 0, 00 \text{ sent}) \\ &+P_{\Phi_3}(\varepsilon_{\mathrm{d}}, i_1\Big||\Omega_2| = l, |\Omega_3| = 0, 01 \text{ sent}) + P_{\Phi_3}(\varepsilon_{\mathrm{d}}, i_1\Big||\Omega_2| = l, |\Omega_3| = 0, 10 \text{ sent}) \\ &+P_{\Phi_3}(\varepsilon_{\mathrm{d}}, i_1\Big||\Omega_2| = l, |\Omega_3| = 0, 11 \text{ sent})\Big\} \\ &= \mathbb{E}_{\gamma_{\mathrm{sd}},\gamma_{\mathrm{rd}}}\left\{\frac{1}{2}Q\left(\frac{\frac{(\alpha+1)}{\sqrt{\alpha^2+1}}\gamma_{\mathrm{sd}} + \gamma_{\mathrm{rd}}}{\sqrt{(\gamma_{\mathrm{sd}}+\gamma_{\mathrm{rd}})/2}}\right) + \frac{1}{2}Q\left(\frac{\frac{(\alpha-1)}{\sqrt{\alpha^2+1}}\gamma_{\mathrm{sd}} + \gamma_{\mathrm{rd}}}{\sqrt{(\gamma_{\mathrm{sd}}+\gamma_{\mathrm{rd}})/2}}\right)\right\} \quad (4.40) \end{aligned}$$

4.B BER Calculations when $k \in \Omega_3$

4.B.1 Case Φ_4

In this case, the received signals at the destination in two phases are:

$$y_{\mathrm{sd}} = \sqrt{E_{\mathrm{s}}}h_{\mathrm{sd}}(\alpha s_1 + s_2) + n_{\mathrm{sd}} \quad (4.41)$$

$$y_{\mathrm{rd}} = \sqrt{E_{\mathrm{r}}}h_{\mathrm{rd}}(\alpha\widehat{s}_1 + \widehat{s}_2) + n_{\mathrm{rd}} \quad (4.42)$$

where $s_1, s_2 = \pm d_2 = \pm\frac{1}{\sqrt{\alpha^2+1}}$, $\widehat{s}_1 = s_1$ and $\widehat{s}_2 = s_2$. Using MRC to combine the two signals gives:

$$\begin{aligned} y_{\mathrm{d}} &= \sqrt{E_{\mathrm{s}}}|h_{\mathrm{sd}}|^2(\alpha s_1 + s_2) + \sqrt{E_{\mathrm{r}}}|h_{\mathrm{rd}}|^2(\alpha\widehat{s}_1 + \widehat{s}_2) + h_{\mathrm{sd}}^* n_{\mathrm{sd}} + h_{\mathrm{rd}}^* n_{\mathrm{rd}} \\ &= \alpha\left(\sqrt{E_{\mathrm{s}}}|h_{\mathrm{sd}}|^2 + \sqrt{E_{\mathrm{r}}}|h_{\mathrm{rd}}|^2\right)s_1 + \left(\sqrt{E_{\mathrm{s}}}|h_{\mathrm{sd}}|^2 + \sqrt{E_{\mathrm{r}}}|h_{\mathrm{rd}}|^2\right)s_2 + h_{\mathrm{sd}}^* n_{\mathrm{sd}} + h_{\mathrm{rd}}^* n_{\mathrm{rd}} \end{aligned} \quad (4.43)$$

The probabilities of error of i_1 and i_2 are given, respectively, as

$$\begin{aligned} &P_{\Phi_4}(\varepsilon_{\mathrm{d}}, i_1\Big||\Omega_3| = l) = \\ &\mathbb{E}_{\gamma_{\mathrm{sd}},\gamma_{\mathrm{rd}}}\left\{\frac{1}{2}Q\left(\frac{(\alpha+1)\sqrt{2(\gamma_{\mathrm{sd}}+\gamma_{\mathrm{rd}})}}{\sqrt{\alpha^2+1}}\right) + \frac{1}{2}Q\left(\frac{(\alpha-1)\sqrt{2(\gamma_{\mathrm{sd}}+\gamma_{\mathrm{rd}})}}{\sqrt{\alpha^2+1}}\right)\right\} \end{aligned} \quad (4.44)$$

$$P_{\Phi_4}(\varepsilon_{\rm d}, i_2\Big||\Omega_3| = l) = \mathbb{E}_{\gamma_{\rm sd},\gamma_{\rm rd}}\left\{Q\left(\frac{\sqrt{2(\gamma_{\rm sd}+\gamma_{\rm rd})}}{\sqrt{\alpha^2+1}}\right)\right.$$
$$\left. - \frac{1}{2}Q\left(\frac{(2\alpha+1)\sqrt{2(\gamma_{\rm sd}+\gamma_{\rm rd})}}{\sqrt{\alpha^2+1}}\right) + \frac{1}{2}Q\left(\frac{(2\alpha-1)\sqrt{2(\gamma_{\rm sd}+\gamma_{\rm rd})}}{\sqrt{\alpha^2+1}}\right)\right\} \quad (4.45)$$

The pdf of $\gamma_{\rm rd}$ given $|\Omega_3| = l$ can be calculated as

$$f_{\gamma_{\rm rd}\Big||\Omega_3|=l}(\gamma_{\rm rd}) = \frac{l}{\sigma_{\rm rd}^2}\sum_{j=0}^{l-1}\binom{l-1}{j}(-1)^j \exp\left(-(j+1)\frac{\gamma_{\rm rd}}{\sigma_{\rm rd}^2}\right) \quad (4.46)$$

Therefore, one can easily verify that

$$P_{\Phi_4}(\varepsilon_{\rm d}, i_1\Big||\Omega_3| = l)$$
$$= \mathbb{E}_{\gamma_{\rm sd},\gamma_{\rm rd}}\left\{\frac{1}{2}Q\left(\frac{(\alpha+1)\sqrt{2(\gamma_{\rm sd}+\gamma_{\rm rd})}}{\sqrt{\alpha^2+1}}\right) + \frac{1}{2}Q\left(\frac{(\alpha-1)\sqrt{2(\gamma_{\rm sd}+\gamma_{\rm rd})}}{\sqrt{\alpha^2+1}}\right)\right\}$$
$$= \frac{1}{2}\sum_{j=0}^{l-1}\binom{l-1}{j}\frac{(-1)^j}{j+1}\left[I_2\left(\sigma_{\rm sr}^2, \frac{\sigma_{\rm rd}^2}{j+1}, \frac{(\alpha+1)^2}{\alpha^2+1}\right) + I_2\left(\sigma_{\rm sr}^2, \frac{\sigma_{\rm rd}^2}{j+1}, \frac{(\alpha-1)^2}{\alpha^2+1}\right)\right] \quad (4.47)$$

$$P_{\Phi_4}(\varepsilon_{\rm d}, i_2\Big||\Omega_3| = l) = \mathbb{E}_{\gamma_{\rm sd},\gamma_{\rm rd}}\left\{Q\left(\frac{\sqrt{2(\gamma_{\rm sd}+\gamma_{\rm rd})}}{\sqrt{\alpha^2+1}}\right)\right.$$
$$\left. - \frac{1}{2}Q\left(\frac{(2\alpha+1)\sqrt{2(\gamma_{\rm sd}+\gamma_{\rm rd})}}{\sqrt{\alpha^2+1}}\right) + \frac{1}{2}Q\left(\frac{(2\alpha-1)\sqrt{2(\gamma_{\rm sd}+\gamma_{\rm rd})}}{\sqrt{\alpha^2+1}}\right)\right\}$$
$$= \frac{1}{2}\sum_{j=0}^{l-1}\binom{l-1}{j}\frac{(-1)^j}{j+1}\left[I_2\left(\sigma_{\rm sr}^2, \frac{\sigma_{\rm rd}^2}{j+1}, \frac{1}{\alpha^2+1}\right)\right.$$
$$\left. - I_2\left(\sigma_{\rm sr}^2, \frac{\sigma_{\rm rd}^2}{j+1}, \frac{(2\alpha+1)^2}{\alpha^2+1}\right) + I_2\left(\sigma_{\rm sr}^2, \frac{\sigma_{\rm rd}^2}{j+1}, \frac{(2\alpha-1)^2}{\alpha^2+1}\right)\right] \quad (4.48)$$

where

$$I_2(\sigma_{\rm sr}^2, \sigma_{\rm rd}^2, \beta) = \begin{cases} \frac{1}{2}\left(1 - \sqrt{\frac{\beta\sigma_{\rm rd}^2}{1+\beta\sigma_{\rm rd}^2}}\right)^2\left(1 + \frac{1}{2}\sqrt{\frac{\beta\sigma_{\rm rd}^2}{1+\beta\sigma_{\rm rd}^2}}\right), & \text{if } \sigma_{\rm rd}^2 = \sigma_{\rm sd}^2; \\ \frac{1}{2}\left(1 - \frac{\sigma_{\rm sd}^2\sqrt{\frac{\beta\sigma_{\rm sd}^2}{1+\beta\sigma_{\rm sd}^2}} - \sigma_{\rm rd}^2\sqrt{\frac{\beta\sigma_{\rm rd}^2}{1+\beta\sigma_{\rm rd}^2}}}{\sigma_{\rm sd}^2 - \sigma_{\rm rd}^2}\right), & \text{if } \sigma_{\rm rd}^2 \neq \sigma_{\rm sd}^2. \end{cases} \quad (4.49)$$

4.B.2 Cases Φ_5 to Φ_7

Similar to the case Φ_4, the combination of two received signals by using MRC is

$$\begin{aligned} y_{\rm d} &= \sqrt{E_{\rm s}}|h_{\rm sd}|^2(\alpha s_1 + s_2) + \sqrt{E_{\rm r}}|h_{\rm rd}|^2(\alpha\widehat{s}_1 + \widehat{s}_2) + h_{\rm sd}^* n_{\rm sd} + h_{\rm rd}^* n_{\rm rd} \\ &= \alpha\left(\sqrt{E_{\rm s}}|h_{\rm sd}|^2 s_1 + \sqrt{E_{\rm r}}|h_{\rm rd}|^2\widehat{s}_1\right) + \left(\sqrt{E_{\rm s}}|h_{\rm sd}|^2 s_2 + \sqrt{E_{\rm r}}|h_{\rm rd}|^2\widehat{s}_2\right) + h_{\rm sd}^* n_{\rm sd} + h_{\rm rd}^* n_{\rm rd} \end{aligned} \tag{4.50}$$

where $s_1, s_2 = \pm d_2 = \pm\frac{1}{\sqrt{\alpha^2+1}}$, $\widehat{s}_1 = \pm s_1$ and $\widehat{s}_2 = \pm s_2$.

With the case Φ_5, the first bit is decoded incorrectly at the selected relay, however, the second bit is decoded correctly, i.e., $\widehat{s}_1 = -s_1$ and $\widehat{s}_2 = s_2$. Therefore (4.50) becomes

$$y_{\rm d} = \alpha\left(\sqrt{E_{\rm s}}|h_{\rm sd}|^2 - \sqrt{E_{\rm r}}|h_{\rm rd}|^2\right)s_1 + \left(\sqrt{E_{\rm s}}|h_{\rm sd}|^2 + \sqrt{E_{\rm r}}|h_{\rm rd}|^2\right)s_2 + h_{\rm sd}^* n_{\rm sd} + h_{\rm rd}^* n_{\rm rd} \tag{4.51}$$

The average BERs of i_1 and i_2 can be calculated as

$$\begin{aligned} P_{\Phi_5}(\varepsilon_{\rm d}, i_1\Big||\Omega_3| = l) &= \frac{1}{4}\Big\{P_{\Phi_5}(\varepsilon_{\rm d}, i_1\Big||\Omega_3| = l, 00 \text{ sent}) + P_{\Phi_5}(\varepsilon_{\rm d}, i_1\Big||\Omega_3| = l, 01 \text{ sent}) \\ &\quad + P_{\Phi_5}(\varepsilon_{\rm d}, i_1\Big||\Omega_3| = l, 10 \text{ sent}) + P_{\Phi_5}(\varepsilon_{\rm d}, i_1\Big||\Omega_3| = l, 11 \text{ sent})\Big\} \\ &= \mathbb{E}_{\gamma_{\rm sd},\gamma_{\rm rd}}\left\{\frac{1}{2}Q\left(\frac{\frac{(\alpha+1)}{\sqrt{\alpha^2+1}}\gamma_{\rm sd} - \frac{(\alpha+1)}{\sqrt{\alpha^2+1}}\gamma_{\rm rd}}{\sqrt{(\gamma_{\rm sd}+\gamma_{\rm rd})/2}}\right) + \frac{1}{2}Q\left(\frac{\frac{(\alpha-1)}{\sqrt{\alpha^2+1}}\gamma_{\rm sd} - \frac{(\alpha-1)}{\sqrt{\alpha^2+1}}\gamma_{\rm rd}}{\sqrt{(\gamma_{\rm sd}+\gamma_{\rm rd})/2}}\right)\right\} \end{aligned} \tag{4.52}$$

$$\begin{aligned} &P_{\Phi_5}(\varepsilon_{\rm d}, i_2\Big||\Omega_3| = l) = \\ &\quad \mathbb{E}_{\gamma_{\rm sd},\gamma_{\rm rd}}\left\{\frac{1}{2}Q\left(\frac{\frac{1}{\sqrt{\alpha^2+1}}\gamma_{\rm sd} - \frac{(2\alpha+1)}{\sqrt{\alpha^2+1}}\gamma_{\rm rd}}{\sqrt{(\gamma_{\rm sd}+\gamma_{\rm rd})/2}}\right) - \frac{1}{2}Q\left(\frac{\frac{(2\alpha+1)}{\sqrt{\alpha^2+1}}\gamma_{\rm sd} - \frac{1}{\sqrt{\alpha^2+1}}\gamma_{\rm rd}}{\sqrt{(\gamma_{\rm sd}+\gamma_{\rm rd})/2}}\right)\right. \\ &\quad \left. + \frac{1}{2}Q\left(\frac{\frac{1}{\sqrt{\alpha^2+1}}\gamma_{\rm sd} + \frac{(2\alpha-1)}{\sqrt{\alpha^2+1}}\gamma_{\rm rd}}{\sqrt{(\gamma_{\rm sd}+\gamma_{\rm rd})/2}}\right) + \frac{1}{2}Q\left(\frac{\frac{(2\alpha-1)}{\sqrt{\alpha^2+1}}\gamma_{\rm sd} + \frac{1}{\sqrt{\alpha^2+1}}\gamma_{\rm rd}}{\sqrt{(\gamma_{\rm sd}+\gamma_{\rm rd})/2}}\right)\right\} \end{aligned} \tag{4.53}$$

With the pdf of $\gamma_{\rm rd}$ given in (4.46), one can approximate the average BERs of i_1 and

i_2 based on (4.37) as follows:

$$\begin{aligned}
&P_{\Phi_5}(\varepsilon_{\rm d}, i_1 \Big| |\Omega_3| = l) \\
&\quad = \mathbb{E}_{\gamma_{\rm sd},\gamma_{\rm rd}} \left\{ \frac{1}{2} Q\left(\frac{\frac{(\alpha+1)}{\sqrt{\alpha^2+1}}\gamma_{\rm sd} - \frac{(\alpha+1)}{\sqrt{\alpha^2+1}}\gamma_{\rm rd}}{\sqrt{(\gamma_{\rm sd}+\gamma_{\rm rd})/2}} \right) + \frac{1}{2} Q\left(\frac{\frac{(\alpha-1)}{\sqrt{\alpha^2+1}}\gamma_{\rm sd} - \frac{(\alpha-1)}{\sqrt{\alpha^2+1}}\gamma_{\rm rd}}{\sqrt{(\gamma_{\rm sd}+\gamma_{\rm rd})/2}} \right) \right\} \\
&\qquad \approx \frac{l}{2} \sum_{j=0}^{l-1} \binom{l-1}{j} \frac{(-1)^j}{(j+1)^2} \left(\frac{\sigma_{\rm rd}^2}{\sigma_{\rm sd}^2 + \frac{\sigma_{\rm rd}^2}{j+1}} + \frac{\sigma_{\rm rd}^2}{\sigma_{\rm sd}^2 + \frac{\sigma_{\rm rd}^2}{j+1}} \right) \quad (4.54)
\end{aligned}$$

$$\begin{aligned}
&P_{\Phi_5}(\varepsilon_{\rm d}, i_2 \Big| |\Omega_3| = l) \\
&\quad = \mathbb{E}_{\gamma_{\rm sd},\gamma_{\rm rd}} \left\{ Q\left(\frac{\frac{1}{\sqrt{\alpha^2+1}}\gamma_{\rm sd} - \frac{1}{\sqrt{\alpha^2+1}}\gamma_{\rm rd}}{\sqrt{(\gamma_{\rm sd}+\gamma_{\rm rd})/2}} \right) + \frac{1}{2} Q\left(\frac{\frac{(2\alpha+1)}{\sqrt{\alpha^2+1}}\gamma_{\rm sd} + \frac{(2\alpha-1)}{\sqrt{\alpha^2+1}}\gamma_{\rm rd}}{\sqrt{(\gamma_{\rm sd}+\gamma_{\rm rd})/2}} \right) \right. \\
&\quad \left. + \frac{1}{2} Q\left(\frac{\frac{(2\alpha-1)}{\sqrt{\alpha^2+1}}\gamma_{\rm sd} + \frac{(2\alpha+1)}{\sqrt{\alpha^2+1}}\gamma_{\rm rd}}{\sqrt{(\gamma_{\rm sd}+\gamma_{\rm rd})/2}} \right) \right\} \approx \frac{l}{2} \sum_{j=0}^{l-1} \binom{l-1}{j} \frac{(-1)^j}{j+1} \frac{2\sigma_{\rm rd}^2}{\sigma_{\rm sd}^2 + (j+1)\sigma_{\rm rd}^2} \quad (4.55)
\end{aligned}$$

Similarly, one can verify that

$$\begin{aligned}
&P_{\Phi_7}(\varepsilon_{\rm d}, i_1 \Big| |\Omega_3| = l) \\
&\quad = \mathbb{E}_{\gamma_{\rm sd},\gamma_{\rm rd}} \left\{ \frac{1}{2} Q\left(\frac{\frac{(\alpha+1)}{\sqrt{\alpha^2+1}}\gamma_{\rm sd} - \frac{(\alpha-1)}{\sqrt{\alpha^2+1}}\gamma_{\rm rd}}{\sqrt{(\gamma_{\rm sd}+\gamma_{\rm rd})/2}} \right) + \frac{1}{2} Q\left(\frac{\frac{(\alpha-1)}{\sqrt{\alpha^2+1}}\gamma_{\rm sd} - \frac{(\alpha+1)}{\sqrt{\alpha^2+1}}\gamma_{\rm rd}}{\sqrt{(\gamma_{\rm sd}+\gamma_{\rm rd})/2}} \right) \right\} \\
&\quad \approx \frac{l}{2} \sum_{j=0}^{l-1} \binom{l-1}{j} \frac{(-1)^j}{(j+1)^2} \left(\frac{(\alpha-1)\sigma_{\rm rd}^2}{(\alpha+1)\sigma_{\rm sd}^2 + \frac{\alpha-1}{j+1}\sigma_{\rm rd}^2} + \frac{(\alpha+1)\sigma_{\rm rd}^2}{(\alpha+1)\sigma_{\rm sd}^2 + \frac{\alpha+1}{j+1}\sigma_{\rm rd}^2} \right) \quad (4.56)
\end{aligned}$$

$$\begin{aligned}
&P_{\Phi_6}(\varepsilon_{\rm d}, i_2 \Big| |\Omega_3| = l) \\
&\quad = \mathbb{E}_{\gamma_{\rm sd},\gamma_{\rm rd}} \left\{ \frac{1}{2} Q\left(\frac{\frac{1}{\sqrt{\alpha^2+1}}\gamma_{\rm sd} - \frac{(2\alpha+1)}{\sqrt{\alpha^2+1}}\gamma_{\rm rd}}{\sqrt{(\gamma_{\rm sd}+\gamma_{\rm rd})/2}} \right) - \frac{1}{2} Q\left(\frac{\frac{(2\alpha+1)}{\sqrt{\alpha^2+1}}\gamma_{\rm sd} - \frac{1}{\sqrt{\alpha^2+1}}\gamma_{\rm rd}}{\sqrt{(\gamma_{\rm sd}+\gamma_{\rm rd})/2}} \right) \right. \\
&\quad \left. + \frac{1}{2} Q\left(\frac{\frac{1}{\sqrt{\alpha^2+1}}\gamma_{\rm sd} + \frac{(2\alpha-1)}{\sqrt{\alpha^2+1}}\gamma_{\rm rd}}{\sqrt{(\gamma_{\rm sd}+\gamma_{\rm rd})/2}} \right) + \frac{1}{2} Q\left(\frac{\frac{(2\alpha-1)}{\sqrt{\alpha^2+1}}\gamma_{\rm sd} + \frac{1}{\sqrt{\alpha^2+1}}\gamma_{\rm rd}}{\sqrt{(\gamma_{\rm sd}+\gamma_{\rm rd})/2}} \right) \right\} \\
&\quad \approx \frac{l}{2} \sum_{j=0}^{l-1} \binom{l-1}{j} \frac{(-1)^j}{(j+1)^2} \left(\frac{(2\alpha+1)\sigma_{\rm rd}^2}{\sigma_{\rm sd}^2 + \frac{2\alpha+1}{j+1}\sigma_{\rm rd}^2} - \frac{\sigma_{\rm rd}^2}{(2\alpha+1)\sigma_{\rm sd}^2 + \frac{\sigma_{\rm rd}^2}{j+1}} \right) \quad (4.57)
\end{aligned}$$

$$
\begin{aligned}
&P_{\Phi_7}(\varepsilon_{\mathrm{d}}, i_2 \big| |\Omega_3| = l) \\
&\quad = \mathbb{E}_{\gamma_{\mathrm{sd}},\gamma_{\mathrm{rd}}} \left\{ \frac{1}{2} Q\left(\frac{\frac{1}{\sqrt{\alpha^2+1}}\gamma_{\mathrm{sd}} - \frac{(2\alpha-1)}{\sqrt{\alpha^2+1}}\gamma_{\mathrm{rd}}}{\sqrt{(\gamma_{\mathrm{sd}}+\gamma_{\mathrm{rd}})/2}} \right) - \frac{1}{2} Q\left(\frac{\frac{(2\alpha+1)}{\sqrt{\alpha^2+1}}\gamma_{\mathrm{sd}} + \frac{1}{\sqrt{\alpha^2+1}}\gamma_{\mathrm{rd}}}{\sqrt{(\gamma_{\mathrm{sd}}+\gamma_{\mathrm{rd}})/2}} \right) \right. \\
&\qquad \left. + \frac{1}{2} Q\left(\frac{\frac{1}{\sqrt{\alpha^2+1}}\gamma_{\mathrm{sd}} + \frac{(2\alpha+1)}{\sqrt{\alpha^2+1}}\gamma_{\mathrm{rd}}}{\sqrt{(\gamma_{\mathrm{sd}}+\gamma_{\mathrm{rd}})/2}} \right) + \frac{1}{2} Q\left(\frac{\frac{(2\alpha-1)}{\sqrt{\alpha^2+1}}\gamma_{\mathrm{sd}} - \frac{1}{\sqrt{\alpha^2+1}}\gamma_{\mathrm{rd}}}{\sqrt{(\gamma_{\mathrm{sd}}+\gamma_{\mathrm{rd}})/2}} \right) \right\} \\
&\qquad \approx \frac{l}{2} \sum_{j=0}^{l-1} \binom{l-1}{j} \frac{(-1)^j}{(j+1)^2} \left(\frac{(2\alpha-1)\sigma_{\mathrm{rd}}^2}{\sigma_{\mathrm{sd}}^2 + \frac{2\alpha-1}{j+1}\sigma_{\mathrm{rd}}^2} + \frac{\sigma_{\mathrm{rd}}^2}{(2\alpha-1)\sigma_{\mathrm{sd}}^2 + \frac{\sigma_{\mathrm{rd}}^2}{j+1}} \right) \qquad (4.58)
\end{aligned}
$$

References

[C4-1] A. Sendonaris, E. Erkip, and B. Aazhang, "User cooperation diversity, Part I: System description," *IEEE Trans. Commun.*, vol. 51, no. 11, pp. 1927–1938, November 2003.

[C4-2] A. Sendonaris, E. Erkip, and B. Aazhang, "User cooperation diversity, Part II: Implementation aspects and performance analysis," *IEEE Trans. Commun.*, vol. 51, no. 11, pp. 1939–1948, November 2003.

[C4-3] Y. Jing and B. Hassibi, "Distributed space-time coding in wireless relay networks," *IEEE Trans. Wireless Commun.*, vol. 5, no. 12, pp. 3524–3536, December 2006.

[C4-4] J. Laneman and G. Wornell, "Distributed space-time-coded protocols for exploiting cooperative diversity in wireless networks," *IEEE Trans. Inform. Theory*, vol. 49, pp. 2415–2425, October 2003.

[C4-5] A. Ribeiro, X. Cai, and G. Giannakis, "Symbol error probabilities for general cooperative links," *IEEE Trans. Wireless Commun.*, vol. 4, pp. 1264–1273, May 2005.

[C4-6] A. Bletsas, H. Shin, and M. Win, "Outage optimality of opportunistic amplify-

and-forward relaying," *IEEE Commun. Letters*, vol. 11, pp. 261–263, March 2007.

[C4-7] E. Beres and R. Adve, "Selection cooperation in multi-source cooperative networks," *IEEE Trans. Wireless Commun.*, vol. 7, pp. 118–127, January 2008.

[C4-8] D. Michalopoulos and G. Karagiannidis, "Performance analysis of single relay selection in Rayleigh fading," *IEEE Trans. Wireless Commun.*, vol. 7, pp. 3718–3724, October 2008.

[C4-9] A. Calderbank and N. Seshadri, "Multilevel codes for unequal error protection," *IEEE Trans. Inform. Theory*, vol. 39, pp. 1234–1248, July 1993.

[C4-10] M. Pursley and J. Shea, "Nonuniform phase-shift-key modulation for multimedia multicast transmission in mobile wireless networks," *IEEE J. Select. Areas in Commun.*, vol. 17, pp. 774–783, May 1999.

[C4-11] M. Aydinlik and M. Salehi, "Turbo coded modulation for unequal error protection," *IEEE Trans. Commun.*, vol. 56, pp. 555–564, April 2008.

[C4-12] M. Hossain, P. Vitthaladevuni, M.-S. Alouini, V. Bhargava, and A. Goldsmith, "Adaptive hierarchical modulation for simultaneous voice and multiclass data transmission over fading channels," *IEEE Trans. Veh. Technol.*, vol. 55, pp. 1181–1194, July 2006.

[C4-13] P. Vitthaladevuni and M.-S. Alouini, "Exact BER computation of generalized hierarchical PSK constellations," *IEEE Trans. Commun.*, vol. 51, pp. 2030–2037, December 2003.

[C4-14] P. Vitthaladevuni and M.-S. Alouini, "A recursive algorithm for the exact BER computation of generalized hierarchical QAM constellations," *IEEE Trans. Inform. Theory*, vol. 49, pp. 297–307, January 2003.

[C4-15] Z. Pereira, M. Pellenz, R. Souza, and M. A. Siqueira, "Unequal error protection for LZSS compressed data using Reed-Solomon codes," *IET Communications*, vol. 1, no. 4, pp. 612–617, 2007.

[C4-16] J. Kim and G. Pottie, "Unequal error protection TCM codes," *IEE Proceedings - Communications*, vol. 148, no. 5, pp. 265–272, 2001.

[C4-17] M. Chiu and C. Chao, "Low-decoding-complexity TDM coded modulation with unequal error protection," *IEE Proceedings - Communications*, vol. 144, no. 6, pp. 372–379, 1997.

[C4-18] T. Wang, A. Cano, G. Giannakis, and J. Ramos, "Multi-tier cooperative broadcasting with hierarchical modulations," *IEEE Trans. Wireless Commun.*, vol. 6, pp. 3047–3057, August 2007.

[C4-19] M.-K. Chang and S.-Y. Lee, "Performance analysis of cooperative communication system with hierarchical modulation over Rayleigh fading channel," *IEEE Trans. Wireless Commun.*, vol. 8, pp. 2848–2852, June 2009.

[C4-20] H. X. Nguyen, H. H. Nguyen, and T. Le-Ngoc, "Signal transmission with unequal error protection in wireless relay networks," *to appear in IEEE Trans. Veh. Technol.*

[C4-21] P. Herhold, E. Zimmermann, and G. Fettweis, "A simple cooperative extension to wireless relaying," *International Zurich Seminar on Communications*, pp. 36–39, 2004.

[C4-22] I. S. Gradshteyn, I. M. Ryzhik, A. Jeffrey, and D. Zwillinger, *Table of Integrals, Series, and Products*. Academic Press, 2000.

[C4-23] D. P. Bertsekas, *Constrained Optimization and Lagrange Multiplier Methods*. Athena Scientific, 1996.

[C4-24] F. Onat, A. Adinoyi, Y. Fan, H. Yanikomeroglu, J. Thompson, and I. Marsland, "Threshold selection for SNR-based selective digital relaying in cooperative wireless networks," *IEEE Trans. Wireless Commun.*, vol. 7, pp. 4226–4237, November 2008.

5. Adaptive Relaying in Noncoherent Cooperative Networks

Published as:

Ha X. Nguyen and Ha H. Nguyen, "Adaptive Relaying in Noncoherent Cooperative Networks", *IEEE Transactions on Signal Processing*, vol. 58, pp. 3938-3945, July 2010.

Most of the works on cooperative networks consider simple and optimistic scenarios, for example, the receivers (at relays and destination) have perfect knowledge of CSI of all the transmission links propagated by their received signals. Such an assumption is clearly unrealistic in fast fading environment. Moreover, the complexity of channel estimation increases with the number of relays.

The manuscript in this chapter studies a DF cooperative network in which BFSK modulation is employed to facilitate noncoherent communications, so that the receivers do not need the CSI. Furthermore, the issue of error propagation is also addressed. In particular, the manuscript proposes an adaptive cooperative scheme that employs two thresholds as follows. One threshold is used to select retransmitting relays: a relay retransmits to the destination if its decision variable is larger than the threshold, otherwise it remains silent. In essence this first threshold is used to alleviate error propagation. The second threshold is used at the destination for detection: the destination marks a relay as a retransmitting relay if the decision variable corresponding to the relay is larger than the threshold, otherwise, the destination marks it as a silent relay. Therefore this second threshold is used to decide whether

a relay transmits in the second phase. Then MRC is employed to combine the signals from the retransmitting relays and from the source to make the final decision. With the closed-form expression of the average BER for a two-relay network, the optimal thresholds or jointly optimal thresholds and power allocation are numerically determined to minimize the average BER. Simulation results show that, compared to the previously proposed detection scheme, the scheme proposed in this chapter yields a superior performance under a wide range of channel conditions when optimal thresholds or jointly optimal thresholds and power allocation are employed.

Adaptive Relaying in Noncoherent Cooperative Networks

Ha X. Nguyen, *Student Member, IEEE*, and Ha H. Nguyen, *Senior Member, IEEE*

Abstract

This letter considers a cooperative network in which binary frequency-shift-keying (BFSK) modulation is employed to facilitate noncoherent communications between a source and a destination with the help of relays. Proposed is an adaptive cooperative scheme that employs two thresholds as follows. One threshold is used to select retransmitting relays: a relay retransmits to the destination if its decision variable is larger than the threshold, otherwise it remains silent. The other threshold is used at the destination for detection: the destination marks a relay as a retransmitting relay if the decision variable corresponding to the relay is larger than the threshold, otherwise, the destination marks it as a silent relay. Then the destination combines the signals from the retransmitting relays and from the source to make the final decision. The average end-to-end (e2e) bit-error-rate (BER) is derived in a closed-form expression for a two-relay network. The problems of selecting optimal thresholds or jointly optimal thresholds and power allocation to minimize the average BER are investigated. Simulation results are provided to validate our analysis. Compared to the previously proposed piecewise-linear (PL) detection scheme, our proposed scheme yields a superior performance under a wide range of channel conditions when optimal thresholds or jointly optimal thresholds and power allocation are employed.

Index terms

Cooperative diversity, relay communications, frequency-shift-keying, fading channel, decode-and-forward protocol.

Manuscript received September 03, 2009; accepted March 05, 2010. The associate editor coordinating the review of this manuscript and approving it for publication was Prof. Huaiyu Dai.

Ha X. Nguyen (*contact author) and Ha H. Nguyen are with the Department of Electrical and Computer Engineering, University of Saskatchewan, 57 Campus Drive, Saskatoon, Sask., Canada, S7N 5A9 (e-mails: hxn201@mail.usask.ca, ha.nguyen@usask.ca).

5.1 Introduction

Cooperative (or relay) diversity has recently emerged as a promising technique to combat fading experienced in wireless transmission. In particular, the end-to-end (e2e) bit-error-rate (BER) performance in a wireless network can be improved by having nodes (users) in the network cooperate with each other [C5-1, C5-2, C5-3]. Two of the most well-known cooperative protocols are amplify-and-forward (AF) and decode-and-forward (DF). With DF, relays decode the source's messages, re-encode and re-transmit to the destination. However, with the DF protocol, cooperation does not achieve full diversity if the relays always re-transmit the received message. This is due to possible retransmission of erroneously decoded bits of the message by the relays. An approach to reduce retransmission of erroneous bits is based on the instantaneous signal-to-noise ratio (SNR) of the source-relay link. When the source-relay SNR is larger than a threshold, the probability of decoding error at the relay is negligible and hence the relay retransmits the message. Otherwise, the relay remains silent. References [C5-4, C5-5] study asymptotic SNR thresholds to minimize the e2e BER in *coherent* cooperative networks.

Most of the previous works assume that the receivers (at relays and destination) have perfect knowledge of channel state information (CSI) of all the transmission links propagated by their received signals. Such an assumption is unrealistic in fast fading environment. Moreover, the complexity of channel estimation increases with the number of relays. To overcome these disadvantages, noncoherent modulation and demodulation have been proposed and considered as more robust methods for both AF and DF protocols in relay processing (see, e.g. [C5-6], for the discussion of possible applications of noncoherent modulation/demodulation in strongly resource-limited systems, such as sensor networks). References [C5-7, C5-8, C5-9, C5-10] focus on the differential phase-shift keying (DPSK) for both AF and DF protocols. Frequency shift keying (FSK) is another popular candidate in noncoherent communications. Reference [C5-11] proposes a framework of noncoherent cooperative transmission for the DF protocol employing FSK signals. Due to the complexity of the nonlinear

maximum likelihood (ML) decoding, a suboptimal piecewise linear (PL) scheme was also proposed in [C5-11]. However, the continuous retransmission of the relays in both ML and PL schemes can still induce error propagation, hence limiting the BER performance of the system [C5-4].

This work is also concerned with noncoherent cooperative networks in which binary FSK (BFSK) is employed. The transmission protocol proposed in this letter is based on the use of two thresholds as follows. After receiving the signal in the first phase from the source, each relay decodes and retransmits if its decision variable is larger than the first threshold, $\theta_{\mathrm{r}}^{\mathrm{th}}$. Otherwise it remains silent in the second phase. At the destination, if the decision variable corresponding to a given relay is larger than the second threshold, $\theta_{\mathrm{d}}^{\mathrm{th}}$, the destination marks the relay as a retransmitting relay. Otherwise it marks the relay as a silent relay. Finally, the destination combines all the signals from the retransmitting relays and from the source to make a final decision. In essence, the first threshold enables each relay to adapt its operation according to the instantaneous source-relay channel quality, while the second threshold helps the destination to decide on what would be the retransmitting relays in the second phase. The average BER of the proposed scheme is analytically derived for the case of a two-relay network. The optimal threshold values or jointly optimal threshold values and power allocation are determined to minimize the average BER. Numerical and simulation results verify that our obtained BER expression is accurate. Compared to the piecewise-linear (PL) scheme in [C5-11], our proposed scheme with the optimal thresholds or jointly optimal thresholds and power allocation provides a superior performance under different channel conditions. It should be mentioned that while our engineering framework is applicable for a general network with an arbitrary number of relays, deriving the average BER for more than two relays is very tedious and involved and hence it is not pursued in this letter.

The remainder of this letter is organized as follows. Section 5.2 describes the system model. The average BER for a two-relay cooperative network is derived in Sections 5.3. Analytical and simulation results are presented in Section 5.4. Finally,

Section 5.5 concludes the letter.

5.2 System Model

Consider a wireless network in which K relays help one source node to communicate with its destination. Every node has only one antenna and operates in a half-duplex mode. The K relays communicate with the destination over orthogonal channels. For convenience, the source, relays, and destination are denoted and indexed by node 0, node i, $i = 1, \ldots, K$, and node $K + 1$, respectively.

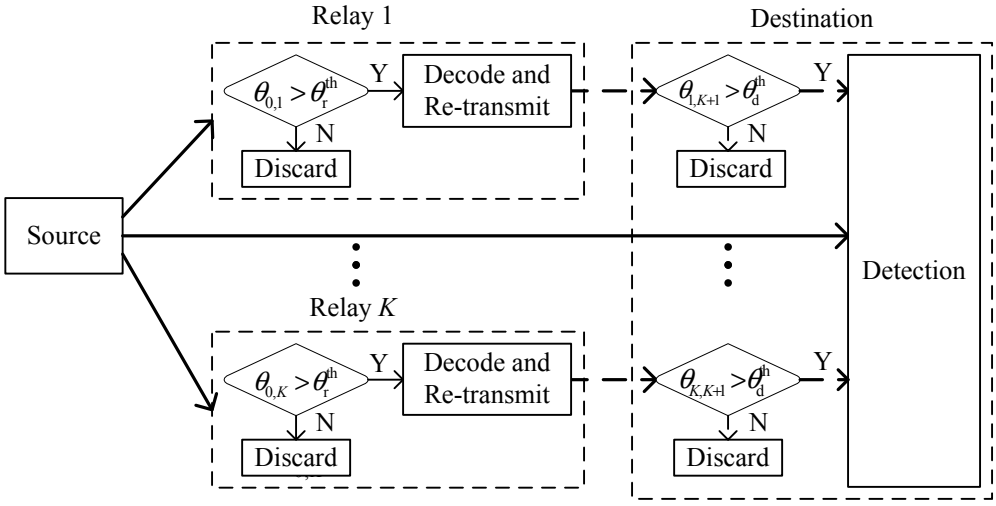

Figure 5.1 System description of the proposed scheme.

Signal transmission from the source to destination is completed in two phases as illustrated in Fig. 5.1. In the first phase, the source broadcasts a BFSK signal. The received signals at node i in baseband can be written as

$$y_{0,i,0} = (1 - x_0)\sqrt{E_0}h_{0,i} + n_{0,i,0}, \tag{5.1}$$

$$y_{0,i,1} = x_0\sqrt{E_0}h_{0,i} + n_{0,i,1}, \tag{5.2}$$

where $h_{0,i}$ is the channel fading coefficient between node 0 and node i, $n_{0,i,k}$ is the noise component at node i, $i = 1, \ldots, K+1$, and E_0 is the average transmitted symbol energy of the source. In (5.1) and (5.2), the third subscript $k \in \{0, 1\}$ denotes the two frequency subbands used in BFSK. The source symbol $x_0 = 0$ if the first frequency subband is used and $x_0 = 1$ if the second frequency subband is used.

After receiving the signal from the source, node i decodes and retransmits a BFSK signal if the magnitude of the energy difference in the two subbands, given by $\theta_{0,i} = \left||y_{0,i,0}|^2 - |y_{0,i,1}|^2\right|$, satisfies $\theta_{0,i} > \theta_{\rm r}^{\rm th}$. When node i transmits in the second phase, the received signals at the destination in the two subbands are

$$y_{i,K+1,0} = (1-x_i)\sqrt{E_i}h_{i,K+1} + n_{i,K+1,0}, \tag{5.3}$$

$$y_{i,K+1,1} = x_i\sqrt{E_i}h_{i,K+1} + n_{i,K+1,1}, \tag{5.4}$$

where E_i is the average symbol energy *assigned* to node i and $n_{i,K+1,k}$ is the noise component at the destination in the second phase. Note that if the ith relay makes a correct detection, then $x_i = x_0$. Otherwise $x_i \neq x_0$.

If $\theta_{0,i} \leqslant \theta_{\rm r}^{\rm th}$, node i remains silent in the second phase and the outputs in the two subbands are

$$y_{i,K+1,0} = n_{i,K+1,0}, \tag{5.5}$$

$$y_{i,K+1,1} = n_{i,K+1,1}. \tag{5.6}$$

Finally, the destination compares the magnitude of the energy difference in the two subbands of each relay-destination link, i.e., $\theta_{i,K+1} = \left||y_{i,K+1,0}|^2 - |y_{i,K+1,1}|^2\right|$ for $i = 1, \ldots, K$, with the second threshold $\theta_{\rm d}^{\rm th}$. If $\theta_{i,K+1} > \theta_{\rm d}^{\rm th}$, the destination marks the ith relay as a retransmitting relay. Otherwise it marks it as a silent relay. Assume that the noise components at both the relay and destination are modeled as[1] $\mathcal{CN}(0, N_0)$ random variables and the channel between nodes i and j is Rayleigh flat fading, modeled as $\mathcal{CN}(0, \sigma_{i,j}^2)$. The average SNR is defined as $\overline{\gamma}_{i,j} = E_i\sigma_{i,j}^2/N_0$. Given the available information about average SNRs and which relays marked by the destination as the retransmitting ones, the optimum detector at the destination is of the following form [C5-11]:

$$\Lambda = \sum_{i=0}^{K} \frac{\overline{\gamma}_{i,K+1}}{(\overline{\gamma}_{i,K+1}+1)N_0}\left(|y_{i,K+1,0}|^2 - |y_{i,K+1,1}|^2\right)\delta_i \underset{1}{\overset{0}{\gtrless}} 0, \tag{5.7}$$

where $\delta_i = 1$ if node i is marked as a retransmitting relay, and $\delta_i = 0$ otherwise.

[1] $\mathcal{CN}(0, \sigma^2)$ denotes a circularly symmetric complex Gaussian random variable with variance σ^2.

An intuitive explanation of the proposed scheme is as follows. As mentioned earlier, the continuous retransmission conducted by relays in both the ML and PL schemes[2] can readily cause error propagation, which limits the e2e BER performance [C5-4]. When error detection and/or instantaneous CSI are unavailable at a relay, an alternative approach to alleviate error propagation is to examine the reliability of the decision statistics at the relays. Given BFSK as the employed modulation technique, this can be accomplished by examining the energy difference in the two subbands at each relay. In particular, if the magnitude of the energy difference is above a threshold, the probability of error at the relay is small and hence the relay forwards the signal. Otherwise, the relay remains silent in the second phase. On the other hand, since whether a relay transmits in the second phase is not exactly known at the destination, a second threshold is employed to decide on this information. From the above discussion one can also expect that the role of the threshold used at the relays is more important than that in the destination since the former deals with the problem of error propagation. Nevertheless simulation results in Section 5.4 demonstrate performance advantage by also implementing a proper threshold at the destination in the scenario that the quality of the source-relay links is poor.

5.3 BER Analysis and Optimization of Thresholds and Power Allocation

As mentioned earlier, the derivation of the average BER shall be presented for the case of a 2-relay network with $\overline{\gamma}_{0,1} = \overline{\gamma}_{0,2} = \overline{\gamma}_1$ and $\overline{\gamma}_{1,3} = \overline{\gamma}_{2,3} = \overline{\gamma}_2$ (balanced network). Although the derivation method can be extended to a network with more than two relays and arbitrary SNRs, it becomes very tedious and involved. We first classify different cases (or events) that result in different conditioned BERs at the destination as summarized in Fig. 5.2. Basically ten different cases, parameterized by Φ_i, $i = 1, \ldots, 10$, arise depending on the values of $\theta_{1,3}$, $\theta_{2,3}$ and the retransmitting/decoding status of each relay. Note that in this section, by "retransmitting"

[2]Due to space limitation, the reader is referred to [C5-11] for the expressions of the ML and PL schemes.

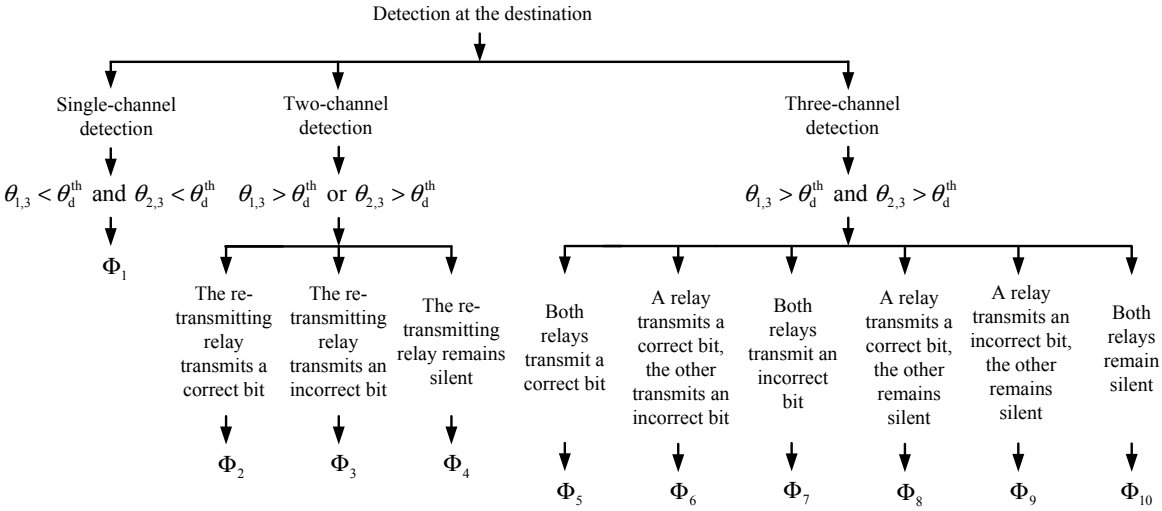

Figure 5.2 Ten possible cases that result in different BERs at the destination in a two-relay network.

relay we mean a relay marked by the destination as the one retransmits in the second phase. The actual action of a relay is, of course, not known to the destination in our study.

Using the law of total probability, the average BER can be found as

$$\mathrm{BER}_{K=2}\left(\theta_{\mathrm{r}}^{\mathrm{th}}, \theta_{\mathrm{d}}^{\mathrm{th}}\right) = \sum_{i=1}^{10} P(\varepsilon|\Phi_i)P(\Phi_i). \tag{5.8}$$

where $P(\varepsilon|\Phi_i)$ is the conditioned BER given Φ_i and $P(\Phi_i)$ is the probability of event Φ_i. In the following subsections, $P(\Phi_i)$ is first determined. The derivation of $P(\varepsilon|\Phi_i)$ is quite straightforward but lengthy. As such only the derivation of $P(\varepsilon|\Phi_2)$ is provided in some detail, while the expressions of other conditioned BERs are simply given.

5.3.1 Case Probabilities

Case Φ_1

As described in Fig. 5.2, this case happens when $\theta_{1,3} < \theta_{\rm d}^{\rm th}$ and $\theta_{2,3} < \theta_{\rm d}^{\rm th}$. Therefore,

$$\begin{aligned} P(\Phi_1) &= P(\theta_{1,3} < \theta_{\rm d}^{\rm th}, \theta_{2,3} < \theta_{\rm d}^{\rm th}) \\ &= P(\theta_{1,3} < \theta_{\rm d}^{\rm th}, \theta_{2,3} < \theta_{\rm d}^{\rm th}, \theta_{0,1} < \theta_{\rm r}^{\rm th}, \theta_{0,2} < \theta_{\rm r}^{\rm th}) \\ &\quad + P(\theta_{1,3} < \theta_{\rm d}^{\rm th}, \theta_{2,3} < \theta_{\rm d}^{\rm th}, \theta_{0,1} < \theta_{\rm r}^{\rm th}, \theta_{0,2} > \theta_{\rm r}^{\rm th}) \\ &\quad + P(\theta_{1,3} < \theta_{\rm d}^{\rm th}, \theta_{2,3} < \theta_{\rm d}^{\rm th}, \theta_{0,1} > \theta_{\rm r}^{\rm th}, \theta_{0,2} < \theta_{\rm r}^{\rm th}) \\ &\quad + P(\theta_{1,3} < \theta_{\rm d}^{\rm th}, \theta_{2,3} < \theta_{\rm d}^{\rm th}, \theta_{0,1} > \theta_{\rm r}^{\rm th}, \theta_{0,2} > \theta_{\rm r}^{\rm th}) \\ &= \left[I_1\left(\theta_{\rm r}^{\rm th}, \overline{\gamma}_1\right) I_2\left(\theta_{\rm d}^{\rm th}\right) + \left(1 - I_1\left(\theta_{\rm r}^{\rm th}, \overline{\gamma}_1\right)\right) I_1\left(\theta_{\rm d}^{\rm th}, \overline{\gamma}_2\right) \right]^2, \end{aligned} \tag{5.9}$$

where the function $I_1\left(\theta^{\rm th}, \overline{\gamma}\right)$ is the probability that the magnitude of the energy difference θ is smaller than the threshold $\theta^{\rm th}$ and $\overline{\gamma}$ is the average SNR of the channel between two nodes over which the information is transmitted. The pdf of θ is given in Lemma 2 of Appendix 5.A, from which $I_1\left(\theta^{\rm th}, \overline{\gamma}\right)$ can be computed as

$$I_1\left(\theta^{\rm th}, \overline{\gamma}\right) = \int_0^{\theta^{\rm th}} f_\theta(x) {\rm d}x = \frac{1}{2+\overline{\gamma}} \left[(1+\overline{\gamma}) \left(1 - {\rm e}^{-\theta^{\rm th}/(1+\overline{\gamma})}\right) + \left(1 - {\rm e}^{-\theta^{\rm th}}\right) \right]. \tag{5.10}$$

On the other hand, $I_2\left(\theta^{\rm th}\right)$ is the probability that the magnitude of the energy difference θ is smaller than the threshold $\theta^{\rm th}$ when the information data is not transmitted from the relay. From the pdf of θ given in Lemma 4 of Appendix 5.A, $I_2\left(\theta^{\rm th}\right)$ is simply computed as

$$I_2\left(\theta^{\rm th}\right) = \int_0^{\theta^{\rm th}} {\rm e}^{-x} {\rm d}x = 1 - {\rm e}^{-\theta^{\rm th}}. \tag{5.11}$$

Cases Φ_2 to Φ_4

These cases correspond to the events that $\theta_{1,3} < \theta_{\rm d}^{\rm th} < \theta_{2,3}$ or $\theta_{2,3} < \theta_{\rm d}^{\rm th} < \theta_{1,3}$. The difference among three cases is whether a relay retransmits in the second phase and the decoded bit is correct. Under Φ_2, the "retransmitting" relay forwards a correct

bit, while the other relay forwards or remains silent in the second phase. Therefore

$$\begin{aligned} P(\Phi_2) &= 2\left[1-I_1\left(\theta_{\mathrm{r}}^{\mathrm{th}},\overline{\gamma}_1\right)\right]\left[1-I_1\left(\theta_{\mathrm{d}}^{\mathrm{th}},\overline{\gamma}_2\right)\right] \\ &\quad\times\left[1-I_3\left(\theta_{\mathrm{r}}^{\mathrm{th}},\overline{\gamma}_1\right)\right]\left[I_1\left(\theta_{\mathrm{r}}^{\mathrm{th}},\overline{\gamma}_1\right)I_2\left(\theta_{\mathrm{d}}^{\mathrm{th}}\right)\right. \\ &\quad\left.+\left(1-I_1\left(\theta_{\mathrm{r}}^{\mathrm{th}},\overline{\gamma}_1\right)\right)I_1\left(\theta_{\mathrm{d}}^{\mathrm{th}},\overline{\gamma}_2\right)\right] \end{aligned} \tag{5.12}$$

where $I_3\left(\theta^{\mathrm{th}},\overline{\gamma}\right)$ is the probability of error of the source-relay link given that the magnitude of the energy difference θ is larger than the threshold θ^{th} and $\overline{\gamma}$ is the average SNR of the channel between two nodes. It can be computed as

$$I_3\left(\theta^{\mathrm{th}},\overline{\gamma}\right) = \frac{1}{1-I_1(\theta^{\mathrm{th}},\overline{\gamma})}\int_{-\infty}^{-\theta^{\mathrm{th}}}\frac{1}{2+\overline{\gamma}_1}\mathrm{e}^{-x}\mathrm{d}x = \frac{1}{1-I_1(\theta^{\mathrm{th}},\overline{\gamma})}\frac{\mathrm{e}^{-\theta^{\mathrm{th}}}}{2+\overline{\gamma}}. \tag{5.13}$$

Case Φ_3 corresponds to the event that one "retransmitting" relay forwards an incorrect bit, the other relay forwards or remains silent in the second phase. It can be determined that

$$\begin{aligned} P(\Phi_3) = 2\left[1-I_1\left(\theta_{\mathrm{r}}^{\mathrm{th}},\overline{\gamma}_1\right)\right]\left[1-I_1\left(\theta_{\mathrm{d}}^{\mathrm{th}},\overline{\gamma}_2\right)\right]I_3\left(\theta_{\mathrm{r}}^{\mathrm{th}},\overline{\gamma}_1\right) \\ \times\left[I_1\left(\theta_{\mathrm{r}}^{\mathrm{th}},\overline{\gamma}_1\right)I_2\left(\theta_{\mathrm{d}}^{\mathrm{th}}\right)+\left(1-I_1\left(\theta_{\mathrm{r}}^{\mathrm{th}},\overline{\gamma}_1\right)\right)I_1\left(\theta_{\mathrm{d}}^{\mathrm{th}},\overline{\gamma}_2\right)\right]. \end{aligned} \tag{5.14}$$

Finally, case Φ_4 happens when the "retransmitting" relay remains silent in the second phase. One has

$$\begin{aligned} P(\Phi_4) = I_1\left(\theta_{\mathrm{r}}^{\mathrm{th}},\overline{\gamma}_1\right)\left[1-I_2\left(\theta_{\mathrm{d}}^{\mathrm{th}}\right)\right]\left[I_1\left(\theta_{\mathrm{r}}^{\mathrm{th}},\overline{\gamma}_1\right)I_2\left(\theta_{\mathrm{d}}^{\mathrm{th}}\right)\right. \\ \left.+\left(1-I_1\left(\theta_{\mathrm{r}}^{\mathrm{th}},\overline{\gamma}_1\right)\right)I_1\left(\theta_{\mathrm{d}}^{\mathrm{th}},\overline{\gamma}_2\right)\right]. \end{aligned} \tag{5.15}$$

Cases Φ_5 to Φ_{10}

These cases happen when $\theta_{1,3} > \theta_{\mathrm{d}}^{\mathrm{th}}$ and $\theta_{2,3} > \theta_{\mathrm{d}}^{\mathrm{th}}$. For case Φ_5, both the relays forward a correct bit. Therefore

$$P(\Phi_5) = \left\{\left[1-I_1\left(\theta_{\mathrm{r}}^{\mathrm{th}},\overline{\gamma}_1\right)\right]\left[1-I_1\left(\theta_{\mathrm{d}}^{\mathrm{th}},\overline{\gamma}_2\right)\right]\left[1-I_3\left(\theta_{\mathrm{r}}^{\mathrm{th}},\overline{\gamma}_1\right)\right]\right\}^2 \tag{5.16}$$

Under case Φ_6 one relay forwards a correct bit, but the other forwards an incorrect bit. Hence

$$P(\Phi_6) = 2\left[1-I_1\left(\theta_{\mathrm{r}}^{\mathrm{th}},\overline{\gamma}_1\right)\right]^2\left[1-I_1\left(\theta_{\mathrm{d}}^{\mathrm{th}},\overline{\gamma}_2\right)\right]^2\left[1-I_3\left(\theta_{\mathrm{r}}^{\mathrm{th}},\overline{\gamma}_1\right)\right]I_3\left(\theta_{\mathrm{r}}^{\mathrm{th}},\overline{\gamma}_1\right). \tag{5.17}$$

For case Φ_7, both relays forward an incorrect bit and

$$P(\Phi_7) = \left\{ \left[1 - I_1\left(\theta_{\mathrm{r}}^{\mathrm{th}}, \overline{\gamma}_1\right)\right] \left[1 - I_1\left(\theta_{\mathrm{d}}^{\mathrm{th}}, \overline{\gamma}_2\right)\right] I_3\left(\theta_{\mathrm{r}}^{\mathrm{th}}, \overline{\gamma}_1\right) \right\}^2 \tag{5.18}$$

Case Φ_8 happens when one relay forwards a correct bit and the other remains silent. One has

$$P(\Phi_8) = 2\left[1 - I_1\left(\theta_{\mathrm{r}}^{\mathrm{th}}, \overline{\gamma}_1\right)\right] \left[1 - I_1\left(\theta_{\mathrm{d}}^{\mathrm{th}}, \overline{\gamma}_2\right)\right] \times \left[1 - I_3\left(\theta_{\mathrm{r}}^{\mathrm{th}}, \overline{\gamma}_1\right)\right] I_1\left(\theta_{\mathrm{r}}^{\mathrm{th}}, \overline{\gamma}_1\right) \left[1 - I_2\left(\theta_{\mathrm{d}}^{\mathrm{th}}\right)\right]. \tag{5.19}$$

For case Φ_9, one relay forwards an incorrect bit, while the other remains silent. Then

$$P(\Phi_9) = 2\left[1 - I_1\left(\theta_{\mathrm{r}}^{\mathrm{th}}, \overline{\gamma}_1\right)\right] \left[1 - I_1\left(\theta_{\mathrm{d}}^{\mathrm{th}}, \overline{\gamma}_2\right)\right] I_3\left(\theta_{\mathrm{r}}^{\mathrm{th}}, \overline{\gamma}_1\right) \times I_1\left(\theta_{\mathrm{r}}^{\mathrm{th}}, \overline{\gamma}_1\right) \left[1 - I_2\left(\theta_{\mathrm{d}}^{\mathrm{th}}\right)\right] \tag{5.20}$$

Finally, for case Φ_{10}, both relays remain silent in the second phase. Therefore

$$P(\Phi_{10}) = \left[I_1\left(\theta_{\mathrm{r}}^{\mathrm{th}}, \overline{\gamma}_1\right) \left(1 - I_2\left(\theta_{\mathrm{d}}^{\mathrm{th}}\right)\right)\right]^2. \tag{5.21}$$

5.3.2 Conditioned BERs

For case Φ_1, the destination uses only the signal received directly from the source in the first phase to decode. Hence the average BER conditioned on Φ_1 is the same as that of BFSK over a flat Rayleigh fading channel, namely [C5-12]:

$$P(\varepsilon|\Phi_1) = \frac{1}{2 + \overline{\gamma}_{0,3}} \tag{5.22}$$

In three cases Φ_2 to Φ_4, the destination combines received signals from the source and one relay to decode. The difference among three cases is in the correctness of the decoded bit and the transmission status of the relay in the second phase. Without loss of generality, assume that node 1 (the first relay) transmits in the second phase. Then

the destination combines two received signals using (5.7) and produces the following sufficient statistic:

$$y = \underbrace{\frac{\overline{\gamma}_{0,3}}{1+\overline{\gamma}_{0,3}}}_{\alpha_1} \underbrace{\left(|y_{0,3,0}|^2 - |y_{0,3,1}|^2\right)}_{X_1} + \underbrace{\frac{\overline{\gamma}_{1,3}}{1+\overline{\gamma}_{1,3}}}_{\alpha_2} \underbrace{\left(|y_{1,3,0}|^2 - |y_{1,3,1}|^2\right)}_{X_2} = \alpha_1 X_1 + \alpha_2 X_2, \tag{5.23}$$

Let us examine case Φ_2 in more detail. This case relates to the event that the relay forwards a correct bit (i.e., the relay correctly decodes the signal from the source). Assuming that the transmitted bit is "0", the pdfs of X_1 and X_2 are given, respectively, by[3] (see Appendix 5.A)

$$f_{X_1}(x) = \begin{cases} \frac{1}{2+\overline{\gamma}_{0,3}} \mathrm{e}^{-x/(1+\overline{\gamma}_{0,3})}, & x \geq 0 \\ \frac{1}{2+\overline{\gamma}_{0,3}} \mathrm{e}^{x}, & x < 0 \end{cases}, \tag{5.24}$$

$$f_{X_2}(x) = \begin{cases} \frac{1}{A} \frac{1}{2+\overline{\gamma}_{2}} \mathrm{e}^{-x/(1+\overline{\gamma}_{2})}, & x \geq \theta_{\mathrm{d}}^{\mathrm{th}} \\ \frac{1}{A} \frac{1}{2+\overline{\gamma}_{2}} \mathrm{e}^{x}, & x < -\theta_{\mathrm{d}}^{\mathrm{th}} \end{cases} \tag{5.25}$$

where $A = \frac{(1+\overline{\gamma}_2)\mathrm{e}^{-\theta_{\mathrm{d}}^{\mathrm{th}}/(1+\overline{\gamma}_2)}}{2+\overline{\gamma}_2} + \frac{\mathrm{e}^{-\theta_{\mathrm{d}}^{\mathrm{th}}}}{2+\overline{\gamma}_2}$. Error happens when $y < 0$. Therefore,

$$\begin{aligned} P(\varepsilon|\Phi_2) = P(y<0) = P(\alpha_1 X_1 + \alpha_2 X_2 < 0) &= \int_{-\infty}^{-\infty} f_{X_2}(x_2) \int_{-\infty}^{-\frac{\alpha_2}{\alpha_1}x_2} f_{X_1}(x_1)\mathrm{d}x_1\mathrm{d}x_2 \\ &= \frac{1}{A(2+\overline{\gamma}_{0,3})(2+\overline{\gamma}_2)} \Big[(2+\overline{\gamma}_{0,3})\mathrm{e}^{-\theta_{\mathrm{d}}^{\mathrm{th}}} \\ &\quad - \frac{(1+\overline{\gamma}_{0,3})\mathrm{e}^{-(1+\frac{\alpha_2}{\alpha_1}\frac{1}{1+\overline{\gamma}_{0,3}})\theta_{\mathrm{d}}^{\mathrm{th}}}}{1+\frac{\alpha_2}{\alpha_1}\frac{1}{1+\overline{\gamma}_{0,3}}} + \frac{\mathrm{e}^{-(\frac{1}{1+\overline{\gamma}_2}+\frac{\alpha_2}{\alpha_1})\theta_{\mathrm{d}}^{\mathrm{th}}}}{\frac{1}{1+\overline{\gamma}_2}+\frac{\alpha_2}{\alpha_1}}\Bigg]. \end{aligned} \tag{5.26}$$

Similarly, $P(\varepsilon|\Phi_3)$ and $P(\varepsilon|\Phi_4)$ can be determined as (5.27) and (5.28), respectively, at the top of next page.

$$\begin{aligned} P(\varepsilon|\Phi_3) = \frac{1}{A(2+\overline{\gamma}_{0,3})(2+\overline{\gamma}_2)} \Bigg[&\frac{\alpha_1 \mathrm{e}^{-(1+\frac{\alpha_2}{\alpha_1})\theta_{\mathrm{d}}^{\mathrm{th}}}}{\alpha_1+\alpha_2} + (1+\overline{\gamma}_2)(2+\overline{\gamma}_{0,3})\mathrm{e}^{-\theta_{\mathrm{d}}^{\mathrm{th}}/(1+\overline{\gamma}_2)} \\ &- \frac{(1+\overline{\gamma}_{0,3})\mathrm{e}^{-\left(\frac{1}{1+\overline{\gamma}_2}+\frac{\alpha_2}{\alpha_1}\frac{1}{1+\overline{\gamma}_{0,3}}\right)\theta_{\mathrm{d}}^{\mathrm{th}}}}{\frac{1}{1+\overline{\gamma}_2}+\frac{\alpha_2}{\alpha_1}\frac{1}{1+\overline{\gamma}_{0,3}}} \Bigg] \end{aligned} \tag{5.27}$$

[3]It should be noted that in this case X_2 satisfies $|X_2| > \theta_{\mathrm{d}}^{\mathrm{th}}$.

$$P(\varepsilon|\Phi_4) = \frac{1}{2} + \frac{1}{2(2+\overline{\gamma}_{0,3})}\left(\frac{\mathrm{e}^{-\frac{\alpha_2}{\alpha_1}\theta_{\mathrm{d}}^{\mathrm{th}}}}{1+\frac{\alpha_2}{\alpha_1}} - \frac{(1+\overline{\gamma}_{0,3})\mathrm{e}^{-\frac{\alpha_2}{\alpha_1}\frac{1}{1+\overline{\gamma}_{0,3}}\theta_{\mathrm{d}}^{\mathrm{th}}}}{1+\frac{\alpha_2}{\alpha_1}\frac{1}{1+\overline{\gamma}_{0,3}}}\right) \tag{5.28}$$

For cases Φ_5 to Φ_{10}, the destination combines signals received from both relays and the source to decode. By performing related integrals, we obtain the closed-form expressions of $P(\varepsilon|\Phi_i), i = 5, \ldots, 10$ as displaying in the next page,

$$P(\varepsilon|\Phi_5) = \begin{cases} \frac{1}{2+\overline{\gamma}_{0,3}}\left(\frac{1}{A}\frac{1}{2+\overline{\gamma}_2}\right)^2 \Bigg\{(2+\overline{\gamma}_{0,3})\mathrm{e}^{-2\theta_{\mathrm{d}}^{\mathrm{th}}} - \frac{(1+\overline{\gamma}_{0,3})\mathrm{e}^{-2\left(1+\frac{\alpha_2}{\alpha_1}\frac{1}{1+\overline{\gamma}_{0,3}}\right)\theta_{\mathrm{d}}^{\mathrm{th}}}}{\left(1+\frac{\alpha_2}{\alpha_1}\frac{1}{1+\overline{\gamma}_{0,3}}\right)^2} \\ + \left[\frac{2(1+\overline{\gamma}_2)}{2+\overline{\gamma}_2}\left(2+\overline{\gamma}_{0,3}+\frac{1}{\frac{\alpha_2}{\alpha_1}+\frac{1}{1+\overline{\gamma}_2}}\right) - \frac{2}{\frac{\alpha_2}{\alpha_1}\frac{1}{1+\overline{\gamma}_{0,3}}-\frac{1}{1+\overline{\gamma}_2}}\left(\frac{1+\overline{\gamma}_2}{2+\overline{\gamma}_2} - \frac{1}{1+\frac{\alpha_2}{\alpha_1}\frac{1}{1+\overline{\gamma}_{0,3}}}\right)\right] \\ \times\mathrm{e}^{-\left(1+\frac{1}{1+\overline{\gamma}_2}\right)\theta_{\mathrm{d}}^{\mathrm{th}}} + \frac{\mathrm{e}^{-2\left(\frac{\alpha_2}{\alpha_1}+\frac{1}{1+\overline{\gamma}_2}\right)\theta_{\mathrm{d}}^{\mathrm{th}}}}{\left(\frac{\alpha_2}{\alpha_1}+\frac{1}{1+\overline{\gamma}_2}\right)^2}\Bigg\}, \quad \text{if } \overline{\gamma}_{0,3} \neq \overline{\gamma}_2 \\ \frac{1}{(2+\overline{\gamma}_{0,3})^{K+1}}\sum_{i=0}^{K}\binom{i}{K+i}\left(\frac{1+\overline{\gamma}_{0,3}}{2+\overline{\gamma}_{0,3}}\right)^i, \quad \text{if } \overline{\gamma}_{0,3} = \overline{\gamma}_2 \end{cases} \tag{5.29}$$

$$\begin{aligned} P(\varepsilon|\Phi_6) = {} & T_1(1+\overline{\gamma}_2)\mathrm{e}^{-\frac{2+\overline{\gamma}_2}{1+\overline{\gamma}_2}\theta_{\mathrm{d}}^{\mathrm{th}}} + T_1(1+\overline{\gamma}_{0,3})\Bigg[(1+\overline{\gamma}_2)\mathrm{e}^{-\frac{2+\overline{\gamma}_2}{1+\overline{\gamma}_2}\theta_{\mathrm{d}}^{\mathrm{th}}} - \\ & \frac{\mathrm{e}^{-\left(1+\frac{1}{1+\overline{\gamma}_2}+\frac{\alpha_2}{\alpha_1}\frac{2}{1+\overline{\gamma}_{0,3}}\right)\theta_{\mathrm{d}}^{\mathrm{th}}}}{\left(1+\frac{\alpha_2}{\alpha_1}\frac{1}{1+\overline{\gamma}_{0,3}}\right)\left(\frac{1}{1+\overline{\gamma}_2}+\frac{\alpha_2}{\alpha_1}\frac{1}{1+\overline{\gamma}_{0,3}}\right)}\Bigg] + \frac{3T_1\mathrm{e}^{-2\theta_{\mathrm{d}}^{\mathrm{th}}}}{4} + \frac{T_1(1+\overline{\gamma}_2)^2\mathrm{e}^{-\frac{2}{1+\overline{\gamma}_2}\theta_{\mathrm{d}}^{\mathrm{th}}}}{2} \\ & + \frac{T_1(1+\overline{\gamma}_{0,3})}{2}\left(1-\frac{1}{\frac{\alpha_2}{\alpha_1}\frac{1}{1+\overline{\gamma}_2}+1}\right)\mathrm{e}^{-2\theta_{\mathrm{d}}^{\mathrm{th}}} + \frac{T_1\mathrm{e}^{-\frac{2}{1+\overline{\gamma}_2}\theta_{\mathrm{d}}^{\mathrm{th}}}}{(\frac{\alpha_2}{\alpha_1}+\frac{1}{1+\overline{\gamma}_2})^2} \\ & + \frac{T_1\mathrm{e}^{-\left(1+\frac{2\alpha_2}{\alpha_1}+\frac{1}{1+\overline{\gamma}_2}\right)\theta_{\mathrm{d}}^{\mathrm{th}}}}{\left(\frac{\alpha_2}{\alpha_1}+\frac{1}{1+\overline{\gamma}_2}\right)\left(\frac{\alpha_2}{\alpha_1}+1\right)} + J_1 \end{aligned} \tag{5.30}$$

$$\begin{aligned} P(\varepsilon|\Phi_7) = {} & \frac{1}{2+\overline{\gamma}_{0,3}}\frac{1}{(A(2+\overline{\gamma}_2))^2}\Big\{(1+\overline{\gamma}_2)^2(2+\overline{\gamma}_{0,3})\mathrm{e}^{-2\theta_{\mathrm{d}}^{\mathrm{th}}/(1+\overline{\gamma}_2)} \\ & - \frac{(1+\overline{\gamma}_{0,3})\mathrm{e}^{-2\left(\frac{1}{1+\overline{\gamma}_2}+\frac{\alpha_2}{\alpha_1}\frac{1}{1+\overline{\gamma}_{0,3}}\right)\theta_{\mathrm{d}}^{\mathrm{th}}}}{\left(\frac{1}{1+\overline{\gamma}_2}+\frac{\alpha_2}{\alpha_1}\frac{1}{1+\overline{\gamma}_{0,3}}\right)^2} + \frac{\mathrm{e}^{-\frac{2(\alpha_1+\alpha_2)}{\alpha_1}\theta_{\mathrm{d}}^{\mathrm{th}}}}{\left(\frac{\alpha_2}{\alpha_1}+1\right)^2} + 2\Bigg[\frac{(1+\overline{\gamma}_2)^2}{2+\overline{\gamma}_2}(2+\overline{\gamma}_{0,3}) \\ & - \frac{1+\overline{\gamma}_{0,3}}{\frac{\alpha_2}{\alpha_1}\frac{1}{1+\overline{\gamma}_{0,3}}-1}\left(\frac{1+\overline{\gamma}_2}{2+\overline{\gamma}_2} - \frac{1}{\frac{1}{1+\overline{\gamma}_2}+\frac{\alpha_2}{\alpha_1}\frac{1}{1+\overline{\gamma}_{0,3}}}\right) + \frac{1}{1+\frac{\alpha_2}{\alpha_1}}\frac{1+\overline{\gamma}_2}{2+\overline{\gamma}_2}\Bigg]\mathrm{e}^{-\frac{2+\overline{\gamma}_2}{1+\overline{\gamma}_2}\theta_{\mathrm{d}}^{\mathrm{th}}}\Big\} \end{aligned} \tag{5.31}$$

$$P(\varepsilon|\Phi_8) = \frac{1}{2}T_2\mathrm{e}^{-\theta_{\mathrm{d}}^{\mathrm{th}}} + T_2(1+\overline{\gamma}_{0,3})\left[\mathrm{e}^{-\theta_{\mathrm{d}}^{\mathrm{th}}} - \frac{\mathrm{e}^{-\left(1+\frac{\alpha_2}{\alpha_1}\frac{2}{1+\overline{\gamma}_{0,3}}\right)\theta_{\mathrm{d}}^{\mathrm{th}}}}{(1+\frac{\alpha_2}{\alpha_1}\frac{1}{1+\overline{\gamma}_{0,3}})^2}\right]$$
$$+ (1+\overline{\gamma}_{0,3})T_2\left[\frac{1}{2} - \frac{1}{\frac{\alpha_2}{\alpha_1}\frac{1}{1+\overline{\gamma}_{0,3}}-1}\left(\frac{1}{2} - \frac{1}{1+\frac{\alpha_2}{\alpha_1}\frac{1}{1+\overline{\gamma}_{0,3}}}\right)\right]\mathrm{e}^{-\theta_{\mathrm{d}}^{\mathrm{th}}}$$
$$+ \frac{T_2\mathrm{e}^{-\frac{1}{1+\overline{\gamma}_2}\theta_{\mathrm{d}}^{\mathrm{th}}}}{1+\frac{1}{1+\overline{\gamma}_2}} + (1+\overline{\gamma}_{0,3})T_2\left(1 - \frac{1}{\frac{\alpha_2}{\alpha_1}\frac{1}{1+\overline{\gamma}_{0,3}}+1}\right)\frac{1+\overline{\gamma}_2}{2+\overline{\gamma}_2}\mathrm{e}^{-\frac{1}{1+\overline{\gamma}_2}\theta_{\mathrm{d}}^{\mathrm{th}}} +$$
$$\frac{T_2\mathrm{e}^{-\theta_{\mathrm{d}}^{\mathrm{th}}}}{2(\frac{\alpha_2}{\alpha_1}+1)} + \frac{T_2}{\frac{\alpha_2}{\alpha_1}+\frac{1}{1+\overline{\gamma}_2}}\frac{\mathrm{e}^{-\left(\frac{2\alpha_2}{\alpha_1}+\frac{1}{1+\overline{\gamma}_2}\right)\theta_{\mathrm{d}}^{\mathrm{th}}}}{\frac{\alpha_2}{\alpha_1}+1} + J_2 \quad (5.32)$$

$$P(\varepsilon|\Phi_9) = T_2(1+\overline{\gamma}_2)\mathrm{e}^{-\frac{1}{1+\overline{\gamma}_2}\theta_{\mathrm{d}}^{\mathrm{th}}} + T_2(1+\overline{\gamma}_{0,3})\left[(1+\overline{\gamma}_2)\mathrm{e}^{-\frac{1}{1+\overline{\gamma}_2}\theta_{\mathrm{d}}^{\mathrm{th}}} - \right.$$
$$\left.\frac{\mathrm{e}^{-\left(\frac{1}{1+\overline{\gamma}_2}+\frac{\alpha_2}{\alpha_1}\frac{2}{1+\overline{\gamma}_{0,3}}\right)\theta_{\mathrm{d}}^{\mathrm{th}}}}{(1+\frac{\alpha_2}{\alpha_1}\frac{1}{1+\overline{\gamma}_{0,3}})(\frac{1}{1+\overline{\gamma}_2}+\frac{\alpha_2}{\alpha_1}\frac{1}{1+\overline{\gamma}_{0,3}})}\right] + \frac{T_2(1+\overline{\gamma}_2)^2\mathrm{e}^{-\frac{\theta_{\mathrm{d}}^{\mathrm{th}}}{1+\overline{\gamma}_2}}}{2+\overline{\gamma}_2}$$
$$+(1+\overline{\gamma}_{0,3})T_2\left[\frac{(1+\overline{\gamma}_2)^2}{2+\overline{\gamma}_2} - \frac{1}{\frac{\alpha_2}{\alpha_1}\frac{1}{1+\overline{\gamma}_{0,3}}-1}\left(\frac{1+\overline{\gamma}_2}{2+\overline{\gamma}_2} - \frac{1}{\frac{1}{1+\overline{\gamma}_2}+\frac{\alpha_2}{\alpha_1}\frac{1}{1+\overline{\gamma}_{0,3}}}\right)\right]\mathrm{e}^{-\frac{\theta_{\mathrm{d}}^{\mathrm{th}}}{1+\overline{\gamma}_2}} + \frac{T_2\mathrm{e}^{-\theta_{\mathrm{d}}^{\mathrm{th}}}}{2}$$
$$+\frac{(1+\overline{\gamma}_{0,3})T_2}{2}\left(1 - \frac{1}{\frac{\alpha_2}{\alpha_1}\frac{1}{1+\overline{\gamma}_2}+1}\right)\mathrm{e}^{-\theta_{\mathrm{d}}^{\mathrm{th}}} + \frac{T_2\mathrm{e}^{-\frac{1}{1+\overline{\gamma}_2}\theta_{\mathrm{d}}^{\mathrm{th}}}}{(\frac{\alpha_2}{\alpha_1}+1)(1+\frac{1}{1+\overline{\gamma}_2})} + \frac{T_2\mathrm{e}^{-\left(1+2\frac{\alpha_2}{\alpha_1}\right)\theta_{\mathrm{d}}^{\mathrm{th}}}}{(\frac{\alpha_2}{\alpha_1}+1)^2} + J_3 \quad (5.33)$$

$$P(\varepsilon|\Phi_{10}) = \frac{1}{4(2+\overline{\gamma}_{0,3})}\left\{2(2+\overline{\gamma}_{0,3}) - \frac{(1+\overline{\gamma}_{0,3})\mathrm{e}^{-\frac{\alpha_2}{\alpha_1}\frac{2}{1+\overline{\gamma}_{0,3}}\theta_{\mathrm{d}}^{\mathrm{th}}}}{\left(1+\frac{\alpha_2}{\alpha_1}\frac{1}{1+\overline{\gamma}_{0,3}}\right)^2}\right.$$
$$\left. - \frac{2(1+\overline{\gamma}_{0,3})}{\frac{\alpha_2}{\alpha_1}\frac{1}{1+\overline{\gamma}_{0,3}}-1}\left(\frac{1}{2} - \frac{1}{1+\frac{\alpha_2}{\alpha_1}\frac{1}{1+\overline{\gamma}_{0,3}}}\right) + \frac{1}{\frac{\alpha_2}{\alpha_1}+1} + \frac{\mathrm{e}^{-2\frac{\alpha_2}{\alpha_1}\theta_{\mathrm{d}}^{\mathrm{th}}}}{\left(\frac{\alpha_2}{\alpha_1}+1\right)^2}\right\} \quad (5.34)$$

where $T_1 = \frac{1}{2+\overline{\gamma}_{0,3}}\left(\frac{1}{A}\frac{1}{2+\overline{\gamma}_2}\right)^2$, $T_2 = \frac{1}{2A(2+\overline{\gamma}_{0,3})(2+\overline{\gamma}_2)}$, and

$$J_1 = \begin{cases} (1+\overline{\gamma}_{0,3})T_1\left[\frac{(1+\overline{\gamma}_2)^2}{2} - \frac{1}{\frac{\alpha_2}{\alpha_1}\frac{1}{1+\overline{\gamma}_{0,3}}-\frac{1}{1+\overline{\gamma}_2}}\right. \\ \left.\left(\frac{1+\overline{\gamma}_2}{2} - \frac{1}{\frac{1}{1+\overline{\gamma}_2}+\frac{\alpha_2}{\alpha_1}\frac{1}{1+\overline{\gamma}_{0,3}}}\right)\right]\mathrm{e}^{-\frac{2}{1+\overline{\gamma}_2}\theta_{\mathrm{d}}^{\mathrm{th}}} + \frac{T_1\alpha_1}{2(\alpha_1+\alpha_2)}, & \text{if } \overline{\gamma}_{0,3} \neq \overline{\gamma}_2 \\ \frac{T_1}{4}(1+\overline{\gamma}_{0,3})(1+\overline{\gamma}_2)^2\mathrm{e}^{-\frac{2}{1+\overline{\gamma}_2}\theta_{\mathrm{d}}^{\mathrm{th}}} + \frac{T_1}{4}\mathrm{e}^{-2\theta_{\mathrm{d}}^{\mathrm{th}}}, & \text{if } \overline{\gamma}_{0,3} = \overline{\gamma}_2 \end{cases}$$

$$J_2 = \begin{cases} \frac{T_2}{1-\frac{\alpha_2}{\alpha_1}} \left(\frac{\mathrm{e}^{-\frac{\alpha_2}{\alpha_1}\theta_{\mathrm{d}}^{\mathrm{th}}}}{\frac{1}{1+\overline{\gamma}_2}+\frac{\alpha_2}{\alpha_1}} - \frac{\mathrm{e}^{-\frac{1}{1+\overline{\gamma}_2}\theta_{\mathrm{d}}^{\mathrm{th}}}}{1+\frac{1}{1+\overline{\gamma}_2}} \right), & \text{if } \overline{\gamma}_{0,3} \neq \overline{\gamma}_2 \\ \frac{T_2 \mathrm{e}^{-\frac{1}{1+\overline{\gamma}_2}\theta_{\mathrm{d}}^{\mathrm{th}}}}{(1+\frac{1}{1+\overline{\gamma}_2})^2}, & \text{if } \overline{\gamma}_{0,3} = \overline{\gamma}_2 \end{cases}$$

$$J_3 = \begin{cases} \frac{T_2}{1-\frac{\alpha_2}{\alpha_1}} \left(\frac{1}{1+\frac{\alpha_2}{\alpha_1}} - \frac{1}{2} \right) \mathrm{e}^{-\theta_{\mathrm{d}}^{\mathrm{th}}}, & \text{if } \overline{\gamma}_{0,3} \neq \overline{\gamma}_2 \\ \frac{T_2}{4} \mathrm{e}^{-\theta_{\mathrm{d}}^{\mathrm{th}}} & \text{if } \overline{\gamma}_{0,3} = \overline{\gamma}_2 \end{cases}$$

In summary, the average BER for a two-relay network[4] with the proposed adaptive relaying method can be evaluated in a closed-form expression by substituting all the related expressions into (5.8). Obviously, the choice of the thresholds and power allocation between the source and relays can strongly affect the BER performance. In fact, as will be seen in Section 5.4, an arbitrary selection of these parameters readily leads to a poorer performance of the proposed scheme as compared to the ML and PL schemes in [C5-11]. In general, one is interested in finding the optimal thresholds and power allocation for the proposed relaying scheme. Unfortunately, an analytical solution for threshold and power allocation values is very difficult, if not impossible to find. Nevertheless with the closed-form BER expressions for the one-relay and two-relay networks, the problems of finding the optimal thresholds or jointly optimal thresholds and power allocation can be done systematically, e.g., using the MATLAB Optimization Toolbox.

It should be noted that the average BERs formulated in (5.8) only require information on the average SNRs of the source-destination, source-relay, and relay-destination links. The optimal thresholds and power allocation can be found centrally and sent to the relays and destination. Otherwise, the relays and destination can find the thresholds for themselves if they have all the average SNR values. Since the average

[4]For the case of a single-relay network, one only needs to classify the errors into four different cases, namely Φ_1, Φ_2, Φ_3, and Φ_4. The conditioned BER for each case in a single-relay network is similar to that in a two-relay network. The case probabilities can be computed, respectively, as $P(\Phi_1) = I_1\left(\theta_{\mathrm{r}}^{\mathrm{th}}, \overline{\gamma}_{0,1}\right) I_2\left(\theta_{\mathrm{d}}^{\mathrm{th}}\right) + \left[1 - I_1\left(\theta_{\mathrm{r}}^{\mathrm{th}}, \overline{\gamma}_{0,1}\right)\right] I_1\left(\theta_{\mathrm{d}}^{\mathrm{th}}, \overline{\gamma}_{1,2}\right)$, $P(\Phi_2) = \left[1 - I_1\left(\theta_{\mathrm{r}}^{\mathrm{th}}, \overline{\gamma}_{0,1}\right)\right]\left[1 - I_1\left(\theta_{\mathrm{d}}^{\mathrm{th}}, \overline{\gamma}_{1,2}\right)\right]\left[1 - I_3\left(\theta_{\mathrm{r}}^{\mathrm{th}}, \overline{\gamma}_{0,1}\right)\right]$, $P(\Phi_3) = \left[1 - I_1\left(\theta_{\mathrm{r}}^{\mathrm{th}}, \overline{\gamma}_{0,1}\right)\right]\left[1 - I_1\left(\theta_{\mathrm{d}}^{\mathrm{th}}, \overline{\gamma}_{1,2}\right)\right] I_3\left(\theta_{\mathrm{r}}^{\mathrm{th}}, \overline{\gamma}_{0,1}\right)$, and $P(\Phi_4) = I_1\left(\theta_{\mathrm{r}}^{\mathrm{th}}, \overline{\gamma}_{0,1}\right)\left[1 - I_2\left(\theta_{\mathrm{d}}^{\mathrm{th}}\right)\right]$.

SNR changes much slower compared to the instantaneous SNR (multiple seconds or minutes for the former as compared to miliseconds for the later [C5-13, Chapter 2]), the signaling overhead should not be a major issue in the proposed scheme. Specifically, the change in average SNR depends very much on the density of the obstacles in the physical environment between the transmit and receive antennas and is directly related to the phenomenon of *shadowing*. This is in contrast to the change in the instantaneous SNR, which is governed by the constructive and destructive interference of the multiple signal paths between the transmitter and the receiver, generally known as *multipath fading*. Typically the average SNR changes significantly when the transmitter and/or receiver moves through a distance of the order of cell size, while the change in instantaneous SNR can occurs at the spatial scale of the order of carrier wavelength [C5-13, Chapter 2]. Another possibility is to determine the optimal thresholds and power allocation in advance for typical sets of average SNRs and store them in a look-up table at the relays and destination.

As mentioned earlier, the relays in both ML and PL schemes always retransmit the received signals. However, a relay in the proposed scheme does not transmit in the second phase if the decision variable obtained in the first phase is smaller than a threshold $\theta_{\mathrm{r}}^{\mathrm{th}}$. Therefore, the proposed scheme can actually save some power compared to the ML and PL schemes. This is quantified and discussed further in the next section.

5.4 Simulation Results

This section presents analytical and simulation results to confirm the analysis of the average BERs of the one-relay and two-relay networks. Furthermore, the performances with optimal thresholds/power allocation are provided to illustrate the advantages of the proposed scheme. In all simulations, the noise components at the destination and relays are modeled as i.i.d. $\mathcal{CN}(0,1)$ random variables. For convenience, denote $\sigma_1^2 = \sigma_{0,1}^2 = \sigma_{0,2}^2$ and $\sigma_2^2 = \sigma_{1,3}^2 = \sigma_{2,3}^2$ for the case of a two-relay network. All the optimized values are provided in Appendix 5.1. Note that the value

of r in Appendix 5.1 is the fraction of the total power assigned to the source, while that assigned to each relay is $(1-r)/K$.

First, Figs. 5.3 plots the average BERs at the destination for one-relay and two-relay networks and under different channel conditions. The thresholds are arbitrarily chosen as $\{\theta_{\mathrm{r}}^{\mathrm{th}} = 5, \theta_{\mathrm{d}}^{\mathrm{th}} = 2\}$. In both networks, the assigned symbol energies are set to be the same for the source and relays, i.e., $E_0 = E_1$ when $K = 1$ and $E_0 = E_1 = E_2$ when $K = 2$. The figure clearly shows that analytical results (shown in lines) and simulation results (shown as marker symbols) are basically identical, which confirms that the analytical results are correct.

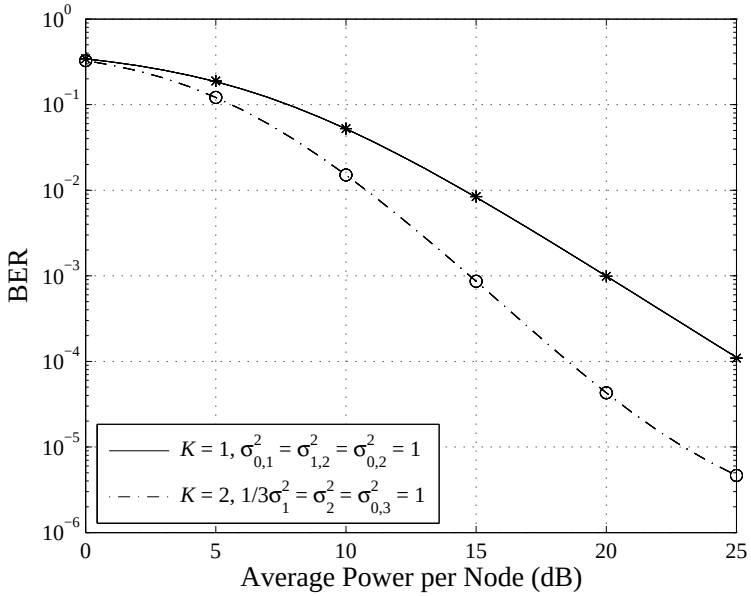

Figure 5.3 BERs of single-relay and two-relay cooperative networks when $\theta_{\mathrm{r}}^{\mathrm{th}} = 5$, $\theta_{\mathrm{d}}^{\mathrm{th}} = 2$. Exact analytical values are shown in lines and simulation results are shown as marker symbols.

Next, Figs. 5.4 and 5.5 illustrate the performance improvements obtained by optimizing the two threshold values alone and by jointly optimizing two threshold values and power allocation in the proposed scheme. The error performance of the PL scheme[5] is also provided in the figure for comparison. It should also be noted that

[5]Since reference [C5-11] does not provide the average BER expression in a two-relay network, we

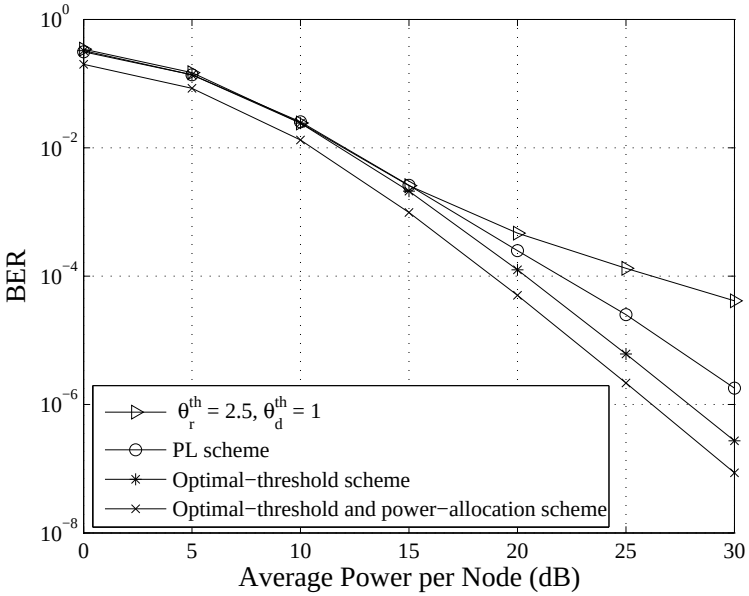

Figure 5.4 BERs of a two-relay network with different schemes when $\sigma_1^2 = \sigma_2^2 = \sigma_{0,3}^2 = 1$.

the channel variances of all communication links are set to be $\sigma_1^2 = \sigma_2^2 = \sigma_{0,3}^2 = 1$ for Fig. 5.4 and $2\sigma_1^2 = 0.1\sigma_2^2 = 5\sigma_{0,3}^2 = 1$ for Fig. 5.5. The figures show that our proposed scheme outperforms the PL scheme. The additional gain obtained by jointly optimizing the thresholds and power allocation over optimizing the thresholds alone is quite significant, about 2 dB and 3 dB at the BER level of 10^{-5} as observed in Figs. 5.4 and 5.5, respectively.

Fig. 5.5 also shows the performance achieved with using only one threshold at the relays. In this one-threshold scheme the second threshold $\theta_{\rm d}^{\rm th}$ is set to zero, while the first threshold value $\theta_{\rm r}^{\rm th}$ is optimized, either separately or jointly with power allocation, to minimize the average BER. The performance improvement offered by the two-threshold method in Fig. 5.5 is expected, but not very significant. It confirms the intuition that the role of the first threshold used at the relays to deal with error propagation is more crucial than the second threshold at the destination. In fact it is simple to realize that if the source-relay links are very strong, the relays likely

do not have the BER performance of the PL scheme with an optimal power allocation.

decodes correctly and forwards the signals and there is no BER improvement by employing/optimizing the threshold at the destination. Taking into account the complexity and modest performance improvement, one could easily prefer the proposed adaptive relaying scheme using only one threshold at the relays.[6]

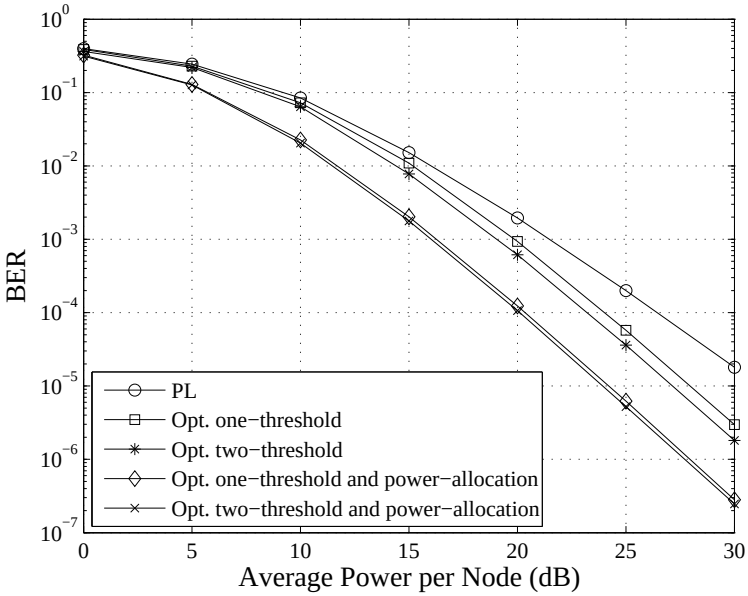

Figure 5.5 BERs of a two-relay network with different schemes when $2\sigma_1^2 = 0.1\sigma_2^2 = 5\sigma_{0,3}^2 = 1$.

The BER performances of the PL and proposed schemes are shown in Fig. 5.6 for the case of a 4-relay network. Since a closed-form BER expression is not available in this case, numerical search is performed to find the optimal thresholds. Briefly, the ranges of two thresholds are limited to reasonable values based on knowledge of the channel conditions (average SNRs). Then a step size for each threshold is set. The BER is then found by simulation for each pair of threshold values. Finally, obtained

[6]A possible detection approach that uses only one threshold at the relays and implicitly rules out a non-forwarding relay is to employ selection combining at the destination. Specifically, the destination makes a decoding decision by considering the received signal with the largest SNR (or the largest signal-plus-noise power). The interested reader can find out more about this approach in the following paper: Ha X. Nguyen and Ha H. Nguyen, "Selection Combining for Noncoherent Decode-and-Forward Relay Networks", *EURASIP Journal of Wireless Communications and Networking*, to appear. *Remark:* This footnote is added to address the external examiner's comment. It is not in the original paper.

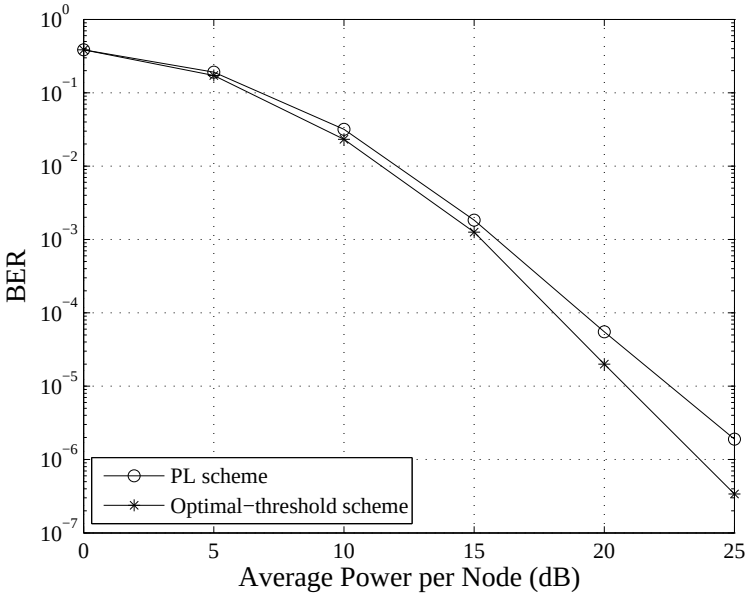

Figure 5.6 BERs of a four-relay network with the proposed and PL schemes when $2\sigma_{0,i}^2 = \sigma_{i,5}^2 = 2\sigma_{0,5}^2 = 1$, $i = 1, 2, 3, 4$.

threshold values are the ones that provide the smallest BER. The figure confirms that the proposed scheme also outperforms the PL scheme in a 4-relay network. In fact a higher diversity order is observed with the proposed scheme.

Finally, it is interesting to quantify the power saving of the proposed scheme compared to the PL scheme. The percentage of power saving can be analytically found to be to $S(\%) = \frac{K}{K+1} I_1(\theta_{\rm r}^{\rm th}, \overline{\gamma}_1)$. Fig. 5.7 illustrates the percentage of power saving for two-relay and four-relay networks presented in Figs. 5.4 and 5.6. The analytical and simulation results are basically identical. Observe that more power saving happens in the lower SNR region. This is expected since a relay likely makes more errors at low SNR and remains silent in the second phase. On the other hand, over the low SNR region the BER performances of both the proposed and PL schemes are similar as shown in Figs. 5.4 and 5.6.

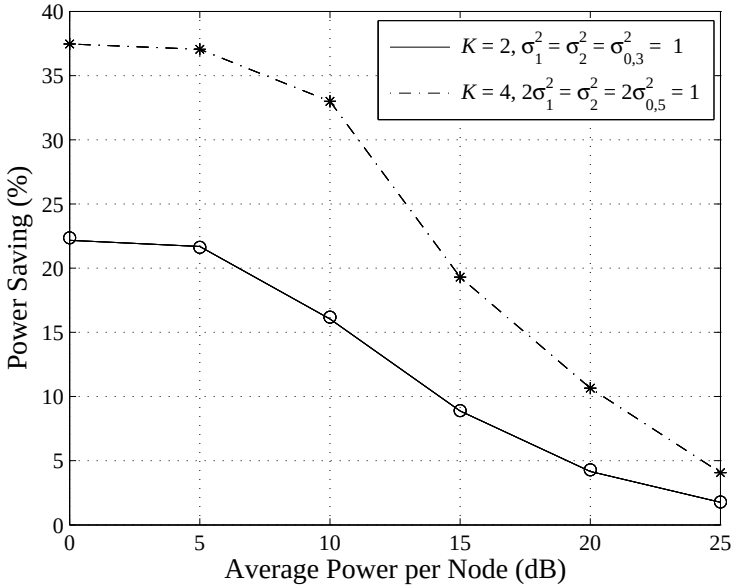

Figure 5.7 Percentages of power saving by the proposed scheme over the PL scheme in two-relay and four-relay networks. Exact analytical values are shown in lines and simulation results are shown as marker symbols.

5.5 Conclusion

In this letter, we have proposed and studied an adaptive relaying scheme for non-coherent cooperative networks. Each node in the network is equipped with a single antenna and the channels are Rayleigh fading. BFSK is used to modulate the signals at both the source and relays. The proposed scheme uses two different thresholds. One threshold is used to select relays for retransmission in the second phase. The other threshold can be used at the destination to detect retransmitting relays. The average BER for a two-relay network is derived in a closed-form expression. Optimal thresholds/power allocation are chosen to minimize the average BER. Performance comparison reveals that by employing optimal thresholds or jointly optimal thresholds and power allocation, our scheme significantly improves the error performance compared to the previously proposed PL scheme, and yet with a similar complexity.

5.A Lemmas used in the Calculation of Error Probabilities

Lemma 1: Consider two random variables $Z_{i,K+1,0} = |y_{i,K+1,0}|$ and $Z_{i,K+1,1} = |y_{i,K+1,1}|$ where $y_{i,K+1,0}$ and $y_{i,K+1,1}$ are as in (5.1) and (5.2), respectively. Assume that the transmitted bit is "0", then the pdfs of $Z_{i,K+1,0}$ and $Z_{i,K+1,1}$ are given by

$$f_{Z_{i,K+1,0}}(z) = \frac{2z}{1+\overline{\gamma}_{i,K+1}} \mathrm{e}^{-z^2/(1+\overline{\gamma}_{i,K+1})}, \quad z \geq 0 \tag{5.35}$$

$$f_{Z_{i,K+1,1}}(z) = 2z\mathrm{e}^{-z^2}, \quad z \geq 0. \tag{5.36}$$

Lemma 2: Consider two random variables $X_{i,K+1} = Z^2_{i,K+1,0} - Z^2_{i,K+1,1}$ and $Y_{i,K+1} = |X_{i,K+1}|$ where $Z_{i,K+1,0}$ and $Z_{i,K+1,1}$ are as in Lemma 1, then the pdfs of $X_{i,K+1}$ and $Y_{i,K+1}$ are

$$f_{X_{i,K+1}}(x) = \begin{cases} \frac{1}{2+\overline{\gamma}_{i,K+1}} \mathrm{e}^{-x/(1+\overline{\gamma}_{i,K+1})}, & x \geq 0 \\ \frac{1}{2+\overline{\gamma}_{i,K+1}} \mathrm{e}^{x}, & x < 0 \end{cases} \tag{5.37}$$

$$f_{Y_{i,K+1}}(x) = \frac{1}{2+\overline{\gamma}_{i,K+1}} \left(\mathrm{e}^{-x/(1+\overline{\gamma}_{i,K+1})} + \mathrm{e}^{-x} \right), \quad x \geq 0. \tag{5.38}$$

Lemma 3: Consider two random variables $Z_{i,K+1,0} = |y_{i,K+1,0}|$ and $Z_{i,K+1,1} = |y_{i,K+1,1}|$ where $y_{i,K+1,0}$ and $y_{i,K+1,1}$ are as in (5.5) and (5.6), respectively. Assume that the transmitted bit is "0", then the pdfs of $Z_{i,K+1,0}$ and $Z_{i,K+1,1}$ are

$$f_{Z_{i,K+1,0}}(z) = f_{Z_{i,K+1,1}}(z) = 2z\mathrm{e}^{-z^2}, \quad z \geq 0. \tag{5.39}$$

Lemma 4: Consider two random variables $X_{i,K+1} = Z^2_{i,K+1,0} - Z^2_{i,K+1,1}$ and $Y_{i,K+1} = |X_{i,K+1}|$ where $Z_{i,K+1,0}$ and $Z_{i,K+1,1}$ are as in Lemma 3, then the pdfs of $X_{i,K+1}$ and $Y_{i,K+1}$ are

$$f_{X_{i,K+1}}(x) = \begin{cases} \frac{1}{2}\mathrm{e}^{-x}, & x \geq 0 \\ \frac{1}{2}\mathrm{e}^{x}, & x < 0 \end{cases} \tag{5.40}$$

$$f_{Y_{i,K+1}}(x) = \mathrm{e}^{-x}, \quad x \geq 0. \tag{5.41}$$

Proof: All the four lemmas above can be easily verified by performing related integrals.

5.B Optimal Thresholds and Power Allocation Factor

Table 5.1 Optimal Thresholds and Power Allocation Factor

Figure	SNR	Opt. two-threshold		Opt. two-threshold & power-allocation			Opt. one-threshold	Opt. one-threshold & power-allocation	
		$\theta_{\mathrm{r}}^{\mathrm{th}}$	$\theta_{\mathrm{d}}^{\mathrm{th}}$	$\theta_{\mathrm{r}}^{\mathrm{th}}$	$\theta_{\mathrm{d}}^{\mathrm{th}}$	r	$\theta_{\mathrm{r}}^{\mathrm{th}}$	$\theta_{\mathrm{r}}^{\mathrm{th}}$	r
Fig. 5.4	0	0.622	0.502	50	50	1			
	5	1.142	0.577	0.725	0	0.761			
	10	2.205	0.697	1.927	0	0.65			
	15	3.702	1.143	3.483	0	0.64			
	20	5.514	1.620	5.328	0	0.653			
	25	7.514	2.016	7.344	0.014	0.67			
	30	9.616	2.345	9.446	0.049	0.686			
Fig. 5.5	0	0.673	0.368	0.649	0.494	0.735	0.622	0.58	0.757
	5	1.17	2.243	1.254	0.813	0.804	1.022	1.252	0.808
	10	1.999	3.968	2.38	1.557	0.833	1.745	2.321	0.841
	15	3.217	4.926	3.892	2.043	0.849	2.906	3.798	0.862
	20	4.795	5.521	5.698	2.376	0.862	4.455	5.577	0.877
	25	6.636	5.925	7.767	2.643	0.872	6.274	7.539	0.889
	30	8.649	5.528	9.628	7.136	0.833	8.253	9.601	0.898
Fig. 5.6	0	0.8	0						
	5	1.2	0.8						
	10	2.4	1.0						
	15	3.7	1.1						
	20	6.3	1.7						
	25	7.3	1.7						

References

[C5-1] J. Laneman, D. Tse, and G. Wornell, "Cooperative diversity in wireless networks: Efficient protocols and outage behavior," *IEEE Trans. Inform. Theory*, vol. 50, pp. 3062–3080, December 2004.

[C5-2] A. Sendonaris, E. Erkip, and B. Aazhang, "User cooperation diversity, Part I: System description," *IEEE Trans. Commun.*, vol. 51, no. 11, pp. 1927–1938, November 2003.

[C5-3] A. Sendonaris, E. Erkip, and B. Aazhang, "User cooperation diversity, Part II: Implementation aspects and performance analysis," *IEEE Trans. Commun.*, vol. 51, no. 11, pp. 1939–1948, November 2003.

[C5-4] F. Onat, A. Adinoyi, Y. Fan, H. Yanikomeroglu, J. Thompson, and I. Marsland, "Threshold selection for SNR-based selective digital relaying in cooperative wireless networks," *IEEE Trans. Wireless Commun.*, vol. 7, pp. 4226–4237, November 2008.

[C5-5] F. Onat, Y. Fan, H. Yanikomeroglu, and J. Thompson, "Asymptotic BER analysis of threshold digital relaying schemes in cooperative wireless systems," *IEEE Trans. Wireless Commun.*, vol. 7, pp. 4938–4947, December 2008.

[C5-6] D. Crouse, C. Berger, S. Zhou, and P. Willett, "Optimal memoryless relays with noncoherent modulation," *IEEE Trans. Signal Process.*, vol. 56, pp. 5962–5975, December 2008.

[C5-7] T. Himsoon, W. Su, and K. Liu, "Differential transmission for amplify-and-forward cooperative communications," *IEEE Signal Process. Letters*, vol. 12, pp. 597–600, September 2005.

[C5-8] T. Himsoon, W. Pam Siriwongpairat, W. Su, and K. Liu, "Differential modulations for multinode cooperative communications," *IEEE Trans. Signal Process.*, vol. 56, pp. 2941–2956, July 2008.

[C5-9] Q. Zhao and H. Li, "Differential modulation for cooperative wireless systems," *IEEE Trans. Signal Process.*, vol. 55, pp. 2273–2283, May 2007.

[C5-10] Q. Zhao, H. Li, and P. Wang, "Performance of cooperative relay with binary modulation in Nakagami-m fading channels," *IEEE Trans. Veh. Technol.*, vol. 57, pp. 3310–3315, September 2008.

[C5-11] D. Chen and J. Laneman, "Modulation and demodulation for cooperative diversity in wireless systems," *IEEE Trans. Wireless Commun.*, vol. 5, pp. 1785–1794, July 2006.

[C5-12] J. G. Proakis, *Digital Communications*. McGraw-Hill, 2000.

[C5-13] D. Tse and P. Viswanath, *Fundamentals of Wireless Communications*. Cambridge University Press, 2005.

6. Throughput Maximization in Noncoherent Cooperative Networks

Published as:

Ha X. Nguyen, Ha H. Nguyen and Tho Le-Ngoc, "Throughput Maximization in Noncoherent Cooperative Networks", to appear in *IET Communications*.

It is important to emphasize again that a cooperative diversity system typically suffers a certain throughput loss because it requires at least two time slots instead of one time slot as compared to the direct transmission. As mentioned in Chapter 2, to overcome this disadvantage, there are two main techniques, namely distributed space-time coding and relay selection. By exploiting limited feedback from the destination, e.g., a single bit indicating the success or failure of the direct transmission, reference [C6-10] introduced incremental relaying protocol, another method to alleviate throughput loss. In particular, a cooperative transmission is employed only when the transmission between the source and destination is not successful. However, those works are based on an amplify-and-forward transmission at the relays and a coherent detection at the destination. Motivated by the above observations, the manuscript included in this chapter studies an incremental relaying protocol based on the adaptive DF relaying scheme for a cooperative wireless network in which BFSK modulation is employed to facilitate noncoherent communications.

Specifically, two different thresholds are employed in order to reduce error propagation and satisfy BER requirement. One threshold is used to select reliable relays, i.e., a relay retransmits when requested only if its decision variable is larger than the

threshold. The other threshold is used at the destination as follows: the destination sends a request to retransmit if the decision variable corresponding to a received signal is smaller than the threshold, otherwise, the destination sends a request to stop retransmissions. Then the destination combines all the received signals to make a final decision. For the case of BFSK, very-tight closed-form upper bounds for both the average BER and throughput are derived. Based on the obtained BER and throughput expressions, optimal thresholds are chosen to maximize the throughput while the BER meets a given constraint. To verify the analytical results, simulation was conducted and the results are in line with the theoretical analysis. Furthermore, the results show that the proposed protocol leads to a considerable improvement in throughput of cooperative diversity systems.

Throughput Maximization in Noncoherent Cooperative Networks

Ha X. Nguyen, Ha H. Nguyen, and Tho Le-Ngoc

Abstract

An incremental relaying protocol based on the adaptive decode-and-forward (DF) relaying scheme is presented for a cooperative wireless network composed of one source, K relays, and one destination and with binary frequency-shift keying (BFSK) modulation. In order to reduce error propagation and satisfy bit error rate (BER) requirement, the proposed protocol employs two thresholds. One threshold is used to select reliable relays: if a relay is requested to retransmit, it will do so if its decision variable is larger than the threshold; otherwise, it remains silent. The other threshold is used at the destination as follows: the destination sends a request to retransmit (RR) if the decision variable corresponding to a received signal is smaller than the threshold, otherwise, the destination sends a request to stop retransmissions (RS). Then the destination combines the signals from the requested relays and from the source to make the final decision. Very-tight closed-form upper bounds for both the average BER and throughput are derived for the proposed protocol. Based on the obtained BER and throughput expressions, the problem of choosing optimal thresholds to maximize the throughput while the BER meets a given constraint is investigated. Simulation results are provided to illustrate and validate analytical results. The results show that our proposed protocol leads to a considerable improvement in the performance of cooperative diversity systems.

Manuscript was submitted to *IET Communications* on September 16, 2010; revised on February 4, 2011; accepted on July 01, 2011.

Ha X. Nguyen (*contact author) and Ha H. Nguyen are with the Department of Electrical and Computer Engineering, University of Saskatchewan, 57 Campus Drive, Saskatoon, Sask., Canada, S7N 5A9 (e-mails: hxn201@mail.usask.ca, ha.nguyen@usask.ca).

Tho Le-Ngoc is with the Department of Electrical and Computer Engineering, McGill University, 3480 University Street, Montreal, Quebec, Canada, H3A 2A7 (e-mail: tho@ece.mcgill.ca).

Index terms

Cooperative diversity, relay communications, frequency-shift-keying, fading channel, decode-and-forward protocol, throughput maximization.

6.1 Introduction

It has been well-known that multiple-input multiple-output (MIMO) techniques can offer a significant performance improvement for data transmission in wireless networks [C6-1]. Unfortunately, packing multiple antennas onto a small mobile terminal faces many difficulties, such as size, cost, and hardware complexity. Such limitations motivate the concept of cooperative/relay communications. The basic idea is that a source node transmits information to the destination not only through a direct link but also through relay links so that the benefits of MIMO technology can be exploited even with single-antenna mobile terminals [C6-2, C6-3, C6-4, C6-5, C6-6, C6-7, C6-8].

Depending on the signal processing performed at relays, cooperative protocols can be classified into three main groups: amplify-and-forward (AF), decode-and-forward (DF), and compress-and-forward (CF) [C6-2, C6-9]. With DF, relays decode the source's messages, re-encode and re-transmit to the destination. However, a major challenge with the DF protocol is that it is not simple to realize the cooperative diversity. This is due to possible retransmission of erroneously decoded bits of the message by the relays in the DF protocol [C6-2, C6-10, C6-5, C6-6]. There are many ways to overcome such a challenge. For example, an error detection code can be added at the source. Based on the decoding result in the first phase, the relay can decide to retransmit or remain silent in the second phase [C6-11, C6-12]. Setting a threshold based on the link signal-to-noise ratio (SNR) is another practical approach to reduce error propagation. Specifically, when the source-relay SNR is larger than a threshold, the probability of decoding error at the relay is negligible and hence the relay retransmits the message [C6-2, C6-10, C6-5, C6-13, C6-6]. In [C6-14], a receiver has been designed to eliminate errors at the relay, which allows the relay to always

forward the received data. In particular, a cooperative maximum-ratio-combining (C-MRC) detector was proposed at the destination to collect the full diversity order by taking into consideration the instantaneous bit-error-rate (BER) of the source-relay link.

It is also important to recognize that a cooperative diversity system typically suffers a certain throughput loss because it requires at least two time slots instead of one time slot as compared to the direct transmission. To overcome this disadvantage, reference [C6-2] proposed to use distributed space-time coding. However, finding codes for a network with more than one relay is still largely open. Further to the work in [C6-2], reference [C6-10] introduced incremental relaying protocol. More specifically, a cooperative transmission is employed only when the transmission between the source and destination is not successful. Reference [C6-5] proposed a simple cooperative diversity protocol, called "opportunistic relaying" in which only the best relay is selected to retransmit. Here the best relay is selected by a certain criterion. Recently, reference [C6-15] combines the above two techniques, and called it "incremental opportunistic relaying", to further improve the throughput of a cooperative diversity system. The protocol works as follows. In the first phase, the source transmits its information to the destination. Then if the source-destination SNR is sufficiently high, the feedback from the destination that indicates a success of the direct transmission is sent to the source and relays, and the relays do nothing. If the source-destination SNR is not sufficiently high for successful direct transmission, then requests are made so that the relays retransmit what they received from the source after processing. In this case, only the best relay is selected to retransmit. The destination then combines the two transmissions to decode the transmitted information. Another approach to improve system throughput is variable-rate transmission [C6-15], [C6-16]. Particularly, the source adapts its rate according to the changing channel conditions. However, those works are based on an amplify-and-forward transmission at the relays.

Most of the papers mentioned above focused on *coherent* communications, i.e., the receivers (at relays and destination) are assumed to have a perfect knowledge

of channel state information (CSI) of all the transmission links propagated by their received signals. However, in practice the exact values of CSI cannot actually be obtained. Since such a perfect CSI assumption might be unrealistic and/or difficult to meet, noncoherent modulation and demodulation have been proposed and considered as more attractive methods in cooperative networks. Differential phase-shift keying (DPSK) has been studied for both AF and DF protocols in [C6-17, C6-18, C6-19, C6-20]. With the DF protocol in [C6-18], the authors considered an ideal case that the relay is able to know exactly whether each decoded symbol is correct. The works in [C6-19, C6-20] examine a very simple cooperative system with one source, one relay, and one destination node. A framework of noncoherent cooperative diversity for the DF protocol employing FSK modulation, a popular modulation scheme in noncoherent communications, has been studied in [C6-21]. The maximum likelihood (ML) demodulation and suboptimal piecewise linear (PL) scheme were proposed to detect the signals at the destination. However, it should be mentioned that either ML or PL demodulation can still suffer from the error propagation phenomenon [C6-7]. To address the issue of error propagation in [C6-21], an adaptive relaying scheme in which one threshold is employed at the relays and one threshold is employed at the destination is investigated in [C6-22]. The results in [C6-22] show that using two thresholds can significantly improve the BER performance as compared to either the ML or PL scheme.

This work is also concerned with noncoherent cooperative networks in which BFSK is employed. Similar to [C6-22] the transmission protocol is based on the use of two thresholds. However, since the focus of this work is on throughput maximization, the proposed protocol is different from the one proposed in [C6-22]. The transmission protocol works as follows. After receiving the signal in the first phase (broadcasting phase) from the source, each relay decodes and marks itself as a reliable relay if its decision variable is larger than the first threshold[1], $\theta_{\mathrm{r}}^{\mathrm{th}}$. Otherwise it marks itself as

[1]It should be emphasized that by employing a threshold to detect the decoding error, the processing at the relays is much simpler than the case employing error detection code, e.g., cyclic redundancy check (CRC).

an unreliable relay. At the destination, if the decision variable corresponding to the source-destination link is larger than the second threshold, $\theta_{\mathrm{d}}^{\mathrm{th}}$, the destination broadcasts an RS to the source and relays. The relays do nothing and the source continues a new transmission. Otherwise an RR is broadcasted by the destination to indicate transmission failure. After receiving the first RR, the first relay retransmits or remains silent depending on the status of the relay (i.e., reliable or unreliable relay). Then if the decision variable corresponding to the source-destination and the relay-destination link is larger than the threshold, an RS is broadcasted and the system starts with a new transmission. Otherwise an RR is broadcasted and the second relay takes turn to retransmit the signal. The relaying phase continues until an RS is broadcasted or all the relays retransmit their signals. Finally, the destination combines all the received signals to make a final decision. In essence, the first threshold enables each relay to adapt its operation according to the instantaneous source-relay channel quality (i.e., to reduce error propagation), while the second threshold helps the destination to decide on whether the relays should continue their retransmission (in order to satisfy the BER requirement) The average upper bounds on BER and throughput of the proposed protocol are analytically derived. Based on these bounds, the optimal threshold values are determined to maximize the average throughput while the BER meets a given constraint. Numerical and simulation results verify that our obtained upper bounds on the BER and throughput expressions are very tight. Moreover, the proposed protocol leads to a considerable improvement in the performance of cooperative diversity systems.

The remainder of this paper is organized as follows. Section 6.2 describes the system model. Section 6.3 presents the average BER analysis and throughput computation and discusses how to find the optimal thresholds. Numerical and simulation results are presented in Section 6.4. Finally, Section 6.5 concludes the paper.

Notations: $\mathbb{E}\{x(\gamma)\}$ is the expectation of $x(\gamma)$ with respect to the random variable γ. $\mathcal{CN}(0, \sigma^2)$ denotes a circularly symmetric complex Gaussian random variable with variance σ^2. The moment-generating function (MGF) of random variable X is

denoted by $M_X(s)$. $P(\cdot)$ denotes the probability measure of some probability space $(\Omega, \mathcal{B})$ where Ω is the finite set and $\mathcal{B}$ is the sigma algebra generated by this set.

6.2 System Model

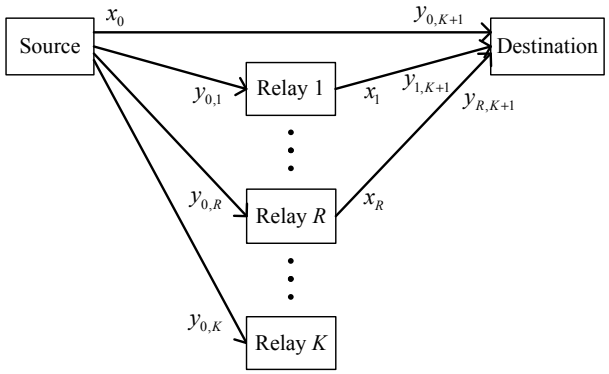

Figure 6.1 A wireless relay network with K relay nodes.

The system model considered in this paper is similar to the one in [C6-22] and it is illustrated in Fig. 6.1. Here a source node transmits information to a destination node with the help of K relay nodes. All nodes are equipped with one antenna and operates in a half-duplex mode (i.e., a node cannot transmit and receive simultaneously). The K relays employ the DF protocol and communicate with the destination over orthogonal channels. The source, relays, and destination are denoted and indexed by node 0, node i, $i = 1, \ldots, K$, and node $K + 1$, respectively[2].

The transmission from the source to destination can be divided into two phases as follows. In the first phase (broadcasting phase), the source broadcasts a BFSK signal. In the baseband model, the received signals at node i are written as

$$y_{0,i,0} = (1 - x_0)\sqrt{E_0}h_{0,i} + n_{0,i,0}, \tag{6.1}$$

$$y_{0,i,1} = x_0\sqrt{E_0}h_{0,i} + n_{0,i,1}, \tag{6.2}$$

where $h_{0,i}$ and $n_{0,i,k}$ are the channel fading coefficient between node 0 and node i and the noise component at node i, $i = 1, \ldots, K + 1$, respectively. E_0 is the aver-

[2]It should be mentioned here that a set up, e.g., numbering the relays, is necessary before any data transmission.

age transmitted symbol energy of the source. In (6.1) and (6.2), the third subscript $k \in \{0, 1\}$ denotes the two frequency subbands used in BFSK signalling. Furthermore, the source symbol $x_0 = 0$ if the first frequency subband is used and $x_0 = 1$ if the second frequency subband is used. In this paper, we assume that the channel between any two nodes is modeled as $\mathcal{CN}(0, \sigma_{ij}^2)$, where i, j refer to transmit and receive nodes, respectively, leading to the well-known Rayleigh flat fading model. The noise components at both the relays and destination are modeled as i.i.d. $\mathcal{CN}(0, N_0)$ random variables. Therefore the instantaneous received SNR for the transmission from node i to node j, denoted by γ_{ij}, is given as $\gamma_{ij} = E_i|h_{i,j}|^2/N_0$. With Rayleigh fading, the pdf of γ_{ij} is exponential and given by $f_{\gamma_{ij}}(\gamma_{ij}) = \frac{1}{\sigma_{ij}^2} \mathrm{e}^{-\gamma_{ij}/\overline{\gamma}_{ij}}$, where $\overline{\gamma}_{ij}$ is the average SNR of the i-j link and defined as $\overline{\gamma}_{ij} = E_i\sigma_{ij}^2/N_0$.

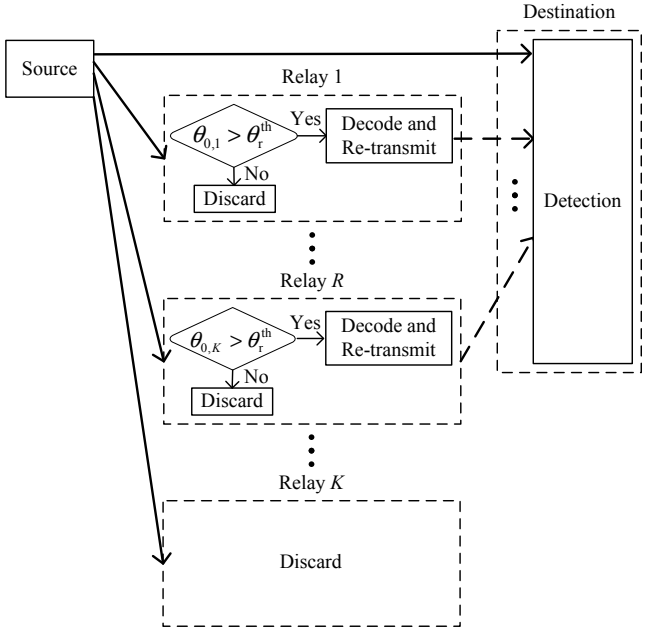

Figure 6.2 System description of the proposed scheme when R relays are requested to retransmit.

After receiving the signal from the source, the relays and destination work as follows (see Fig. 6.2). Each relay decodes and marks itself as a reliable relay if the magnitude of the energy difference in the two subbands, given by $\theta_{0,i} = \frac{\overline{\gamma}_{0,i}}{(\overline{\gamma}_{0,i}+1)N_0}\left||y_{0,i,0}|^2 - |y_{0,i,1}|^2\right|$, satisfies $\theta_{0,i} \geq \theta_{\mathrm{r}}^{\mathrm{th}}$. When node i is requested to retransmit in the second phase (relaying phase) (i.e., the i^{th} RR is broadcasted), the received

signals at the destination in the two subbands are

$$y_{i,K+1,0} = (1-x_i)\sqrt{E_i}h_{i,K+1} + n_{i,K+1,0}, \tag{6.3}$$

$$y_{i,K+1,1} = x_i\sqrt{E_i}h_{i,K+1} + n_{i,K+1,1}, \tag{6.4}$$

where E_i is the average symbol energy *assigned* to node i and $n_{i,K+1,k}$ is the noise component at the destination in the second phase. Note that if the ith relay makes a correct detection, then $x_i = x_0$. Otherwise $x_i \neq x_0$.

If $\theta_{0,i} < \theta_{\mathrm{r}}^{\mathrm{th}}$, node i marks itself as an unreliable relay and remains silent in the second phase when it is requested to retransmit. The outputs in the two subbands are

$$y_{i,K+1,0} = n_{i,K+1,0}, \tag{6.5}$$

$$y_{i,K+1,1} = n_{i,K+1,1}. \tag{6.6}$$

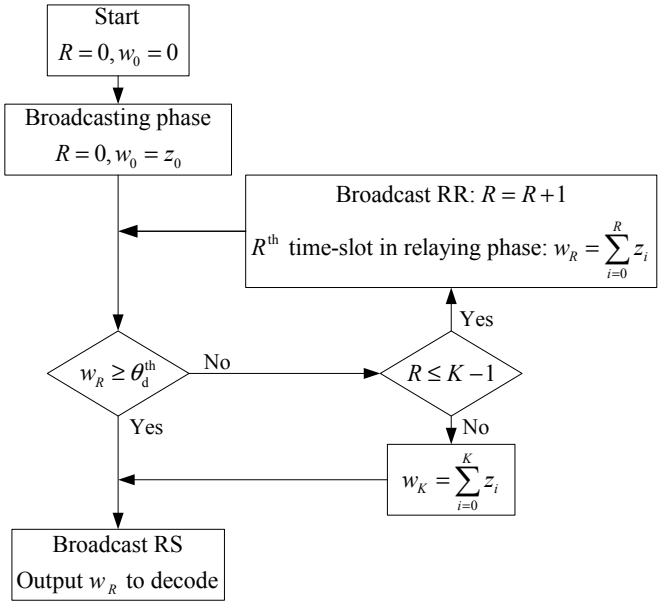

Figure 6.3 Operation description of the proposed scheme at the destination.

The flow-chart in Fig. 6.3 describes the process at the destination. After receiving the signal from the source, the destination broadcasts an RS if the decision variable, given by $w_0 = z_0 = \frac{\overline{\gamma}_{0,K+1}}{(\overline{\gamma}_{0,K+1}+1)N_0}\left||y_{0,K+1,0}|^2 - |y_{0,K+1,1}|^2\right|$, satisfies $w_0 \geq \theta_{\mathrm{d}}^{\mathrm{th}}$. Otherwise an RR is broadcasted to the source and the relays. After

the first RR is broadcasted, the destination receives the signal from the first relay and updates the decision variable. If the updated decision variable is larger than the threshold, an RS is broadcasted. Otherwise another RR is broadcasted. The relaying phase continues until an RS is broadcasted, i.e., $w_R = \sum_{i=0}^{R} z_i \geq \theta_{\mathrm{d}}^{\mathrm{th}}$ where $z_i = \frac{\overline{\gamma}_{i,K+1}}{(\overline{\gamma}_{i,K+1}+1)N_0} \left(|y_{i,K+1,0}|^2 - |y_{i,K+1,1}|^2\right)$ and R is the number of relays that the destination requests to retransmit, or all the relays retransmit their signals.

When an RS is broadcasted by the destination, the destination also combines all the received signals to make a final decision. Given the available information about average SNRs, the optimum detector at the destination is of the following form [C6-21]:

$$w_R = \sum_{i=0}^{R} z_i = \sum_{i=0}^{R} \frac{\overline{\gamma}_{i,K+1}}{(\overline{\gamma}_{i,K+1}+1)N_0} \left(|y_{i,K+1,0}|^2 - |y_{i,K+1,1}|^2\right) \underset{1}{\overset{0}{\gtrless}} 0. \tag{6.7}$$

It should be mentioned here that if $R < K$, then $|w_R| \geq \theta_{\mathrm{d}}^{\mathrm{th}}$.

The basic intuition of using two thresholds for the system is to reduce error propagation and maximize the system throughput while meeting a certain required BER performance. As mentioned earlier, the DF protocol does not provide cooperative diversity if the relays always retransmit the decoded bits. With BFSK, the energy difference in the two subbands can be used to examine the reliability of the decision statistics at each relay [C6-22]. Hence the first threshold is used at the relays to reduce error propagation: if the magnitude of the energy difference is above a threshold, the relay forwards the signal. Otherwise, the relay remains silent in the second phase. Besides, there is a trade-off between throughput and BER performance in any communication systems. How to maximize the system throughput under a constraint on the BER requirement is an important issue. A second threshold is thus employed to address this issue. Specifically, if the decision variable at the destination is smaller than the second threshold, the BER performance is still worse than the BER requirement. Hence the destination needs more signals before making a final decision.[3]

[3]It should be pointed out that the proposed protocol requires one or more RR bits to complete the transmission of one information bit, which implies a high cost. As such the proposed protocol is more

6.3 Performance Analysis

To simplify our analysis, we assume that all the relays have the same average SNRs to the source and to the destination, i.e., $\overline{\gamma}_{0,1} = \overline{\gamma}_{0,2} = \cdots = \overline{\gamma}_{0,K} = \overline{\gamma}_1$ and $\overline{\gamma}_{1,K+1} = \overline{\gamma}_{2,K+1} = \cdots = \overline{\gamma}_{K,K+1} = \overline{\gamma}_2$, i.e., a balanced and symmetrical network. Furthermore, let $\overline{\gamma}_0 = \overline{\gamma}_{0,K+1}$. This assumption implies that the first threshold at all the relays is the same. Generalization of the analysis in this section to networks with arbitrary qualities of source-relay and relay-destination links is rather straightforward.

6.3.1 Derivation of Probability Density Function of Decision Variable w_R

The key in performing BER and throughput analysis of the network under consideration is to obtain the probability distribution functions (pdf) of the decision variable w_R expressed in (6.7). To this end, we first review pdfs and moment-generating functions (MGFs) of some related random variables.

When the transmitted bit at node i is "0", the pdfs of two random variables $z_{i,K+1,0}$ and $z_{i,K+1,1}$, defined as $z_{i,K+1,0} = \frac{\overline{\gamma}_{i,K+1}}{\overline{\gamma}_{i,K+1}+1}|y_{i,K+1,0}|^2$ and $z_{i,K+1,1} = \frac{\overline{\gamma}_{i,K+1}}{\overline{\gamma}_{i,K+1}+1}|y_{i,K+1,1}|^2$ where $y_{i,K+1,0}$ and $y_{i,K+1,1}$ are as in (6.3) and (6.4), respectively, are given by[4]

$$f_{z_{i,K+1,0}}(x) = \frac{1}{\overline{\gamma}_{i,K+1}} \mathrm{e}^{-x/\overline{\gamma}_{i,K+1}}, \quad f_{z_{i,K+1,1}}(x) = \frac{1+\overline{\gamma}_{i,K+1}}{\overline{\gamma}_{i,K+1}} \mathrm{e}^{-x(1+\overline{\gamma}_{i,K+1})/\overline{\gamma}_{i,K+1}}. \quad (6.8)$$

It follows that the MGFs of $z_{i,K+1,0}$ and $z_{i,K+1,1}$ are

$$M_{z_{i,K+1,0}}(s) = \mathbb{E}\left\{\mathrm{e}^{-sz_{i,K+1,0}}\right\} = \frac{1}{1+\overline{\gamma}_{i,K+1}s}, \quad (6.9)$$

$$M_{z_{i,K+1,1}}(s) = \mathbb{E}\left\{\mathrm{e}^{-sz_{i,K+1,1}}\right\} = \frac{1}{1+\frac{\overline{\gamma}_{i,K+1}}{1+\overline{\gamma}_{i,K+1}}s}. \quad (6.10)$$

practical for block fading channels, i.e., when the fading coefficients remain constant over a large block of bits. *Remark:* This footnote is added to address the external examiner's comment. It is not in the original paper.

[4]Lemma 1 in Appendix 6.A of [C6-22] can be used to compute these pdfs.

Likewise, when the transmitted bit at node i is "1", the corresponding MGFs are

$$M_{z_{i,K+1,0}}(s) = \frac{1}{1+\frac{\overline{\gamma}_{i,K+1}}{1+\overline{\gamma}_{i,K+1}}s}, \tag{6.11}$$

$$M_{z_{i,K+1,1}}(s) = \frac{1}{1+\overline{\gamma}_{i,K+1}s}. \tag{6.12}$$

When node i is silent, the pdfs of two random variables $z_{i,K+1,0}$ and $z_{i,K+1,1}$ are the same:

$$f_{z_{i,K+1,0}}(x) = f_{z_{i,K+1,1}}(x) = \frac{1+\overline{\gamma}_{i,K+1}}{\overline{\gamma}_{i,K+1}} \mathrm{e}^{-x(1+\overline{\gamma}_{i,K+1})/\overline{\gamma}_{i,K+1}}, \tag{6.13}$$

and the corresponding MGF is

$$M_{z_{i,K+1,0}}(s) = M_{z_{i,K+1,1}}(s) = \frac{1}{1+\frac{\overline{\gamma}_{i,K+1}}{1+\overline{\gamma}_{i,K+1}}s}. \tag{6.14}$$

Now w_R in (6.7) can be rewritten as

$$w_R = \sum_{i=0}^{R} \frac{\overline{\gamma}_{i,K+1}}{(\overline{\gamma}_{i,K+1}+1)N_0} \left(|y_{i,K+1,0}|^2 - |y_{i,K+1,1}|^2 \right) = \alpha - \beta, \tag{6.15}$$

where $\alpha = \sum_{i=0}^{R} \frac{\overline{\gamma}_{i,K+1}}{(\overline{\gamma}_{i,K+1}+1)N_0} |y_{i,K+1,0}|^2$ and $\beta = \sum_{i=0}^{R} \frac{\overline{\gamma}_{i,K+1}}{(\overline{\gamma}_{i,K+1}+1)N_0} |y_{i,K+1,1}|^2$.

Let the set $\mathcal{S}_{\text{relay}} = \{1, 2, \ldots, R\}$ of R relays be divided into three disjoint subsets Ω_{C}, Ω_{I}, and Ω_{S}. Here Ω_{C}, Ω_{I}, and Ω_{S} are the sets of relays that forward a correct bit, an incorrect bit, and remain silent in the second phase, respectively. Let $|\Omega_{\text{C}}| = M$, $|\Omega_{\text{I}}| = N$, and $|\Omega_{\text{S}}| = L$ where $|\Omega|$ denotes the cardinality of the set Ω. Clearly, $R = M + N + L$. The MGFs of α and β are expressed, respectively, as[5]

$$\begin{aligned} M_\alpha(s) &= (1+\overline{\gamma}_0 s)^{-1} (1+\overline{\gamma}_2 s)^{-M} \left(1+\frac{\overline{\gamma}_2}{1+\overline{\gamma}_2}s\right)^{-N-L} \\ &= A_1 (1+\overline{\gamma}_0 s)^{-1} + \sum_{i=1}^{M} B_i (1+\overline{\gamma}_2 s)^{-i} + \sum_{i=1}^{N+L} C_i \left(1+\frac{\overline{\gamma}_2}{1+\overline{\gamma}_2}s\right)^{-i} \end{aligned} \tag{6.16}$$

$$\begin{aligned} M_\beta(s) &= \left(1+\frac{\overline{\gamma}_0}{1+\overline{\gamma}_0}s\right)^{-1} (1+\overline{\gamma}_2 s)^{-N} \left(1+\frac{\overline{\gamma}_2}{1+\overline{\gamma}_2}s\right)^{-M-L} \\ &= D_1 \left(1+\frac{\overline{\gamma}_0}{1+\overline{\gamma}_0}s\right)^{-1} + \sum_{i=1}^{N} E_i (1+\overline{\gamma}_2 s)^{-i} + \sum_{i=1}^{M+L} F_i \left(1+\frac{\overline{\gamma}_2}{1+\overline{\gamma}_2}s\right)^{-i} \end{aligned} \tag{6.17}$$

[5]With n independent random variables X_1, X_2, ..., X_n, the MGF of random variable $X = \sum_{i=1}^{n} X_n$ is given by $M_X(s) = \prod_{i=1}^{n} M_{X_i}(s)$.

where

$$A_1 = \left(1 - \frac{\overline{\gamma}_2}{\overline{\gamma}_0}\right)^{-M} \left(1 - \frac{\overline{\gamma}_2}{\overline{\gamma}_0(1+\overline{\gamma}_2)}\right)^{-N-L}, \tag{6.18}$$

$$B_i = \frac{\overline{\gamma}_2^{i-M}}{(M-i)!} \frac{\partial^{M-i}}{\partial s^{M-i}} \left[(1+\overline{\gamma}_0 s)^{-1} \left(1 + \frac{\overline{\gamma}_2}{1+\overline{\gamma}_2} s\right)^{-N-L}\right]_{s=-1/\overline{\gamma}_2}, \tag{6.19}$$

$$C_i = \frac{\overline{\gamma}_2^{i-N-L}}{(N+L-i)!} \frac{\partial^{N+L-i}}{\partial s^{N+L-i}} \left[(1+\overline{\gamma}_0 s)^{-1} (1+\overline{\gamma}_2 s)^{-M}\right]_{s=-(1+\overline{\gamma}_2)/\overline{\gamma}_2}, \tag{6.20}$$

$$D_1 = \left(1 + \frac{\overline{\gamma}_2(1+\overline{\gamma}_0)}{\overline{\gamma}_0}\right)^{-N} \left(1 + \frac{\overline{\gamma}_2(1+\overline{\gamma}_0)}{\overline{\gamma}_0(1+\overline{\gamma}_2)}\right)^{-M-L}, \tag{6.21}$$

$$E_i = \frac{\overline{\gamma}_2^{i-N}}{(N-i)!} \frac{\partial^{N-i}}{\partial s^{N-i}} \left[\left(1 + \frac{\overline{\gamma}_0}{1+\overline{\gamma}_0} s\right)^{-1} \left(1 + \frac{\overline{\gamma}_2}{1+\overline{\gamma}_2} s\right)^{-M-L}\right]_{s=-1/\overline{\gamma}_2}, \tag{6.22}$$

$$F_i = \frac{\overline{\gamma}_2^{i-M-L}}{(M+L-i)!} \frac{\partial^{M+L-i}}{\partial s^{M+L-i}} \left[\left(1 + \frac{\overline{\gamma}_0}{1+\overline{\gamma}_0} s\right)^{-1} (1+\overline{\gamma}_2 s)^{-N}\right]_{s=-(1+\overline{\gamma}_2)/\overline{\gamma}_2}. \tag{6.23}$$

Taking the inverse Laplace transforms of $M_\alpha(s)$ and $M_\beta(s)$, the pdfs of α and β are, respectively, as

$$f_\alpha(x) = \frac{A_1}{\overline{\gamma}_0} \mathrm{e}^{-\frac{x}{\overline{\gamma}_0}} + \sum_{i=1}^{M} \frac{B_i (\overline{\gamma}_2)^{-i}}{(i-1)!} x^{i-1} \mathrm{e}^{-\frac{x}{\overline{\gamma}_2}} + \sum_{i=1}^{N+L} \frac{C_i}{(i-1)!} \left(\frac{\overline{\gamma}_2}{1+\overline{\gamma}_2}\right)^{-i} x^{i-1} \mathrm{e}^{-\frac{x(1+\overline{\gamma}_2)}{\overline{\gamma}_2}} \tag{6.24}$$

$$f_\beta(x) = \frac{D_1(1+\overline{\gamma}_0)}{\overline{\gamma}_0} \mathrm{e}^{-\frac{x(1+\overline{\gamma}_0)}{\overline{\gamma}_0}} + \sum_{i=1}^{N} \frac{E_i (\overline{\gamma}_2)^{-i}}{(i-1)!} x^{i-1} \mathrm{e}^{-\frac{x}{\overline{\gamma}_2}} + \sum_{i=1}^{M+L} \frac{F_i}{(i-1)!} \left(\frac{\overline{\gamma}_2}{1+\overline{\gamma}_2}\right)^{-i} x^{i-1} \mathrm{e}^{-\frac{x(1+\overline{\gamma}_2)}{\overline{\gamma}_2}} \tag{6.25}$$

The pdf of random variable w_R where $w_R = \alpha - \beta$ now can be computed as [C6-23]:

$$f_{w_R}(z) = \begin{cases} \int_{y=0}^{\infty} f_{\alpha\beta}(y+z, y)\mathrm{d}y, & z \geq 0 \\ \int_{x=0}^{\infty} f_{\alpha\beta}(x, x-z)\mathrm{d}z, & z < 0 \end{cases}. \tag{6.26}$$

For $z \geq 0$, $f_{w_R}(z)$ can be determined as

$$
\begin{aligned}
f_{w_R}(z) &= \int_{y=0}^{\infty} f_{xy}(y+z, y)\mathrm{d}y \\
&= \frac{A_1 D_1(1+\overline{\gamma}_0)}{\overline{\gamma}_0^2} K_1\left(1, 1, \frac{1}{\overline{\gamma}_0}, \frac{1+\overline{\gamma}_0}{\overline{\gamma}_0}, z\right) \\
&+ \sum_{i=1}^{N} \frac{A_1 E_i (\overline{\gamma}_2)^{-i}}{\overline{\gamma}_0 (i-1)!} K_1\left(1, i, \frac{1}{\overline{\gamma}_0}, \frac{1}{\overline{\gamma}_2}, z\right) \\
&+ \sum_{i=1}^{M+L} \frac{A_1 F_i}{\overline{\gamma}_0 (i-1)!} \left(\frac{\overline{\gamma}_2}{1+\overline{\gamma}_2}\right)^{-i} K_1\left(1, i, \frac{1}{\overline{\gamma}_0}, \frac{1+\overline{\gamma}_2}{\overline{\gamma}_2}, z\right) \\
&+ \sum_{i=1}^{M} \frac{B_i D_1 (1+\overline{\gamma}_0)(\overline{\gamma}_2)^{-i}}{\overline{\gamma}_0 (i-1)!} K_1\left(i, 1, \frac{1}{\overline{\gamma}_2}, \frac{1+\overline{\gamma}_0}{\overline{\gamma}_0}, z\right) \\
&+ \sum_{j=1}^{N} \sum_{i=1}^{M} \frac{B_i E_j (\overline{\gamma}_2)^{-i-j}}{(i-1)!(j-1)!} K_1\left(i, j, \frac{1}{\overline{\gamma}_2}, \frac{2}{\overline{\gamma}_2}, z\right) \\
&+ \sum_{j=1}^{M+L} \sum_{i=1}^{M} \frac{B_i F_j (\overline{\gamma}_2)^{-i}}{(i-1)!(j-1)!} \left(\frac{\overline{\gamma}_2}{1+\overline{\gamma}_2}\right)^{-j} K_1\left(i, j, \frac{1}{\overline{\gamma}_2}, \frac{1+\overline{\gamma}_2}{\overline{\gamma}_2}, z\right) \\
&+ \sum_{i=1}^{N+L} \frac{D_1 C_i (1+\overline{\gamma}_0)}{\overline{\gamma}_0 (i-1)!} \left(\frac{\overline{\gamma}_2}{1+\overline{\gamma}_2}\right)^{-i} K_1\left(i, 1, \frac{1+\overline{\gamma}_0}{\overline{\gamma}_0} + \frac{1+\overline{\gamma}_2}{\overline{\gamma}_2}, \frac{1+\overline{\gamma}_2}{\overline{\gamma}_2}, z\right) \\
&+ \sum_{j=1}^{N} \sum_{i=1}^{N+L} \frac{C_i E_j (\overline{\gamma}_2)^{-j}}{(i-1)!(j-1)!} \left(\frac{\overline{\gamma}_2}{1+\overline{\gamma}_2}\right)^{-i} K_1\left(i, j, \frac{1+\overline{\gamma}_2}{\overline{\gamma}_2}, \frac{1}{\overline{\gamma}_2}, z\right) \\
&+ \sum_{j=1}^{M+L} \sum_{i=1}^{N+L} \frac{C_i F_j}{(i-1)!(j-1)!} \left(\frac{\overline{\gamma}_2}{1+\overline{\gamma}_2}\right)^{-i-j} K_1\left(i, j, \frac{1+\overline{\gamma}_2}{\overline{\gamma}_2}, \frac{1+\overline{\gamma}_2}{\overline{\gamma}_2}, z\right) \quad (6.27)
\end{aligned}
$$

where

$$
\begin{aligned}
K_1(m, n, \rho_1, \rho_2, z) &= \int_0^{\infty} (y+z)^{m-1} \mathrm{e}^{-\rho_1(y+z)} y^{n-1} \mathrm{e}^{-\rho_2 y} \\
&= \sum_{k=0}^{m-1} \binom{m-1}{k} z^{m-1-k} \mathrm{e}^{-\rho_1 z} \int_0^{\infty} x^{k+n-1} \mathrm{e}^{-(\rho_1+\rho_2)y} \mathrm{d}y \\
&= \sum_{k=0}^{m-1} \binom{m-1}{k} \frac{(k+n-1)!}{(\rho_1+\rho_2)^{k+n}} z^{m-1-k} \mathrm{e}^{-\rho_1 z} \quad (6.28)
\end{aligned}
$$

Similarly, for $z < 0$, $f_{w_R}(z)$ can be computed as

$$\begin{aligned}
f_{w_R}(z) &= \int_{x=0}^{\infty} f_{xy}(x, x-z)\mathrm{d}x \\
&= \frac{A_1 D_1(1+\overline{\gamma}_0)}{\overline{\gamma}_0^2} K_1\left(1, 1, \frac{1+\overline{\gamma}_0}{\overline{\gamma}_0}, \frac{1}{\overline{\gamma}_0}, -z\right) \\
&+ \sum_{i=1}^{N} \frac{A_1 E_i (\overline{\gamma}_2)^{-i}}{\overline{\gamma}_0 (i-1)!} K_1\left(i, 1, \frac{1}{\overline{\gamma}_2}, \frac{1}{\overline{\gamma}_0}, -z\right) \\
&+ \sum_{i=1}^{M+L} \frac{A_1 F_i}{\overline{\gamma}_0 (i-1)!} \left(\frac{\overline{\gamma}_2}{1+\overline{\gamma}_2}\right)^{-i} K_1\left(i, 1, \frac{1}{\overline{\gamma}_0}, \frac{1+\overline{\gamma}_2}{\overline{\gamma}_2}, -z\right) \\
&+ \sum_{i=1}^{M} \frac{B_i D_1 (1+\overline{\gamma}_0)(\overline{\gamma}_2)^{-i}}{\overline{\gamma}_0 (i-1)!} K_1\left(1, i, \frac{1+\overline{\gamma}_0}{\overline{\gamma}_0}, \frac{1}{\overline{\gamma}_2}, -z\right) \\
&+ \sum_{j=1}^{N} \sum_{i=1}^{M} \frac{B_i E_j (\overline{\gamma}_2)^{-i-j}}{(i-1)!(j-1)!} K_1\left(j, i, \frac{1}{\overline{\gamma}_2}, \frac{1}{\overline{\gamma}_2}, -z\right) \\
&+ \sum_{j=1}^{M+L} \sum_{i=1}^{M} \frac{B_i F_j (\overline{\gamma}_2)^{-i}}{(i-1)!(j-1)!} \left(\frac{\overline{\gamma}_2}{1+\overline{\gamma}_2}\right)^{-j} K_1\left(j, i, \frac{1+\overline{\gamma}_2}{\overline{\gamma}_2}, \frac{1}{\overline{\gamma}_2}, -z\right) \\
&+ \sum_{i=1}^{N+L} \frac{D_1 C_i (1+\overline{\gamma}_0)}{\overline{\gamma}_0 (i-1)!} \left(\frac{\overline{\gamma}_2}{1+\overline{\gamma}_2}\right)^{-i} K_1\left(1, i, \frac{1+\overline{\gamma}_0}{\overline{\gamma}_0}, \frac{1+\overline{\gamma}_2}{\overline{\gamma}_2}, -z\right) \\
&+ \sum_{j=1}^{N} \sum_{i=1}^{N+L} \frac{C_i E_j (\overline{\gamma}_2)^{-j}}{(i-1)!(j-1)!} \left(\frac{\overline{\gamma}_2}{1+\overline{\gamma}_2}\right)^{-i} K_1\left(j, i, \frac{1}{\overline{\gamma}_2}, \frac{1+\overline{\gamma}_2}{\overline{\gamma}_2}, -z\right) \\
&+ \sum_{j=1}^{M+L} \sum_{i=1}^{N+L} \frac{C_i F_j}{(i-1)!(j-1)!} \left(\frac{\overline{\gamma}_2}{1+\overline{\gamma}_2}\right)^{-i-j} K_1\left(j, i, \frac{1+\overline{\gamma}_2}{\overline{\gamma}_2}, \frac{1+\overline{\gamma}_2}{\overline{\gamma}_2}, -z\right) \qquad (6.29)
\end{aligned}$$

We further define two more functions that are useful in obtaining the average BER and throughput of the system. First,

$$\begin{aligned}
K_2(m, n, \rho_1, \rho_2, \rho_3, \theta^{\mathrm{th}}) &= \int_0^{\theta^{\mathrm{th}}} K_1(m, n, \rho_1, \rho_2, z) \mathrm{e}^{-\rho_3 z} \mathrm{d}z \\
&= \int_0^{\theta^{\mathrm{th}}} \sum_{k=0}^{m-1} \binom{m-1}{k} \frac{(k+n-1)!}{(\rho_1+\rho_2)^{k+n}} z^{m-1-k} \mathrm{e}^{-\rho_1 z} \mathrm{e}^{-\rho_3 z} \mathrm{d}z \\
&= \sum_{k=0}^{m-1} \binom{m-1}{k} \frac{(k+n-1)!}{(\rho_1+\rho_2)^{k+n}} K_3\left(m-1-k, \rho_1+\rho_3, \theta^{\mathrm{th}}\right) \qquad (6.30)
\end{aligned}$$

where

$$K_3(n, \mu, u) = \int_0^u x^n \mathrm{e}^{-\mu x} \mathrm{d}x = \frac{n!}{\mu^{n+1}} - \mathrm{e}^{\mu u} \sum_{k=0}^{n} \frac{n!}{k!} \frac{u^k}{\mu^{n-k+1}}. \qquad (6.31)$$

Second,

$$K_4(m,n,\rho_1,\rho_2,\rho_3,\theta^{\text{th}}) = \int_{-\theta^{\text{th}}}^{0} K_1(m,n,\rho_1,\rho_2,-z)\mathrm{e}^{-\rho_3 z}\mathrm{d}z$$
$$= \int_{-\theta^{\text{th}}}^{0} \sum_{k=0}^{m-1} \binom{m-1}{k} \frac{(k+n-1)!}{(\rho_1+\rho_2)^{k+n}} (-z)^{m-1-k}\mathrm{e}^{\rho_1 z}\mathrm{e}^{-\rho_3 z}\mathrm{d}z$$
$$= \sum_{k=0}^{m-1} \binom{m-1}{k} \frac{(k+n-1)!}{(\rho_1+\rho_2)^{k+n}} K_3\left(m-1-k, \rho_1-\rho_3, \theta^{\text{th}}\right) \tag{6.32}$$

6.3.2 Average Bit Error Rate Analysis

To compute the average BER of the network, we first classify all different cases that result in different conditioned BERs at the destination. Three major cases can be classified and parameterized by variable Θ as follows. The first case, $\Theta = 1$, is when $|w_0| \geq \gamma_{\text{d}}^{\text{th}}$, i.e., no relay retransmission is requested from the destination ($R = 0$). The second case, parameterized by $\Theta = 2$, corresponds to $|w_0| < \gamma_{\text{d}}^{\text{th}}, \ldots, |w_{R-1}| < \gamma_{\text{d}}^{\text{th}}$ and $|w_R| > \gamma_{\text{d}}^{\text{th}}$ where $1 \leq R \leq K-1$, i.e., R relays are requested to retransmit by the destination. Lastly, the third case, $\Theta = 3$, happens if $|w_{K-1}| < \gamma_{\text{d}}^{\text{th}}$, i.e, K relays are requested to retransmit. Under all three cases, it should be noted that the destination combines $R+1$ received signals, i.e., uses w_R, to decode the transmitted information. The average BER of the network can be expressed as

$$\text{BER}(\theta_{\text{r}}^{\text{th}}, \theta_{\text{d}}^{\text{th}}) = \sum_{i=1}^{3} \text{BER}(\theta_{\text{r}}^{\text{th}}, \theta_{\text{d}}^{\text{th}}, \Theta = i) \tag{6.33}$$

where $\text{BER}(\theta_{\text{r}}^{\text{th}}, \theta_{\text{d}}^{\text{th}}, \Theta = i)$ is the average joint probability of error at the destination and the case $\Theta = i$. They are obtained in the following for each case of $\Theta \in \{1, 2, 3\}$.

Case $\Theta = 1$

The BER for this case is easily computed as

$$\text{BER}(\theta_{\text{r}}^{\text{th}}, \theta_{\text{d}}^{\text{th}}, \Theta = 1) = P(w_0 < -\theta_{\text{d}}^{\text{th}} \Big| |w_0| \geq \theta_{\text{d}}^{\text{th}})$$
$$= \frac{1}{1 - I_1\left(\frac{\theta_{\text{d}}^{\text{th}}(1+\overline{\gamma}_0)}{\overline{\gamma}_0}, \overline{\gamma}_0\right)} \frac{\mathrm{e}^{-\frac{\theta_{\text{d}}^{\text{th}}(1+\overline{\gamma}_0)}{\overline{\gamma}_0}}}{2+\overline{\gamma}_0} = I_2\left(\frac{\theta_{\text{d}}^{\text{th}}(1+\overline{\gamma}_0)}{\overline{\gamma}_0}, \overline{\gamma}_0\right) \tag{6.34}$$

where $I_1(\theta^{\text{th}}, \overline{\gamma})$ is the probability that the magnitude of the energy difference in the two subbands at node i is smaller than the threshold, i.e., $\theta_{0,i} < \theta^{\text{th}}$, and $\overline{\gamma}$ is the

average SNR of the channel between two nodes over which the data is transmitted. The pdf of $\theta_{0,i}$ is given in Lemma 2 of [C6-22], which is used to obtain the following expression for $I_1(\theta^{\rm th}, \overline{\gamma}_1)$:

$$I_1(\theta^{\rm th}, \overline{\gamma}_1) = \int_0^{\theta^{\rm th}} f_{\theta_{0,i}}(x){\rm d}x = \int_0^{\theta^{\rm th}} \frac{1}{2+\overline{\gamma}_1}\left({\rm e}^{-x/(1+\overline{\gamma}_1)} + {\rm e}^{-x}\right){\rm d}x$$
$$= \frac{1+\overline{\gamma}_1}{2+\overline{\gamma}_1}\left[1-{\rm e}^{-\theta^{\rm th}/(1+\overline{\gamma}_1)}\right] + \frac{1}{2+\overline{\gamma}_1}\left[1-{\rm e}^{-\theta^{\rm th}}\right] \quad (6.35)$$

On the other hand, $I_2(\theta^{\rm th}, \overline{\gamma})$ is the probability of error at node i, $i = 1, \ldots, K$, given that the magnitude of the energy difference in the two subbands is larger than the threshold, i.e., $\theta_{0,i} > \theta^{\rm th}$. Therefore $I_2(\theta^{\rm th}, \overline{\gamma})$ can be computed as

$$I_2(\theta^{\rm th}, \overline{\gamma}) = \frac{1}{1-I_1(\theta^{\rm th}, \overline{\gamma})}\int_{-\infty}^{-\theta^{\rm th}} \frac{1}{2+\overline{\gamma}_1}{\rm e}^{-x}{\rm d}x = \frac{1}{2+\overline{\gamma}}\frac{1}{1-I_1(\theta^{\rm th}, \overline{\gamma})}{\rm e}^{-\theta^{\rm th}} \quad (6.36)$$

Case $\Theta = 2$

In this case, R relays are requested to retransmit to the destination where $1 \leq R \leq K-1$. Since the last relay, i.e., relay R, may forward a correct bit, an incorrect bit, and remain silent, three different sub-cases, parameterized by $\Phi = \{1, 2, 3\}$, can be further separated under $\Theta = 2$. By using the law of total probability, the average BER for this case can be expressed as

$${\rm BER}(\theta_{\rm r}^{\rm th}, \theta_{\rm d}^{\rm th}, \Theta = 2) = \sum_{i=1}^{3}\sum_{R=1}^{K-1}\sum_{M=0}^{R-1}\sum_{N=R-1-M}^{R-1} P(\Phi = i, M, N, L)P(\varepsilon|\Phi = i, M, N, L) \quad (6.37)$$

where $P(\varepsilon|\Phi = i, M, N, L)$ and $P(\Phi = i, M, N, L)$ denote the conditioned BER and case probability for the specific set dimensions $\{\Phi, M, N, L\}$. It should be mentioned here that M, N, and L are the numbers of relays that forward a correct bit, an incorrect bit, and remain silent, respectively among $(R-1)$ relays (excluding the last relay, i.e., relay R). Clearly $R-1 = M+N+L$. The probability of occurrence for the specific set dimensions $\{\Phi, M, N, L\}$ can be determined to be

$$P(\Phi = 1, M, N, L) = \binom{R-1}{M}\binom{R-1-M}{N}\left[1-I_1(\theta_{\rm r}^{\rm th}, \overline{\gamma}_1)\right]^{M+N+1}$$
$$\times \left[1-I_2(\theta_{\rm r}^{\rm th}, \overline{\gamma}_1)\right]^{M+1}\left[I_2(\theta_{\rm r}^{\rm th}, \overline{\gamma}_1)\right]^{N}\left[I_1(\theta_{\rm r}^{\rm th}, \overline{\gamma}_1)\right]^{L} \quad (6.38)$$

$$P(\Phi=2,M,N,L)=\binom{R-1}{M}\binom{R-1-M}{N}\left[1-I_1(\theta_{\rm r}^{\rm th},\overline{\gamma}_1)\right]^{M+N+1}$$
$$\times\left[1-I_2(\theta_{\rm r}^{\rm th},\overline{\gamma}_1)\right]^{M}\left[I_2(\theta_{\rm r}^{\rm th},\overline{\gamma}_1)\right]^{N+1}\left[I_1(\theta_{\rm r}^{\rm th},\overline{\gamma}_1)\right]^{L} \quad (6.39)$$

$$P(\Phi=3,M,N,L)=\binom{R-1}{M}\binom{R-1-M}{N}\left[1-I_1(\theta_{\rm r}^{\rm th},\overline{\gamma}_1)\right]^{M+N}$$
$$\times\left[1-I_2(\theta_{\rm r}^{\rm th},\overline{\gamma}_1)\right]^{M}\left[I_2(\theta_{\rm r}^{\rm th},\overline{\gamma}_1)\right]^{N}\left[I_1(\theta_{\rm r}^{\rm th},\overline{\gamma}_1)\right]^{L+1} \quad (6.40)$$

On the other hand, the conditioned BER can be written as

$$P(\varepsilon|\Phi,M,N,L)=P\left(w_R<-\theta_{\rm d}^{\rm th},|w_0|<\theta_{\rm d}^{\rm th},|w_1|<\theta_{\rm d}^{\rm th},\ldots,\left|w_{R-1}\right|<\theta_{\rm d}^{\rm th}\right) \quad (6.41)$$

To simplify and keep the analysis tractable, the above expression can be upper bounded as

$$P(\varepsilon|\Phi,M,N,L)\le P\left(w_R<-\theta_{\rm d}^{\rm th},\left|w_{R-1}\right|<\theta_{\rm d}^{\rm th}\right)=P\left(w_{R-1}+z_R<-\theta_{\rm d}^{\rm th},\left|w_{R-1}\right|<\theta_{\rm d}^{\rm th}\right)$$
$$=\int_{-\theta_{\rm d}^{\rm th}}^{\theta_{\rm d}^{\rm th}}f_{w_{R-1}}(w_{R-1})\int_{-\infty}^{-\theta_{\rm d}^{\rm th}-w_{R-1}}f_{z_R}(z_R){\rm d}z_R{\rm d}w_{R-1}. \quad (6.42)$$

Let $C_1(M,N,L,\rho,\theta^{\rm th})$, $C_2(M,N,L,\rho,\theta^{\rm th})$, and $C_3(M,N,L,\rho,\theta^{\rm th})$ be defined as follows:

$$C_1(M,N,L,\rho,\theta^{\rm th})=\int_{-\theta_{\rm d}^{\rm th}}^{\theta_{\rm d}^{\rm th}}f_{w_{R-1}}(w_{R-1}){\rm e}^{-\rho w_{R-1}}{\rm d}w_{R-1}$$
$$=\underbrace{\int_{-\theta_{\rm d}^{\rm th}}^{0}f_{w_{R-1}}(w_{R-1}){\rm e}^{-\rho w_{R-1}}{\rm d}w_{R-1}}_{C_2(M,N,L,\rho,\theta^{\rm th})}+\underbrace{\int_{0}^{\theta_{\rm d}^{\rm th}}f_{w_{R-1}}(w_{R-1}){\rm e}^{-\rho w_{R-1}}{\rm d}w_{R-1}}_{C_3(M,N,L,\rho,\theta^{\rm th})} \quad (6.43)$$

where $C_2(M,N,L,\rho,\theta^{\rm th})$ can be found by replacing $K_1(m,n,\rho_1,\rho_2,-z)$ in (6.29) by $K_4(m,n,\rho_1,\rho_2,\rho,\theta^{\rm th})$ in (6.32) and $C_3(M,N,L,\rho,\theta^{\rm th})$ can be found by replacing $K_1(m,n,\rho_1,\rho_2,-z)$ in (6.27) by $K_2(m,n,\rho_1,\rho_2,\rho,\theta^{\rm th})$ in (6.30). With the pdf of z_R for three sub-cases given in Appendix 6.A, the conditioned BER can be computed from (6.42) as follows:

$$P(\varepsilon|\Phi=1,M,N,L)\le\frac{1}{2+\overline{\gamma}_2}{\rm e}^{-\frac{1+\overline{\gamma}_2}{\overline{\gamma}_2}\theta_{\rm d}^{\rm th}}C_1\left(M,N,L,\frac{1+\overline{\gamma}_2}{\overline{\gamma}_2},\theta_{\rm d}^{\rm th}\right) \quad (6.44)$$

$$P(\varepsilon|\Phi=2,M,N,L) \leq \frac{1+\overline{\gamma}_2}{2+\overline{\gamma}_2}\mathrm{e}^{-\frac{1}{\overline{\gamma}_2}\theta_{\mathrm{d}}^{\mathrm{th}}} C_1\left(M,N,L,\frac{1}{\overline{\gamma}_2},\theta_{\mathrm{d}}^{\mathrm{th}}\right) \tag{6.45}$$

$$P(\varepsilon|\Phi=3,M,N,L) \leq \frac{1}{2}\mathrm{e}^{-\frac{1+\overline{\gamma}_2}{\overline{\gamma}_2}\theta_{\mathrm{d}}^{\mathrm{th}}} C_1\left(M,N,L,\frac{1+\overline{\gamma}_2}{\overline{\gamma}_2},\theta_{\mathrm{d}}^{\mathrm{th}}\right) \tag{6.46}$$

Hence the average upper-bound on the BER for the case $\Theta = 2$ can be computed by substituting Equations (6.38)–(6.40), (6.44)–(6.46) into Equation (6.37).

Case $\Theta = 3$

Similar to the case $\Theta = 2$, the average BER for $\Theta = 3$ can be computed as (6.37) where $R = K$. The difference is the conditioned BER. It can be upper bound as

$$P(\varepsilon|\Phi,M,N,L) \leq P\left(w_K < 0, \left|w_{K-1}\right| < \theta_{\mathrm{d}}^{\mathrm{th}}\right) \tag{6.47}$$

With $M + N + L = K - 1$, one can obtain the conditioned BERs as follows:

$$\begin{aligned} P(\varepsilon|\Phi=1,M,N,L) &= C_2(M,N,L,0,\theta_{\mathrm{d}}^{\mathrm{th}}) \\ &-\tfrac{1+\overline{\gamma}_2}{2+\overline{\gamma}_2}C_2(M,N,L,-\tfrac{1}{\overline{\gamma}_2},\theta_{\mathrm{d}}^{\mathrm{th}}) + \tfrac{1}{2+\overline{\gamma}_2}C_3(M,N,L,-\tfrac{1+\overline{\gamma}_2}{\overline{\gamma}_2},\theta_{\mathrm{d}}^{\mathrm{th}}) \end{aligned} \tag{6.48}$$

$$\begin{aligned} P(\varepsilon|\Phi=2,M,N,L) &= C_2(M,N,L,0,\theta_{\mathrm{d}}^{\mathrm{th}}) \\ &-\tfrac{1}{2+\overline{\gamma}_2}C_2(M,N,L,-\tfrac{1+\overline{\gamma}_2}{\overline{\gamma}_2},\theta_{\mathrm{d}}^{\mathrm{th}}) + \tfrac{1+\overline{\gamma}_2}{2+\overline{\gamma}_2}C_3(M,N,L,-\tfrac{1}{\overline{\gamma}_2},\theta_{\mathrm{d}}^{\mathrm{th}}) \end{aligned} \tag{6.49}$$

$$\begin{aligned} P(\varepsilon|\Phi=3,M,N,L) &= C_2(M,N,L,0,\theta_{\mathrm{d}}^{\mathrm{th}}) \\ &-\tfrac{1}{2}C_2(M,N,L,-\tfrac{1+\overline{\gamma}_2}{\overline{\gamma}_2},\theta_{\mathrm{d}}^{\mathrm{th}}) + \tfrac{1}{2}C_3(M,N,L,-\tfrac{1+\overline{\gamma}_2}{\overline{\gamma}_2},\theta_{\mathrm{d}}^{\mathrm{th}}) \end{aligned} \tag{6.50}$$

6.3.3 Throughput Analysis

In this paper, the throughput of a cooperative network is computed as $\mathcal{R}/\kappa$ where $\mathcal{R}$ is the bit rate for a single transmission and κ is the number of time slots for a completed transmission from the source to the destination. For instance, when BFSK is employed and R relays are requested to assist the source, the throughput is $\frac{1}{R+1}$

(bps/Hz). Thus, with the three cases that we classify to compute the average BER, the throughput of the network can be determined by

$$\mathcal{T}(\theta_{\rm r}^{\rm th},\theta_{\rm d}^{\rm th})=\sum_{i=1}^{3}\mathcal{T}(\theta_{\rm r}^{\rm th},\theta_{\rm d}^{\rm th},\Theta=i) \tag{6.51}$$

where $\mathcal{T}(\theta_{\rm r}^{\rm th},\theta_{\rm d}^{\rm th},\Theta=i)$ is the joint throughput of the network and the case $\Theta=i$.

Case $\Theta=1$

The throughput of the network for this case can be computed as

$$\mathcal{T}(\theta_{\rm r}^{\rm th},\theta_{\rm d}^{\rm th},\Theta=1)=P(|w_0|\geq\theta_{\rm d}^{\rm th})=1-I_1\left(\frac{\theta_{\rm d}^{\rm th}(1+\overline{\gamma}_0)}{\overline{\gamma}_0},\overline{\gamma}_0\right) \tag{6.52}$$

Case $\Theta=2$

With three sub-cases we separate in the previous section, the throughput can be determined to be

$$\mathcal{T}(\theta_{\rm r}^{\rm th},\theta_{\rm d}^{\rm th},\Theta=2)=\sum_{i=1}^{3}\sum_{R=1}^{K-1}\sum_{M=0}^{R-1}\sum_{N=R-1-M}^{R-1}P(\Phi=i,M,N,L)P(\eta|\Phi=i,M,N,L) \tag{6.53}$$

where $P(\eta|\Phi=i,M,N,L)$ and $P(\Phi=i,M,N,L)$ denote the conditional throughput and case probability for the specific set dimensions $\{\Phi,M,N,L\}$. It should be mentioned that the case probabilities are computed as in (6.38)–(6.40). The conditional throughput can be expressed as

$$P(\eta|\Phi,M,N,L)=\frac{1}{R+1}P\left(\left|w_R\right|\geq\theta_{\rm d}^{\rm th},|w_0|<\theta_{\rm d}^{\rm th},|w_1|<\theta_{\rm d}^{\rm th},\ldots,\left|w_{R-1}\right|<\theta_{\rm d}^{\rm th}\right) \tag{6.54}$$

Similarly, it can be upper bounded as

$$\begin{aligned}P(\eta|\Phi,M,N,L)&\leq\frac{1}{R+1}P\left(\left|w_R\right|\geq\theta_{\rm d}^{\rm th},\left|w_{R-1}\right|<\theta_{\rm d}^{\rm th}\right)\\&=\tfrac{1}{R+1}\underbrace{P\left(w_R<-\theta_{\rm d}^{\rm th},\left|w_{R-1}\right|<\theta_{\rm d}^{\rm th}\right)}_{P(\eta_1|\Phi,M,N,L)}+\tfrac{1}{R+1}\underbrace{P\left(w_R\geq\theta_{\rm d}^{\rm th},\left|w_{R-1}\right|<\theta_{\rm d}^{\rm th}\right)}_{P(\eta_2|\Phi,M,N,L)}\end{aligned} \tag{6.55}$$

The first term in (6.55) can be computed as in (6.42) in which the upper bound expressions are in (6.44)–(6.46). Therefore we only need to compute the second term,

i.e., $P(\eta_2|\Phi, M, N, L)$. This is determined as

$$P(\eta_2|\Phi, M, N, L) = P\left(w_{R-1} + z_R \geq \theta_{\rm d}^{\rm th}, \left|w_{R-1}\right| < \theta_{\rm d}^{\rm th}\right)$$
$$= \int_{-\theta_{\rm d}^{\rm th}}^{\theta_{\rm d}^{\rm th}} f_{w_{R-1}}(w_{R-1}) \int_{\theta_{\rm d}^{\rm th}-w_{R-1}}^{\infty} f_{z_R}(z_R) {\rm d}z_R {\rm d}w_{R-1} \quad (6.56)$$

By performing the above integral, it can be easily verified that

$$P(\eta_2|\Phi = 1, M, N, L) = \frac{1+\overline{\gamma}_2}{2+\overline{\gamma}_2} {\rm e}^{-\frac{1}{\overline{\gamma}_2}\theta_{\rm d}^{\rm th}} C_1\left(M, N, L, -\frac{1}{\overline{\gamma}_2}, \theta_{\rm d}^{\rm th}\right) \quad (6.57)$$

$$P(\eta_2|\Phi = 2, M, N, L) = \frac{1}{2+\overline{\gamma}_2} {\rm e}^{-\frac{1+\overline{\gamma}_2}{\overline{\gamma}_2}\theta_{\rm d}^{\rm th}} C_1\left(M, N, L, -\frac{1+\overline{\gamma}_2}{\overline{\gamma}_2}, \theta_{\rm d}^{\rm th}\right) \quad (6.58)$$

$$P(\eta_2|\Phi = 3, M, N, L) = \frac{1}{2} {\rm e}^{-\frac{1+\overline{\gamma}_2}{\overline{\gamma}_2}\theta_{\rm d}^{\rm th}} C_1\left(M, N, L, -\frac{1+\overline{\gamma}_2}{\overline{\gamma}_2}, \theta_{\rm d}^{\rm th}\right) \quad (6.59)$$

Case $\Theta = 3$

With $M + N + L = K - 1$, the conditional throughput can be verified to be

$$P(\eta|\Phi, M, N, L) = \frac{1}{K+1} P\left(\left|w_{R-1}\right| < \theta_{\rm d}^{\rm th}\right) = \frac{1}{K+1} C_1(M, N, L, 0, \theta_{\rm d}^{\rm th}) \quad (6.60)$$

To summarize, all the expressions involved in the upper-bound expressions of the average BER in (6.33) and throughput in (6.51) can be calculated analytically. The tightness of the obtained upper bounds shall be verified in Section 6.4 by comparing them with simulation results. On the other hand, the choice of the thresholds employed at the relays and the destination strongly affect the overall BER performance and throughput of the network. With the upper bounds on the BER and throughput just obtained, the optimization of the threshold values can be set up as follows:

$$(\widehat{\theta}_{\rm r}^{\rm th}, \widehat{\theta}_{\rm d}^{\rm th}) = \arg \min_{(\theta_{\rm r}^{\rm th}, \theta_{\rm d}^{\rm th})} -\mathcal{T}(\theta_{\rm r}^{\rm th}, \theta_{\rm d}^{\rm th}) \text{ subject to } {\rm BER}(\theta_{\rm r}^{\rm th}, \theta_{\rm d}^{\rm th}) \leq {\rm BER}_{\rm T} \quad (6.61)$$

where ${\rm BER}_{\rm T}$ is the target BER of the network.

Unfortunately, an analytical solution for the two threshold values in the general case is very difficult to obtain due to the exponential terms in the final expressions of

the objective and constraint. Therefore, we pursue numerical optimization by using the MATLAB Optimization Toolbox. Specifically, we use the routine "fmincon", which is designed to find the minimum of a given constrained nonlinear multivariate function. Furthermore, since it is difficult to prove the cost function to be convex or not, to have a good confidence in the numerical results, the optimization problem is solved with many initial conditions and the best value is retained.

6.4 Simulation Results

This section presents analytical and simulation results to confirm the analysis of the average BER and throughput of the networks with the proposed protocol. In all simulations, transmitted powers are set to be the same for the source and the relay (i.e., $E_{\mathrm{s}} = E_{\mathrm{r}}$). The noise components at both the source and relay are modeled as i.i.d. $\mathcal{CN}(0, 1)$ random variables. The channel variances of all the transmission links in the network are denoted set to be $\sigma_0^2 = \sigma_{0,K+1}^2$, $\sigma_{0,1}^2 = \sigma_{0,2}^2 = \cdots = \sigma_{0,K}^2 = \sigma_1^2$ and $\sigma_{1,K+1}^2 = \sigma_{2,K+1}^2 = \cdots = \sigma_{K,K+1}^2 = \sigma_2^2$.

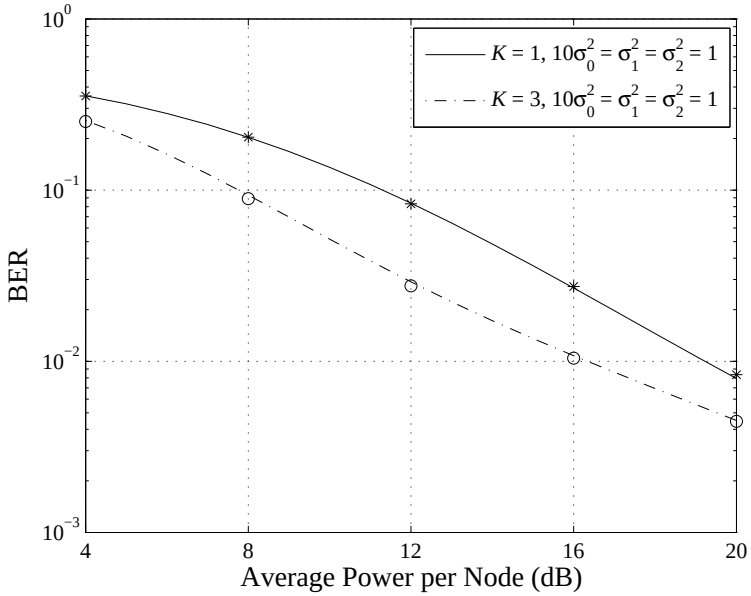

Figure 6.4 BERs of single-relay and three-relay cooperative networks when $\theta_{\mathrm{r}}^{\mathrm{th}} = 1$, $\theta_{\mathrm{d}}^{\mathrm{th}} = 3$. Analytical values are shown in lines and simulation results are shown as marker symbols.

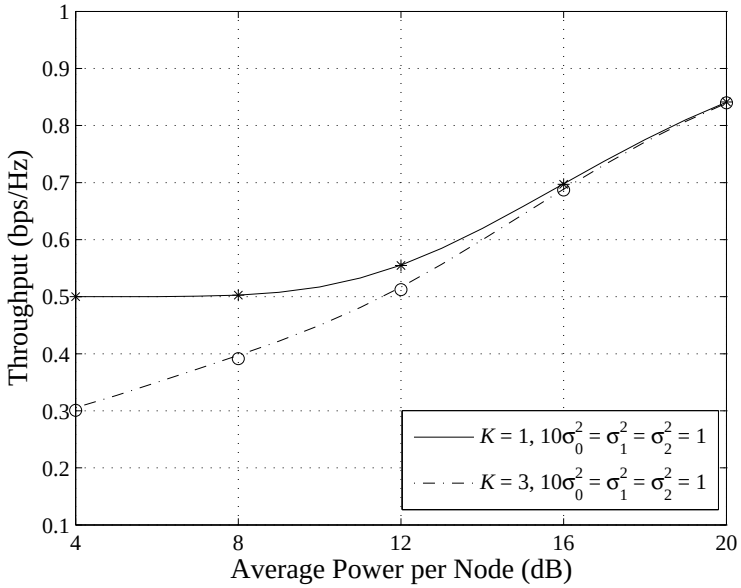

Figure 6.5 Throughput of single-relay and three-relay cooperative networks when $\theta_{\mathrm{r}}^{\mathrm{th}} = 1$, $\theta_{\mathrm{d}}^{\mathrm{th}} = 3$. Analytical values are shown in lines and simulation results are shown as marker symbols.

Figs. 6.4 and 6.5 plot the average BERs and throughput for one-relay and three-relay networks and under different channel conditions. The thresholds are arbitrarily chosen as $\{\theta_{\mathrm{r}}^{\mathrm{th}} = 1, \theta_{\mathrm{d}}^{\mathrm{th}} = 3\}$. The figure clearly shows that analytical upper bound results (shown in lines) and simulation results (shown as marker symbols) are basically identical, which confirms that the upper bounds are very tight and provide a useful tool in calculating the average BER and throughput as well as to optimize the relaying and destination thresholds.

Next, Fig. 6.6 compares the throughput of the proposed protocol for different target BERs for two-relay networks when the variances of Rayleigh fading channels are set to be $10\sigma_0^2 = 0.5\sigma_1^2 = 0.5\sigma_2^2 = 1$. Note that the figure only shows the throughput in the SNR region in which the BER requirement is satisfied. For example, Fig. 6.6 presents the throughput in the region of SNR ≥ 14 dB for $\mathrm{BER_T} = 10^{-2}$. It can be seen that there is a tradeoff between throughput and error performance. With the optimal threshold values obtained by numerically solving (6.61), an additional SNR of about 5 dB is required to maintain the same throughput of 0.7 (bps/Hz) when the

target BER is decreased from 10^{-1} to 10^{-2}. The figure also shows that the analytical results give very tight upper bound as compared to the simulation results.

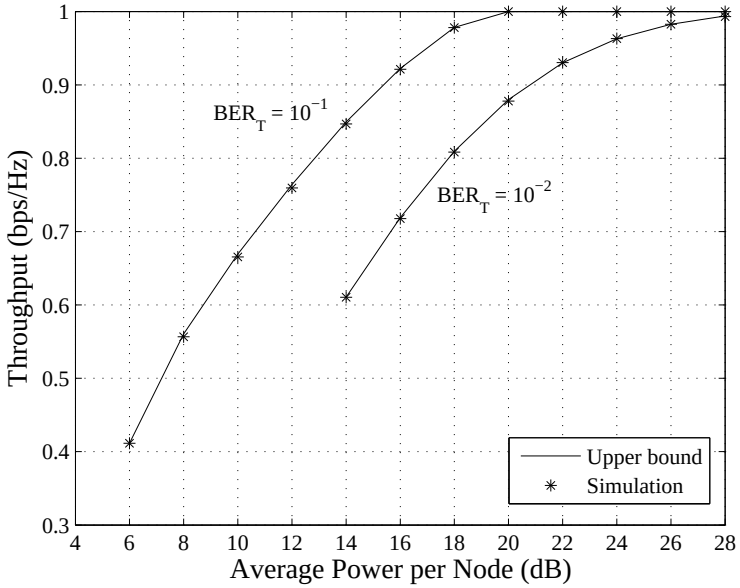

Figure 6.6 Throughput of two-relay cooperative network with different target BERs when $10\sigma_0^2 = 0.5\sigma_1^2 = 0.5\sigma_2^2 = 1$.

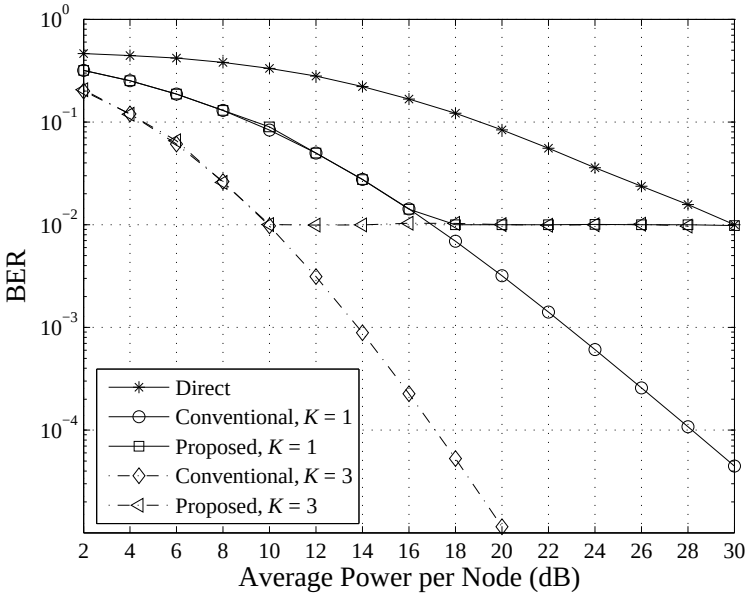

Figure 6.7 BERs of single-relay and three-relay cooperative networks when $10\sigma_0^2 = 0.2\sigma_1^2 = \sigma_2^2 = 1$.

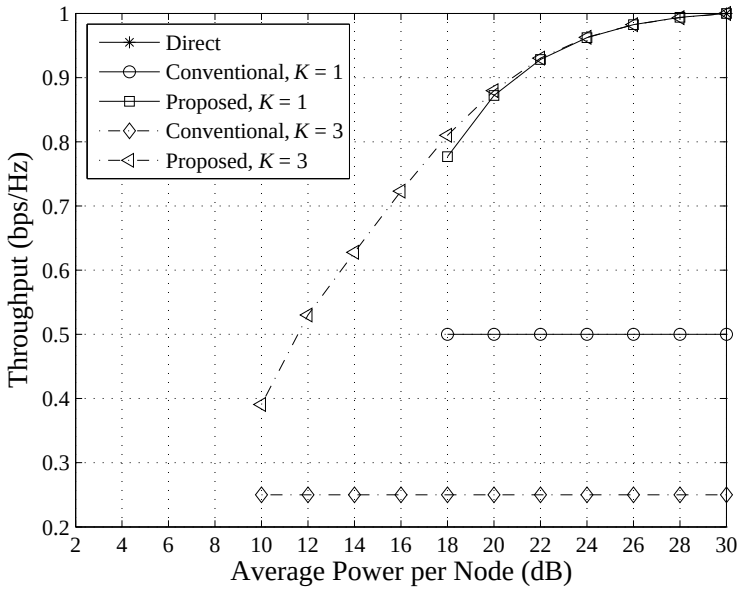

Figure 6.8 Throughput of single-relay and three-relay cooperative networks when $\mathrm{BER_T} = 10^{-2}$ and $10\sigma_0^2 = 0.2\sigma_1^2 = \sigma_2^2 = 1$.

Finally, Figs. 6.7 and 6.8 show the average BERs and throughput obtained by simulation for one-relay and three-relay networks. The channel variances of all communication links are set to be $10\sigma_0^2 = 0.2\sigma_1^2 = \sigma_2^2 = 1$. The BER requirement is $\mathrm{BER_T} = 10^{-2}$. The adaptive relaying scheme, referred to as the conventional scheme, uses only one threshold at the relays and works as follows: a relay retransmits to the destination if its decision variable is larger than the threshold; otherwise, it remains silent. The destination then combines all the received signals for the detection of transmitted information. The average BER of the conventional scheme can be found to be the average BER of the proposed scheme with $\theta_{\mathrm{d}}^{\mathrm{th}} \to \infty$. One can also find the optimal threshold value of the conventional scheme to minimize the average BER by numerical optimization. As can be seen from Fig. 6.7, the BER curves start to meet the requirement when the average SNRs are 10 dB and 18 dB for $K = 1$ and $K = 3$, respectively. Similar to Fig. 6.6, Fig. 6.8 only shows the throughput over the SNR region that the BER requirement is satisfied. The improvement of the throughput by the proposed protocol is observed when compared with the conventional scheme. This is expected since the proposed protocol does not need to use all the relays to

retransmit to satisfy the BER requirement when the average SNR is high enough. It also explains why the throughput of the proposed protocol reverts to that of the direct link in the high average SNR region, e.g., SNR = 30 dB in Fig. 6.8.

6.5 Conclusion

In this paper, we have proposed and studied an incremental relaying protocol for noncoherent cooperative networks. Each node in the network is equipped with a single antenna and the channels are Rayleigh fading. BFSK is used to modulate the signals at both the source and relays. The proposed scheme uses two different thresholds. One threshold is used to select reliable relays for retransmission in the second phase. The other threshold can be used at the destination to satisfy the BER requirement. Very-tight closed-form upper bounds for both the average BER and throughput are derived. Optimal thresholds are chosen to maximize the throughput while the BER meets a given requirement. Performance comparison reveals that by employing optimal thresholds, our proposed protocol leads to a considerable improvement in the performance of cooperative diversity systems.

6.A Lemmas used in the Calculation of Probability of Error

Lemma 1: Consider a random variable $X_{i,K+1} = \frac{\overline{\gamma}_{i,K+1}}{(\overline{\gamma}_{i,K+1}+1)N_0}\left(|y_{i,K+1,0}|^2 - |y_{i,K+1,1}|^2\right)$ where $y_{i,K+1,0}$ and $y_{i,K+1,1}$ are as in (6.1) and (6.2), respectively. The pdf of $X_{i,K+1}$ when the transmitted bit is "0" and "1" are given, respectively, by

$$f_{X_{i,K+1}}(x) = \begin{cases} \frac{1+\overline{\gamma}_{i,K+1}}{\overline{\gamma}_{i,K+1}(2+\overline{\gamma}_{i,K+1})} \mathrm{e}^{-x/\overline{\gamma}_{i,K+1}}, & x \geq 0 \\ \frac{1+\overline{\gamma}_{i,K+1}}{\overline{\gamma}_{i,K+1}(2+\overline{\gamma}_{i,K+1})} \mathrm{e}^{x(1+\overline{\gamma}_{i,K+1})/\overline{\gamma}_{i,K+1}}, & x < 0 \end{cases} \tag{6.62}$$

$$f_{X_{i,K+1}}(x) = \begin{cases} \frac{1+\overline{\gamma}_{i,K+1}}{\overline{\gamma}_{i,K+1}(2+\overline{\gamma}_{i,K+1})} \mathrm{e}^{-x(1+\overline{\gamma}_{i,K+1})/\overline{\gamma}_{i,K+1}}, & x \geq 0 \\ \frac{1+\overline{\gamma}_{i,K+1}}{\overline{\gamma}_{i,K+1}(2+\overline{\gamma}_{i,K+1})} \mathrm{e}^{x/\overline{\gamma}_{i,K+1}}, & x < 0 \end{cases} \tag{6.63}$$

Lemma 2: Consider a random variable $X_{i,K+1} = \frac{\overline{\gamma}_{i,K+1}}{(\overline{\gamma}_{i,K+1}+1)N_0}\left(|y_{i,K+1,0}|^2 - |y_{i,K+1,1}|^2\right)$ where $y_{i,K+1,0}$ and $y_{i,K+1,1}$ are as in (6.5) and (6.6), respectively. The pdf of $X_{i,K+1}$

is given by

$$f_{X_{i,K+1}}(x) = \begin{cases} \frac{1+\overline{\gamma}_{i,K+1}}{2\overline{\gamma}_{i,K+1}} \mathrm{e}^{-x(1+\overline{\gamma}_{i,K+1})/\overline{\gamma}_{i,K+1}}, & x \geq 0 \\ \frac{1+\overline{\gamma}_{i,K+1}}{2\overline{\gamma}_{i,K+1}} \mathrm{e}^{x(1+\overline{\gamma}_{i,K+1})/\overline{\gamma}_{i,K+1}}, & x < 0 \end{cases} \tag{6.64}$$

Proof: The above two lemmas above can be easily verified by performing related integrals.

References

[C6-1] D. Tse and P. Viswanath, *Fundamentals of Wireless Communications*. Cambridge University Press, 2005.

[C6-2] J. Laneman and G. Wornell, "Distributed space-time-coded protocols for exploiting cooperative diversity in wireless networks," *IEEE Trans. Inform. Theory*, vol. 49, pp. 2415–2425, October 2003.

[C6-3] A. Sendonaris, E. Erkip, and B. Aazhang, "User cooperation diversity, Part I: System description," *IEEE Trans. Commun.*, vol. 51, no. 11, pp. 1927–1938, November 2003.

[C6-4] A. Sendonaris, E. Erkip, and B. Aazhang, "User cooperation diversity, Part II: Implementation aspects and performance analysis," *IEEE Trans. Commun.*, vol. 51, no. 11, pp. 1939–1948, November 2003.

[C6-5] A. Bletsas, A. Khisti, D. Reed, and A. Lippman, "A simple cooperative diversity method based on network path selection," *IEEE J. Select. Areas in Commun.*, vol. 24, pp. 659–672, March 2006.

[C6-6] A. Bletsas, H. Shin, and M. Win, "Cooperative communications with outage-optimal opportunistic relaying," *IEEE Trans. Wireless Commun.*, vol. 6, pp. 3450–3460, September 2007.

[C6-7] F. Onat, A. Adinoyi, Y. Fan, H. Yanikomeroglu, J. Thompson, and I. Marsland, "Threshold selection for SNR-based selective digital relaying in coopera-

tive wireless networks," *IEEE Trans. Wireless Commun.*, vol. 7, pp. 4226–4237, November 2008.

[C6-8] F. Onat, Y. Fan, H. Yanikomeroglu, and J. Thompson, "Asymptotic BER analysis of threshold digital relaying schemes in cooperative wireless systems," *IEEE Trans. Wireless Commun.*, vol. 7, pp. 4938–4947, December 2008.

[C6-9] J. Hi and R. Hu, "Slepian-Wolf cooperation: A practical and effcient compress-and-forward relay scheme," in *Allerton Conf. Commun. Contr. and Comp.*, November 2005.

[C6-10] J. Laneman, D. Tse, and G. Wornell, "Cooperative diversity in wireless networks: Efficient protocols and outage behavior," *IEEE Trans. Inform. Theory*, vol. 50, pp. 3062–3080, December 2004.

[C6-11] T. Hunter and A. Nosratinia, "Diversity through coded cooperation," *IEEE Trans. Wireless Commun.*, vol. 5, pp. 283–289, February 2006.

[C6-12] T. Hunter, S. Sanayei, and A. Nosratinia, "Outage analysis of coded cooperation," *IEEE Trans. Inform. Theory*, vol. 52, pp. 375–391, February 2006.

[C6-13] A. Bletsas, H. Shin, and M. Win, "Outage optimality of opportunistic amplify-and-forward relaying," *IEEE Commun. Letters*, vol. 11, pp. 261–263, March 2007.

[C6-14] T. Wang, A. Cano, G. Giannakis, and J. Laneman, "High-performance cooperative demodulation with decode-and-forward relays," *IEEE Trans. Commun.*, vol. 55, pp. 1427–1438, july 2007.

[C6-15] K.-S. Hwang, Y.-C. Ko, and M.-S. Alouini, "Performance analysis of incremental opportunistic relaying over identically and non-identically distributed cooperative paths," *IEEE Trans. Wireless Commun.*, vol. 8, pp. 1953 –1961, April 2009.

[C6-16] T. Nechiporenko, K. Phan, C. Tellambura, and H. H. Nguyen, "On the capacity of Rayleigh fading cooperative systems under adaptive transmission," *IEEE Trans. Wireless Commun.*, vol. 8, pp. 1626 –1631, April 2009.

[C6-17] T. Himsoon, W. Su, and K. Liu, "Differential transmission for amplify-and-forward cooperative communications," *IEEE Signal Process. Letters*, vol. 12, pp. 597–600, September 2005.

[C6-18] T. Himsoon, W. Siriwongpairat, W. Su, and K. Liu, "Differential modulation with threshold-based decision combining for cooperative communications," *IEEE Trans. Signal Process.*, vol. 55, pp. 3905–3923, July 2007.

[C6-19] Q. Zhao and H. Li, "Differential modulation for cooperative wireless systems," *IEEE Trans. Signal Process.*, vol. 55, pp. 2273–2283, May 2007.

[C6-20] Q. Zhao, H. Li, and P. Wang, "Performance of cooperative relay with binary modulation in Nakagami-m fading channels," *IEEE Trans. Veh. Technol.*, vol. 57, pp. 3310–3315, September 2008.

[C6-21] D. Chen and J. Laneman, "Modulation and demodulation for cooperative diversity in wireless systems," *IEEE Trans. Wireless Commun.*, vol. 5, pp. 1785–1794, July 2006.

[C6-22] H. X. Nguyen and H. H. Nguyen, "Adaptive relaying in noncoherent cooperative networks," *IEEE Trans. Signal Process.*, vol. 58, pp. 3938–3945, July 2010.

[C6-23] A. Papoulis and S. U. Pillai, *Probability, Random Variables and Stochastic Processes*. 4th edition, McGraw Hill, 2002.

7. Noncoherent Amplify-and-Forward Relaying with Implicit Channel Estimation

Published as:

Ha X. Nguyen, Ha H. Nguyen and Tho Le-Ngoc, "Noncoherent Amplify-and-Forward Relaying with Implicit Channel Estimation", submitted to *IEEE Transactions on Communications*.

As mentioned in Chapter 2, the two main signal processing methods performed at the relays are AF and DF. The manuscripts in Chapters 3, 4, 5, and 6 have concentrated on various protocols for the relaying systems with DF. However, the AF method is also attractive since it puts a less processing burden on the relays. Furthermore, the fixed-gain AF relaying scheme does not need the instantaneous CSI, but the average signal-to-noise ratio of the source-relay link in order to maintain a fixed average transmit power at each relay. On the other hand, with AF, the destination requires the knowledge of CSI of all the transmission links propagated by its received signals in order to perform a coherent detection. This requirement implies a high cost for a network with multiple relay transmission links, especially in a fast fading environment.

The manuscript included in this chapter studies a noncoherent detection scheme for a fixed-gain AF multiple-relay network. Built on the fact that every transmitted symbol from the source to the destination can be considered as a pilot symbol, i.e., implicit pilot symbol, the destination first estimates the overall channels after receiving signals from the source and all the relays. Then the MRC is employed to make a

final decision. With BFSK, a tight upperbound on the error performance is derived in a closed-form expression for a multiple-relay network. In addition, it is proven that the proposed scheme achieves a full diversity order. Simulation results are also provided to confirm that the proposed scheme can significantly improve the BER performance when compared to previously proposed schemes in a temporally-correlated fading environment.

Noncoherent Amplify-and-Forward Relaying with Implicit Channel Estimation

Ha X. Nguyen, *Student Member, IEEE*, Ha H. Nguyen, *Senior Member, IEEE*, and Tho Le-Ngoc, *Fellow, IEEE*

Abstract

This paper develops a detection scheme based on implicit pilot-symbol-assisted architecture for non-coherent amplify-and-forward (AF) relay networks. The networks use M-ary frequency-shift-keying (FSK) modulation and multiple relays to assist communication from a source to a destination. Built on the fact that every transmitted symbol from the source to the destination can be considered as a pilot symbol, the destination combines the signals from the source and the relays to perform detection by using the estimated channels obtained from the implicit pilot symbols. Although the exact performance analysis of the developed scheme is complicated due to the non-Gaussian nature of the source-relay-destination links, a tight upper bound on the bit-error-rate (BER) is provided and used to show that the proposed scheme achieves a full diversity order. Moreover, simulation results reveal that the proposed scheme can significantly improve the BER performance when compared to previously proposed schemes in a temporally-correlated fading environment.

Index terms

Cooperative diversity, relay communications, frequency-shift-keying, fading channel, amplify-and-forward protocol.

Manuscript was submitted to *IEEE Transactions on Communications* on January 25, 2011.

Ha X. Nguyen (*contact author) and Ha H. Nguyen are with the Department of Electrical and Computer Engineering, University of Saskatchewan, 57 Campus Drive, Saskatoon, Sask., Canada, S7N 5A9 (e-mails: hxn201@mail.usask.ca, ha.nguyen@usask.ca).

Tho Le-Ngoc is with the Department of Electrical and Computer Engineering, McGill University, 3480 University Street, Montreal, Quebec, Canada, H3A 2A7 (e-mail: tho@ece.mcgill.ca).

7.1 Introduction

The last decade has witnessed an explosive interest in wireless relay communications, from both industry and research community. This is due mainly to its ability to provide spatial diversity (or cooperative diversity) in mobile units that cannot be equipped with multiple antennas. Specifically, a relay communication network can be designed so that one mobile in the network sends (or receives) its signal to (or from) the base station via other mobiles or base station in the network. With such a configuration, a virtual multiple antenna system is created although the multiple antennas are not collocated, hence providing spatial diversity [C7-1, C7-2, C7-3].

The cooperative diversity transmission is typically divided into two phases. In the first phase, the source broadcasts its signal to all the relays and destination. In the second phase, the relays either amplify-and-forward the received signal, or decode, re-encode, and forward the re-encoded signal. The former process is commonly referred to as amplify-and-forward (AF), whereas the latter is known as decode-and-forward (DF) [C7-1, C7-2, C7-3, C7-4]. The AF protocol is quite attractive since it puts a less processing burden on the relays. The AF protocol is further categorized as variable-gain or fixed-gain relaying based on the availability of channel state information (CSI) at the relays. The variable-gain AF relaying scheme requires the instantaneous CSI of the source-relay link at the corresponding relay to maintain a fixed transmit power at all time. On the other hand, the fixed-gain AF relaying scheme does not need the instantaneous CSI, but the average signal-to-noise ratio of the source-relay link in order to maintain a fixed average transmit power at each relay [C7-3,C7-5,C7-6,C7-7].

A majority of previous research works in wireless relay communications assumes that all the receivers in the network (i.e., at relays and destination) have the perfect knowledge of CSI of all the transmission links propagated by their received signals in order to perform a coherent detection. However, such an assumption is unrealistic or implies a high cost for a network with multiple relay transmission links, especially in a fast fading environment. To alleviate the need of requiring CSI at the receivers, differential or noncoherent modulation/demodulation techniques can be used. In par-

ticular, references [C7-8,C7-9,C7-10,C7-11] focus on the differential phase-shift keying (DPSK) for both AF and DF protocols. In [C7-12], the maximum-likelihood (ML) receiver and a suboptimal non-coherent AF receiver have been studied for on-off keying (OOK) and binary frequency-shift-keying (BFSK). The paper shows that a full diversity order is achieved for BFSK but not for OOK. However, the ML receiver involves integrals and hence is very complicated for implementation. Reference [C7-13] shows that there is no closed-form ML detector for a non-coherent AF network. Reference [C7-14] proposes a non-coherent detection scheme based on the generalized likelihood ratio test (GLRT) method, in which the likelihood function of each hypothesis is evaluated using the maximum-likelihood estimation of the channel gain. For the case of BFSK and single-relay transmission, the paper shows that the GLRT receiver achieves near full diversity order. More recently, the maximum energy selection (MES) receiver was developed in [C7-15] by selecting the maximum output from the square-law detectors of all branches, and was shown to achieve the full spatial diversity. The GLRT receiver in [C7-14] requires only the average noise power at the relays and destination, while the MES receiver does not need any CSI nor noise information [C7-15]. These two receivers therefore have low complexity.

It should be pointed out that references [C7-12,C7-14,C7-15] assume that there is no temporal correlation in any wireless channel of the network. As such, the receivers developed in these references might not work well when temporal channel correlation exists. This observation motivates our study of yet another detection scheme for non-coherent AF relay networks that makes use of the implicit pilot-symbol-assisted technique. Such a technique was originally developed in [C7-16] for point-to-point communications with multiple antennas. Although the main concept is inspired by the work in [C7-16], there are significant differences between our development and analysis of the technique for AF relay networks and those reported in [C7-16] for point-to-point multiple-antenna systems.

Specifically, the detection framework that shall be developed for AF relay networks is as follows (detailed description and performance analysis are presented in

Section 7.2). After receiving signals from the source and all the relays over orthogonal channels, the destination first estimates the *overall* channels using the implicit pilot symbols with the linear minimum mean square error (LMMSE) estimation algorithm. The maximal ratio combining (MRC) is then employed to make a final decision. The upper-bound on the bit-error-rate (BER) is derived in a closed-form expression for a multiple-relay AF network with BFSK in Section 7.3. Compared to previously proposed schemes, our proposed scheme can significantly improve the BER performance under different channel conditions (numerical and simulation results are provided in Section 7.5). The framework developed in this paper can be applied to a general AF cooperative networks when the source, relays and destination are also equipped with multiple antennas. As an illustration, the extension to the scenario that the source is equipped with two antennas while the relays and destination are equipped with a single antenna is presented in Section 7.4.

Notations: Superscripts $(\cdot)^*$, $(\cdot)^t$ and $(\cdot)^H$ stand for conjugate, transpose, and Hermitian transpose operations, respectively. $\mathrm{Re}(x)$ takes the real part of a complex number x. For a random variable (RV) X, $f_X(\cdot)$ denotes its probability density function (pdf), and $\mathbb{E}_X\{\cdot\}$ denotes its expectation. $\mathcal{CN}(0,\sigma^2)$ denotes a circularly symmetric complex Gaussian random variable with variance σ^2. The Q-function is defined as $Q(x) = (1/\sqrt{2\pi})\int_x^\infty \exp(-t^2/2)\mathrm{d}t$. The notation $E_1(x)$ is used to denote the exponential integral, i.e., $E_1(x) = \int_x^\infty(\exp(-t)/t)\mathrm{d}t$. The gamma function is defined as $\Gamma(x) = \int_0^\infty \exp(-t)t^{x-1}\mathrm{d}t$, $\mathrm{Re}(x) > 0$. $J_0(x)$ is the zero-th order Bessel function of the first kind. The moment-generating function (MGF) of random variable X is denoted by $M_X(s)$, i.e., $M_X(s) = \mathbb{E}_X\{\exp(-sX)\}$.

7.2 Proposed Framework for Noncoherent AF Relay Systems

7.2.1 System Model

Consider a wireless relay network with one source, K relays, and one destination as illustrated in Fig. 7.1. The K relays retransmit signals to the destination over orthogonal channels. For convenience, the source, relays, and destination are denoted

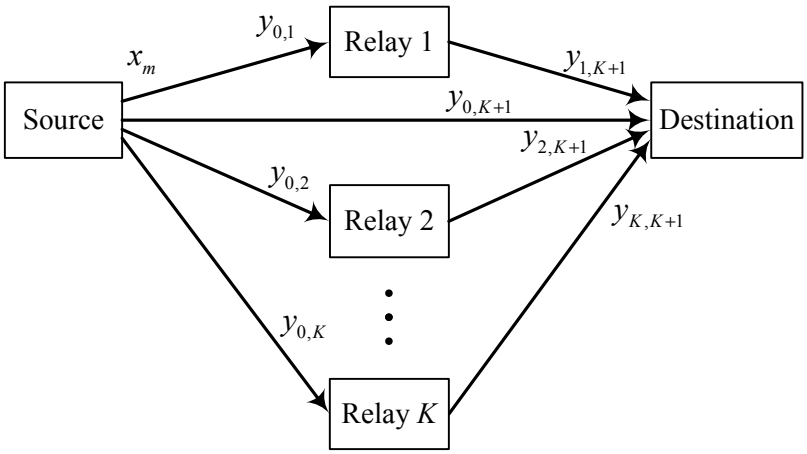

Figure 7.1 A wireless multiple-relay network.

and indexed by node 0, node i, $i = 1, \ldots, K$, and node $K + 1$, respectively. Every node is equipped with one antenna and operates in a half-duplex mode, i.e., a node cannot transmit and receive simultaneously. Fixed-gain AF protocol is employed at the relays.

Without loss of generality, assume that orthogonal channels are made available by means of time-division multiplexing. This implies that signal transmission from the source to destination is completed in $(K + 1)$ time slots, i.e., the duration is $(K + 1)T$ where T is the symbol duration (or time slot duration). In the following discussion, we adopt the convention that epoch k starts at $t = k(K + 1)T$ and ends at $(k+1)(K+1)T$. In the first time slot at epoch k, the source broadcasts a M-FSK signal and the received signal at node i, $i = 1, \ldots, K + 1$, is written as

$$y_{0,i}(t) = \sqrt{E_0} h_{0,i}[k] x_m(t) + n_{0,i}(t), \quad t \in \mathbf{T}_{k,0} \tag{7.1}$$

where $\mathbf{T}_{k,j} = [k(K+1)T + jT, k(K+1)T + (j+1)T)$ denotes the interval of time slot $(j + 1)$ at epoch k, $h_{0,i}[k]$ denotes the channel fading coefficient between node 0 and node i at epoch k, which is assumed to be fixed during time slot $\mathbf{T}_{k,0}$, and $n_{0,i}(t)$ is zero-mean additive white Gaussian noise (AWGN) at node i whose two-sided power spectral density (PSD) is $N_0/2$. The quantity E_0 is the average transmitted symbol energy of the source. The transmitted waveform $x_m(t)$, chosen from an M-ary FSK

constellation, is given in complex baseband as

$$x_m(t) = \frac{1}{\sqrt{T}} \exp\left(\frac{j\pi t}{T}(2m - M - 1)\right), \quad m = 1, \ldots, M \tag{7.2}$$

The channel between any two nodes is assumed to be constant over $(K+1)$ time slots, but varies dependently every $(K+1)$ time slots. In particular, the channel gains are modeled as circularly symmetric complex Gaussian random variables (i.e., the magnitudes of the channel gains have the flat Rayleigh fading property) with the following Jake's autocorrelation function:

$$\phi_{i,j}[l] = \mathbb{E}\left\{h^*_{i,j}[l+m]h_{i,j}[m]\right\} = \sigma^2_{i,j} J_0(2\pi f_{i,j} l) \tag{7.3}$$

In the above equation, the indices i, j refer to transmit and receive nodes, respectively and $f_{i,j}$ is the maximum Doppler frequency experienced by the transmission between node i and node j.

For AF with fixed-gain relaying, the ith relay node amplifies and retransmits the received signal with a fixed scaling factor given by

$$\beta_i = \sqrt{\frac{E_i}{\mathbb{E}\{|y_{0,i}(t)|^2\}}} = \sqrt{\frac{E_i}{E_0\sigma^2_{0,i} + N_0}} \tag{7.4}$$

where E_i is the average transmitted symbol energy of relay i. The received signal at the destination via the ith relay node at epoch k, i.e., during the time interval $t \in \mathbf{T}_{k,i}$ is written as

$$\begin{aligned}
y_{i,K+1}(t) &= \beta_i h_{i,K+1}[k] y_{0,i}(t - iT) + n_{i,K+1}(t) \\
&= \beta_i \sqrt{E_0} h_{0,i}[k] h_{i,K+1}[k] x_m(t - iT) + \beta_i h_{i,K+1}[k] n_{0,i}(t - iT) + n_{i,K+1}(t) \\
&= \beta_i \sqrt{E_0} h_{0,i,K+1}[k] x_m(t - iT) + \beta_i h_{i,K+1}[k] n_{0,i}(t - iT) + n_{i,K+1}(t) \\
&= \beta_i \sqrt{E_0} h_{0,i,K+1}[k] x_m(t - iT) + w_{0,i,K+1}(t)
\end{aligned} \tag{7.5}$$

where $h_{0,i,K+1}[k] = h_{0,i}[k] h_{i,K+1}[k]$ denotes the ith overall relay channel between the source and destination at epoch k, and $w_{0,i,K+1}(t) = \beta_i h_{i,K+1}[k] n_{0,i}(t - iT) + n_{i,K+1}(t)$ is the total additive noise corrupting the received signal. The noise $n_{i,K+1}(t)$ is also a zero-mean AWGN with two-sided PSD of $N_0/2$.

Similar to [C7-16], it shall be pointed out in the next section that every transmitted symbol from the source to the destination can be considered as an implicit pilot symbol. Hence the first task at the destination is to estimate the overall channels of all the links from the source to destination using these implicit pilot symbols. Then based on the estimated overall channels, the destination performs a MRC detection as if the overall channels are perfectly known. The details are presented in the next sections.

7.2.2 Channel Estimation

Exploiting the orthogonal property of FSK signalling [C7-17, C7-16], the received signals at the destination are correlated with the following sum waveform, $r(t)$, in order to estimate the overall channels:

$$r(t) = \sum_{m=1}^{M} x_m(t) = \sum_{m=1}^{M} \frac{1}{\sqrt{T}} \exp\left(\frac{j\pi t}{T}(2m - M - 1)\right) = \sum_{l=1}^{\frac{M}{2}} \frac{2}{\sqrt{T}} \cos\left((2l-1)\frac{\pi t}{T}\right) \tag{7.6}$$

The outputs of the correlators are

$$\begin{aligned} g_{0,K+1}[k] &= \int_{\mathbf{T}_{k,0}} y_{0,K+1}(t) r(t) \mathrm{d}t = \sqrt{E_0} h_{0,K+1}[k] + v_{0,K+1}[k], & (7.7) \\ g_{0,i,K+1}[k] &= \int_{\mathbf{T}_{k,i}} y_{i,K+1}(t) r(t) \mathrm{d}t \\ &= \beta_i \sqrt{E_0} h_{0,i,K+1}[k] + \beta_i h_{i,K+1}[k] v_{0,i}[k] + v_{i,K+1}[k] \\ &= \beta_i \sqrt{E_0} h_{0,i,K+1}[k] + u_{0,i,K+1}[k], \quad i = 1, \ldots, K & (7.8) \end{aligned}$$

where $\int_{\mathbf{T}_{k,i}}$ means $\int_{k(K+1)T+iT}^{k(K+1)T+(i+1)T}$ and $u_{0,i,K+1}[k] = \beta_i h_{i,K+1}[k] v_{0,i}[k] + v_{i,K+1}[k]$. The noise term $v_{i,K+1}[k]$, $i = 0, \ldots, K$, is

$$v_{i,K+1}[k] = \int_{\mathbf{T}_{k,i}} n_{i,K+1}(t) r(t) \mathrm{d}t \tag{7.9}$$

which is a zero-mean complex Gaussian random variable with variance MN_0. Similarly, the noise term $v_{0,i}[k]$, $i = 1, \ldots, K$, is also a zero-mean complex Gaussian random variable with variance MN_0. Observe from (7.7) and (7.8) that $g_{0,K+1}[k]$ and $g_{0,i,K+1}[k]$ are independent of the transmitted waveform $x_m(t)$. This implies that

one can estimate the overall channels $h_{0,K+1}[k]$ and $h_{0,i,K+1}[k]$ without explicit pilot symbols from the source.

By employing the LMMSE estimation algorithm [C7-18, C7-19], the estimation of $h_{0,K+1}[k]$ and $h_{0,i,K+1}[k]$, denoted by $\hat{h}_{0,K+1}[k]$ and $\hat{h}_{0,i,K+1}[k]$ respectively, can be obtained as follows:

$$\hat{h}_{0,i}[k] = \Psi_{h\mathbf{g}}^{(0)} \left(\Phi_{\mathbf{gg}}^{(0)}\right)^{-1} \mathbf{g}_{0,K+1}[k], \tag{7.10}$$

$$\hat{h}_{0,i,K+1}[k] = \Psi_{h\mathbf{g}}^{(i)} \left(\Phi_{\mathbf{gg}}^{(i)}\right)^{-1} \mathbf{g}_{0,i,K+1}[k], \quad i = 1, \ldots, K \tag{7.11}$$

where $\mathbf{g}_{0,K+1}[k]$ and $\mathbf{g}_{0,i,K+1}[k]$ are the $2P \times 1$ vectors formed by stacking $2P$ consecutive values of $g_{0,K+1}[k+l]$ and $g_{0,i,K+1}[k+l]$, $l = -P, \ldots, P$, respectively. That is,

$$\mathbf{g}_{0,K+1}[k] = \begin{pmatrix} g_{0,K+1}[k-P] \\ g_{0,K+1}[k-P+1] \\ \vdots \\ g_{0,K+1}[k+P] \end{pmatrix},$$

$$\mathbf{g}_{0,i,K+1}[k] = \begin{pmatrix} g_{0,i,K+1}[k-P] \\ g_{0,i,K+1}[k-P+1] \\ \vdots \\ g_{0,i,K+1}[k+P] \end{pmatrix}, \quad i = 1, \ldots, K, \tag{7.12}$$

Furthermore, $\Psi_{h\mathbf{g}}^{(i)}$ is the correlation vector between $h_{0,K+1}[k]$ and $\mathbf{g}_{0,K+1}[k]$ for $i = 0$ or between $h_{0,i,K+1}[k]$ and $\mathbf{g}_{0,i,K+1}[k]$ for $i = 1, \ldots, K$. The matrix $\Phi_{\mathbf{gg}}^{(i)}$ is $2P \times 2P$ auto-correlation matrix of $\mathbf{g}_{0,K+1}[k]$ for $i = 0$ or $\mathbf{g}_{0,i,K+1}[k]$ for $i = 1, \ldots, K$. In essence, the estimations in (7.10) and (7.11) use the P closest data symbols from the past and P closet data symbols from the future to estimate the channel at a given symbol time. It should be noted that there is a trade-off between complexity and performance. Additional pilot symbols may be used to improve the performance but that will increase the complexity.

With the system model and channel properties described in the previous section,

$\Psi_{h\mathbf{g}}^{(i)}$ can be computed as

$$\Psi_{h\mathbf{g}}^{(0)} = \mathbb{E}\left\{h_{0,K+1}[k]\mathbf{g}_{0,K+1}^{H}[k]\right\} = \left(\sqrt{E_0}\phi_{0,K+1}[k-P] \quad \sqrt{E_0}\phi_{0,K+1}[k-P+1] \quad \ldots \quad \sqrt{E_0}\phi_{0,K+1}[k+P] \right), \quad (7.13)$$

$$\Psi_{h\mathbf{g}}^{(i)} = \mathbb{E}\left\{h_{0,i,K+1}[k]\mathbf{g}_{0,i,K+1}^{H}[k]\right\} = \left(\beta_i\sqrt{E_0}\phi_{0,i,K+1}[k-P] \right.$$
$$\left. \ldots \quad \beta_i\sqrt{E_0}\phi_{0,i,K+1}[k-P+1] \quad \beta_i\sqrt{E_0}\phi_{0,i,K+1}[k+P] \right), \quad i=1,\ldots,K, \quad (7.14)$$

where $\phi_{0,i,K+1}[l]$ is the auto-correlation function of the overall channel $h_{0,i,K+1}$. Assuming a channel model based on fixed relays as in [C7-18], one has

$$\phi_{0,i,K+1}[l] = \phi_{0,i,K+1}[l]\phi_{0,i,K+1}[l] = \sigma_{0,i}^2\sigma_{i,K+1}^2 J_0(2\pi f_{0,i}l)J_0(2\pi f_{i,K+1}l) \quad (7.15)$$

The (n,m)-th element of $\Phi_{\mathbf{gg}}^{(i)}$ can be computed as

$$\Phi_{\mathbf{gg}}^{(i)}(n,m) = \begin{cases} E_0\phi_{0,K+1}[(n-m)] + MN_0\delta[n-m], & i=0, \\ \beta_i^2 E_0\phi_{0,i,K+1}[(n-m)] + \beta_i^2\sigma_{0,i}^2 MN_0\delta[n-m] & \\ +MN_0\delta[n-m], & i=1,\ldots,K. \end{cases} \quad (7.16)$$

where $\delta[\cdot]$ is the discrete-time Dirac delta function.

Let the estimation errors of channels $h_{0,K+1}[k]$ and $h_{0,i,K+1}[k]$ be $e_{0,K+1}[k] = h_{0,K+1}[k] - \hat{h}_{0,K+1}[k]$ and $e_{0,i,K+1}[k] = h_{0,i,K+1}[k] - \hat{h}_{0,i,K+1}[k]$, respectively. From the LMMSE property [C7-20], the estimation errors $e_{0,K+1}[k]$ and $e_{0,i,K+1}[k]$ are zero-mean complex random variables with variances given, respectively, as

$$\tilde{\sigma}_{0,K+1}^2 = \sigma_{0,K+1}^2 - \Psi_{h\mathbf{g}}^{(0)}\left(\Phi_{\mathbf{gg}}^{(0)}\right)^{-1}\left(\Psi_{h\mathbf{g}}^{(0)}\right)^{H} \quad (7.17)$$

$$\tilde{\sigma}_{0,i,K+1}^2 = \sigma_{0,i,K+1}^2 - \Psi_{h\mathbf{g}}^{(i)}\left(\Phi_{\mathbf{gg}}^{(i)}\right)^{-1}\left(\Psi_{h\mathbf{g}}^{(i)}\right)^{H}, \quad i=1,\ldots,K \quad (7.18)$$

where $\sigma_{0,i,K+1}^2 = \sigma_{0,i}^2\sigma_{i,K+1}^2$ denotes the overall channel variance.

7.2.3 Data Detection

For the purpose of data detection, the received signals at the destination in (7.1) and (7.5) are rewritten as

$$y_{0,K+1}(t) = \sqrt{E_0}\hat{h}_{0,K+1}[k]x_m(t) + \sqrt{E_0}e_{0,K+1}[k]x_m(t) + n_{0,K+1}(t), \quad (7.19)$$

$$y_{i,K+1}(t) = \beta_i\sqrt{E_0}\hat{h}_{0,i,N+1}[k]x_m(t-iT) + \beta_i\sqrt{E_0}e_{0,i,N+1}[k]x_m(t-iT) + w_{0,i,K+1}(t) \quad (7.20)$$

First, the destination correlates the received signals in (7.19) and (7.20) with the following vector of basis waveforms in M-FSK:

$$x(t) = \left[\begin{array}{cccc} x_1^*(t) & x_2^*(t) & \ldots & x_M^*(t) \end{array} \right]^t. \quad (7.21)$$

The outputs of the correlators can be shown to be:

$$\mathbf{y}_{0,K+1}[k] = \sqrt{E_0}\widehat{\mathbf{H}}_{0,K+1}[k]\mathbf{x}_m[k] + \sqrt{E_0}\mathbf{E}_{0,K+1}[k]\mathbf{x}_m[k] + \mathbf{n}_{0,K+1}[k], \quad (7.22)$$

$$\mathbf{y}_{i,K+1}[k] = \beta_i\sqrt{E_0}\widehat{\mathbf{H}}_{0,i,N+1}[k]\mathbf{x}_m[k] + \beta_i\sqrt{E_0}\mathbf{E}_{0,i,N+1}[k]\mathbf{x}_m[k] + \mathbf{w}_{0,i,K+1}[k], \quad (7.23)$$

where the $M \times 1$ vector $\mathbf{x}_m[k]$, $m = 1, \ldots, M$, represents the transmitted symbol at epoch k. Note that $\mathbf{x}_m[k]$ has 1 as its mth element and 0 as its other elements. The estimated channel matrix (or channel error matrix) between node i and node j, $\widehat{\mathbf{H}}_{i,j}$ (or $\mathbf{E}_{i,j}$), is an $M \times M$ matrix containing estimated channel gains (or channel estimation errors) $\hat{h}_{i,j}$ (or $e_{i,j}$) on its main diagonal and 0 at its other elements. Similarly, the estimated overall channel matrix (or overall channel error matrix), $\widehat{\mathbf{H}}_{0,i,K+1}$ (or $\mathbf{E}_{0,i,K+1}$), is also an $M \times M$ matrix containing overall channel gains (or overall channel estimation errors) $\hat{h}_{0,i,K+1}$ (or $e_{0,i,K+1}$) on its main diagonal and 0 at its other elements. The elements of $M \times 1$ noise vectors $\mathbf{n}_{0,K+1}[k]$ and $\mathbf{w}_{0,i,K+1}[k]$ are i.i.d. zero-mean random variables with variance N_0 and $\left(\beta_i^2\sigma_{i,K+1}^2 + 1\right)N_0$, respectively.

The destination then combines the received signals in (7.22) and (7.23) to detect the transmitted information. Using the channel estimations $\widehat{\mathbf{H}}_{0,K+1}[k]$ and $\widehat{\mathbf{H}}_{0,i,K+1}[k]$ as they are the correct channels, the output of the maximum ratio combiner is

$$\mathbf{r}[k] = \varepsilon_0\widehat{\mathbf{H}}_{0,K+1}^H[k]\mathbf{y}_{0,K+1}[k] + \sum_{i=1}^{K}\varepsilon_i\widehat{\mathbf{H}}_{0,i,K+1}^H[k]\mathbf{y}_{i,K+1}[k], \quad (7.24)$$

where the combining weights $\varepsilon_0 = \frac{1}{E_0\widetilde{\sigma}^2_{0,K+1}+N_0}$ and $\varepsilon_i = \frac{1}{\beta_i^2 E_0\widetilde{\sigma}^2_{0,i,K+1}+\beta_i^2\sigma^2_{i,K+1}N_0+N_0}$ are used to maximize the SNR of the combiner's output. The destination subsequently decides the transmitted symbol as

$$\hat{m} = \arg \max_{m=1,\ldots,M} \mathrm{Re}(r_m[k]) \tag{7.25}$$

where $r_m[k]$ is the mth element of the $M \times 1$ vector $\mathbf{r}[k]$.

7.3 Analysis of Upper Bound on BER Performance and Diversity Order

The exact BER performance analysis of the proposed detection scheme appears difficult due to the non-Gaussian nature of the noise in (7.23). Instead, this section shall derive an upper bound on the BER by assuming that the noise is Gaussian.

It follows from (7.24) that the instantaneous SNR at the combiner's output can be written as

$$\gamma = \sum_{i=0}^{K} \gamma_i \tag{7.26}$$

where

$$\gamma_0 = \frac{E_0|\hat{h}_{0,K+1}|^2}{E_0\widetilde{\sigma}^2_{0,K+1}+N_0}, \quad \text{and} \quad \gamma_i = \frac{\beta_i^2 E_0|\hat{h}_{0,i,K+1}|^2}{\beta_i^2 E_0\widetilde{\sigma}^2_{0,i,K+1}+\beta_i^2\sigma^2_{i,K+1}N_0+N_0}. \tag{7.27}$$

The upper-bound on BER can be evaluated using the moment-generating function (MGF) method [C7-21]. To simplify the analysis, it is assumed that BFSK is employed[1], i.e., $M = 2$. The average BER can be upper bounded as

$$P_{\mathrm{e}} \leq \frac{1}{\pi}\int_0^{\frac{\pi}{2}} M_\gamma\left(\frac{g}{\sin^2\theta}\right)\mathrm{d}\theta = \frac{1}{\pi}\int_0^{\frac{\pi}{2}} \prod_{i=0}^{K} M_{\gamma_i}\left(\frac{g}{\sin^2\theta}\right)\mathrm{d}\theta \tag{7.28}$$

where $g = \frac{1}{2}$ for BFSK.

The MGF of γ_i, $M_{\gamma_i}(s)$, can be obtained by performing integration over the pdf of $|\hat{h}_{0,K+1}|^2$ for $i = 0$, or $|\hat{h}_{0,i,K+1}|^2$ for $i = 1, \ldots, K$. One can verify that [C7-18]

$$M_{\gamma_0}(s) = (1 + s\overline{\gamma}_0)^{-1}, \tag{7.29}$$

[1]It should be noted that for $M > 2$ the pairwise error probability can be upper bounded as $P_{\mathrm{e}}^{(M-\mathrm{FSK})} < \frac{M}{2}P_{\mathrm{e}}^{(\mathrm{BFSK})}$ [C7-16]. It implies that if the network can achieve a full diversity order with $M = 2$, it also achieves a full diversity order with arbitrary values of M.

and[2]

$$M_{\gamma_i}(s) = \frac{1}{\overline{\gamma}_i s} \exp\left(\frac{1}{\overline{\gamma}_i s}\right) E_1\left(\frac{1}{\overline{\gamma}_i s}\right) \tag{7.30}$$

where

$$\overline{\gamma}_0 = \mathbb{E}\{\gamma_0\} = \frac{E_0(\sigma^2_{0,K+1} - \widetilde{\sigma}^2_{0,K+1})}{E_0\widetilde{\sigma}^2_{0,K+1} + N_0}, \quad \overline{\gamma}_i = \mathbb{E}\{\gamma_i\} = \frac{\beta_i^2 E_0(\sigma^2_{0,i,K+1} - \widetilde{\sigma}^2_{0,i,K+1})}{\beta_i^2 E_0\widetilde{\sigma}^2_{0,i,K+1} + \beta_i^2\sigma^2_{i,K+1}N_0 + N_0}. \tag{7.31}$$

By substituting (7.29) and (7.30) into (7.28), an upper bound on the BER can be obtained by performing a single integration. Although such an upper bound can be calculated numerically, it does not readily tell us about the diversity order achieved by the proposed detection method. To analyze the diversity order, a looser upper bound on the BER is presented next that does not involve any integration.

By using the following inequality [C7-22]

$$\frac{1}{1+x} < \exp(x)E_1(x) \leq \frac{1}{\eta + x}, \quad \forall x > 0, \quad 0 < \eta < 1 \tag{7.32}$$

one has

$$P_{\mathrm{e}} \leq \frac{1}{\pi}\int_0^{\frac{\pi}{2}} M_\gamma\left(\frac{g}{\sin^2\theta}\right)\mathrm{d}\theta \leq \frac{1}{\pi}\int_0^{\frac{\pi}{2}} \frac{1}{1+s\overline{\gamma}_0}\prod_{i=1}^{K}\frac{1}{1+\eta\overline{\gamma}_i s}\bigg|_{s=\frac{g}{\sin^2\theta}}\mathrm{d}\theta \tag{7.33}$$

Then the Chernoff bound can be used to further upper bound the BER by setting $\theta = \pi/2$ in the above expression, which results in

$$P_{\mathrm{e}} \leq \frac{1}{\pi}\frac{1}{1+s\overline{\gamma}_0}\prod_{i=1}^{K}\frac{1}{1+\eta\overline{\gamma}_i s}\bigg|_{s=g} = \frac{1}{\pi(1+\overline{\gamma}_0/2)\prod_{i=1}^{K}(1+\eta\overline{\gamma}_i/2)} \tag{7.34}$$

It is now clearly seen that, when the transmitted powers at the source and relays are sufficiently large, the variances of the estimation errors approach zero (i.e., $\widetilde{\sigma}^2_{0,K+1}, \widetilde{\sigma}^2_{0,i,K+1} \to 0$), hence $\overline{\gamma}_0 \to \frac{E_0\sigma^2_{0,K+1}}{N_0}, \overline{\gamma}_i \to \frac{\beta_i^2 E_0\sigma^2_{0,i,K+1}}{\beta_i^2\sigma^2_{i,K+1}N_0+N_0}$. This means that in the high signal-to-noise ratio region, a full diversity order of $K+1$ is achieved by the

[2]To compute the MGF of γ_i, $i = 1, \ldots, K$, one needs the pdf of $|\hat{h}_{0,i,K+1}|^2$, $i = 1, \ldots, K$. Since it is very difficult, if not impossible, to obtain the exact pdf of $|\hat{h}_{0,i,K+1}|^2$ it is assumed that $\hat{h}_{0,i,K+1}$ has the same pdf form as the pdf of $h_{0,i,K+1}$ (remember that $\hat{h}_{0,i,K+1}$ is an estimate of $h_{0,i,K+1}$). *Remark:* This footnote is added to address the external examiner's comment. It is not in the original paper.

proposed detection scheme. This result agrees with the conclusion in [C7-19] that the presence of channel estimation errors does not affect the diversity order. The result of full diversity order shall also be confirmed by the BER curves obtained by simulation in Section 7.5.

7.4 Extension to Space-Time FSK Implemented at the Source

The previous two sections focus on a scenario where all the nodes in the network are equipped with a single antenna. However, the developed framework can be extended to a more generalized multi-antenna AF relay networks, i.e., when the source, relays and destination are equipped with multiple antennas. As an example and also a practical scenario, a relay network in which the source is equipped with two transmit antennas while the relays and destination are equipped with a single antenna is considered in this section. Naturally, an Alamouti space-time block code is employed at the source to transmit the signal to the destination.

Let $x_m^{(1)}(t)$ and $x_n^{(2)}(t)$ be the data symbols that enter the Alamouti space-time encoder during the time $t \in [k(K+1)2T, k(K+1)2T+2T)$, i.e., at epoch k. Different from the single-antenna scenario, here the time duration to complete a transmission from the source to the destination is $(K+1)2T$, i.e., epoch k starts at $t = k(K+1)2T$ and ends at $(k+1)(K+1)2T$. Assuming that the channel does not change over one space-time block code, the received signal at node i, $i = 1, \ldots, K+1$, at epoch k is written as

$$y_{0,i}(t) = \begin{cases} \sqrt{E_0} h_{0,i}^{(1)}[k] x_m^{(1)}(t) + \sqrt{E_0} h_{0,i}^{(2)}[k] x_n^{(2)}(t) + n_{0,i}(t), & t \in \mathbf{T}_{k,0} \\ -\sqrt{E_0} h_{0,i}^{(1)}[k] \left(x_n^{(2)}(t)\right)^* + \sqrt{E_0} h_{0,i}^{(2)}[k] \left(x_m^{(2)}(t)\right)^* + n_{0,i}(t), & t \in \mathbf{T}_{k,1} \end{cases} \tag{7.35}$$

where $\mathbf{T}_{k,j} = [k(K+1)2T + jT, k(K+1)2T + (j+1)T)$ denotes time slot $(j+1)$ of epoch k, and $h_{0,i}^{(1)}[k]$ and $h_{0,i}^{(2)}[k]$ are the channel fading coefficients between the first and second antennas of node 0 and node i at epoch k, respectively. Similar to the single-antenna scenario, the channel between any two antennas is assumed to be constant over one epoch. The channel gains are modeled as circularly symmetric

complex Gaussian random variables with the following Jake's autocorrelation function

$$\phi_{i,j}^{(k)}[l] = \mathbb{E}\left\{\left(h_{i,j}^{(k)}\right)^* [l+m] h_{i,j}^{(k)}[m]\right\} = \left(\sigma_{i,j}^{(k)}\right)^2 J_0\left(2\pi f_{i,j}^{(k)} l\right), \quad k = 1, 2 \tag{7.36}$$

where i, j denote the node number, while k is the antenna number of node i. Throughout this section, the superscript (k) is used only if there are two antennas at the transmitting node, i.e., for the links from the source to the relays and destination. Otherwise, the superscript (k) is dropped.

The scaling factor at the ith relay node in this scenario is given by

$$\beta_i = \sqrt{\frac{E_i}{\mathbb{E}\{|y_{0,i}(t)|^2\}}} = \sqrt{\frac{E_i}{E_0\left(\sigma_{0,i}^{(1)}\right)^2 + E_0\left(\sigma_{0,i}^{(2)}\right)^2 + N_0}}. \tag{7.37}$$

Therefore the received signal at the destination via the ith relay node can be written as

$$\begin{aligned} y_{i,K+1}(t) &= \beta_i h_{i,K+1}[k] y_{0,i}(t - i2T) + n_{i,K+1}(t) = \\ &\begin{cases} \beta_i \sqrt{E_0} h_{0,i,K+1}^{(1)}[k] x_m^{(1)}(t - i2T) & \\ +\beta_i \sqrt{E_0} h_{0,i,K+1}^{(2)}[k] x_n^{(2)}(t - i2T) + w_{0,i,K+1}(t), & t \in \mathbf{T}_{k,2i} \\ -\beta_i \sqrt{E_0} h_{0,i,K+1}^{(1)}[k] \left(x_n^{(2)}(t - i2T)\right)^* & \\ +\beta_i \sqrt{E_0} h_{0,i,K+1}^{(2)}[k] \left(x_m^{(1)}(t - i2T)\right)^* + w_{0,i,K+1}(t), & t \in \mathbf{T}_{k,2i+1} \end{cases} \end{aligned} \tag{7.38}$$

where $h_{0,i,N+1}^{(1)}[k] = h_{0,i}^{(1)}[k] h_{i,K+1}[k]$ and $h_{0,i,N+1}^{(2)}[k] = h_{0,i}^{(2)}[k] h_{i,K+1}[k]$ are the overall channels from the first and second antennas of the source to the destination via relay i, respectively. The waveform $w_{0,i,K+1}(t) = \beta_i h_{i,K+1}[k] n_{0,i}(t - i2T) + n_{i,K+1}(t)$ is the total additive noise corrupting the received signal. It should be noted that $h_{i,K+1}[k]$ is constant during epoch k.

Similar to the single-antenna scenario, the destination first estimates the overall channels of all the links from the source to the destination. Then it performs a MRC for the final detection decision. To estimate the overall channels, the received signals at the destination in (7.35) and (7.38) are correlated with the waveform $r(t)$ in (7.6)

as follows:

$$g^{(1)}_{0,K+1}[k] = \int_{\mathbf{T}_{k,0}} y_{0,K+1}(t)r(t)\mathrm{d}t = \sqrt{E_0}h^{(1)}_{0,K+1}[k] + \sqrt{E_0}h^{(2)}_{0,K+1}[k] + v^{(1)}_{0,K+1}[k], \quad (7.39)$$

$$g^{(2)}_{0,K+1}[k] = \int_{\mathbf{T}_{k,1}} y_{0,K+1}(t)r(t)\mathrm{d}t = -\sqrt{E_0}h^{(1)}_{0,K+1}[k] + \sqrt{E_0}h^{(2)}_{0,K+1}[k] + v^{(2)}_{0,K+1}[k] \quad (7.40)$$

$$\begin{aligned} g^{(1)}_{0,i,K+1}[k] &= \int_{\mathbf{T}_{k,2i}} y_{i,K+1}(t)r(t)\mathrm{d}t \\ &= \beta_i\sqrt{E_0}h^{(1)}_{0,i,K+1}[k] + \beta_i\sqrt{E_0}h^{(2)}_{0,i,K+1}[k] + w^{(1)}_{0,i,K+1}[k], \quad i = 1,\ldots,K \end{aligned} \quad (7.41)$$

$$\begin{aligned} g^{(2)}_{0,i,K+1}[k] &= \int_{\mathbf{T}_{k,2i+1}} y_{i,K+1}(t)r(t)\mathrm{d}t \\ &= -\beta_i\sqrt{E_0}h^{(1)}_{0,i,K+1}[k] + \beta_i\sqrt{E_0}h^{(2)}_{0,i,K+1}[k] + w^{(2)}_{0,i,K+1}[k], \quad i = 1,\ldots,K \end{aligned} \quad (7.42)$$

where $w^{(1)}_{0,i,K+1}[k] = \beta_i h_{i,K+1}[k]v^{(1)}_{0,i}[k] + v^{(1)}_{i,K+1}[k]$ and $w^{(2)}_{0,i,K+1} = \beta_i h_{i,K+1}[k]v^{(2)}_{0,i}[k] + v^{(2)}_{i,K+1}[k]$. The noise terms $v^{(j)}_{0,i}[k]$, $i = 0,\ldots,K+1, j = 1,2$ and $v^{(j)}_{i,K+1}[k]$, $i = 0,\ldots,K+1, j = 1,2$, are zero-mean complex Gaussian random variables with variance MN_0. Moreover, the above equations lead to the following computations:

$$\begin{aligned} \overline{g}^{(1)}_{0,K+1}[k] &= \frac{1}{2}\left(g^{(1)}_{0,K+1}[k] - g^{(2)}_{0,K+1}[k]\right) = \sqrt{E_0}h^{(1)}_{0,K+1}[k] + \frac{1}{2}\left(v^{(1)}_{0,K+1}[k] - v^{(2)}_{0,K+1}[k]\right) \\ \overline{g}^{(2)}_{0,K+1}[k] &= \frac{1}{2}\left(g^{(1)}_{0,K+1}[k] + g^{(2)}_{0,K+1}[k]\right) = \sqrt{E_0}h^{(2)}_{0,K+1}[k] + \frac{1}{2}\left(v^{(1)}_{0,K+1}[k] + v^{(2)}_{0,K+1}[k]\right) \\ \overline{g}^{(1)}_{0,i,K+1}[k] &= \frac{1}{2}\left(g^{(1)}_{0,i,K+1}[k] - g^{(2)}_{0,i,K+1}[k]\right) = \beta_i\sqrt{E_0}h^{(1)}_{0,i,K+1}[k] + \frac{1}{2}\left(w^{(1)}_{0,i,K+1}[k] - w^{(2)}_{0,i,K+1}[k]\right) \\ \overline{g}^{(2)}_{0,i,K+1}[k] &= \frac{1}{2}\left(g^{(1)}_{0,i,K+1}[k] + g^{(2)}_{0,i,K+1}[k]\right) = \beta_i\sqrt{E_0}h^{(2)}_{0,i,K+1}[k] + \frac{1}{2}\left(w^{(1)}_{0,i,K+1}[k] + w^{(2)}_{0,i,K+1}[k]\right) \end{aligned}$$

It means that the estimations of $h^{(j)}_{0,K+1}[k]$ and $h^{(j)}_{0,i,K+1}[k]$, denoted by $\hat{h}^{(j)}_{0,K+1}[k]$ and $\hat{h}^{(j)}_{0,i,K+1}[k]$ respectively, can be obtained by employing the following LMMSE estimation algorithm[3]:

$$\hat{h}^{(j)}_{0,i}[k] = \Psi^{(0)}_{h^{(j)}\overline{\mathbf{g}}^{(j)}}\left(\Phi^{(0)}_{\overline{\mathbf{g}}^{(j)}\overline{\mathbf{g}}^{(j)}}\right)^{-1}\overline{\mathbf{g}}^{(j)}_{0,K+1}[k], \quad j = 1,2 \quad (7.43)$$

$$\hat{h}^{(j)}_{0,i,K+1}[k] = \Psi^{(i)}_{h^{(j)}\overline{\mathbf{g}}^{(j)}}\left(\Phi^{(i)}_{\overline{\mathbf{g}}^{(j)}\overline{\mathbf{g}}^{(j)}}\right)^{-1}\overline{\mathbf{g}}^{(j)}_{0,i,K+1}[k], \quad i = 1,\ldots,K, j = 1,2 \quad (7.44)$$

[3]Since the noise terms $\left(w^{(1)}_{0,i,K+1}[k] - w^{(2)}_{0,i,K+1}[k]\right)$ and $\left(w^{(1)}_{0,i,K+1}[k] + w^{(2)}_{0,i,K+1}[k]\right)$ are not statistically independent, one may jointly estimate the overall channels $h^{(1)}_{0,i,K+1}[k]$ and $h^{(2)}_{0,i,K+1}[k]$ to get a better result. Unfortunately, the pdfs of $\left(w^{(1)}_{0,i,K+1}[k] - w^{(2)}_{0,i,K+1}[k]\right)$ and $\left(w^{(1)}_{0,i,K+1}[k] + w^{(2)}_{0,i,K+1}[k]\right)$ are not available in a closed form and we propose to estimate the overall channels separately. *Remark:* This footnote is added to address the external examiner's comment. It is not in the original paper.

In the above expressions, $\overline{\mathbf{g}}^{(j)}_{0,K+1}[k]$ and $\overline{\mathbf{g}}^{(j)}_{0,i,K+1}[k]$ are the $2P \times 1$ vectors formed by stacking $2P$ consecutive values of $\overline{g}^{(j)}_{0,K+1}[k+l]$ and $\overline{g}^{(j)}_{0,i,K+1}[k+l]$, $l = -P, \ldots, P$, respectively, $\Psi^{(i)}_{h^{(j)}\overline{\mathbf{g}}^{(j)}}$ is the correlation vector between $h^{(j)}_{0,K+1}[k]$ and $\overline{\mathbf{g}}^{(j)}_{0,K+1}[k]$ for $i = 0$ or between $h^{(j)}_{0,i,K+1}[k]$ and $\overline{\mathbf{g}}^{(j)}_{0,i,K+1}[k]$ for $i = 1, \ldots, K$, and $\Phi^{(i)}_{\overline{\mathbf{g}}^{(j)}\overline{\mathbf{g}}^{(j)}}$ is the auto-correlation matrix of $\overline{\mathbf{g}}^{(j)}_{0,K+1}[k]$ for $i = 0$ or $\overline{\mathbf{g}}^{(j)}_{0,i,K+1}[k]$ for $i = 1, \ldots, K$. The vector $\Psi^{(i)}_{h^{(j)}\overline{\mathbf{g}}^{(j)}}$ and matrix $\Phi^{(i)}_{\overline{\mathbf{g}}^{(j)}\overline{\mathbf{g}}^{(j)}}$ can be computed as

$$\begin{aligned}\Psi^{(0)}_{h^{(j)}\overline{\mathbf{g}}^{(j)}} &= \mathbb{E}\left\{h^{(j)}_{0,K+1}[k]\left(\overline{\mathbf{g}}^{(j)}_{0,K+1}[k]\right)^H\right\} \\ &= \left(\begin{array}{cccc}\sqrt{E_0}\phi^{(j)}_{0,K+1}[k-P] & \sqrt{E_0}\phi^{(j)}_{0,K+1}[k-P+1] & \ldots & \sqrt{E_0}\phi^{(j)}_{0,K+1}[k+P]\end{array}\right),\end{aligned} \tag{7.45}$$

$$\begin{aligned}\Psi^{(i)}_{h^{(j)}\overline{\mathbf{g}}^{(j)}} = \mathbb{E}\left\{h^{(j)}_{0,i,K+1}[k]\left(\overline{\mathbf{g}}^{(j)}_{0,i,K+1}[k]\right)^H\right\} = \Big(\ \beta_i\sqrt{E_0}\phi^{(j)}_{0,i,K+1}[k-P] \\ \beta_i\sqrt{E_0}\phi^{(j)}_{0,i,K+1}[k-P+1]\ \ldots\ \ \beta_i\sqrt{E_0}\phi^{(j)}_{0,i,K+1}[k+P]\ \Big), \quad i = 1, \ldots, K,\end{aligned} \tag{7.46}$$

$$\Phi^{(i)}_{\overline{\mathbf{g}}^{(j)}\overline{\mathbf{g}}^{(j)}}(n,m) = \begin{cases} E_0\phi^{(j)}_{0,K+1}[(n-m)] + \frac{1}{2}MN_0\delta[n-m], & i = 0, \\ \beta_i^2 E_0\phi^{(j)}_{0,i,K+1}[(n-m)] + \frac{1}{2}\beta_i^2\sigma^2_{i,K+1}MN_0\delta[n-m] & \\ \qquad\qquad + \frac{1}{2}MN_0\delta[n-m], & i = 1, \ldots, K. \end{cases} \tag{7.47}$$

Similarly, the estimation errors $e^{(j)}_{0,K+1}[k] = h^{(j)}_{0,K+1}[k] - \hat{h}^{(j)}_{0,K+1}[k]$ and $e^{(j)}_{0,i,K+1}[k] = h^{(j)}_{0,i,K+1}[k] - \hat{h}^{(j)}_{0,i,K+1}[k]$ are zero-mean complex random variables with variances given, respectively, as

$$\left(\tilde{\sigma}^{(j)}_{0,K+1}\right)^2 = \left(\sigma^{(j)}_{0,K+1}\right)^2 - \Psi^{(0)}_{h^{(j)}\overline{\mathbf{g}}^{(j)}}\left(\Phi^{(0)}_{\overline{\mathbf{g}}^{(j)}\overline{\mathbf{g}}^{(j)}}\right)^{-1}\left(\Psi^{(0)}_{h^{(j)}\overline{\mathbf{g}}^{(j)}}\right)^H \tag{7.48}$$

$$\left(\tilde{\sigma}^{(j)}_{0,i,K+1}\right)^2 = \left(\sigma^{(j)}_{0,i,K+1}\right)^2 - \Psi^{(i)}_{h^{(j)}\overline{\mathbf{g}}^{(j)}}\left(\Phi^{(i)}_{\overline{\mathbf{g}}^{(j)}\overline{\mathbf{g}}^{(j)}}\right)^{-1}\left(\Psi^{(i)}_{h^{(j)}\overline{\mathbf{g}}^{(j)}}\right)^H, \quad i = 1, \ldots, K \tag{7.49}$$

where $\left(\sigma^{(j)}_{0,i,K+1}\right)^2 = \left(\sigma^{(j)}_{0,i}\right)^2\sigma^2_{i,K+1}$.

To detect the transmitted data, the destination first stacks the received waveforms in (7.35) and (7.38) as

$$\mathbf{y}_{i,K+1}(t) = \left(\begin{array}{c} y_{i,K+1}(t) \\ y^*_{i,K+1}(t) \end{array}\right), \quad i = 0, \ldots, K. \tag{7.50}$$

Then it correlates the above with the vector of basis waveforms in (7.21) to yield

$$\mathbf{y}_{0,K+1}[k] = \sqrt{E_0}\widehat{\mathbf{H}}_{0,K+1}[k]\mathbf{x}_q[k] + \sqrt{E_0}\mathbf{E}_{0,K+1}[k]\mathbf{x}_q[k] + \mathbf{n}_{0,K+1}[k], \tag{7.51}$$

$$\mathbf{y}_{i,K+1}[k] = \beta_i\sqrt{E_0}\widehat{\mathbf{H}}_{0,i,N+1}[k]\mathbf{x}_q[k] + \beta_i\sqrt{E_0}\mathbf{E}_{0,i,N+1}[k]\mathbf{x}_q[k] + \mathbf{w}_{0,i,K+1}[k], i = 1,\ldots,K \tag{7.52}$$

where $\widehat{\mathbf{H}}_{0,K+1}[k]$, $\widehat{\mathbf{H}}_{0,i,K+1}[k]$, $\mathbf{E}_{0,K+1}[k]$, and $\mathbf{E}_{0,i,K+1}[k]$ are defined, respectively, as

$$\widehat{\mathbf{H}}_{0,K+1}[k] = \begin{pmatrix} \widehat{\mathbf{H}}^{(1)}_{0,K+1}[k] & \widehat{\mathbf{H}}^{(2)}_{0,K+1}[k] \\ -\left(\widehat{\mathbf{H}}^{(2)}_{0,K+1}[k]\right)^* & \left(\widehat{\mathbf{H}}^{(1)}_{0,K+1}[k]\right)^* \end{pmatrix}, \tag{7.53}$$

$$\widehat{\mathbf{H}}_{0,i,K+1}[k] = \begin{pmatrix} \widehat{\mathbf{H}}^{(1)}_{0,i,K+1}[k] & \widehat{\mathbf{H}}^{(2)}_{0,i,K+1}[k] \\ -\left(\widehat{\mathbf{H}}^{(2)}_{0,i,K+1}[k]\right)^* & \left(\widehat{\mathbf{H}}^{(1)}_{0,i,K+1}[k]\right)^* \end{pmatrix}, \tag{7.54}$$

$$\mathbf{E}_{0,K+1}[k] = \begin{pmatrix} \mathbf{E}^{(1)}_{0,K+1}[k] & \mathbf{E}^{(2)}_{0,K+1}[k] \\ -\left(\mathbf{E}^{(2)}_{0,K+1}[k]\right)^* & \left(\mathbf{E}^{(1)}_{0,K+1}[k]\right)^* \end{pmatrix}, \tag{7.55}$$

$$\mathbf{E}_{0,i,K+1}[k] = \begin{pmatrix} \mathbf{E}^{(1)}_{0,i,K+1}[k] & \mathbf{E}^{(2)}_{0,i,K+1}[k] \\ -\left(\mathbf{E}^{(2)}_{0,i,K+1}[k]\right)^* & \left(\mathbf{E}^{(1)}_{0,i,K+1}[k]\right)^* \end{pmatrix}. \tag{7.56}$$

The $M \times M$ matrices $\widehat{\mathbf{H}}^{(j)}_{0,K+1}$, $\widehat{\mathbf{H}}^{(j)}_{0,i,K+1}$, $\mathbf{E}^{(j)}_{0,K+1}$, and $\mathbf{E}^{(j)}_{0,i,K+1}$ are defined as before (i.e., after equation (7.23)) but with elements $\widehat{h}^{(j)}_{0,K+1}$, $\widehat{h}^{(j)}_{0,i,K+1}$, $e^{(j)}_{0,K+1}$, and $e^{(j)}_{0,i,K+1}$, respectively. It should be noted that $\widehat{\mathbf{H}}^{(j)}_{0,K+1}[k]$ and $\widehat{\mathbf{H}}^{(j)}_{0,i,K+1}[k]$ are obtained from (7.43) and (7.44), which in turn give $\widehat{\mathbf{H}}_{0,K+1}[k]$ and $\widehat{\mathbf{H}}_{0,K+1}[k]$. Lastly the vector $\mathbf{x}_q[k]$ is defined as

$$\mathbf{x}_q[k] = \begin{pmatrix} \mathbf{x}^{(1)}_m[k] \\ \mathbf{x}^{(2)}_n[k] \end{pmatrix}. \tag{7.57}$$

To maximize the SNR, the destination uses the following combining weights

$$\varepsilon_0 = \frac{1}{E_0\left(\widetilde{\sigma}^{(1)}_{0,K+1}\right)^2 + E_0\left(\widetilde{\sigma}^{(2)}_{0,K+1}\right)^2 + 2N_0} \tag{7.58}$$

$$\varepsilon_i = \frac{1}{\beta_i^2 E_0\left(\widetilde{\sigma}^{(1)}_{0,i,K+1}\right)^2 + \beta_i^2 E_0\left(\widetilde{\sigma}^{(2)}_{0,i,K+1}\right)^2 + 2\beta_i^2\sigma^2_{i,K+1}N_0 + 2N_0} \tag{7.59}$$

to combine the received signals in (7.51) and (7.52) and produces:

$$\mathbf{r}[k] = \varepsilon_0\widehat{\mathbf{H}}^H_{0,K+1}[k]\mathbf{y}_{0,K+1}[k] + \sum_{i=1}^{K}\varepsilon_i\widehat{\mathbf{H}}^H_{0,i,K+1}[k]\mathbf{y}_{i,K+1}[k] \tag{7.60}$$

The transmitted symbols are finally decided by

$$\hat{m} = \arg \max_{m=1,\ldots,M} \mathrm{Re}(r_m[k]) \tag{7.61}$$

$$\hat{n} = \arg \max_{n=1,\ldots,M} \mathrm{Re}(r_{n+M}[k]) \tag{7.62}$$

where $r_i[k]$ is the ith element of the $2M \times 1$ vector $\mathbf{r}[k]$.

Furthermore, an instantaneous SNR at the combiner's output in this scenario can also be written as

$$\gamma = \sum_{i=0}^{K} \gamma_i \tag{7.63}$$

where

$$\gamma_0 = \frac{E_0 \left|\hat{h}_{0,K+1}^{(1)}\right|^2 + E_0 \left|\hat{h}_{0,K+1}^{(2)}\right|^2}{E_0 \left(\widetilde{\sigma}_{0,K+1}^{(1)}\right)^2 + E_0 \left(\widetilde{\sigma}_{0,K+1}^{(2)}\right)^2 + 2N_0} \tag{7.64}$$

$$\gamma_i = \frac{\beta_i^2 E_0 \left|\hat{h}_{0,i,K+1}^{(1)}\right|^2 + \beta_i^2 E_0 \left|\hat{h}_{0,i,K+1}^{(2)}\right|^2}{\beta_i^2 E_0 \left(\widetilde{\sigma}_{0,i,K+1}^{(1)}\right)^2 + \beta_i^2 E_0 \left(\widetilde{\sigma}_{0,i,K+1}^{(2)}\right)^2 + 2\beta_i^2 \sigma_{i,K+1}^2 N_0 + 2N_0} \tag{7.65}$$

To simplify the analysis, it is assumed that $\left(\sigma_{0,i}^{(1)}\right)^2 = \left(\sigma_{0,i}^{(2)}\right)^2 = \sigma_{0,i}^2$, $i = 1, \ldots, K+1$, which means $\left(\sigma_{0,i,K+1}^{(1)}\right)^2 = \left(\sigma_{0,i,K+1}^{(2)}\right)^2 = \sigma_{0,i,K+1}^2$, $i = 1, \ldots, K$. The MGF of γ_i can be evaluated as (see Appendix 7.A)

$$M_{\gamma_0}(s) = \frac{1}{(1 + s\overline{\gamma}_0)^2} \tag{7.66}$$

$$M_{\gamma_i}(s) = \frac{1}{\overline{\gamma}_i s} \tag{7.67}$$

where

$$\overline{\gamma}_0 = \frac{E_0 \left(\sigma_{0,K+1}^2 - \widetilde{\sigma}_{0,K+1}^2\right)}{E_0 \widetilde{\sigma}_{0,K+1}^2 + N_0} \tag{7.68}$$

$$\overline{\gamma}_i = \frac{\beta_i^2 E_0 \left(\sigma_{0,i,K+1}^2 - \widetilde{\sigma}_{0,i,K+1}^2\right)}{\sigma_{0,i}^2 \left(\beta_i^2 E_0 \widetilde{\sigma}_{0,i,K+1}^2 + \beta_i^2 \sigma_{i,K+1}^2 N_0 + N_0\right)} \tag{7.69}$$

By substituting (7.66) and (7.67) into (7.28), one can easily find an upper bound on the BER performance in this scenario when BFSK is used. Under the high SNR assumption, $\widetilde{\sigma}_{i,K+1}^2$ $(i = 0, \ldots, K)$, and $\widetilde{\sigma}_{0,i,K+1}^2$ $(i = 1, \ldots, K)$ approach 0. Therefore $\overline{\gamma}_0 \to \frac{E_0 \sigma_{0,K+1}^2}{N_0}$, and $\overline{\gamma}_i \to \frac{\beta_i^2 E_0 \sigma_{i,K+1}^2}{\sigma_{0,i}^2 \left(\beta_i^2 \sigma_{i,K+1}^2 N_0 + N_0\right)}$. It then can be concluded that a diversity

order of $K+2$ is achieved in this scenario. This maximum achievable diversity order is due to the bottleneck of the source-relay-destination links because there is only one antenna at the relays. If the relays are equipped with two antennas, the maximum achievable diversity of the network would be $2(K+1)$ [C7-23, C7-24].

7.5 Simulation Results

In all simulations discussed in this section, the transmitted powers are set to be the same for the source and all the relays, i.e., $E_i = E,\ i = 0, \ldots, K$. The noise components at the relays and destination are modeled as i.i.d. $\mathcal{CN}(0,1)$ random variables. The average quality of a transmission link is assumed to be a function of the relative distance between a transmitting node and a receiving node. In particular we set $\sigma_{i,j}^2 = d_{i,j}^{-\nu}$ (or $(\sigma_{i,j}^{(k)})^2 = d_{i,j}^{-\nu}$ for the multiple-antenna scenario) where ν is the path loss exponent and $d_{i,j}$ is the distance between node i and node j. All the simulation results are reported with $\nu = 4$. Also for simplicity, we assume that all the relays have the same distances to the source and to the destination, i.e., $d_{0,1} = d_{0,2} = \cdots = d_{0,K} = d_1$, $d_{1,K+1} = d_{2,K+1} = \cdots = d_{K,K+1} = d_2$, and $d_{0,K+1} = d_0$. Unless other stated, the parameter P (which defines the size of observations used in channel estimation – see (7.12)) is set to 2 and the Doppler frequencies are normalized as $10 f_{0,i} T = f_{i,K+1} T = f_{0,K+1} T = 0.01$, $i = 1, \ldots, K$. It should be emphasized again that the fading coefficients are independent among different transmission links, but they are time correlated according to the Jake's model.

Figs. 7.2, 7.3, and 7.4 compare the performance of the proposed detection scheme with that of three previously proposed schemes, namely GLRT [C7-14], MES [C7-15], and the "optimum" detection scheme in [C7-12]. The comparison is done for a two-relay network with BFSK modulation and under three different scenarios: the relays are placed close to the source (Fig. 7.2), close to the destination (Fig. 7.3), and at the midpoint between the source and the destination (Fig. 7.4). Plots of the upper bound from (7.28) and performance of the coherent detection scheme (i.e., when the destination has perfect knowledge of CSI of all the transmission links) are also

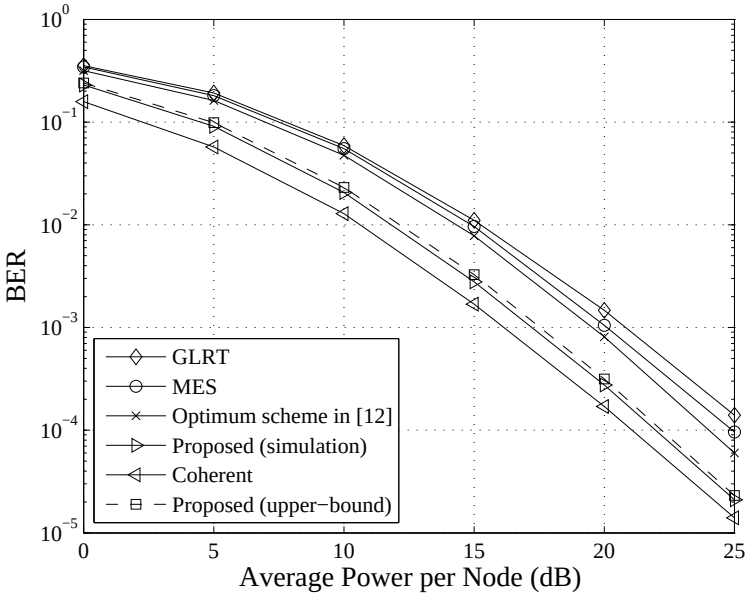

Figure 7.2 Error performance of a two-relay network by different detection schemes when $M = 2$ (BFSK), $d_0 = 1, d_1 = 0.5, d_2 = 1.5$ (the relays are placed close to the source).

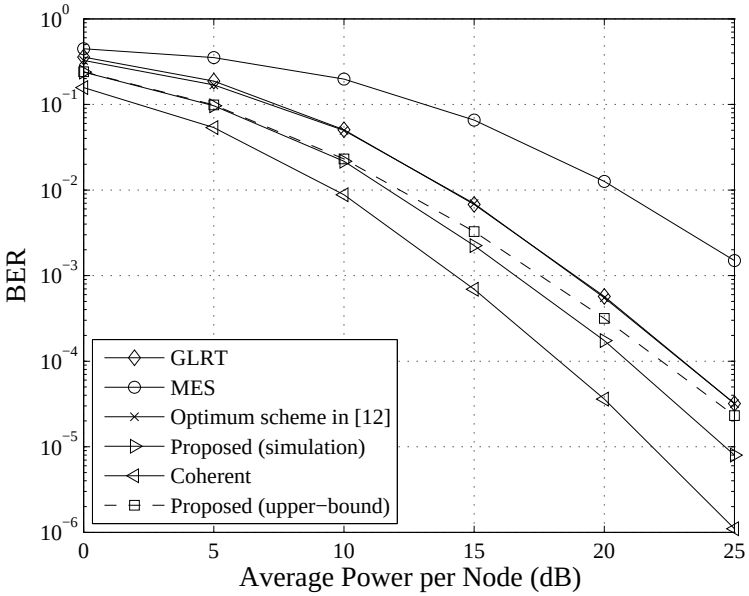

Figure 7.3 Error performance of a two-relay network by different detection schemes when $M = 2$ (BFSK), $d_0 = 1, d_1 = 1.5, d_2 = 0.5$ (the relays are placed close to the destination).

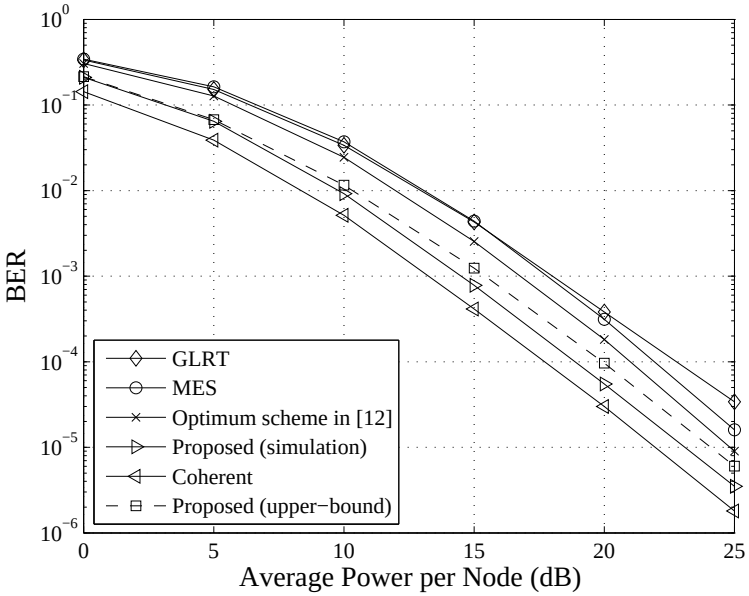

Figure 7.4 Error performance of a two-relay network by different detection schemes when $M = 2$ (BFSK), $d_0 = 1, d_1 = 1, d_2 = 1$ (the relays are placed at the midpoint between the source and the destination).

included in these figures. The three figures show that our proposed scheme outperforms other schemes in all three considered scenarios of relay positions (i.e., different channel conditions). The superior performance of our proposed scheme comes from the fact that it can make use of the correlation information to aid in the estimation of the overall channels. It is also noted that the performance gap to the coherent scheme is becomes smaller for the proposed scheme when the relays are close to the source or at the midpoint between the source and destination. This observation is intuitively satisfying since in such scenarios the destination is affected by less noise amplification from the relays. The tightness of the derived upper bound on the BER performance of our proposed scheme can also be confirmed from these figures.

Next, Fig. 7.5 illustrates how the size of observations (determined by the parameter P) used for channel estimation, affects the average BER of the proposed scheme. Investigated here is a single-relay network with BFSK modulation and when the relay is placed close to the source. It can be seen that the BER performance improves as P

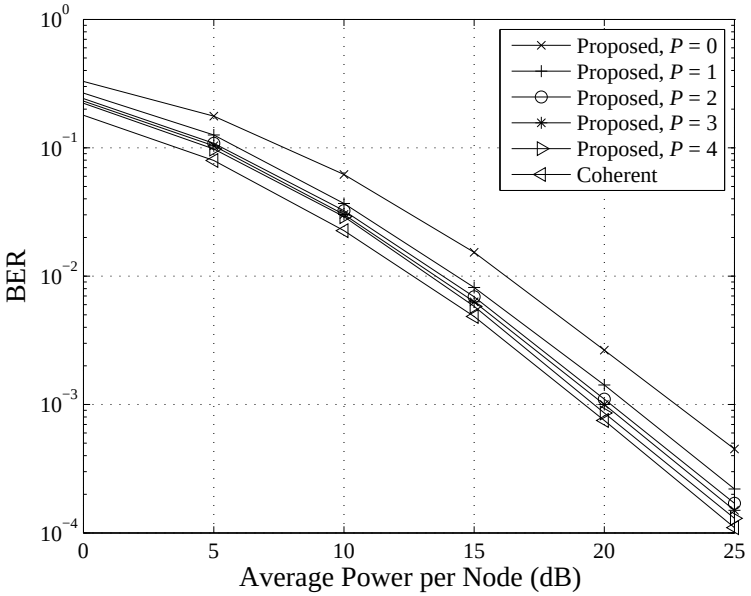

Figure 7.5 Error performance of a single-relay network with various values of P when $M = 2$ (BFSK), $d_0 = 1, d_1 = 0.5, d_2 = 1.5$ (the relays are placed close to the source).

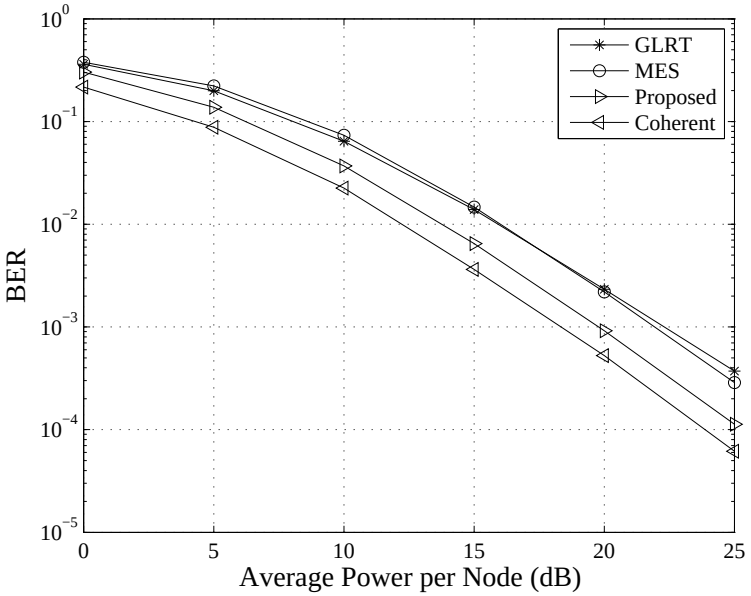

Figure 7.6 Error performance of a single-relay network by different schemes when $M = 4$ (4-FSK), $d_0 = 1, d_1 = 1, d_2 = 1$ (the relays are placed at the midpoint between the source and the destination).

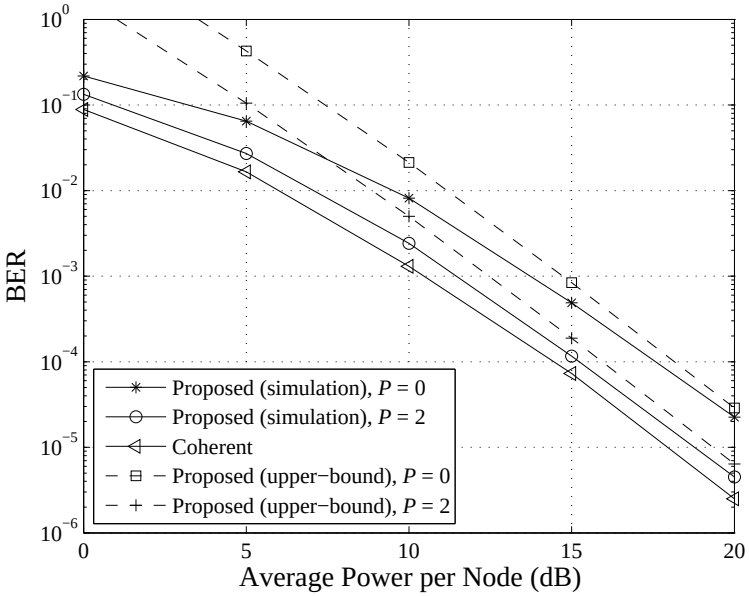

Figure 7.7 Error performance of a single-relay network with Alamouti space-time code when $M = 2$ (BFSK), $d_0 = 1, d_1 = 1, d_2 = 1$ (the relays are placed at the midpoint between the source and the destination).

increases. In general, the parameter P should be chosen to tradeoff among different system requirements, such as the BER performance, implementation complexity, and decoding delay. As observed from the figure, when P increases from 0 to 1, there is a gain of about 2 dB in average transmitted power per node. However, the power gain is quite insignificant when P increases from 2 to 3. Such a behavior is also expected since when the estimation error reaches a saturation point, increasing P will not result in a significant BER improvement. However, in the high SNR region, the performance of the proposed scheme can be made to approach that of the coherent scheme by keep increasing P.

The BER comparison of the proposed scheme and other schemes is shown in Fig. 7.6 for the case of a single-relay network and 4-FSK modulation ($M = 4$). In this comparison, the relay is placed at the midpoint between the source and the destination. The figure again confirms that the proposed scheme outperforms other previously proposed schemes for 4-FSK. A diversity order of 2 is also observed with

all the schemes from the figure.

Finally, the performance of the proposed scheme when the source is equipped with two antennas as presented in Section 7.4 is illustrated in Fig. 7.7 for a single-relay network. Here the relay is placed close to the destination and BFSK modulation is employed. One can observe that the diversity order of 3 is achieved by the proposed scheme for this dual-antenna implementation at the source. The BER performance is improved when the parameter P increases. With $P = 2$, a gap of only 1.5 dB is observed when compared to the coherent detection.

7.6 Conclusions

In this paper, we have considered amplify-and-forward multiple-relay networks in which the source transmits to the destination with the help of K relays and the channels are temporally-correlated Rayleigh flat fading. The networks are invested when M-FSK is employed at both the source and relays to facilitate noncoherent communications. Making use of the orthogonal property of FSK signalling, the destination first estimates the overall channel coefficients based on a LMMSE approach and then detects the information symbol with a (approximate) maximum ratio combiner. An upper-bound of the BER expression was also derived and used to show that the proposed scheme achieves a full diversity order. Simulation results were presented to corroborate the analysis. Performance comparison reveals that the proposed scheme outperforms the previously proposed schemes.

7.A Derivation of (7.67)

Let $Y = \left|\hat{h}^{(1)}_{0,i,K+1}\right|^2 + \left|\hat{h}^{(2)}_{0,i,K+1}\right|^2 = \left|\hat{h}_{i,K+1}\right|^2 \left(\left|\hat{h}^{(1)}_{0,i}\right|^2 + \left|\hat{h}^{(2)}_{0,i}\right|^2\right) = X_1 X_2$ where $X_1 = \left|\hat{h}_{i,K+1}\right|^2$ and $X_2 = \left|\hat{h}^{(1)}_{0,i}\right|^2 + \left|\hat{h}^{(2)}_{0,i}\right|^2$. Due to the fact that $\hat{h}_{i,K+1}$, $\hat{h}^{(1)}_{0,i}$, and $\hat{h}^{(2)}_{0,i}$ are the estimates of $h_{i,K+1}$, $h^{(1)}_{0,i}$, and $h^{(2)}_{0,i}$, one can approximate that the pdfs of $\hat{h}_{i,K+1}$, $\hat{h}^{(1)}_{0,i}$, and $\hat{h}^{(2)}_{0,i}$ have the same form as the pdfs of $h_{i,K+1}$, $h^{(1)}_{0,i}$, and $h^{(2)}_{0,i}$, respectively. Then $f_{X_1}(x) = \frac{1}{\hat{\sigma}^2_{i,K+1}} \mathrm{e}^{-\frac{x}{\hat{\sigma}^2_{i,K+1}}}$ and $f_{X_2}(x) = \frac{x}{\hat{\sigma}^2_{0,i}} \mathrm{e}^{-\frac{x}{\hat{\sigma}^2_{0,i}}}$. The MGF of Y can then be

computed as: [C7-25]

$$M_Y(s) = \int_0^\infty f_{X_2}(x) M_{X_1}(sx) \mathrm{d}x = \int_0^\infty \frac{x}{\hat{\sigma}_{0,i}^2} \mathrm{e}^{-\frac{x}{\hat{\sigma}_{0,i}^2}} \frac{1}{1+\hat{\sigma}_{i,K+1}^2 sx} \mathrm{d}x$$
$$\simeq \int_0^\infty \frac{x}{\hat{\sigma}_{0,i}^2} \mathrm{e}^{-\frac{x}{\hat{\sigma}_{0,i}^2}} \frac{1}{\hat{\sigma}_{i,K+1}^2 sx} \mathrm{d}x = \frac{1}{\hat{\sigma}_{i,K+1}^2 s} \leq \frac{\sigma_{0,i}^2}{\hat{\sigma}_{0,i,K+1}^2 s} \quad (7.70)$$

References

[C7-1] A. Sendonaris, E. Erkip, and B. Aazhang, "User cooperation diversity, Part I: System description," *IEEE Trans. Commun.*, vol. 51, no. 11, pp. 1927–1938, November 2003.

[C7-2] A. Sendonaris, E. Erkip, and B. Aazhang, "User cooperation diversity, Part II: Implementation aspects and performance analysis," *IEEE Trans. Commun.*, vol. 51, no. 11, pp. 1939–1948, November 2003.

[C7-3] J. Laneman, D. Tse, and G. Wornell, "Cooperative diversity in wireless networks: Efficient protocols and outage behavior," *IEEE Trans. Inform. Theory*, vol. 50, pp. 3062–3080, December 2004.

[C7-4] J. Laneman and G. Wornell, "Distributed space-time-coded protocols for exploiting cooperative diversity in wireless networks," *IEEE Trans. Inform. Theory*, vol. 49, pp. 2415–2425, October 2003.

[C7-5] M. Hasna and M.-S. Alouini, "A performance study of dual-hop transmissions with fixed gain relays," *IEEE Trans. Wireless Commun.*, vol. 3, pp. 1963–1968, November 2004.

[C7-6] R. Nabar, H. Bolcskei, and F. Kneubuhler, "Fading relay channels: Performance limits and space-time signal design," *IEEE J. Select. Areas in Commun.*, vol. 22, pp. 1099–1109, August 2004.

[C7-7] D. Chen and J. Laneman, "Modulation and demodulation for cooperative diversity in wireless systems," *IEEE Trans. Wireless Commun.*, vol. 5, pp. 1785–1794, July 2006.

[C7-8] T. Himsoon, W. Su, and K. Liu, "Differential transmission for amplify-and-forward cooperative communications," *IEEE Signal Process. Letters*, vol. 12, pp. 597–600, September 2005.

[C7-9] T. Himsoon, W. Pam Siriwongpairat, W. Su, and K. Liu, "Differential modulations for multinode cooperative communications," *IEEE Trans. Signal Process.*, vol. 56, pp. 2941–2956, July 2008.

[C7-10] Q. Zhao and H. Li, "Differential modulation for cooperative wireless systems," *IEEE Trans. Signal Process.*, vol. 55, pp. 2273–2283, May 2007.

[C7-11] Q. Zhao, H. Li, and P. Wang, "Performance of cooperative relay with binary modulation in Nakagami-m fading channels," *IEEE Trans. Veh. Technol.*, vol. 57, pp. 3310–3315, September 2008.

[C7-12] R. Annavajjala, P. Cosman, and L. Milstein, "On the performance of optimum noncoherent amplify-and-forward reception for cooperative diversity," *Proc. IEEE Military Commun. Conf.*, pp. 3280–3288, October 2005.

[C7-13] Y. Zhu, P.-Y. Kam, and Y. Xin, "Non-coherent detection for amplify-and-forward relay systems in a Rayleigh fading environment," *Proc. IEEE Global Telecommun. Conf.*, pp. 1658–1662, November 2007.

[C7-14] M. R. Souryal, "Non-coherent amplify-and-forward generalized likelihood ratio test receiver," *IEEE Trans. Wireless Commun.*, vol. 9, pp. 2320–2327, July 2010.

[C7-15] G. Farhadi and N. Beaulieu, "A low complexity receiver for noncoherent amplify-and-forward cooperative systems," *IEEE Trans. Commun.*, vol. 58, pp. 2499–2504, September 2010.

[C7-16] P. Ho, Z. Songhua, and K. P. Yuen, "Space-time FSK: An implicit pilot symbol assisted modulation scheme," *IEEE Trans. Wireless Commun.*, vol. 6, pp. 2602–2611, July 2007.

[C7-17] P. Y. Kam, P. Sinha, and Y. Some, "Generalized quadratic receivers for orthogonal signals over the Gaussian channel with unknown phase/fading," *IEEE Trans. Commun.*, vol. 43, pp. 2050–2059, June 1995.

[C7-18] C. Patel and G. Stuber, "Channel estimation for amplify and forward relay based cooperation diversity systems," *IEEE Trans. Wireless Commun.*, vol. 6, pp. 2348–2356, June 2007.

[C7-19] B. Gedik and M. Uysal, "Impact of imperfect channel estimation on the performance of amplify-and-forward relaying," *IEEE Trans. Wireless Commun.*, vol. 8, pp. 1468–1479, March 2009.

[C7-20] S. M. Kay, *Fundamentals of Statistical Signal Processing, Volume I: Estimation Theory*. Prentice Hall, 1998.

[C7-21] M. K. Simon and M.-S. Alouini, *Digital Communication over Fading Channels*. Wiley, 2005.

[C7-22] T. Wang, A. Cano, and G. Giannakis, "Link-adaptive cooperative communications without channel state information," in *Proc. IEEE Military Commun. Conf.*, pp. 1–7, October 2006.

[C7-23] H. Muhaidat and M. Uysal, "Cooperative diversity with multiple-antenna nodes in fading relay channels," *IEEE Trans. Wireless Commun.*, vol. 7, pp. 3036–3046, August 2008.

[C7-24] S. Muhaidat, J. Cavers, and P. Ho, "Transparent amplify-and-forward relaying in MIMO relay channels," *IEEE Trans. Wireless Commun.*, vol. 9, pp. 3144–3154, October 2010.

[C7-25] J. G. Proakis, *Digital Communications*. McGraw-Hill, 2000.

8. Summary and Suggestions for Further Studies

8.1 Summary

This thesis mainly focused on how to utilize the thresholds to improve the error performance/throughput in coherent/noncoherent DF cooperative networks with/without unequal error protection. The thesis also developed a transmission framework for noncoherent AF cooperative networks. The main contributions for each topic are summarized as follows:

1. Signal Transmission with Unequal Error Protection in Wireless Relay Networks

   - The use of two different SNR thresholds at the relay has been studied for a single-relay DF network with unequal error protection in Chapter 3. The average e2e BERs for two different protection classes have been derived when a hierarchical 2/4-ASK constellation is employed at the source. Optimal thresholds that are chosen to minimize the BER for the less protection class while the BER of the more protection class satisfies a given requirement have been found numerically. The BER performance comparison has been conducted and shown that the optimal thresholds improve the error performance significantly.
   - The SNR-threshold-based relaying in DF cooperative networks using hierarchical modulation has been developed and studied in the context of relay selection in Chapter 4. The average BERs for two different information classes have been derived. Optimal thresholds for the relays have been found numerically. The simulation results have shown that the optimal

thresholds significantly improve the error performance.

2. Adaptive Relaying in Noncoherent Cooperative Networks

   - An adaptive relaying scheme for noncoherent DF cooperative networks in which BFSK is used to modulate the signals at both the source and relays has been proposed and studied in Chapter 5. The average BER for a two-relay network has been derived in a closed-form expression when MRC is employed at the destination. Optimal thresholds/power allocation are chosen to minimize the average BER. Simulations results have shown that by employing optimal thresholds or jointly optimal thresholds and power allocation, the proposed protocol significantly improves the error performance compared to the previously proposed PL scheme, and yet with a similar complexity.

3. Throughput Maximization in Cooperative Networks

   - An incremental relaying protocol for noncoherent DF cooperative networks was proposed and studied in Chapter 6. For BFSK, very-tight closed-form upper bounds for both the average BER and throughput have been derived. Optimal thresholds are chosen to maximize the throughput while the BER meets a given requirement. The performance comparison has revealed that by employing optimal thresholds, the proposed protocol leads to a considerable improvement in the performance of cooperative diversity systems.

4. Noncoherent Amplify-and-Forward Relaying with Implicit Channel Estimation

   - Multiple-relay AF networks in which M-FSK is employed at both the source and relays to facilitate noncoherent communications when the channels are temporally-correlated Rayleigh flat fading have been studied in Chapter 7. An upper-bound of the BER expression has been derived and used to show that the proposed scheme achieves a full diversity order. Sim-

ulation results show that the proposed scheme outperforms the previously proposed schemes.

8.2 Suggestions for Further Studies

The concept of cooperative communications presents many challenges as well as opportunities for research in wireless networks. Possible continuing research works are summarized below.

1. Signal Transmission with Unequal Error Protection in Wireless Relay Networks

   - As presented in Chapters 3 and 4, our works concentrated on the use of a hierarchical 2/4-ASK constellation. However, given the advantages of nonuniform PSK constellations, a study on finding optimum thresholds in cooperative networks employing nonuniform PSK constellations is of interest.
   - The threshold-based relaying protocol with UEP assumes that the full CSI is available at the receivers. It is useful to investigate the use of thresholds with noncoherent modulation/demodulation in UEP cooperative networks. For example, the nonuniform M-DPSK signals can be employed to modulate different protection bits at the source and the relays.

2. Adaptive Relaying in Noncoherent Cooperative Networks

   - The work in Chapter 5 investigated the optimum thresholds in cooperative networks in which simple BFSK is employed. Considering M-FSK in a multiple-relay network is an important and interesting extension. In particular, one can investigate how to reduce error propagation with M-FSK to improve the error performance of the network.

3. Distributed Space-Time FSK in Wireless Relay Networks

   - In this thesis, the repetition-based cooperative schemes have been considered, i.e., the multiple relays communicate with the destination over orthogonal channels to achieve the spatial diversity order. However, such schemes suffer a poor spectral efficiency. To overcome this disadvantage, distributed space time coding (DSTC) could be designed to provide diversity without a significant loss in spectral efficiency. Previous works along this line assumed that perfect CSI is available at the receivers to employ coherent detection. It is therefore necessary to find out how to design a distributed space-time FSK for AF/DF relay networks with noncoherent detection.

4. Noncoherent Cooperative Networks under the Presence of Interference

   - Although the cooperative technique has been extensively studied in the literature, most existing works have assumed that the effect of interference is ignored. Although this assumption simplifies theoretical studies, it does not always represent practical scenarios with simultaneous multi-user transmissions. Hence studying cooperative networks affected by interference is relevant and of practical interest. In particular, how to handle the interference during the cooperation process in noncoherent cooperative systems should be investigated.